

University of Tasmania Open Access Repository

Cover sheet

Title

Hellyer host rock alteration

Author

Jack, DJ

Bibliographic citation

Jack, DJ (1989). Hellyer host rock alteration. University Of Tasmania. Thesis.
<https://doi.org/10.25959/23210243.v1>

Is published in:

Copyright information

This version of work is made accessible in the repository with the permission of the copyright holder/s under the following,

Licence.

Rights statement: Copyright the Author - The University is continuing to endeavour to trace the copyright owner(s) and in the meantime this item has been reproduced here in good faith. We would be pleased to hear from the copyright owner(s).

If you believe that this work infringes copyright, please email details to: oa.repository@utas.edu.au

Downloaded from University of Tasmania Open Access Repository

Please do not remove this coversheet as it contains citation and copyright information.

University of Tasmania Open Access Repository

Library and Cultural Collections

University of Tasmania

Private Bag 3

Hobart, TAS 7005 Australia

E oa.repository@utas.edu.au

CRICOS Provider Code 00586B | ABN 30 764 374 782

utas.edu.au

HELLYER HOST ROCK ALTERATION

BY

DOUGLAS JAMES JACK, BSc (Eng) (Mining Geology) (Witwatersrand)

Submitted in fulfilment of the requirements
for the degree of Master of Science

UNIVERSITY OF TASMANIA

HOBART

FEBRUARY 1989

This thesis contains no material that has been accepted for the award of any degree or diploma in any university. To the best of the candidate's knowledge this thesis contains no copy or paraphrase of material previously written or published by another person, except where due reference is made.

D. J. Jack

Signed: D. J. Jack

CONTENTS

	<u>PAGE</u>
ABSTRACT	1
 <u>CHAPTER 1 INTRODUCTION</u>	 3
The Hellyer Deposit and its Discovery	3
Aims	3
Physiography, Vegetation and Climate	4
Previous Literature and Research	4
Outline of Thesis	6
Work Completed	7
Acknowledgements	8
 <u>CHAPTER 2 GEOLOGICAL SETTING</u>	 10
<u>Regional Geology</u>	10
<u>Hellyer District Geology</u>	15
Stratigraphy	
Structure	
Metamorphism	
Mineralization and Ore Deposits	
 <u>CHAPTER 3 THE ORE BODY</u>	 19
<u>Introduction</u>	19
<u>Zoning</u>	19
<u>Textures and Mineralogy</u>	24
<u>Interpretation</u>	26
 <u>CHAPTER 4 PRIMARY PETROLOGY AND GEOCHEMISTRY OF THE HOST SEQUENCE</u>	 27
<u>Introduction</u>	27
<u>Petrography</u>	27
Macroscopic Textures	
Microscopic Textures	

	<u>PAGE</u>
<u>Regional Metamorphic Imprint</u>	34
<u>Interpretation of Petrographic Textures</u>	34
<u>Primary Mineral Chemistry (Relict Primary Phases)</u>	35
<u>Primary Whole-Rock Geochemistry</u>	38
<u>Tectonic Setting based on Geochemistry</u>	47
<u>The Hellyer Core Lava</u>	48
<u>Comparison with other VMS Host Rocks</u>	51
 <u>CHAPTER 5 EFFECTS OF HYDROTHERMAL ALTERATION</u>	 53
<u>Introduction</u>	53
<u>Textures and Mineralogy</u>	54
<u>Whole Rock Geochemistry</u>	63
Introduction	63
Element Distribution on Cross Sections	67
Through the Hydrothermal Centre	
Isocon Diagram	87
Rare Earth Elements	96
Interpretation	99
<u>Mineral Chemistry</u>	104
<u>Comparison with other VMS Alteration</u>	110
 <u>CHAPTER 6 SULPHUR ISOTOPES</u>	 113
<u>Introduction</u>	113
<u>Results</u>	113
<u>Interpretation</u>	119
 <u>CHAPTER 7 CONCLUSIONS AND RECOMMENDATIONS</u>	 132
<u>REFERENCES</u>	136

APPENDICES

Appendix 1	Cross Sections through Stringer Zone Core and Orebody	145
Appendix 2	Whole-Rock Geochemical Analyses	154

FIGURES

FIGURE 1	Distribution of Mount Read Volcanics in Western Tasmania	11
FIGURE 2	Hellyer District Geology	13
FIGURE 3	Que River - Hellyer Stratigraphy Schematic Sections	14
FIGURE 4	Hellyer Long Section Projection Showing Drill Holes Sampled	20
FIGURE 5	Hellyer Cross Section 10900N	21
FIGURE 6	Hellyer Cross Section 10750N	22
FIGURE 7	Hellyer Schematic Cross Section	23
FIGURE 8	Composition of Augites at Hellyer	37
FIGURE 9	Cr.100/(Cr+Al) versus Mg.100/(Mg+Fe ²⁺) in Hellyer Hangingwall Basalt Chromites.	39
FIGURE 10	SiO ₂ versus Ti/Zr for all Hellyer Rock Types Outside the Stringer Zone.	41
FIGURE 11	Ti/Zr versus Nb/Y for all Hellyer Rock Types Outside the Stringer Zone.	42
FIGURE 12	Ti/100-Zr-Yx3 Ternary Plot for all Hellyer Volcanic Rocks Outside the Stringer Zone.	44
FIGURE 13	Rare-Earth Element Chondrite-normalized Spidergram for Hellyer Andesites and Basalts compared with High-K Lavas from Java.	45
FIGURE 14	Rare-Earth and Other Element Chondrite-normalized Spidergram for Continuous Core Grinds Through the Hellyer Hangingwall Core Basalt and the Surrounding Basalt.	46
FIGURE 15	Hellyer Research Section. Ti/Zr Ratio Distribution.	49
FIGURE 16	Ppm Zr versus % TiO ₂ for the Hellyer Hangingwall Basalt in Drill Hole HL55 through the Hellyer Hangingwall Alteration Plume.	50
FIGURE 17	Hellyer Research Section. Drill Hole Locations and Transpositions.	64
FIGURE 18	Silica Distribution.	72

		<u>PAGE</u>
FIGURE 19	Alumina Distribution.	73
FIGURE 20	Total Iron Distribution.	74
FIGURE 21	Manganese Distribution.	75
FIGURE 22	Magnesium Distribution.	76
FIGURE 23	Calcium Distribution.	77
FIGURE 24	Sodium Distribution.	78
FIGURE 25	Potassium Distribution.	79
FIGURE 26	Sulphur Distribution.	80
FIGURE 27	Copper Distribution.	81
FIGURE 28	Lead Distribution.	82
FIGURE 29	Zinc Distribution.	83
FIGURE 30	Chromium Distribution.	84
FIGURE 31	Barium Distribution.	85
FIGURE 32	Quartz-barite Alteration Isocon	90
FIGURE 33	Sericite-pyrite Alteration Isocon	91
FIGURE 34	Mg-chlorite Alteration Isocon	92
FIGURE 35	Quartz-sericite Stringer-envelope-zone Alteration Isocon	93
FIGURE 36	Mean Fuchsite Alteration Isocon	94
FIGURE 37	Albite Alteration Isocon	95
FIGURE 38	REE Chondrite-normalized Spidergram for Stringer Zone Rocks 1.	97
FIGURE 39	REE Chondrite-normalized Spidergram for Stringer Zone Rocks 2.	98
FIGURE 40,41	Element abundances in DDH HL55 through the calcite fuchsite-pyrite plume - Major Elements.	100
FIGURE 42,43	Element abundances in DDH HL55 through the calcite fuchsite-pyrite plume - Trace Elements.	102

		<u>PAGE</u>
FIGURE 44	Hellyer Sulphur Isotopes - Histogram	118
FIGURE 45	Sulphur Isotopes in Mount Read Volcanic Ore Deposits.	122
FIGURE 46	Hellyer Sulphur Isotopes - Models	124
FIGURE 47	Log f_{O_2} versus pH at 250°C Showing the Isotopic Composition of Sulphur in Pyrite.	125
FIGURE 48	Progressive Reduction of Seawater with a Non-replenished Supply by Rayleigh Fractionation.	126
FIGURE 49	(SO_4^{2-} - H_2S) Sulphate - sulphide Isotopic Fractionation versus T.	130

TABLES

TABLE 1	Augite Microprobe Analyses	36
TABLE 2	Chromite Microprobe Analyses	36
TABLE 3	Rare-earth Element Analyses	43
TABLE 4	Transformations Used in Constructing the Hellyer Pre-Jack Fault Research Section.	65
TABLE 5	Major Additions and Losses of Elements during Alteration.	89
TABLE 6	Mica Microprobe Analyses	105
TABLE 7	Variations in Illite Composition with Reference to Muscovite.	106
TABLE 8	Chlorite Carbonate Albite Apatite and Titanite Microprobe Analyses.	109
TABLE 9	Sulphur Isotope Data	114
TABLE 10	Sulphur Isotopes Summary	120

PLATES

PLATE 1	The Que-Hellyer area looking south.	5
PLATE 2	Textures in albite porphyritic andesite.	28
PLATE 3	Textures in polymict ash volcanoclastic.	30
PLATE 4	Textures in Hellyer hangingwall basalt (unaltered).	31
PLATE 5	Textures in the stringer zone core.	55
PLATE 6	Textures in the stringer envelope zone.	58
PLATE 7	Textures in calcite-fuchsite alteration.	60
PLATE 8	A mat of albite alteration and a K-feldspar veinlet in interpillow sediment.	62

APPENDIX

Appendix 1	Cross Sections through Stringer Zone Core and Orebody.	145
Figure i	Orebody and Upper Stringer Zone - Copper Distribution.	146
Figure ii	Orebody and Upper Stringer Zone - Lead Distribution.	147
Figure iii	Orebody and Upper Stringer Zone - Zinc Distribution.	148
Figure iv	Orebody and Upper Stringer Zone - Silver Distribution.	149
Figure v	Orebody and Upper Stringer Zone - Gold Distribution.	150
Figure vi	Orebody and Upper Stringer Zone - Barium Distribution.	151
Figure vii	Orebody and Upper Stringer Zone - Arsenic Distribution.	152
Figure viii	Orebody and Upper Stringer Zone - Density Distribution.	153
Appendix 2i	Element Analyses, Holes, Sample Intervals, Rock Descriptions.	154
Appendix 2ii	Northings, Eastings, RLs, Ratios	165
Appendix 2iii	Transformed co-ordinates for Sample Points used in the Research Section.	176
Appendix 2iv	Abbreviations. Definition of Ratios. Rock Type Key.	180

ABSTRACT

Hellyer is a large (16 million tonne plus), Kuroko-style, polymetallic, volcanogenic massive sulphide deposit in Cambrian high-K, calc-alkaline, arc-like, volcanics in western Tasmania. Hydrothermal alteration in the Hellyer host lavas is preserved in a near pristine condition, overprinted only by low-grade prehnite-pumpellyite facies metamorphism.

The massive sulphide deposit occurs at the time break between an albite porphyritic andesite footwall and a hangingwall basalt. Within the Hellyer hangingwall basalt is a lava flow directly above the Hellyer deposit with regionally high Ti/Zr ~53, higher primary MgO, Ni, Cr and lower primary SiO₂, TiO₂, P₂O₅, Y, Zr, La and Nb than the surrounding basalt. The structure which localized the Hellyer hydrothermal system is thought to have also provided the locus for the extrusion of this deeper sourced, more-primitive lava.

Not only is an excellent example of a hydrothermal feeder system developed in the footwall andesite, but a plume shaped zone of chrome green alteration occurs in the hangingwall basalt. The basalt was extruded while the hydrothermal system was still active. The Cu, Pb, Zn mineralized stringer-zone core consists of quartz barite surrounded by quartz sericite pyrite grading outwards into a chlorite rich zone including massive Mg-chlorite schists. This is surrounded by an envelope zone of quartz sericite pyrite alteration. K-feldspar develops across the outer margins of the envelope zone. The green hangingwall plume consists of pervasive calcite-fuchsite, accessory Fe-chlorite patches, calcite veining and increased quantities of interpillow pyrite. Albite alteration extends out from the plume.

Element distributions highlight the stringer zone with a Na_2O low, and more complexly, with SiO_2 , Fe_2O_3 , MgO , S , Cu , Pb , Zn , Ba highs. CaO and Sr depletion in the footwall is more widespread than the Na_2O depletion and extends outside the stringer zone. In the hangingwall, the plume is highlighted by increased S (2-4 times background S), increased CaO (2 times background CaO), and elevated Ba . Na_2O highs trace albite alteration.

In the hangingwall calcite-fuchsite alteration there has been a major mass addition of CaO , K_2O , Al_2O_3 , Ba and depletion in Fe_2O_3 , MgO , and SiO_2 , with relative enrichment in As , Rb and Mn . Zr , TiO_2 , Y , Nb and the rare-earth elements remain immobile as evidenced by unchanged ratios of these elements regardless of the degree of alteration. In the footwall stringer zone core there is some mobility of all elements.

Sulphur isotopes show a progressive decrease in $\delta^{34}\text{S}$ (pyrite) values inwards and up the stringer zone from +13 per mil at depth through +8 per mil to consistent values of +7 per mil in the orebody. This is due either to an increase in oxygen fugacity towards the quartz barite stringer-zone top and into a narrow oxygen fugacity field for the deposition of the orebody, or to mixing a hydrothermal fluid with a value of +7 per mil with a variable supply of reduced seawater sulphate. Sulphur in light pyrite (-14 per mil) in hangingwall interpillow areas is produced from reduced seawater sulphate rapidly replenished by a high seawater flux.

CHAPTER 1

INTRODUCTION

The Hellyer deposit and its Discovery

Hellyer is a large (16 million tonne plus) Kuroko-style volcanogenic sulphide deposit in Cambrian andesitic and basaltic lavas in western Tasmania (McArthur, 1986). The deposit was discovered in August 1983 (Sise and Jack, 1984; Eadie et al., 1985) by drilling an electromagnetic conductor which occurred below bright chrome-green alteration and a barite pod exposed at surface in the hinge of an anticline. Hellyer occurs three kilometres north of Que River (Webster and Skey, 1979), a 2.6 million tonne volcanogenic deposit that also has bright chrome-green alteration in its hangingwall and which has been interpreted to occur in a tightly folded synform (Large et al., 1987b).

Aims

This study aimed to document mineralogical and geochemical changes due to hydrothermal alteration in the Hellyer host rocks and to relate these changes to the ore forming process. A cross section extensively drilled to aid geologic understanding during the resource establishment programme was chosen to construct a series of diagrams detailing the distribution of elements in host rocks on a section through the centre of the ore body. It was hoped to develop criteria useful for exploration based on this documentation and to use the results of this research as they became available.

Physiography, Vegetation and Climate

The Que River-Hellyer area comprises densely forested rugged terrain typical of the west coast of Tasmania. The present physiography is dominated by the Southwell River gorge in the east with the Cambrian volcanics forming a prominent ridge to the west (Plate 1). On this ridge, Mt. Charter is a low high (840 metres) and the Sharks Fin is a prominent spine on the edge of the ridge. Quaternary-Recent glaciation has formed some of the valleys down into the Southwell River. However, little till has developed and Cambrian rocks are only covered by a rare, thin veneer of glacial sediment.

Temperate rainforest covers the entire Que River-Hellyer area except for patches of sedgeland which develop more especially on the more acid intrusions and sediment-rich areas.

The climate is cold and wet with most rain falling in winter. Average annual rainfall at Hellyer is 2083mm.

Previous Literature and Research

The only published account of the geology at Hellyer is McArthur (1986). Unpublished Aberfoyle reports include Jack (1983) and Jack (1984), in which the host stratigraphy, way up, and gross character of the alteration system and orebody was first described, and McArthur (1985), a detailed account of the resource drilling programme, geostatistics, calculation of ore reserves and description of the host



Plate 1 The Que-Hellyer area looking south. Photography D. Jack 1984

The Que-Hellyer Volcanics form a prominent ridge with the Southwell River gorge and Lake Mackintosh just visible in the east (top left of photograph). The cleared area along the ridge is a powerline and Que River Mine can be seen in the background as a clearing east of the powerline. Hellyer is below the logged area in the foreground. Access to Hellyer is through an adit in the Southwell River gorge. Logging above Hellyer was done by Associated Forest Holdings immediately prior to and during Hellyer's discovery in 1983.

rocks and alteration. W. Fander, in a series of unpublished petrographic reports, described many Hellyer rocks from both the orebody and host rocks. The CSIRO produced a series of unpublished reports on the mineralogy of the orebody (Ramsden and Creelman, 1984; Ramsden et al., 1986; Whitford et al., 1984, 1985). G.R. Green researched the oxygen and carbon isotopes around Hellyer. More recently, Large et al. (in press), produced a paper on gold in western Tasmania which includes some data on Hellyer. The first report (unpublished) on recent research in the stringer system (Gemmell, 1988) recently became available but is restricted. Harris, 1986 completed a regional study on the hangingwall volcanoclastic rocks. Waters (1988) has issued three unpublished progress reports on a PhD on the regional vulcanology and sedimentology. Recently, McArthur and Dronseika have completed a paper on the geology of Que River and Hellyer, (McArthur and Dronseika, in press).

Outline of Thesis

In order to describe the alteration in the Hellyer host rocks, their original character needed description. Therefore after brief introductions to the regional setting (Chapter 2), and geology of the orebody (Chapter 3), Chapter 4 is devoted to the primary geology and geochemistry of the host rocks. Chapter 5 describes the effects of hydrothermal alteration, an important part being presented diagrammatically depicted element distribution around the orebody. The question of element mobility in various alteration facies is also addressed. Finally, in Chapter 6 the distribution of sulphur isotope ratios is discussed and interpreted.

Work Completed

A series of drill holes covering all the rock types and as wide as possible a distribution around the orebody were selected for sampling concentrating on a section drilled extensively in the early resource drilling. This section passes close to the centre of the hydrothermal system as established by subsequent underground drilling. 140 continuous core grinds covering intervals logged macroscopically by the author were analysed for whole-rock geochemistry (Appendix 2). In addition a further 208 split core samples, most from within the core grind intervals, were analysed for whole-rock geochemistry (Appendix 2). All split core samples have an accompanying polished thin section and these were examined and related to the geochemical analysis. These are filed together with photographs and offcuts in Aberfoyle's thin section library in Burnie. In addition 19 rocks were selected for rare-earth element analysis. Most analyses, including all the rare-earth element analyses, were done or supervised by P. Robinson at the University of Tasmania as detailed in Appendix 2 and Table 3, (XRF and XRF-ion exchange). Some samples (see Appendix 2) were analysed by AMDEL laboratories in Adelaide and by the Tasmanian Mines Department Laboratories in Launceston by a combination of ICP and XRF methods (see Appendix 2). All the data is stored on Aberfoyle's HP1000 computer 'DMAP' programme with selected data stored on Macintosh P.C. 'Cricket' and 'Excel' systems. Aberfoyle's Appollo computer and an 'Eagle-Condor' gridding and interpolated programme were used to produce a series of .pa element and element ratio distribution diagrams which are stored in

Aberfoyle's Burnie file together with numerous other scattergrams, histograms and geostatistical data not presented in this thesis. Selected microprobe analyses were performed at the Central Science Laboratory at the University of Tasmania by the author on a JEOL JXA - 50A microprobe. The detailed 2 metre core grinds through the upper stringer zone and orebody were provided by G. McArthur at Hellyer Mining, analyses being done by Analabs and Aberfoyle's Cleveland Laboratory. Contouring was done by the author. ⁵⁹ Sulphur isotope analyses were performed by Ritchie Woolley at the Central Science Laboratory University of Tasmania and by Dr. Sue Golding at the University of Queensland. All sulphur isotope analyses were performed on samples drilled out using a dentist's drill and are accompanied by a polished thin section filed in the library in Burnie. Most work associated with this thesis was conducted part-time during the period 1985-87 and a series of nine progress reports were produced (Jack, D., 1985 to 1987). Interpretation and writing of this thesis was done part-time in 1988 and early 1989.

Acknowledgements

I would like to thank Dr. Ross Large for guidance, constructive criticism and numerous suggestions while undertaking the research and writing of this thesis. I would also like to thank Dr. Anthony Crawford for similar guidance on the primary character of the rocks. Discussion with numerous other people at the University of Tasmania including David

Huston, Dr. Peter McGoldrick, Dr. Bruce Gemmel, Dr. Ron Berry and Dr. Rick Varne helped consolidate ideas. Phil Robinson supervised the geochemical analyses and Ritchie Woolley and Dr. Sue Golding did the sulphur isotope analyses.

Dr. Geoff Green from the Tasmanian Department of Mines is thanked for arranging some geochemical analyses at their Launceston laboratory, free of charge and for providing data and discussion on carbon oxygen and sulphur isotopes.

Many people at Aberfoyle helped in the production of this thesis: thanks especially to Jacky Cure who typed the thesis and put up with numerous revisions, to Julia Rapier who did most of the drafting, to Rod Paterson and Richard de Bomford who helped with the computer applications, to Gary McArthur who provided the underground drilling analyses and under whom the author worked during the 1984/85 resource drilling at Hellyer, and to Hugh Skey and David Wallace for encouragement and support.

Aberfoyle Resources is thanked for sponsoring this thesis.

CHAPTER 2 GEOLOGICAL SETTING

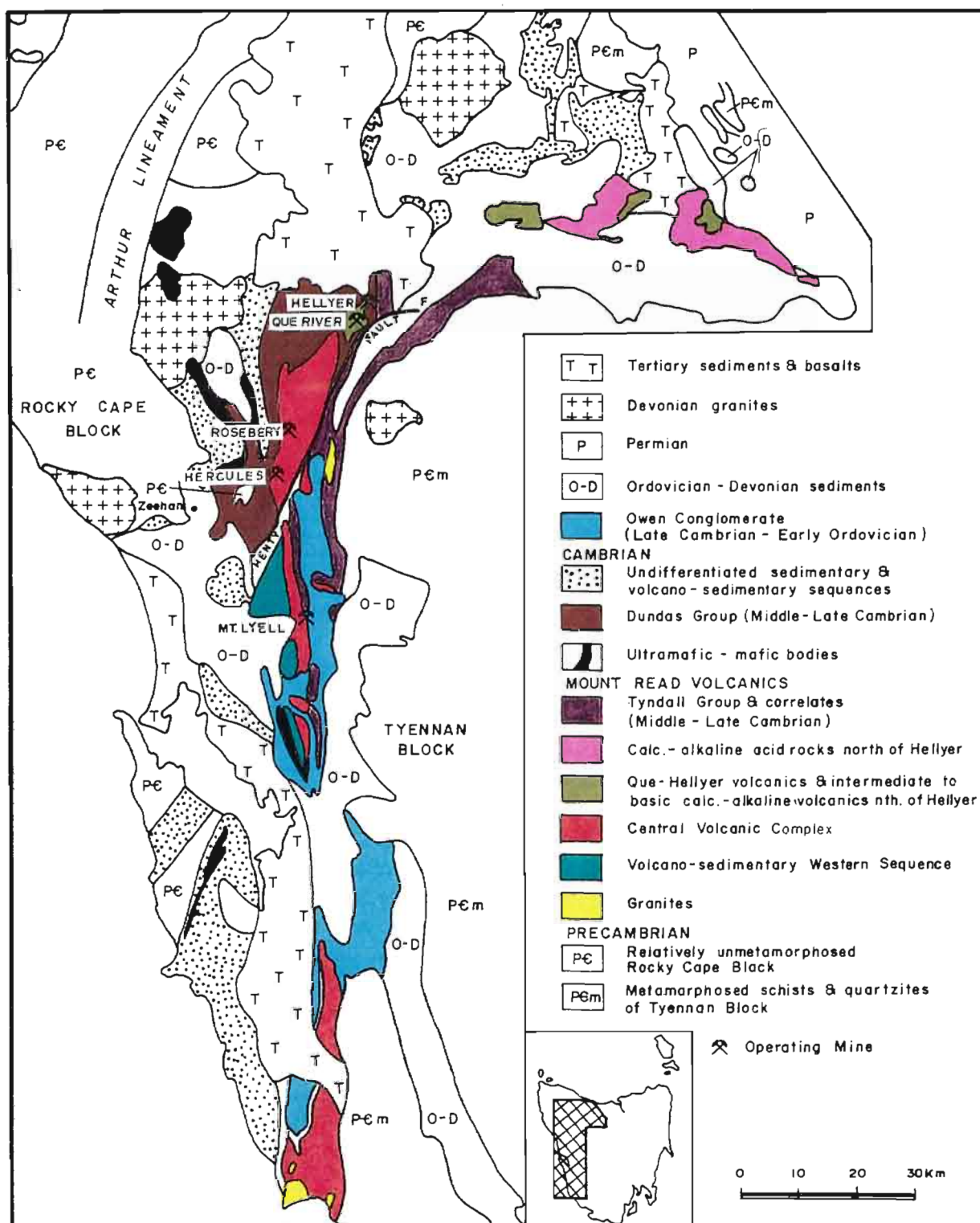
Regional Geology

Hellyer occurs in an arcuate belt of Cambrian calc-alkaline volcanics in western Tasmania described as the Mount Read Volcanics (MRV) (Campana and King, 1963) (Figure 1). The MRV is host to the other volcanogenic massive sulphide (VMS) deposits, Que River, Rosebery, Hercules and Prince Lyell. The MRV are flanked to the west by a volcano-sedimentary sequence deposited in the Dundas Trough. (Campana and King, 1963).

The Dundas Trough and the MRV occur between two Precambrian blocks, the Rocky Cape in north-west Tasmania and the Tyennenean Nucleus of central Tasmania.

The Dundas Trough contains the carbonate-dominated Success Creek Group stratigraphically overlain by greywacke - mudstones and tholeiitic volcanics of the Crimson Creek Formation. Several fault-bounded ultramafic bodies occur. All of these rocks are thought to be older than the MRV. They occur together in the Dundas Trough with younger sediments and volcanics assigned to the Dundas Group (Corbett, 1981). The Dundas Group sediments are at least partly formed from detritus shed off the MRV.

Other volcanogenic deposits in Tasmania (Figure 1) are confined to a division of the MRV that consists predominantly of acid lavas, pyroclastic rocks and intrusive rocks known as the Central Volcanic Complex (Corbett and Solomon, in press). Hellyer and Que River occur in a more mafic package of volcanics, the Que-Hellyer Volcanic interpreted to be younger than the Central Volcanic Complex to the south (Komyshan, 1986).



Aberfoyle Resources Limited

EXPLORATION DIVISION

FIG.1.

REVISIONS				NORTH WEST TASMANIA		Compiled : DJJ
Init.	Date	Init.	Date	DISTRIBUTION OF MOUNT READ VOLCANICS		Drawn :
				IN WESTERN TASMANIA		Traced : JLR
				MODIFIED AFTER LARGE et al., 1987		Checked :
Location Code :				Scale :	Date : June 1988	Plate No. : DT.95

FIGURE 1: The Distribution of Mount Read Volcanics in Western Tasmania. The Mount Read Volcanics are exclusively calc-alkaline. Hellyer occurs in an intermediate to basic member in the north.

The Henty Fault system (Figure 1) transects the MRV, separating the Central Complex into a dacitic-andesitic arc segment immediately south of the Que-Hellyer volcanics from a more rhyolitic arc segment in the southeast (Corbett and Lees, 1987). In the southeast the Central Volcanic Complex is flanked by a western volcano-sedimentary sequence interpreted to be partly older and partly coeval with the Central Complex (Corbett, 1979, 1981).

Quartz-feldspar porphyritic volcanics and volcanoclastic rocks assigned to the Tundall Group in the southeast overly and flank the Central Volcanic Complex, mostly in troughs or grabens. At Hellyer, the mafic lavas containing the orebody are overlain by a black shale and then by younger rhyolitic quartz and feldspar porphyritic lavas and pyroclastics mixed with sediments (Figure 2). Tasmanian Mines Department mapping (Komyshan, 1986) has grouped all these rocks, including the Que-Hellyer volcanics, into the Dundas Group. Berry and Crawford (1988) group the Que-Hellyer volcanics into the western Sequence of Corbett (1981).

Cambrian granites, notably the Murchison granite, intrude the Tyndall Group in the east. The end of volcanism was marked by the deposition, again in grabens, of siliclastic rocks assigned to the Owen Conglomerate. Major folding and greenschist facies metamorphism occurred in the Devonian.

The MRV themselves have been linked to rifting and grabens (Campana et al., 1958; Williams, 1978; Corbett, 1981). Large et al. (1987a), emphasise the importance of rifting in locating the volcanogenic massive sulphides (VMS). Extension of Precambrian continental crust figures in

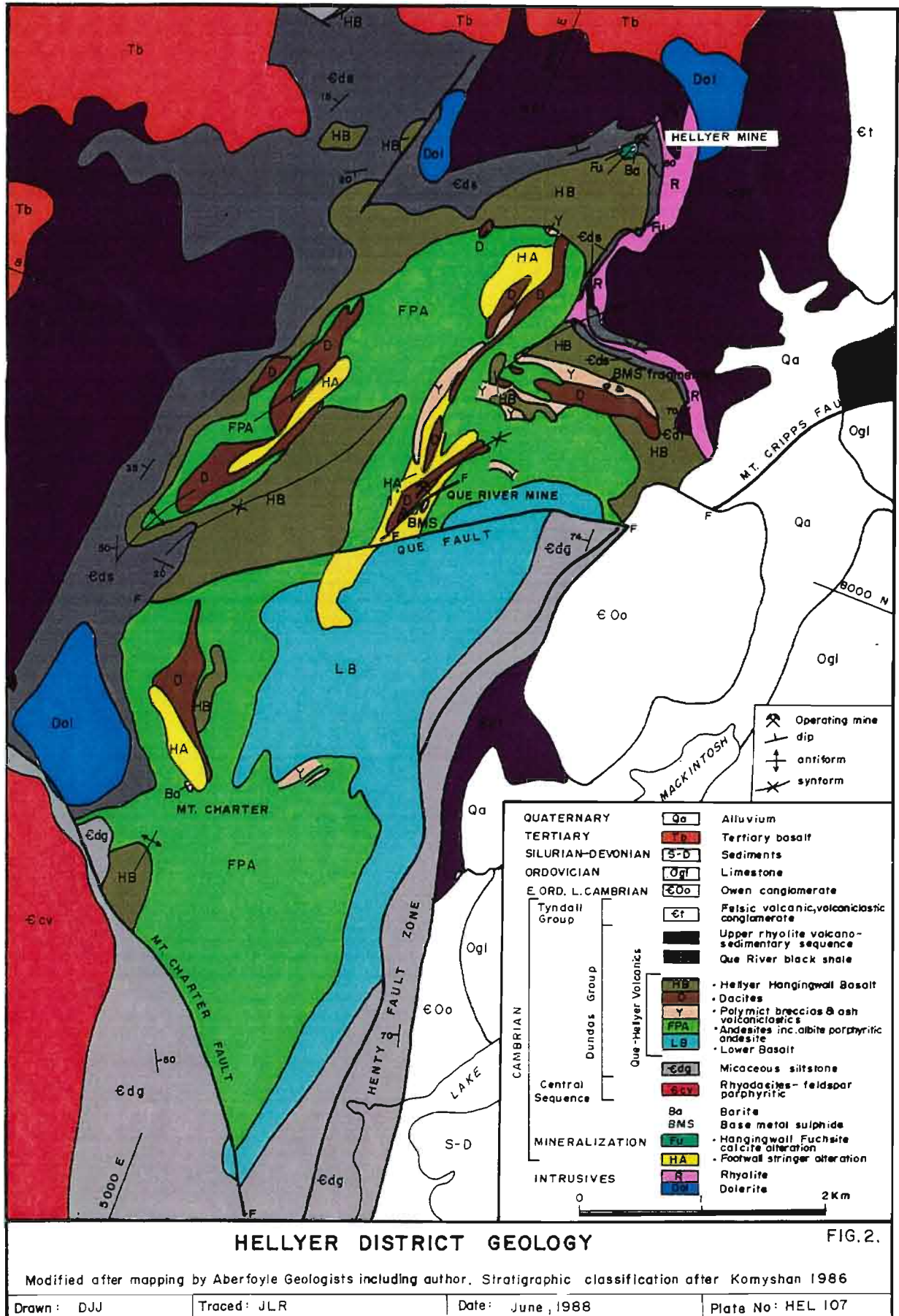
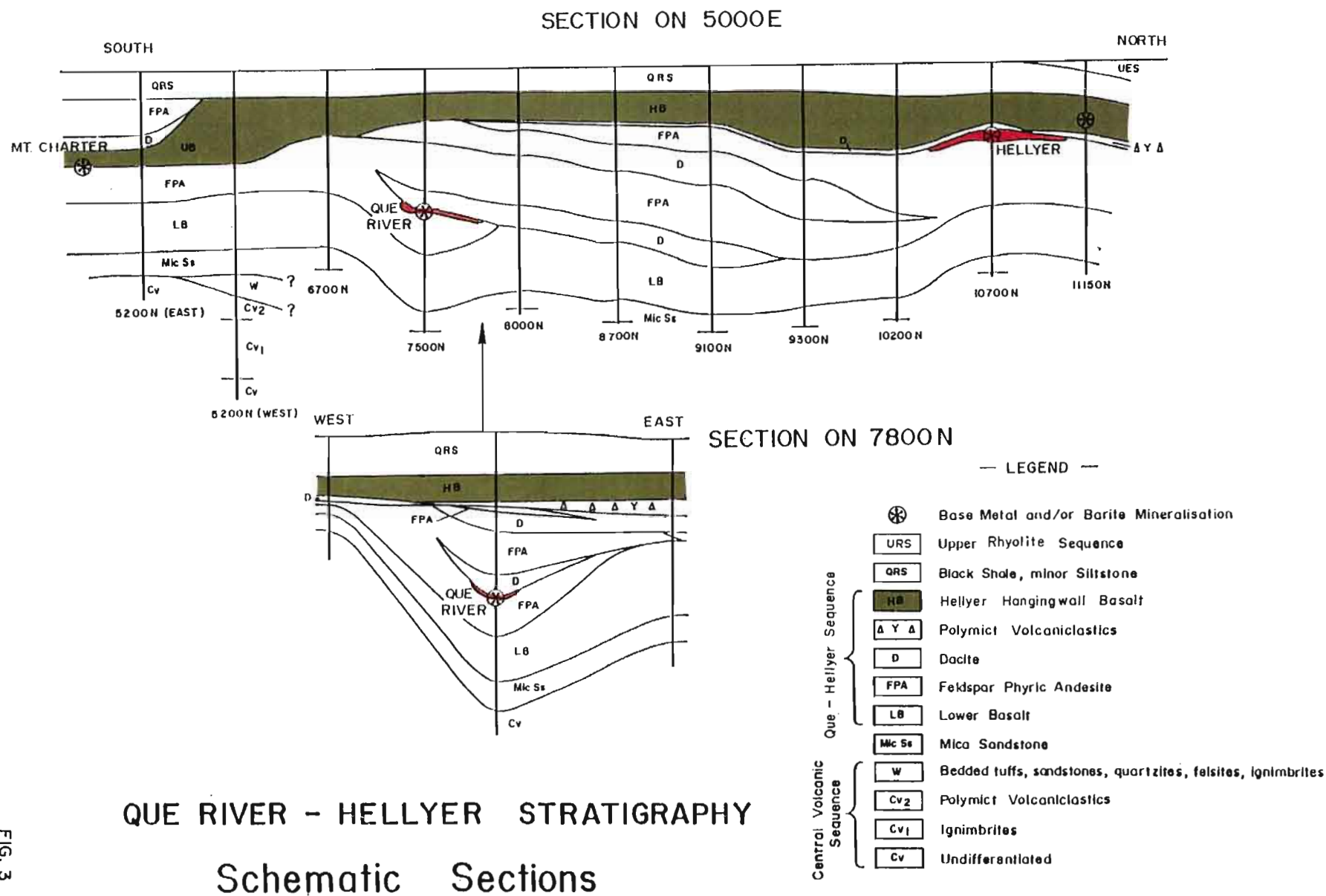


FIGURE 2: Hellyer District Geology. Hellyer occurs in the hinge zone of a prominent regional anticline below bright green calcite-fuchsite altered pillow basalt, 3 kilometres north of the Que River Mine.

FIGURE 3: Que River-Hellyer Stratigraphy. Schematic Sections depict Que River stratigraphically lower than Hellyer but within the same dacite and polymict rock dominated sequence that occurs between the lower and upper basalt extrusions.



many tectonic hypotheses. This varies from analogues to the east African rift system (Williams, 1978; Collins and Williams, 1986), to the incorporation of accretionary prisms, extension tectonics and crustal thinning on the edge of an active continental margin (Varne and Foden, 1987). Corbett and Lees (1987), modifying an hypothesis of Green (1983), have suggested an east-dipping subduction zone below a Cambrian accretionary prism - forearc sequence near Rosebery. Berry and Crawford (1988) draw analogies with present day arc-continent collisions and associate back-arc thrusting.

Hellyer District Geology

A simplified geologic mapping of the Hellyer area is presented as Figure 2 and interpreted schematic long and cross sections as Figure 3.

Stratigraphy

The intermediate lava-dominated package containing Hellyer, is called the Que-Hellyer volcanics (Komyshan, 1986), and this rests on a mica sandstone basement. Lava extrusion begins with a lower basalt which passes into an andesite that often contains prominent albite phenocrysts. Within these lavas are subsidiary dacites and polymict ash volcanoclastics and breccias, many of which are interpreted to be epiclastics. At the top of this lava sequence is the Hellyer hangingwall basalt which directly overlies the Hellyer ore position.

The contacts at the base and the top of this lava package are conformable, the lower lava being inter-calated with the basement mica

sandstone, and the Hellyer hangingwall basalt often having a peperitic contact with the late Middle Cambrian black shale above.

The lava package varies from less than 300 metres thick in the west to in excess of 800 metres in the east and individual units change rapidly in thickness.

The black shale above the lavas passes into a sequence of rhyolitic volcanics and sediments informally called the Upper rhyolitic sequence. Rhyolitic volcanics include possible ignimbritic and subaerial units and the sediments include shales and polymict volcaniclastics. Further to the northeast is another block of sediments, rhyolitic lavas and epiclastics interpreted to belong to the Tyndall Group (Komyshan, 1986).

The whole sequence is intruded by rhyolitic dykes and by dolerites. A K-Ar determination on pyroxene concentrates from the dolerite gave a Devonian age (Webb, 1985), interpreted to be a signature superimposed during Devonian tectonism.

Structure

Major faults have cut and partly bound the Que-Hellyer sequence (Figure 2). Prominent are the Henty fault and Mount Charter fault which together form a V-shaped southern limit to the lavas. The Henty fault contains sheared and folded shales in a horst to the south (Berry 1986), and this is interpreted to extend up the east of the Que-Hellyer volcanics and then to coalesce with the Que fault - Mount Cripps fault to the north (Aberfoyle staff mapping, 1978 - 1988). An anticline has been mapped at Hellyer (Aberfoyle staff mapping 1978-1988) and a synform has been interpreted at Que River (Young 1980, Large et al., 1987). The folding is interpreted to have occurred in the Devonian (Large et al., 1987).

Metamorphism

The rocks have undergone prehnite-pumpellyite grade metamorphism (Whitford et al., 1982). In contrast with Rosebery and Hercules, both of which are subject to intense folding and greenschist facies metamorphism, little internal deformation of the Hellyer VMS has occurred and metamorphic grade is not high enough to develop amphibole in the lavas.

Mineralization and Ore Deposits

Two operating VMS mines Que River and Hellyer occur in the Hellyer district. Que River mine, 3 kilometres south of Hellyer, is hosted by andesitic lavas with minor polymict epiclastic rocks. The major VMS body, PQ lens, occurs in a subvertical, lensoid wedge-shaped body below a dacite lava. The shape and metal distribution within the orebody has led to PQ lens being interpreted as a synform with the centre of the feeder system represented by coarse pyrite at the base of the keel (Large et.al., 1987). This represents a refinement of a proposal by Young (1980) and differs considerably from previous interpretations of stacked vertical lenses in a west facing sequence (Webster and Skey, 1979; Wallace and Green, 1982).

In addition to the PQ - P north lens system, a massive sulphide lens called S lens with a copper rich facies and an equivocal relationship with PQ lens outcrops 130 metres to the east of the main PQ - P north Que River orebody. These massive sulphide lenses occur in a subvertical, footwall-type stringer system of sericite, chlorite,

pyrite, sphalerite, chalcopyrite alteration up to 100 metres wide and more than 300 metres deep. At the top of PQ lens in the core of the interpreted synform is a polymict unit approximately a metre thick, containing basaltic fragments pervasively altered to fuchsite and calcite.

Three kilometres south of Que River mine, a stockwork of barite veinlets and lenses outcrops at Mount Charter. Coarse white and grey barite intercalated with sulphides is underlain by a zone of alteration interpreted to be a footwall stringer system (Figure 2). Other interpreted stringer systems exposed at surface are also shown in Figure 2.

High grade VMS clasts in a polymict volcaniclastic rock one kilometre south-east of Hellyer mine, may be the remnants of a VMS deposit fragmented and redistributed by explosive volcanism.

Calcite-fuchsite alteration occurs above Hellyer and also one kilometre south east of Hellyer, where it forms an exploration target based on data discussed below. There is a barite lens at surface in the middle of the fuchsite calcite alteration above Hellyer.

CHAPTER 3 THE ORE BODY

Introduction

A detailed description of the ore body is outside the scope of this thesis, and only a brief description is provided as background and to relate some features to alteration in the host rocks.

An indicated geological resource of 16.1 million tonnes at 0.38% Cu, 7.4% Pb, 14.4% Zn, 175 g/t Ag, 2.4 g/t Au, 2.3% Ba and 1.1% As is drilled between 10285N and 11075N at Hellyer, (June 1987 Ore Reserve; G. McArthur, pers. comm. 1987). This excludes any stringer zone mineralisation.

The elongate cigar-shaped ore body is depicted on a long section in Figure 4 and on cross sections 10900N and 10750N (Figures 5 and 6). The ore body is transected by a fault major called the Jack fault. By comparing mineral zoning, grade and the shape of the ore body on either side of the fault, the movement has been established as east side 130 metres north up 30 metres (McArthur, 1986).

Hellyer's shape is probably controlled partly by palaeotopography with sulphide deposition occurring in topographic lows and by mounding outwards from a central core. Recent underground exposures suggest some structural modification with occasional parasitic folds on the edges of the ore body and possible tight fold hinges at the top of a possible antiform east of the fault and a possible synform west of the fault.

Zoning

Zoning in the ore body is illustrated on a schematic cross section (Figure 7) and on the detailed contoured cross sections (Figures 1 to

FIGURE 4: Hellyer Long Section Projection Showing Drill Holes Sampled.

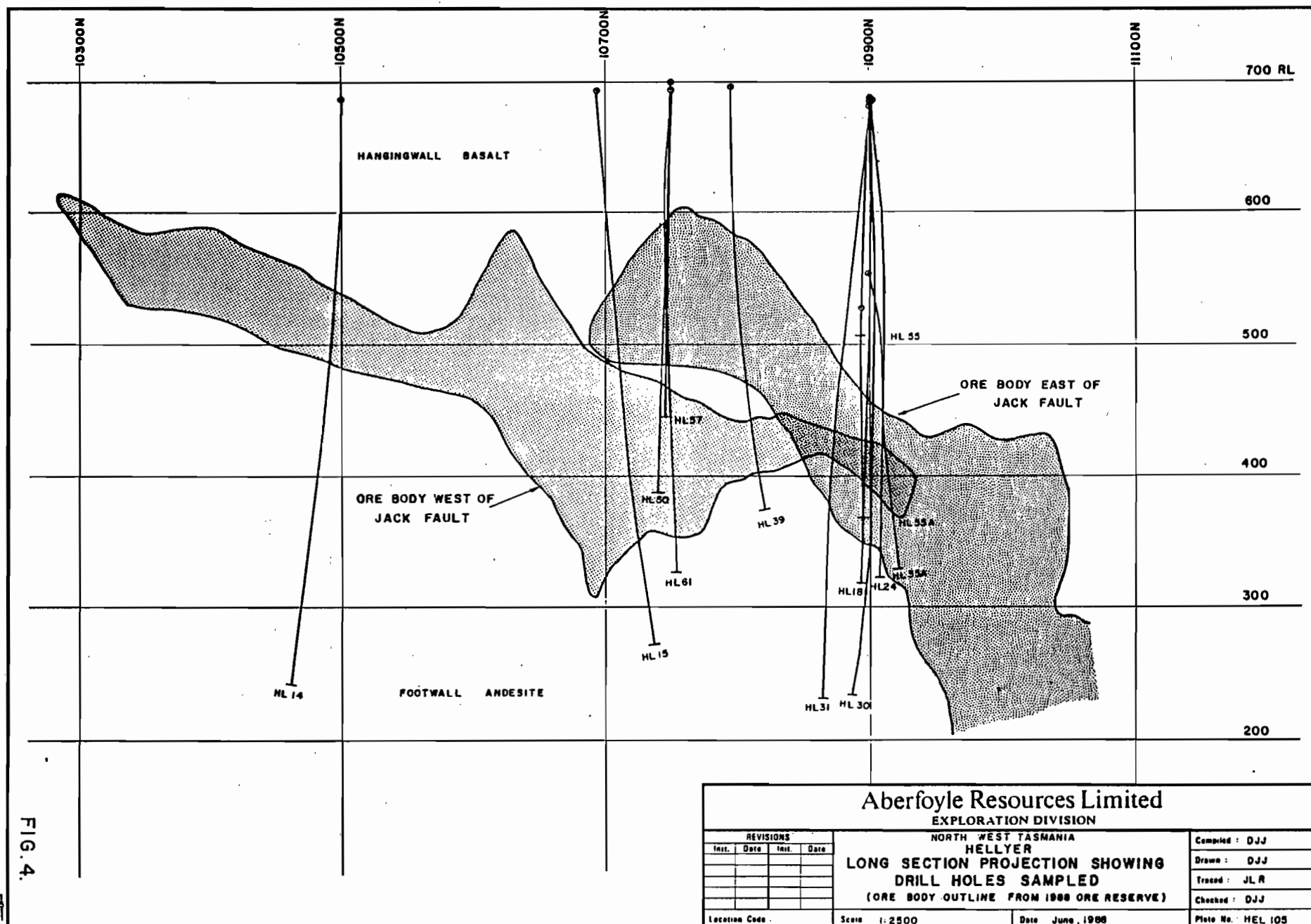


FIGURE 5: Hellyer Cross Section 10900N. Holes sampled are shown. The area in colour is joined with the coloured area in Figure 6 to form the Hellyer Research Section. (Figure 17)

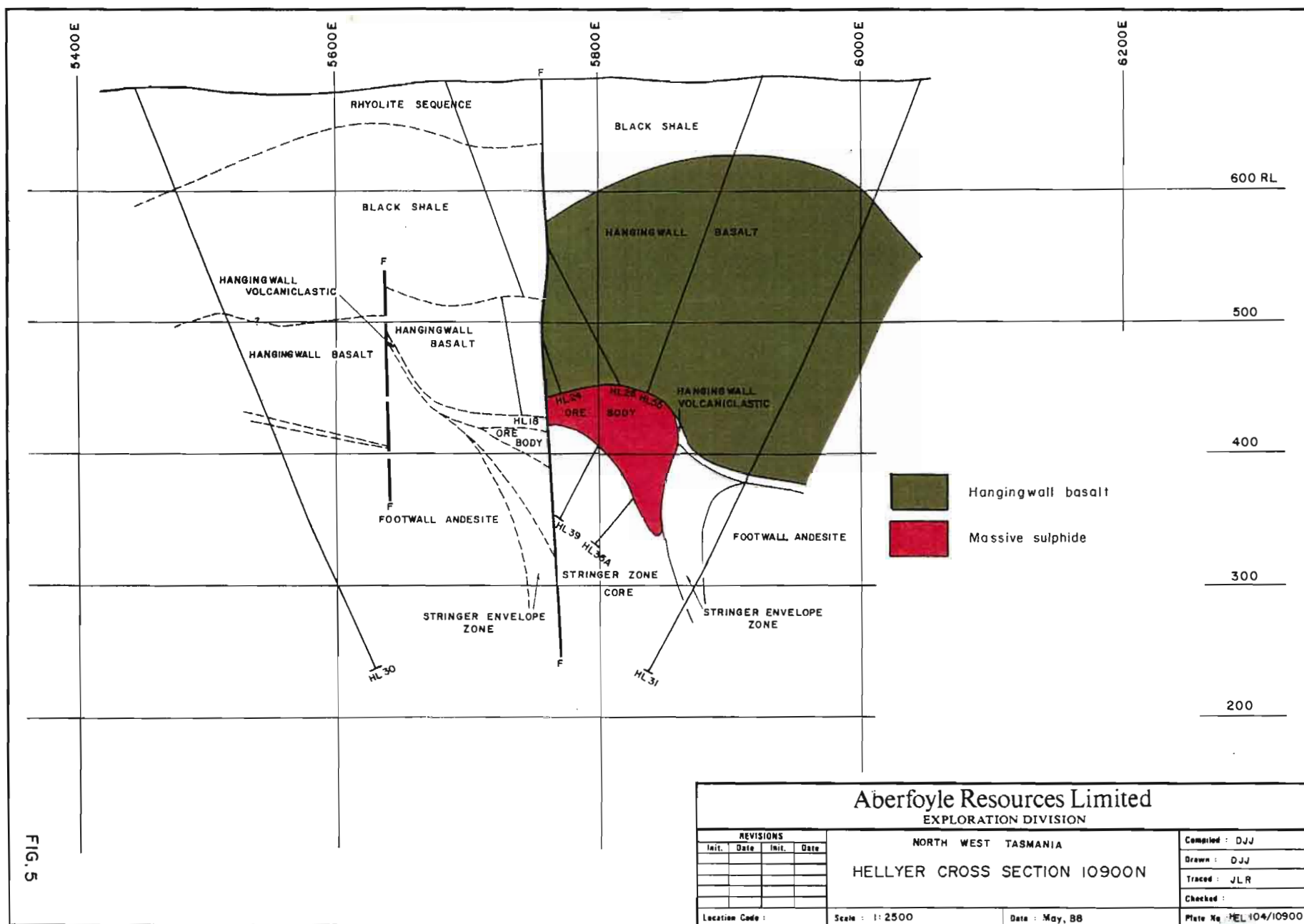


FIGURE 6: Hellyer Cross Section 10750N. Holes sampled are shown. The area in colour is joined with the coloured area in Figure 5 to form the Hellyer Research Section (Figure 17).

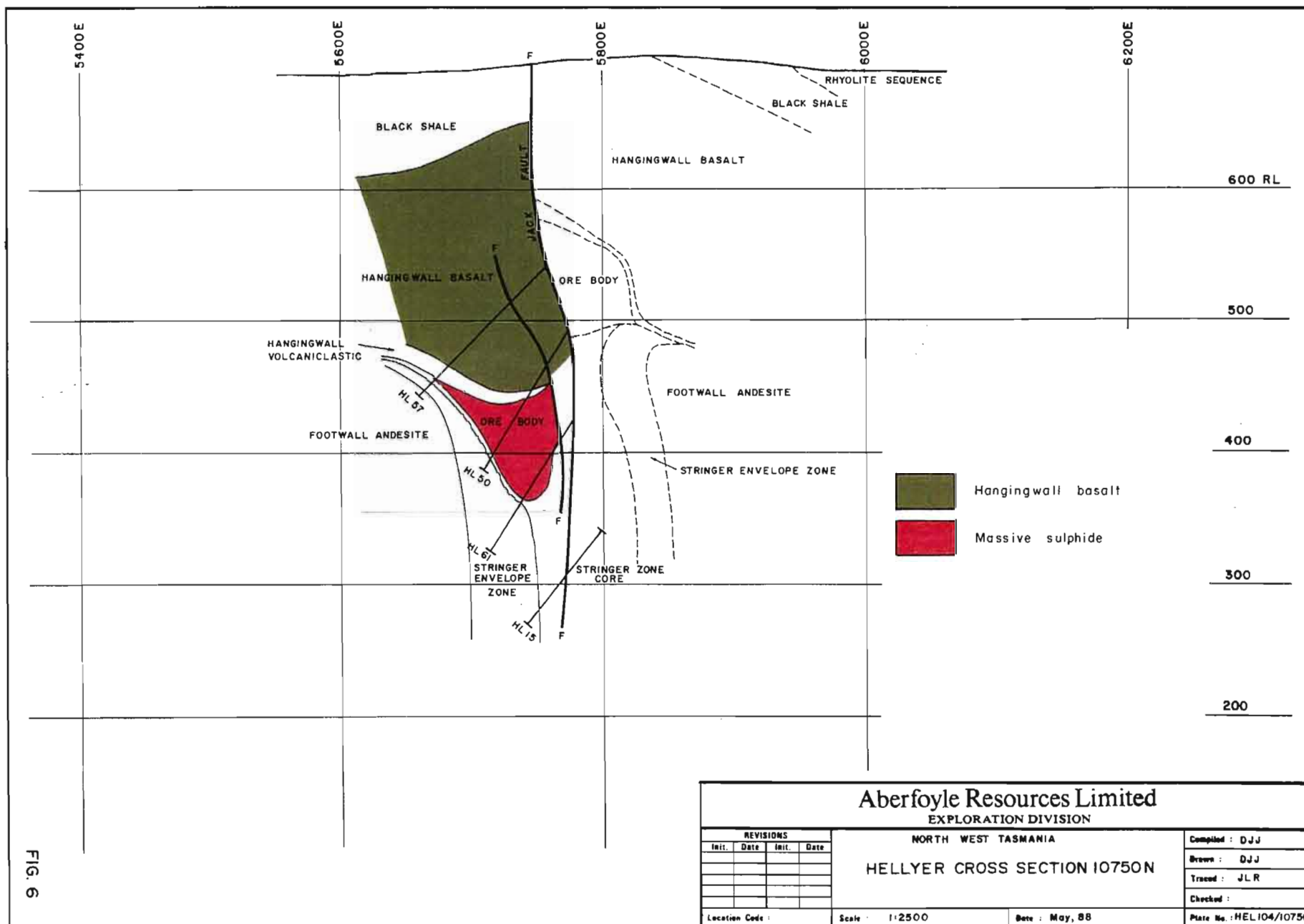


FIG. 6

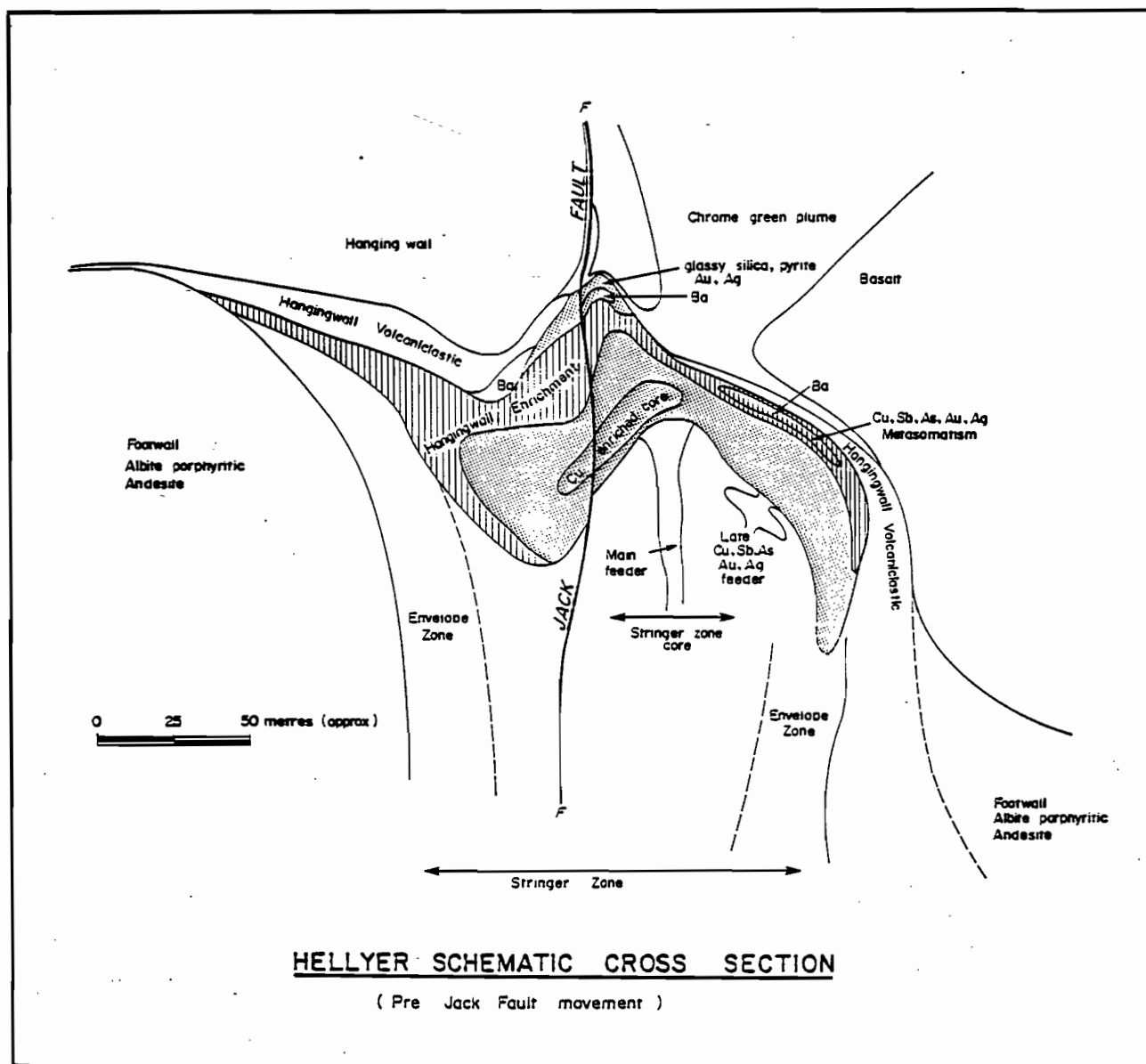


FIGURE 7: Hellyer Schematic Cross Section: This depicts the zoning in the stringer zone and in the massive sulphide. The location of the chrome green hangingwall plume above the "main feeder" in the stringer zone is also shown.

viii in Appendix 1). The zoning consists of a pyrite base at the centre top of the stringer zone, a chalcopyrite-pyrite rich lower ore body, a central massive zone passing upwards and outwards into a Pb, As, Ag, Au and Sb enriched hangingwall zone which extends into the footwall in the trough west of the Jack Fault. There is a barite top to the ore body and an auriferous glassy quartz-pyrite cap.

Textures and Mineralogy

Fragmental textures are rare, and the ore is commonly a featureless pyrite-rich massive variety. Jigsaw-like brecciation, interpreted to be a response to shrinkage and load adjustment phenomena, is common, (Fander, 1984).

In the outer hangingwall enriched-zone, banded brown sphalerite-pyrite-galena occurs. Sphalerite-enriched banding between blocks of massive sulphide has been observed in this enriched zone. The base of ore body is marked by a porous lead-and zinc-poor, pyrite-rich zone. There is a major barite-pyrite and precious-metal cap to the ore body. Pyrite set in glassy silica caps the barite.

The dominant microscopic feature is the complex fine-grained intergrowth of pyrite with galena and sphalerite. Framboids, radial and concentric textures, colloform and banded structures occur in zones in the massive ore. Spongy arsenopyrite is intergrown with other minerals, especially sphalerite and galena. Barite can be interbanded with sulphides that display sedimentary characteristics such as graded bedding. Sphalerite with chalcopyrite disease is especially abundant in the precious metal/barite zone. Fine grained arsenopyrite occurs with

tabular pyrite in veins in the upper precious metal zone (Ramsden et al., 1984, 1985).

The deposit averages 51% pyrite, 22% sphalerite, 8.5% galena, 2% arsenopyrite, and 1% chalcopyrite with trace tetrahedrite. Boulangerite ($5\text{PbS} \cdot 2\text{Sb}_2\text{S}_3$), subsidiary bournonite ($2\text{PbS} \cdot \text{Cu}_2\text{S} \cdot \text{Sb}_2\text{S}_3$) tetrahedrite ($\text{Cu}_{12}\text{Sb}_4\text{S}_{13}$) - tennantite ($\text{Cu}_{12}\text{As}_4\text{S}_{13}$) occur in the precious metal zone (Fander, 1984; Ramsden et al., 1984, 1985).

The principal non-sulphide gangue mineral is calcite which occurs as veinlets, tension gashes and also microscopically between the sulphide grains. The other major gangue mineral is quartz especially in the hangingwall precious-metal zone. Barite increases in quantity from a major barium low in the lower and central parts of the ore body to massive barite in the hangingwall (see Figure iv in Appendix 1). Other gangue minerals include chlorite and sericite, but these occur in zones where there is evidence of faulting and their occurrence is possibly related to deformation. Other less prevalent gangue minerals are ankerite, which occurs with calcite towards the hangingwall in the western trough (Figure 6), and apatite, with the ore having a P_2O_5 content of up to 0.15% (Abermet internal reports).

Little internal deformation or metamorphism of the Hellyer VMS has occurred. Deformation is confined to restricted areas such as the hinge of the trough west of the fault. This is in contrast to Que River which has suffered intense folding, and where banding within the ore may be the result of a metamorphic/structural overprint (Large et al., 1987).

Interpretation

The zoning is interpreted to be the result of remobilization of metals outwards from the stringer zone core. This is evident in the contoured cross sections in Appendix 1 where the hangingwall enriched zone forms a halo around a central metal-depleted zone. This accords broadly with models presented for Kuroko deposits such as these of Eldridge et al., 1983. There also appears to be late Au, Ag, As, Sb and Cu metasomatism interpreted, based on its position, to be related to the secondary stringer system east of the central core (see Figure 7 and Figures i to viii in Appendix 1). Interpretation of the mechanisms involved in this redistribution is beyond the scope of this thesis.

The abundance of calcite in the ore body is important in considering the calcite-fuchsite plume-shaped zone in the hangingwall lavas (see Chapter 5) in that a carbonate-rich phase has clearly penetrated the ore body.

CHAPTER 4 PRIMARY PETROLOGY AND GEOCHEMISTRY OF THE HOST SEQUENCE

Introduction

The Que-Hellyer volcanics, host to the Hellyer deposit, consist of basalt and andesite, with subsidiary polymictic rocks and dacites. At Hellyer, the hangingwall is a basalt lava and the footwall an albite porphyritic andesite lava. At the ore position between these two lavas is a polymict breccia and ash volcanoclastic rock which onlaps onto the sulphide mound.

The primary petrology and geochemistry of these rocks are described to provide a basis for petrographic comparison with altered products and to assess the direction and amount of element mobility.

Petrography

Macroscopic Textures

The Hellyer footwall andesite

The Hellyer footwall andesite is a grey albite porphyritic lava and lava breccia. Plate 2 depicts typical textures in this unit. The lava commonly consists of lapilli-sized andesitic lava fragments set in an andesite matrix. The albite phenocrysts, the grey colour, the absence of pillows, and the scarcity of vesicles are the most striking macroscopic features to contrast with the Hellyer hangingwall basalt.

A secondary lava type in the andesite is a lava breccia with pink siliceous angular fragments set in a green chlorite-rich matrix. Both matrix and fragments are albite porphyritic. These pink fragments may attain angular eutaxitic-like shapes. Other rarer polymict components

Plate 2:

Textures in albite
porphyritic
andesite.

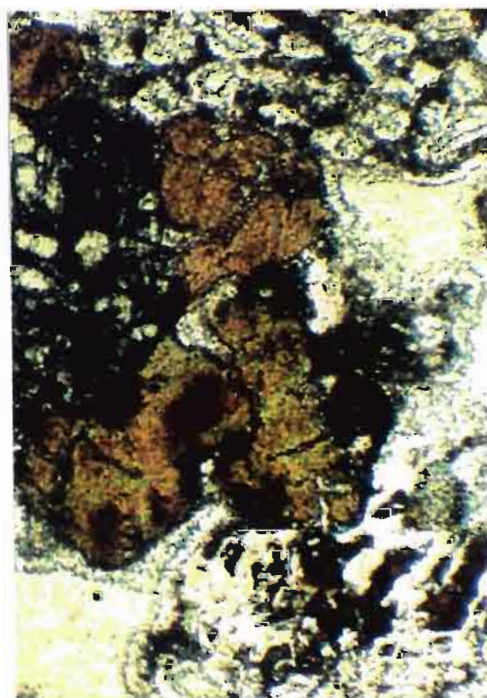
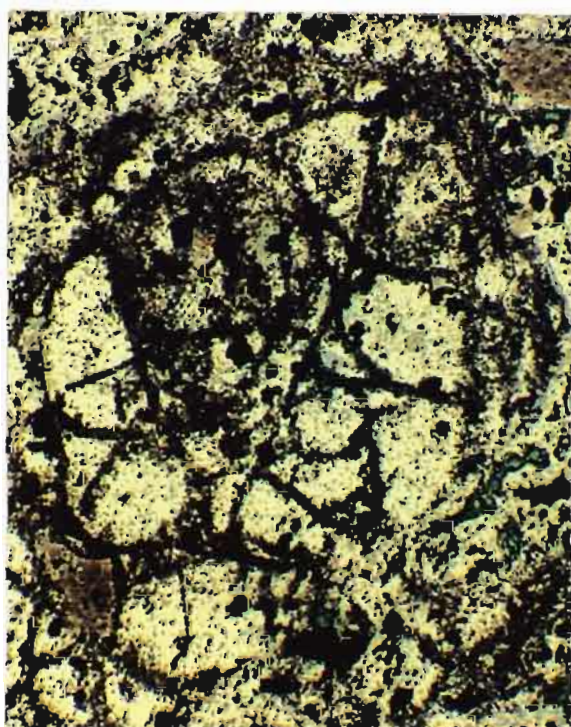
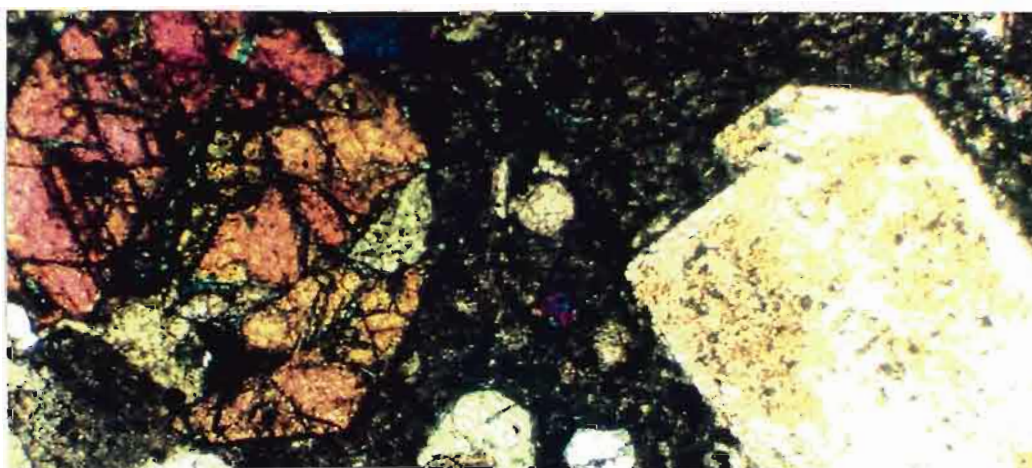
Middle:
augite (left) and
albite (right)
phenocrysts.

Bottom:
Perlitic glass
(left), pumpellyite
at end of augite
phenocryst in glass
fragments altered
to chlorite with
sericite rims(right).



HL030 319.7m 334078

0 5cm (above)



1mm (above)

within the lava include dacite and a variety of lava fragments exhibiting changes in colour and silica content of the andesite. Epidote and distinctive green pumpellyite may be visible with epidote usually developed in the matrix and pumpellyite pseudomorphing the albite.

The Hellyer hangingwall volcanoclastic rocks

The Hellyer hangingwall volcanoclastic rock is a highly polymict, poorly sorted unit of breccia with intercalated bedded ash volcanoclastic rock illustrated in Plate 3. Fragment types in order of abundance include andesite, usually albite porphyritic, basalt usually with prominent carbonate-filled vesicles, leucoandesite normally flow banded and commonly the largest of the fragments, grey felsite, wispy green sericite-altered fragments, rare massive volcanogenic sulphide and pyrite fragments. Finer sericitized, elongate volcanic fragments form the matrix.

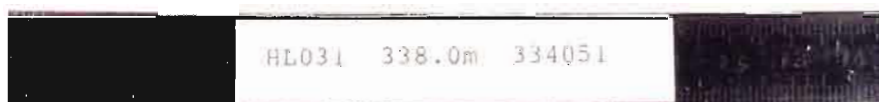
The Hellyer hangingwall basalt

The Hellyer hangingwall basalt is a mixed lava unit with highly vesicular flows intercalated with pillow lavas, massive non-vesicular lavas, lava breccias and increasingly, closer to the shale contact, a mixture of lava and shale with a characteristic peperitic texture. The pillow lavas display a wide variety of pillow shapes, from near spherical to tubular (Plate 4). Grey chert is less common than shale in interpillow areas, and flow margins to pillows are altered to muscovite and chlorite.

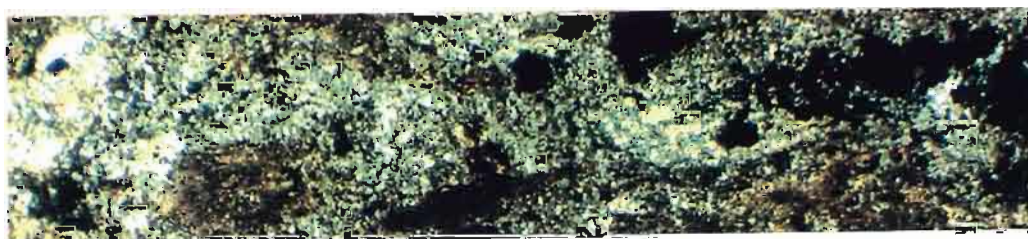
The lava breccias often consist of hyaloclastic quench fragments. Jigsaw-like brecciated flow tops can be identified. Vesicular units are

Plate 3:

Textures in
polymict ash
volcaniclastic.



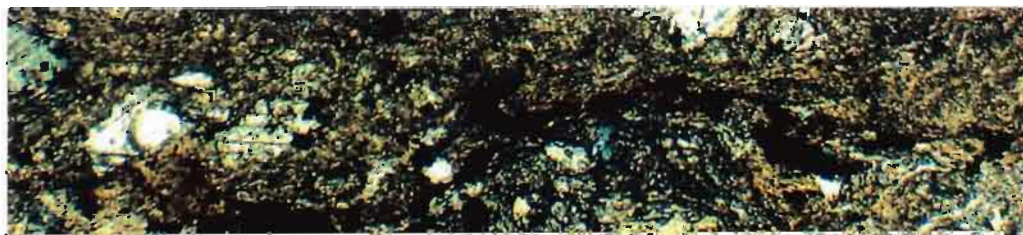
0 5 cm (above)



Cryptocrystalline quartz-pyrite-sericite.
Variably sericitized volcanic fragments (above).



Pervasive sericite (above)



Pervasive sericite-pyrite-calcite.



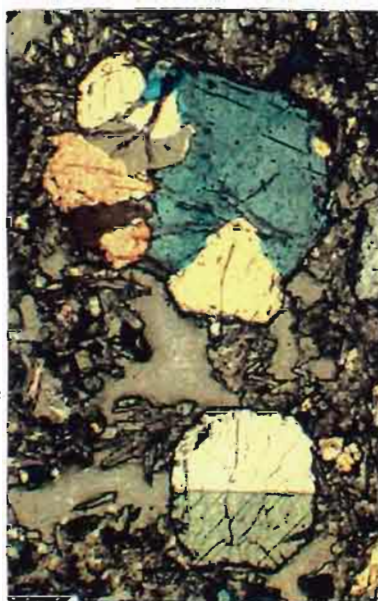
Fe-chlorite altered fragments in sericite.
0 1 mm (above)



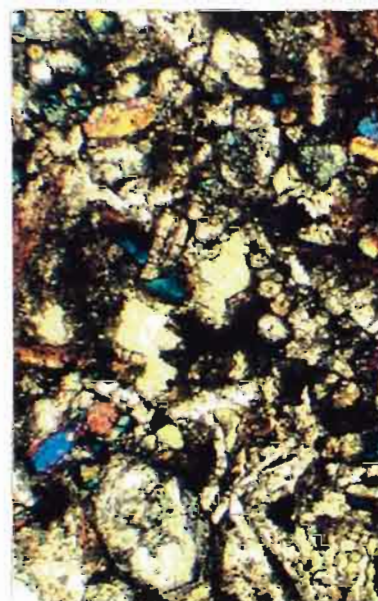
Plate 4:

Textures in hangingwall
basalt (unaltered)

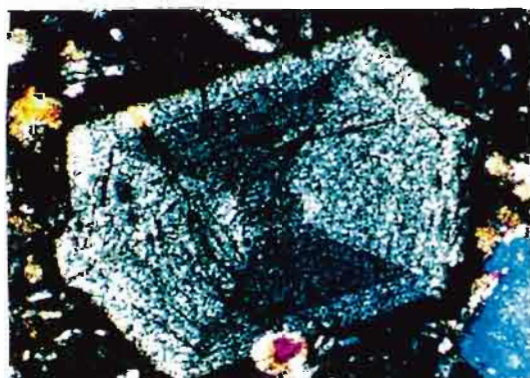
1. Pillow lavas (above)
2. Augite phenocrysts
set in a matrix of
albite microlaths
and Fe-chlorite
altered glass
(opposite)
3. Hourglass zoning
in augite and
augite pseudomorphed
by cryptocrystalline
quartz and calcite
(below).



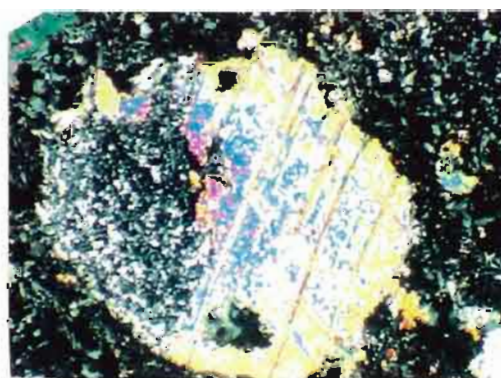
334038



334028



334038



1 mm (above)

locally correlatable using vesicle shapes and concentrations but are not laterally extensive. Vesicles are usually rod-shaped from 1 mm to 1 cm long and filled with chlorite calcite or quartz. Spherical variolites emanate from massive light areas sometimes with a mirror image effect.

The Que River shale

This is a massive to finely bedded carbonaceous black shale. Fine-grained bedded pyrite is prevalent. Subsidiary siltstone zones display graded bedding. There is almost a complete absence of cross bedding or other sedimentary structures. The shale is typically massive but sometimes displays parallel bedding. The unit contains Late Middle Cambrian agnostid trilobites (Gee et al., 1970; Jago, 1979).

The Upper rhyolite sequence

A complex rhyo-dacitic-sedimentary sequence consists of black shale intercalated with highly polymict units, volcaniclastic rocks, siltstone, vitric tuffs, greywacke, and interpreted pyroclastic rocks with prominent eutaxitic, sericite-altered flattened fragments up to several metres long set in a black vitric matrix. Disseminated pyrite and rare volcanic fragments are found in the polymict units. Veinlets of sphalerite, galena, chalcopryrite and pyrite in the shale units are the source of all the Cu, Pb, Zn geochemical anomalies in this study's data set.

Microscopic textures

The Hellyer footwall andesite

The footwall andesite contains abundant albite phenocrysts set in a complex siliceous, often perlitic, matrix (Plate 2). Albite laths and

chloritized glass are also common in the matrix. Epidote is the most abundant metamorphic mineral while distinctive green and brown mottled pumpellyite is found in the matrix and pseudomorphing albite or augite (Plate 2). Prehnite laths are relatively rare. Augite phenocrysts occur in accessory amounts and are much less abundant than in the basalt. Aphanitic footwall andesite is rare at Hellyer.

The Hellyer hangingwall volcanoclastic rocks

The hangingwall volcanoclastic rock matrix consists of andesite and basalt fragments in a finer-grained matrix of quartz, chert and chlorite after glass, including glass shards. All samples are highly sericitized and occasionally fine albite microlaths and phenocrysts are present (Plate 3).

The Hellyer hangingwall basalt

The hangingwall basalt contains abundant stubby augite phenocrysts, normally around 0.5 mm across, set in a matrix of albite microlaths and subordinate volcanic glass altered to chlorite (Plate 4). Augites rarely form larger phenocrysts (to 2mm across) and may constitute up to 50% of the rock. Augites in places display hourglass zoning (Plate 4). The augites are generally euhedral and may form aggregates. Augites are commonly pseudomorphed by calcite, cherty quartz, and less frequently by chlorite (Plate 4). Olivine has not been positively identified and possible olivine pseudomorphs are rare. Albite microlites may increase to phenocryst size but are almost never visible in handspecimen.

Quench textures are widespread in the matrix, defined by spherulitic albite - pyroxene - glass (quartz) intergrowths. Devitrified glass is abundant in thin section and XRD of selected samples (Brown, 1987) suggests a significant amorphous glassy component.

Distinctive, translucent, red euhedral chromites are a major accessory mineral occurring as discrete crystals within the matrix. Titanite (partly altered to leucoxene) after Fe-Ti oxide groundmass grains occurs in small patches pervasively throughout the matrix. There is also accessory apatite.

Variolites consist of coarser radial albite set in chloritized glass while the macroscopically darker matrix in which the spheroids are set is much finer-grained microscopically but has a similar mineralogy.

Regional Metamorphic Imprint

Prehnite-pumpellyite facies metamorphism has been described at Que River (Whitford et al., 1982). This is reflected at Hellyer in the footwall andesites by the development of epidote, pumpellyite and prehnite. The Hellyer hangingwall basalts only rarely develop these Ca silicate minerals. The prominent albite phenocrysts in the footwall andesite are thought to be metamorphic products. Feldspar phenocrysts in the Mt. Read Volcanics are invariably albite (e.g. Corbett, 1981).

Interpretation of Petrographic Textures

The footwall andesite locally contains a polymict component. It is suggested that this is volcanic debris caught up in the lava flow.

Epiclastic rocks prevalent elsewhere in the Que-Hellyer volcanics have only developed in the extreme south at Hellyer. The more felsic angular brown fragments in the footwall andesite may result from local silicification and subsequent spalling and shattering of these solidified areas within the lavas to produce the highly angular and sometimes flattened shapes. The formation of the Hellyer sulphide mound was followed by the deposition of the highly varied and polymict hangingwall volcanoclastic rocks which onlap onto, but do not completely cover, the sulphides which must have been a topographic high at the time (McArthur, 1986). The quench textures, hyaloclastite shattering and the pillows in the hangingwall basalt provide ample evidence of submarine extrusion.

Primary Mineral Chemistry (Relict Primary Phases)

Fresh augites occur in unaltered remnant blocks of lava in the host rocks. Table 1 lists augite microprobe analyses in the hangingwall basalt and the footwall andesite. Figure 8 shows the augite character on a Wollastonite (Wo), Ferrosilite (Fs), Enstatite (En) ternary plot. The low Ti typical "andesitic" nature of the augites is apparent. The high magnesian numbers are notable, reflecting the primitive nature of the magma. A trend of decreasing Wo and increasing Fs occurs in augites in the basalts.

Chromites are widespread in the Hellyer hangingwall basalt. Compositions of Cr - spinels reflect the compositional characteristics and affinities of their host mafic volcanic rock since they are very sensitive to magma bulk composition, temperature and fO_2 variations

TABLE 1 Augite Microprobe Analyses

Rock No.	Description	SiO ₂	TiO ₂	Al ₂ O ₃	V ₂ O ₃	Cr ₂ O ₃	FeO	MgO	CaO	Sum	Mg
											Mg+Fe
334038	Hangingwall core basalt	50.7	0.3	3.4		1.0	4.6	16.4	21.6	98.0	86.3
		52.6		1.4	0.2	0.6	4.6	17.7	20.6	97.8	87.2
		53.2		1.7		0.6	5.2	17.9	20.4	98.9	86.1
		53.2	0.2	3.6		0.9	4.8	16.9	21.7	100.0	86.4
		54.7		1.8		0.6	6.1	18.6	19.5	101.4	84.5
		52.9		2.4		0.8	5.0	17.5	20.8	99.2	86.1
	mean										
334166	High P ₂ O ₅ LEE enriched 'shosonitic' Hangingwall basalt	51.4	0.3	2.4		0.8	3.8	17.1	31.3	97.1	89.0
		53.4	0.3	3.2		0.5	5.3	18.2	20.6	101.5	86.1
334079	Footwall andesite	51.3	0.2	1.5			9.8	15.2	20.6	98.6	73.3
		53.8		1.8		0.4	4.7	18.1	22.4	101.1	87.2
		54.1		1.6		0.9	3.9	18.8	22.4	101.7	89.6

TABLE 2 Chromite Microprobe Analyses

Rock No.	Description	TiO ₂	Al ₂ O ₃	Cr ₂ O ₃	Fe ₂ O ₃	MnO	FeO	MgO	Sum	Mg	Cr
										Mg+Fe	Cr+Al
	Calcite										
	Fuchsite										
	Altered Hangingwall core basalt										
334045	grain centre		12.6	53.4			24.1	9.1	99.1		74.0
	towards edge		12.0	52.9			24.7	8.5	98.1		34.8
	grain edge	0.20	11.5	52.2	25.1	0.6		7.1	97.2		75.3
334171	grain centre		13.6	53.9	4.1		18.3	10.5	99.9	50.5	72.7
	towards edge		13.9	53.8	4.0		17.7	10.9	100.2	52.3	72.2
	on edge		13.8	54.2	3.2		18.6	10.2	99.9	49.4	72.4

AUGITES HELLYER HANGINGWALL BASALT AND ANDESITE

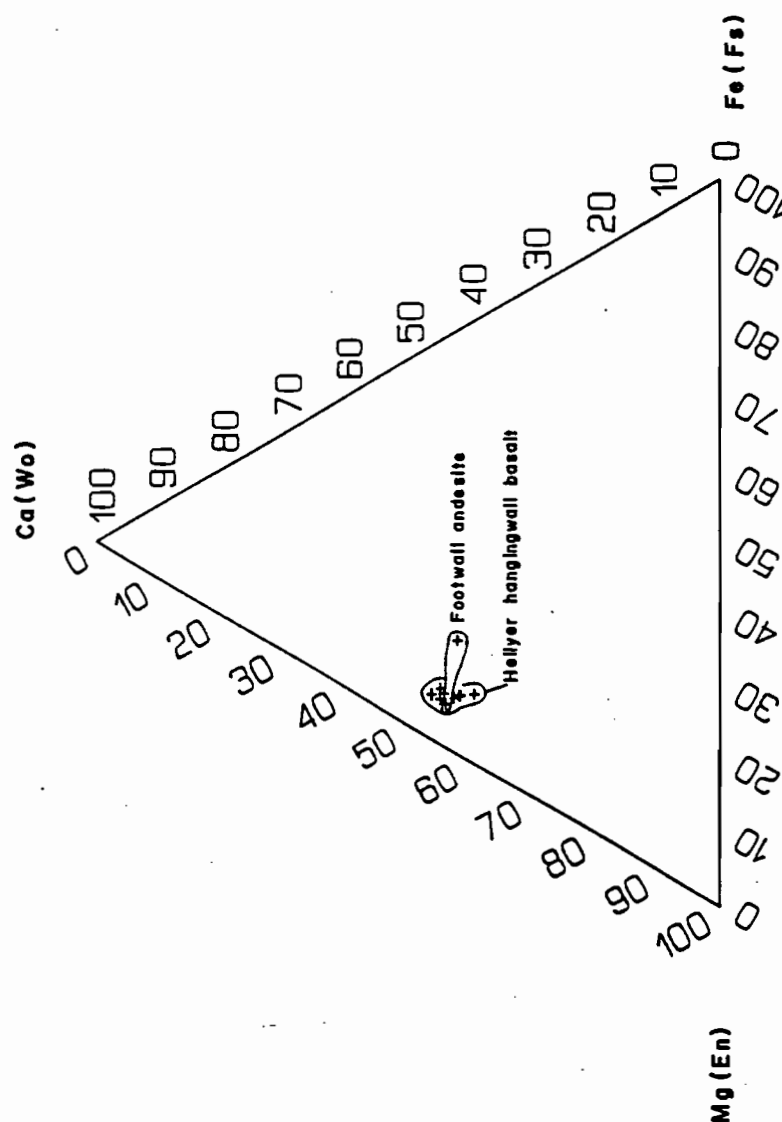


FIG. 8.

FIGURE 8: Composition of Augites at Hellyer. This is shown on a Wollastonite (Wo), Ferrosilite (Fs), Enstatite (En) plot. Note the high magnesium content in the basalt. This reflects the primitive nature of the magma.

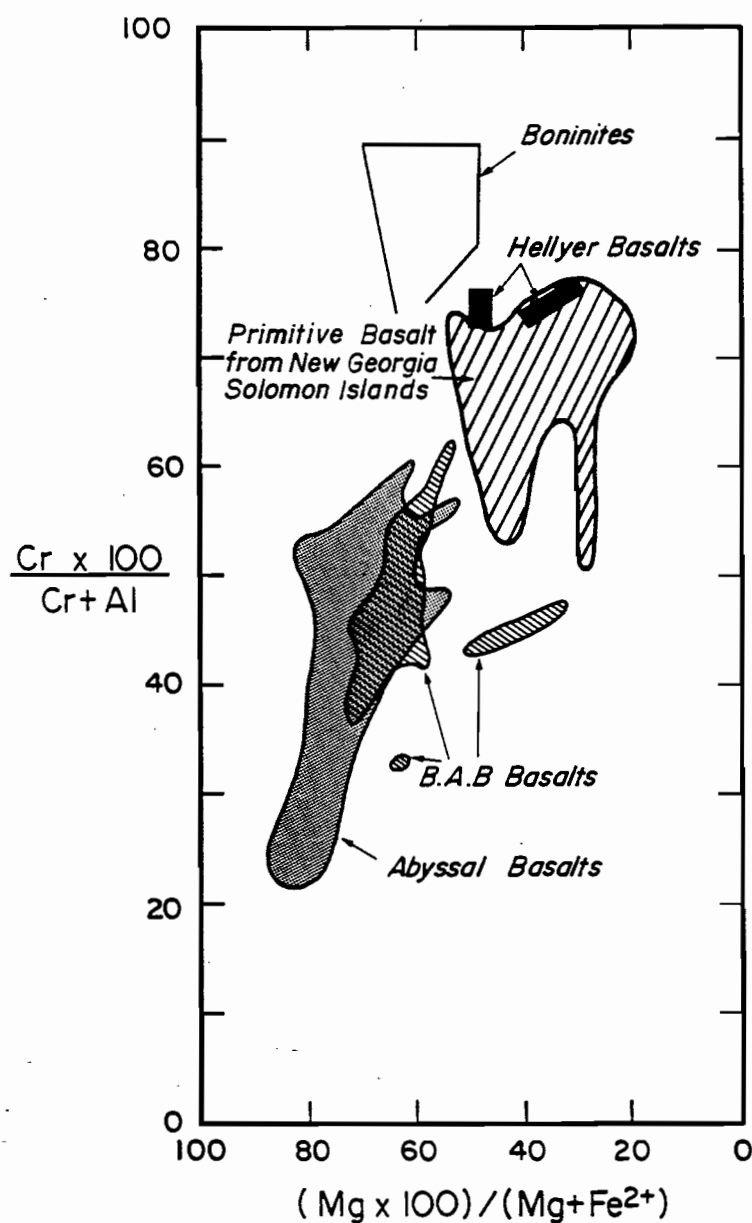
(e.g. Dick and Bullen, 1984), . Table 2 gives compositions of the chromite in the Hellyer hangingwall basalt. $\text{Cr.100}/(\text{Cr}+\text{Al})$ versus $\text{Mg.100}/(\text{Mg}+\text{Fe}^{2+})$ ratios are plotted on Figure 9. The relatively high $\text{Cr}/(\text{Cr}+\text{Al})$ ratios of chromites in the Hellyer hangingwall basalt are typical of chromites in arc basalts (Ramsay et al., 1984), and indicate derivation from a source slightly more refractory than MORB source mantle but less depleted than the source peridotite of boninites (Jaques and Green, 1980). Figure 9 shows that chromites in the Hellyer basalts are clearly unlike those in back-arc basins or abyssal basalts at mid ocean-ridges (MORB) but are similar to primitive arc basalts such as those in the Solomon Islands.

Primary Whole-Rock Geochemistry

All analyses are listed in Appendix 2 grouped by rock type. Analytical methods and laboratories are also listed. All rocks used to characterize primary geochemistry were analysed by XRF at the University of Tasmania.

It is important to find unaltered rocks for comparison with hydrothermally modified rocks in order to document both mineralogical and geochemical changes as well as to describe their primary chemistry. Unaltered footwall andesite is represented by sample 334083 (Plate 2) and pristine hangingwall basalt by 334028 and 334038 (Plate 4). All three samples are petrographically unaltered. The andesite sample is from 150 metres west of Hellyer. The two hangingwall basalt samples are from remnants of unaltered massive lava that occur immediately above Hellyer. They are amongst the least altered rocks anywhere in the Que-Hellyer volcanics.

$\frac{\text{Cr} \times 100}{\text{Cr} + \text{Al}}$ versus $\frac{\text{Mg} \times 100}{\text{Mg} + \text{Fe}^{2+}}$ in Hellyer hangingwall basalt
chromites compared with modern primitive basalt



B.A.B = Back Arc Basin.
Fields for Boninites, B.A.B. Basalts & Abyssal
Basalts from Dick & Bullen, 1984.
Field for Solomon Island Basalts from Ramsay
et al, 1984.

FIG. 9

FIGURE 9: $\text{Cr} \cdot 100 / (\text{Cr} + \text{Al})$ versus $\text{Mg} \cdot 100 / (\text{Mg} + \text{Fe}^{2+})$ in Hellyer Hangingwall Basalt Chromites. Hellyer basalts are similar to modern primitive basalts from the Solomon Islands.

The question of element mobility is addressed in the next chapter in more detail. Essentially Ti, Zr, Y, Nb, Sc and the rare-earth elements are immobile in all rocks except those within the footwall stringer system. Other elements analysed (see Appendix 2) are all extremely mobile. This element mobility creates problems with most standard major-element plots, and they are therefore not presented here.

In spite of the mobility of silica, primary variations in silica content are still evident, providing samples within the stringer zone are excluded. This is illustrated on a SiO_2 versus Ti/Zr scattergram (Figure 10).

Trace elements provide better information on primary geochemical variations. The rock types are categorised by plotting a Ti/Zr versus Nb/Y scattergram (Figure 11). The calc-alkaline nature of the Hellyer host rock is shown and compared with other Cambrian volcanics in Tasmania on a ternary Ti/100-Zr-Y.3 diagram (Figure 12).

Rare-earth elements (Table 3) were analysed at the University of Tasmania by P. Robinson by XRF ion exchange. Chondrite-normalized element variation diagrams (spidergrams) showing REE patterns are depicted on Figures 13 and 14. Figure 13 illustrates the similarity of Hellyer host rocks to Quaternary high - K calc-alkaline lavas from Java. The light rare-earth element (LREE) enrichment, especially in the hangingwall basalt, is characteristic of calc-alkaline rocks. The heavy rare earths in the andesite plot on a flatter line.

Fractionation in co-magmatic lava suites results in REE lines higher on these diagrams (for comparable Mg contents). Decreasing Mg

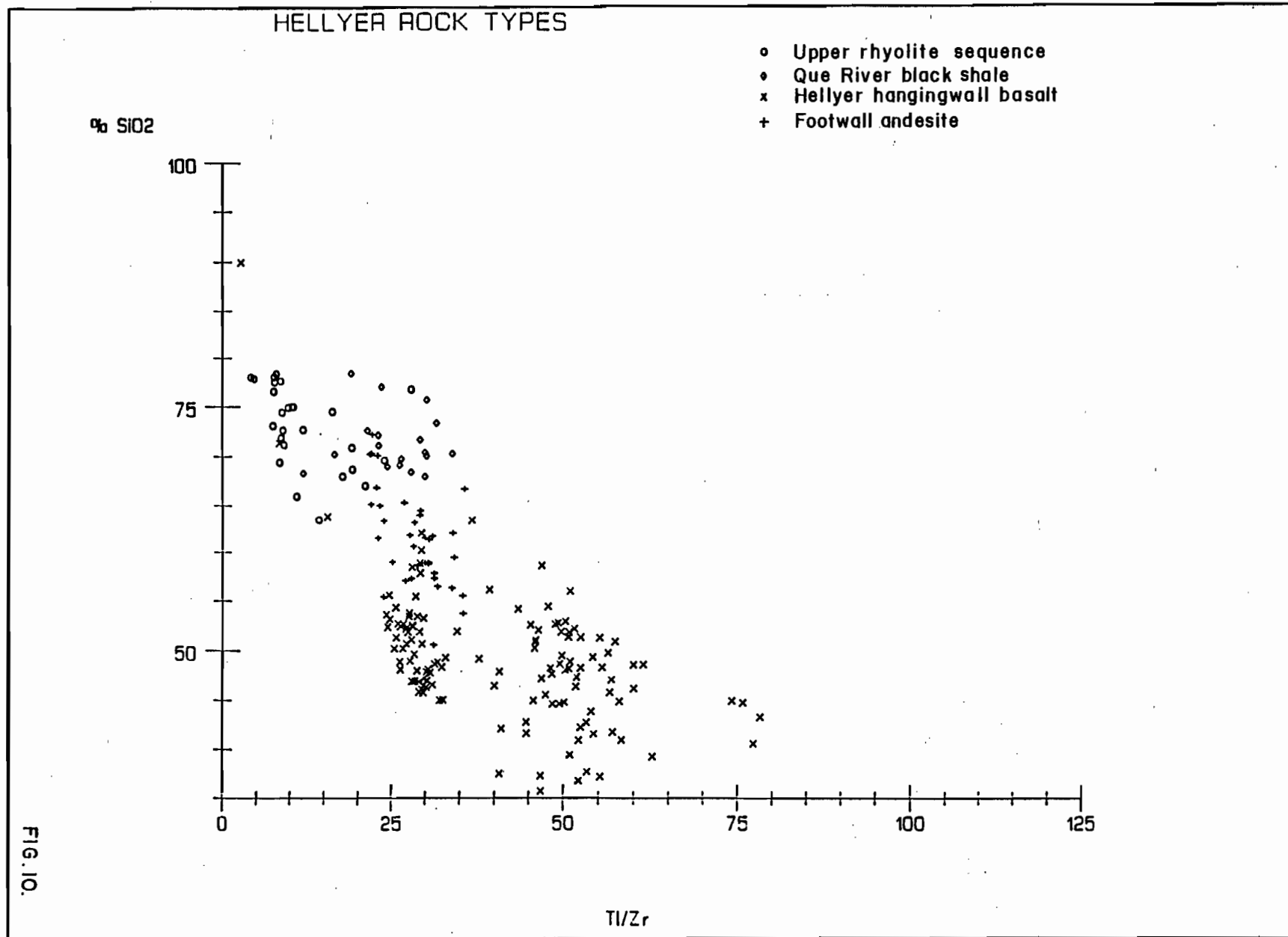


FIGURE 10: SiO₂ versus Ti/Zr for all Hellyer Rock Types Outside the Stringer zone.

FIGURE 11: Ti/Zr versus Nb/Y for all Hellyer Rock Types Outside the Stringer Zone.

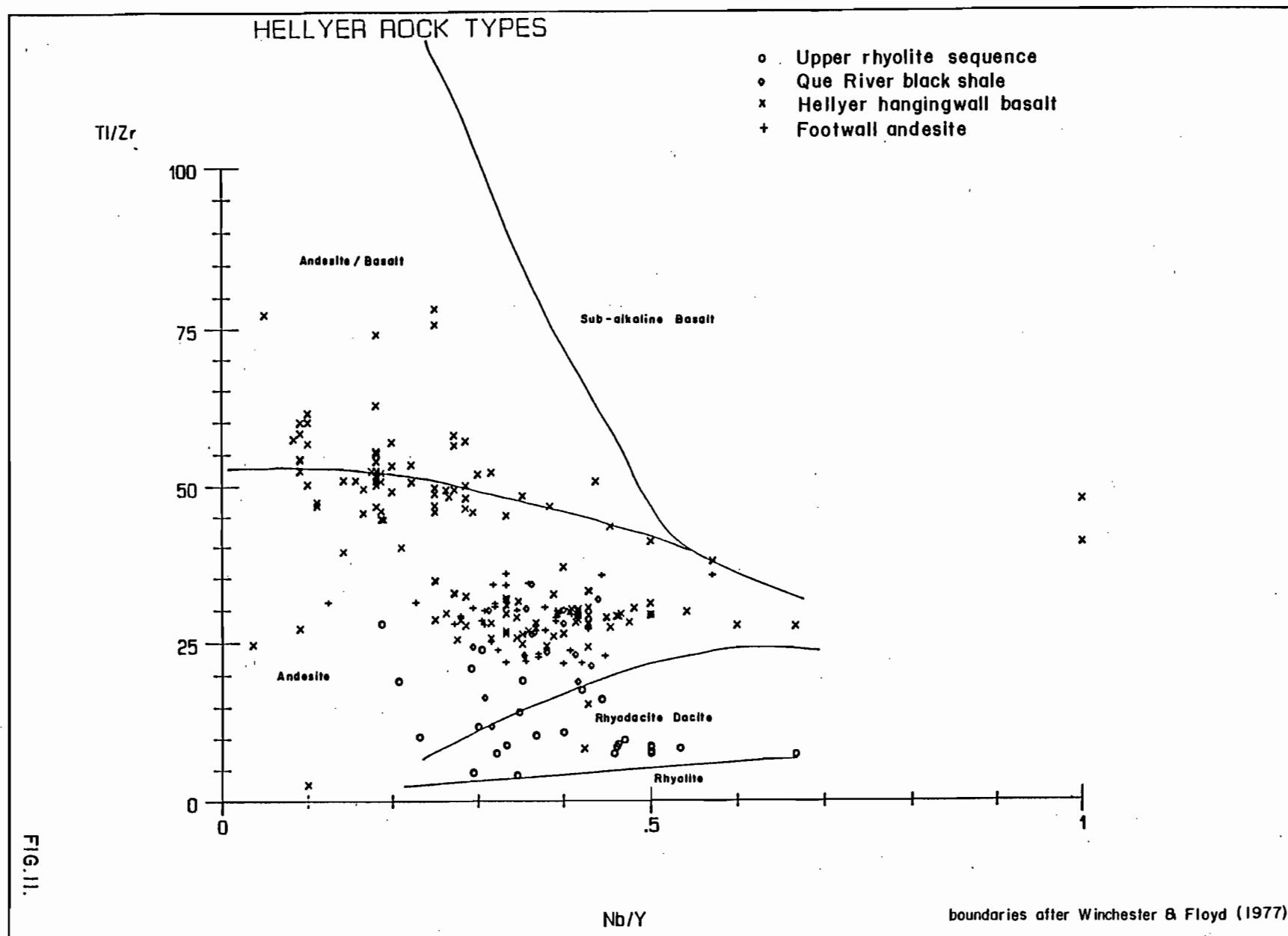


TABLE 3 Rare Earth Element Analyses

Sample No.	Description		La	Ce	Pr	Nd	Sm	Eu	Gd	Dy	Er	Yb
334001	Surrounding Basalt	Hangingwall basalt lava continuous	62.5	136	15.2	63.0	11.1	2.8	8.7	5.9	2.9	2.5
334002	"	core grinds	69.5	146.8	16.8	66.6	11.4	2.5	8.7	5.7	3.0	2.2
334003	"	"	52.5	110.6	12.9	49.6	8.7	2.0	6.8	4.5	2.3	2.1
334004	Core Basalt	"	38.3	74.9	8.5	31.6	5.6	1.3	4.6	3.5	1.88	1.6
334005	"	"	36.7	69.6	7.9	29.1	4.8	1.0	3.9	3.1	1.5	1.3
334006	"	"	36.8	72.1	7.5	30.4	5.1	1.2	4.1	3.2	1.6	1.6
334007	"	"	35.8	69.2	7.3	29.0	4.9	1.2	3.8	2.9	1.5	1.2
334008	"	"	35.6	72.4	8.0	32.0	5.7	1.6	4.8	3.8	2.2	2.1
334009	"	"	30.0	60.1	6.6	25.5	4.3	1.2	3.6	2.9	1.5	1.4
334010	"	"	27.7	56.7	6.9	24.4	4.4	1.1	3.3	2.7	1.6	1.4
334028	Surrounding Basalt	Hangingwall	54	110	13.1	51.8	9.1	2.2	6.9	5.0	2.3	1.9
334038	Core Basalt	"	35	62.1	7.3	26.4	4.4	0.9	3.5	3.1	1.6	1.7
334045	Core Basalt extreme calcite fuchsite alteration	"	36	81.4	8.1	31.2	5.1	1.0	4.1	3.9	2.2	2.2
334171	Core Basalt extreme calcite fuchsite alteration	"	36.1	78.8	9.2	33.7	5.9	1.7	4.8	3.9	2.1	2.0
334063	Chlorite Chlorite Quartz Schist	Stringer Zone	30.0	67.9	8.1	29.7	5.7	0.4	5.3	5.5	4.0	3.9
334064	Quartz Chlorite Quartz Stringer Rocks	"	21.1	44.7	4.9	17.3	3.02	<0.2	2.8	3.0	2.2	1.9
334227	Sericite Sericite quartz pyrite Rock	"	39.6	86.2	9.8	37.3	7.0	1.1	6.6	7.5	5.5	5.1
334087	Chlorite-dolomite schist	"	33.5	74.0	8.6	33.1	6.3	0.6	5.4	4.7	2.8	2.6
334091	Silicified envelope zone	"	14.2	30.5	3.3	12.8	2.5	0.4	2.3	2.6	1.6	1.5

Analyses by P. Robinson Geology Dept. Univ. Tas. by XRF - ion exchange according to the method by P. Robinson et al., (1986)

Normalizing factors used on spidergrams : La 0.315, Ce 0.813, Pr 0.115, Na 0.597, Sm - 0.192, Eu 0.0722, Gd 0.259, Tb 0.047, Dy 0.325, Er 0.2125, Yb 0.208 - 'Leedy/1.2' from Masuda A. et al. (1973). Ba 6.9, Rb 0.35, K 0.01445, Nb 0.35, P 0.0154, Zr 6.84, Ti 0.10342, from R. N. Thompson (1982) Scott. J. Geol.

HELLYER ALL SAMPLES OUTSIDE STRINGER ZONE

+ Calc - alkaline Hellyer Mt Read Volcanics

A & B = Low potassium tholeiite

B = Ocean floor basalt

B & C = Calc - alkali basalt

D = Within plate basalt

(Field A-D after Pearce & Cann(1973))



Field of Crimson Creek Dundas /
Smithton trough Cambrian Tholeiites
(after Brown (1986))



Field of low - titanium basalt
(after Brown (1986))



Field for Mt Read Volcanics
(after McClenaghan & Corbett (1985))

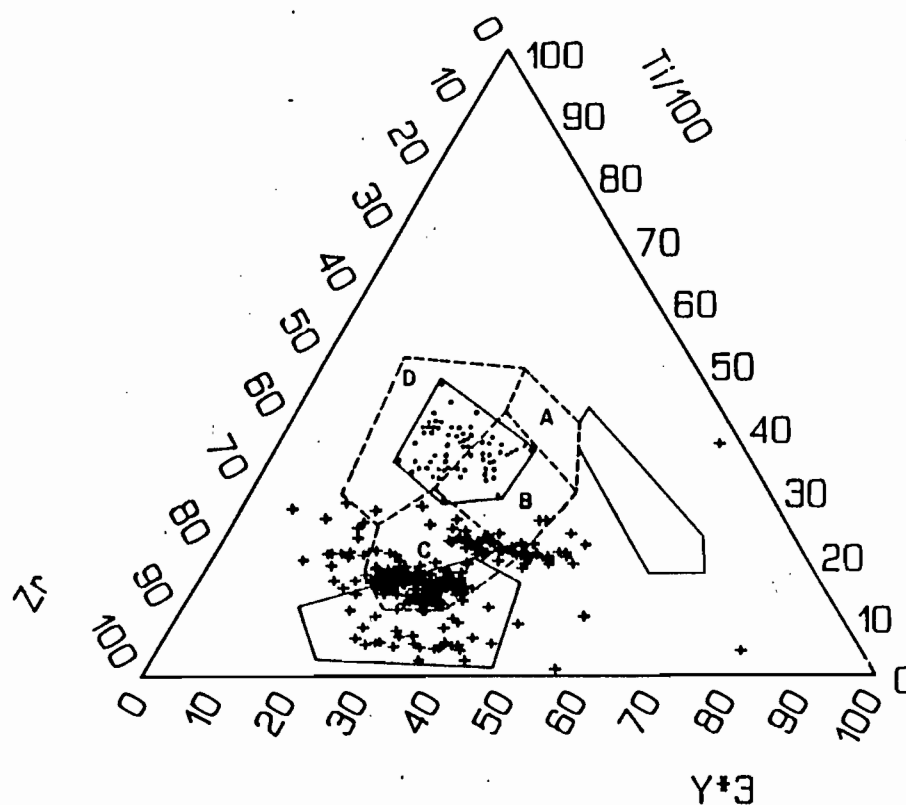


FIG.12

FIGURE 12: Ti/100-Zr-Y*3 Ternary plot for all Hellyer Volcanic Rocks Outside the Stringer Zone. The calc-alkaline character of the Hellyer rocks is readily apparent.

REE for High K Calc-Alkaline Series

ROCK/CHONDRITE

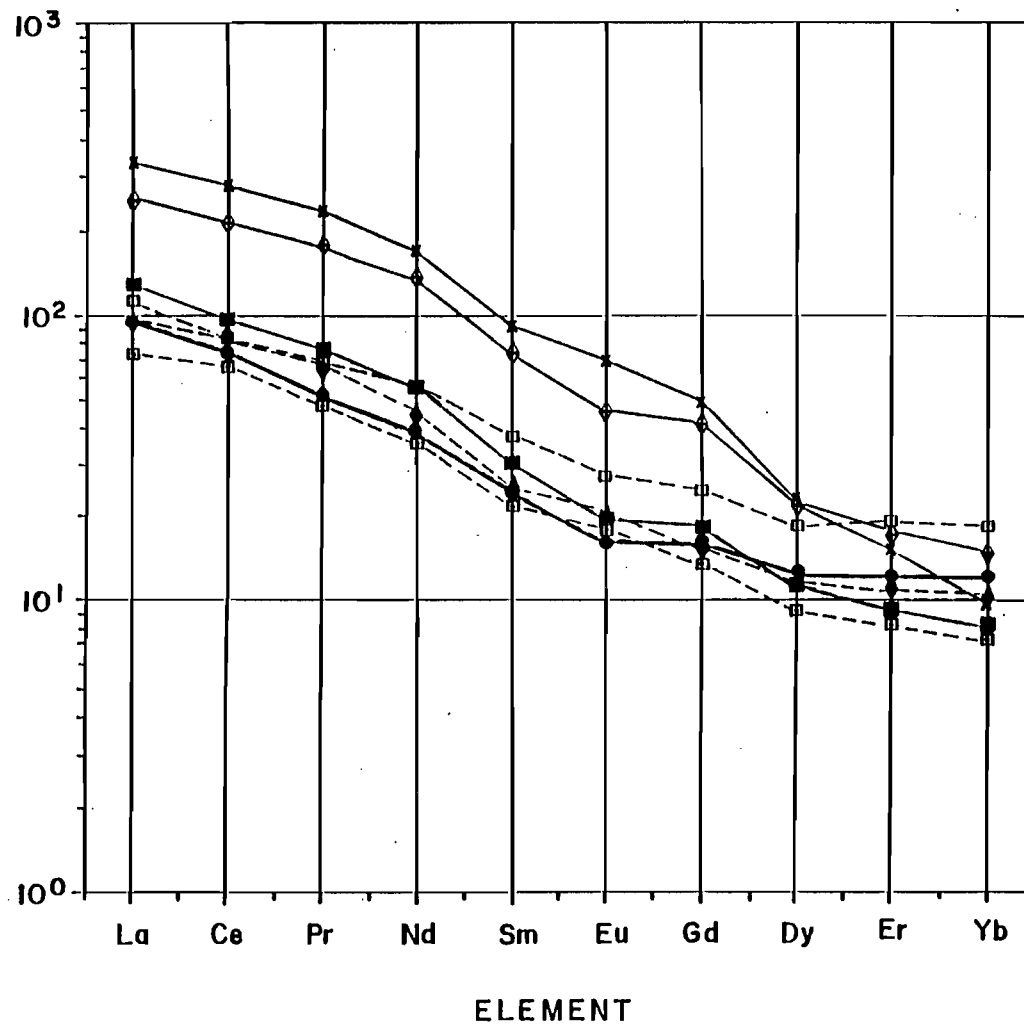


FIG. 13.

FIGURE 13: Rare-earth Element Chondrite-normalized Spidergram for Hellyer Andesites and Basalts compared with High-K Lavas from Java.

Basalt continuous grind HL55

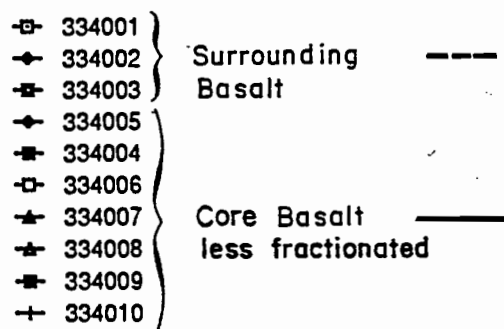
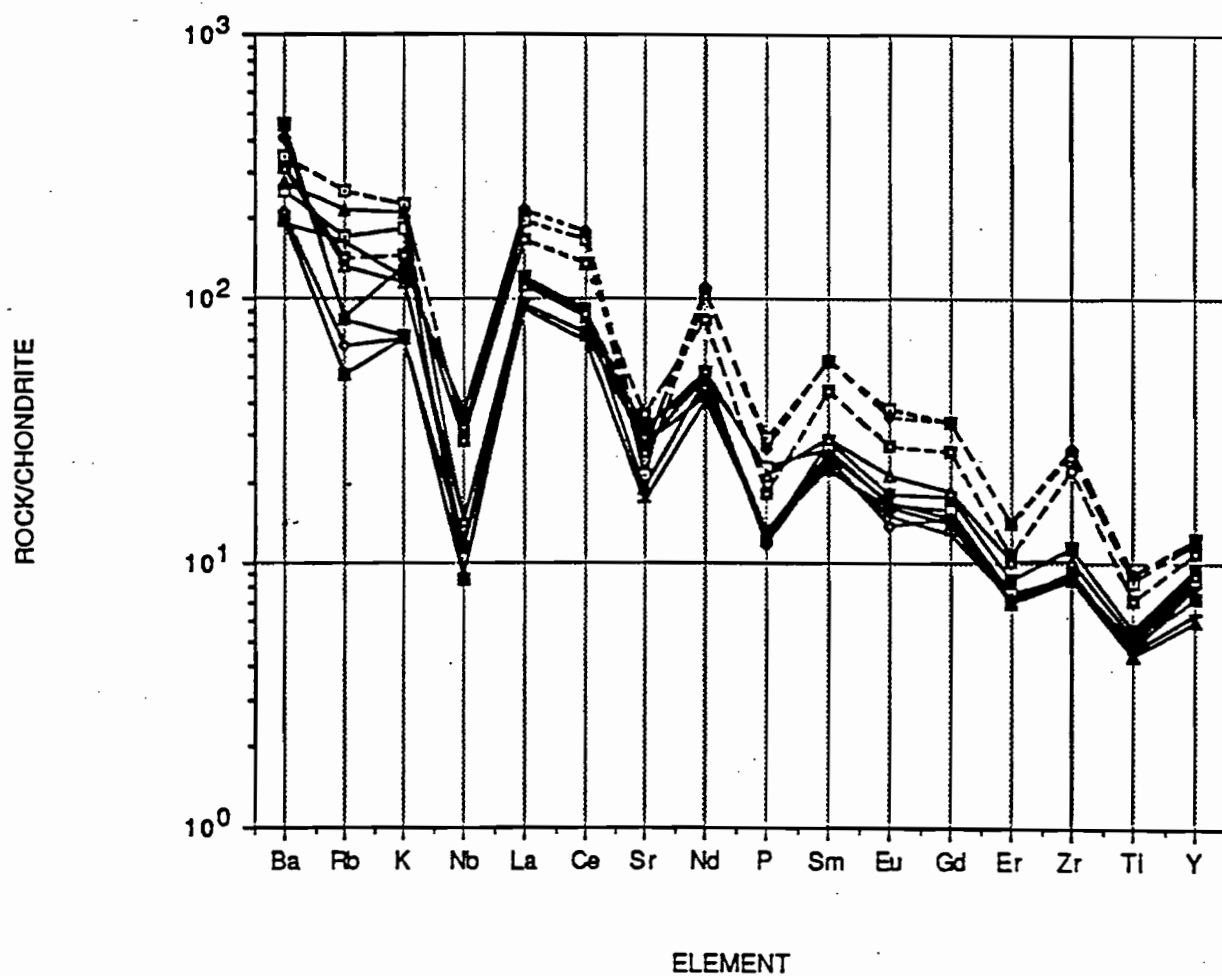


FIG. 14

FIGURE 14: Rare - earth and Other Element Chondrite-normalized Spidergram for Continuous Core Grinds Through the Hellyer Hangingwall Core Basalt and the Surrounding Basalt. Samples from the less fractionated core basalt plot lower on the diagram.

content is also reflected in a parallel line higher on the diagram. The Hellyer footwall andesite, shown on Figure 13 (334083), has a Mg content of 2.38% while the basalts analysed have Mg contents of 10.07% (334028) in the core flow and 12.90% (334038) in the surrounding flow. Figure 13 establishes that the two basalts may be co-magmatic. The older 334038 is less fractionated than 334028. The footwall andesite, however, plots lower than either basalt in spite of its markedly lower Mg content and therefore is unlikely to be co-magmatic with the overlying basalts. Subsidiary basalt lavas intercalated with the Hellyer basalts have extreme P_2O_5 contents up to .6% P_2O_5 and these show extreme LREE enrichment reflecting LREE in apatite (Figure 13).

The immobility of the REE is evident on Figure 14, where continuous core grinds from intervals with markedly different degrees of alteration in the same primary lava cluster tightly. The core grinds include the unaltered islands of massive lava from which the split core samples 334028 and 334038 were taken. Mobile elements Ba, Rb, K and Sr have widely crossing trend lines compared with the REE and other immobile elements plotted.

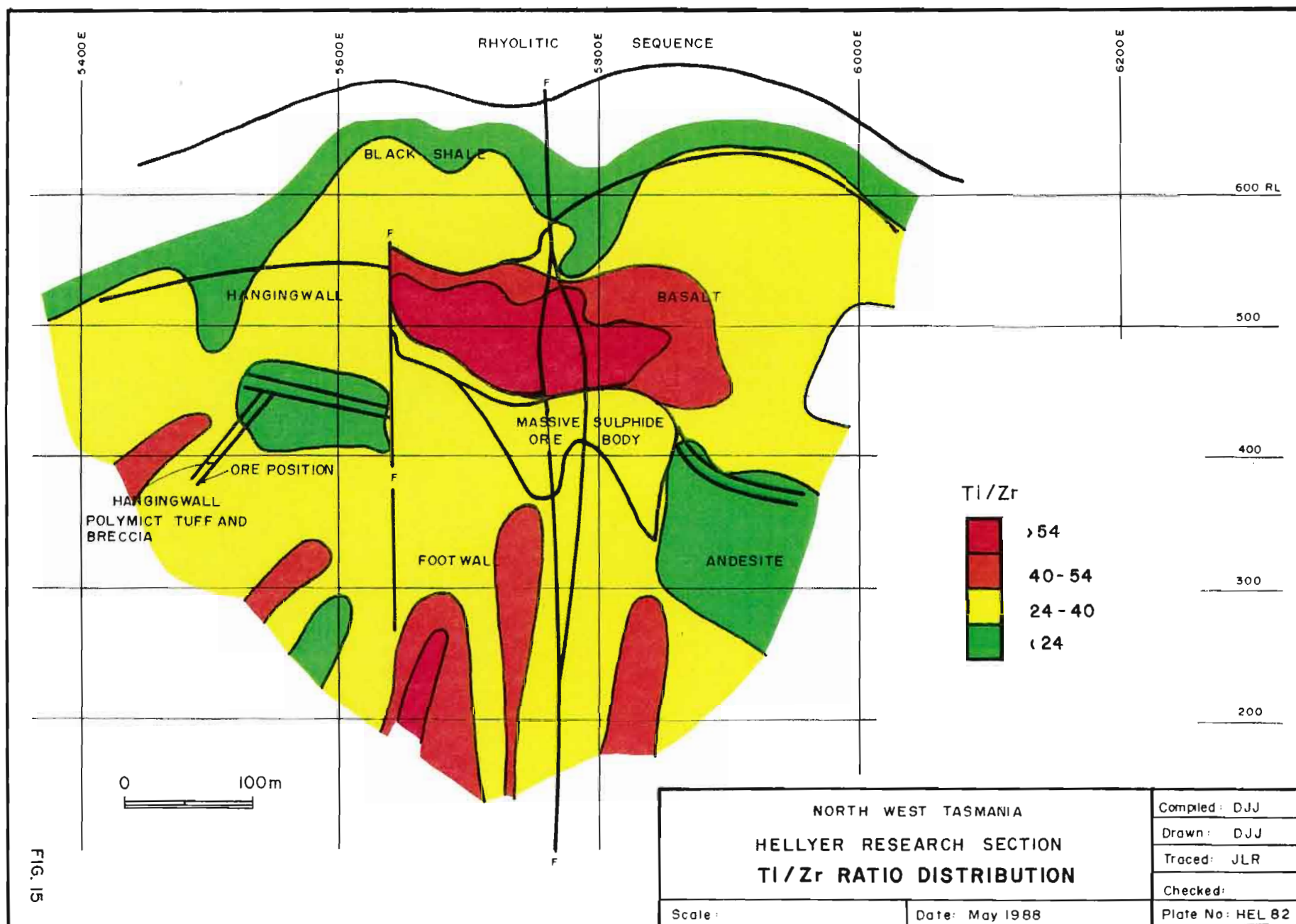
Tectonic Setting based on Geochemistry

The Hellyer basalts show the characteristic low Ti and Nb abundances of arc basalts but are notably enriched in K-group elements (K, Ba, Rb, LREE). The enrichment in K-group elements is a characteristic of subduction related calc-alkaline basalts, in particular high-K calc-alkaline basalts from island arcs such as those from Java. Extreme LREE enrichment is associated with late post collisional "shosonitic" phases in these environments (Morrison, 1980).

The Hellyer Core Lava

Perhaps the most important discovery related to the primary geochemistry at Hellyer is the existence of a lava with regionally high Ti/Zr immediately above the Hellyer ore body (Figure 15). Aberfoyle Resources Ltd. routinely analyse all the exploration holes for these two elements and, out of several thousand samples, only four localities show the high Ti/Zr lavas: 1) above the Hellyer VMS, 2) in possible feeder dykes in the footwall intersected in HL14 at Hellyer, 3) in lava fragments in the polymict unit under the dacite wedge at Que River, and 4) in holes drilled in the vicinity of the abundant VMS fragments south-east of Hellyer. Figure 15 shows the Ti/Zr distribution in Hellyer host rocks on a cross section through Hellyer (see Chapter 5). The basalt with Ti/Zr ~53 is called the core basalt in this thesis. The high ratio is not caused by alteration, as petrographically unaltered rocks in the lava have the same ratio as highly altered rocks. 334038, chosen as a parent rock on the basis of its unaltered character, is from this core lava. Figure 16 plots Zr versus TiO_2 and this shows a strong correlation within the lava flows. It is also apparent from the analyses in Appendix 2i that this core lava in general has lower SiO_2 , TiO_2 , P_2O_5 , Y, Zr, La and Nb and higher Ni, Cr, MgO compared with the surrounding lava. It is suggested that this less fractionated lava is a primitive deeper sourced lava which extruded up the same structure that localised the Hellyer hydrothermal system.

FIGURE 15: Hellyer Research Section. Ti/Zr Ratio Distribution. A lava with regionally high Ti/Zr >54 forms directly above the Hellyer massive sulphide and stringer system.



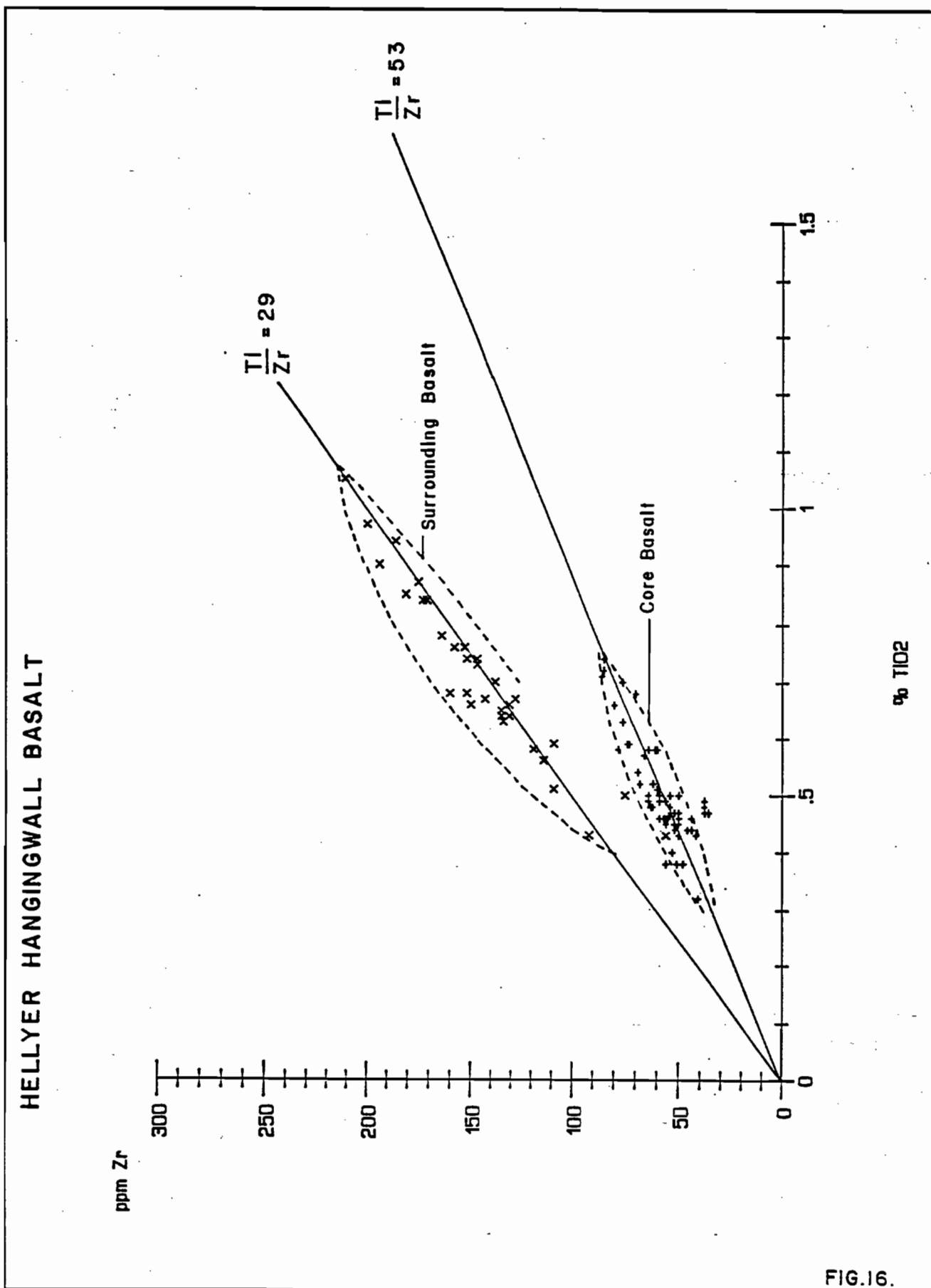


FIGURE 16: Ppm Zr versus % TiO_2 for the Hellyer Hangingwall Basalt in Drillhole HL55 through the Hellyer Hangingwall Alteration Plume. In spite of alteration the ratios remain at an interpreted primary constant value. The core basalt with a primary Ti/Zr ratio ≈ 53 occurs directly above the Hellyer orebody.

Comparison with other Volcanogenic Massive Sulphide Host Rocks

Hellyer is classified as a zinc-lead-copper volcanogenic massive sulphide deposit based on ore body composition (McArthur, 1986; Franklin et al., 1981). Other deposits in this category include the Kuroko deposits in Japan; the Bathurst district deposits New Brunswick; and the Buchans orebodies, Newfoundland, in Canada; the Rosebery, Hercules, Que River deposits in west Tasmania; and the Captains Flat, Woodlawn and Benambra deposits in southeastern Australia (Franklin et al., 1981). However, comparison of the host rocks and alteration (see Chapter 5) at Hellyer with other volcanogenic massive sulphide deposits crosses classification boundaries to include similarities with Archean copper-zinc deposits such as the Canadian Noranda district deposits and even with ophiolite-dominated Cyprus type deposits (Constantinou, 1977).

Hellyer occurs at the time break between a footwall andesite and a hangingwall basalt. There is no evidence of the rhyolite domes typical of most Kuroko deposits (Sato, 1974), or of the subequal amounts of sediments and rhyolitic volcanic host rocks at the Buchans and Bathurst-New Brunswick deposits (Davies, 1980; Thurlow et al., 1975). In fact, the domination of the immediate host sequence by lavas is more like the Cu-rich Cyprus ophiolite-associated deposits (Constantinou, 1976). The existence of a thin (2 metre) intersection of massive sulphide within the Hellyer hangingwall basalt between two interpreted flows north of Hellyer highlights this comparison. The regional occurrence of dacites at the Hellyer ore position south of Hellyer is suggestive of the bimodal volcanism associated with many Kuroko (Ohmoto et al., 1983), Canadian Archean (Franklin et al., 1981), and other VMS (Vivallo,

1987), deposits. Tasmanian deposits, Rosebery and Hercules, are in acid-dominated volcanics. In Tasmania, only Que River 3 kilometres south of Hellyer is in the same intermediate lava dominated sequence as Hellyer. Most Noranda deposits have felsic volcanic hosts, and Hellyer may be more analogous to the Amulet lower and upper A and the Corbett deposits (Knuckley et al., 1982; Knuckley and Watkins, 1982; Beaty and Taylor, 1982) which are also in mafic volcanics. Hellyer, along with the rest of the deposits in the Tasmanian Mount Read Volcanics, occurs in primary calc-alkaline volcanics (e.g. McClenahan and Corbett (1985), as opposed to the tholeiitic affinities (Brown, 1986) of older Tasmanian Cambrian volcanics (which do not contain known VMS deposits). There has by contrast been some debate as to whether the Canadian Archean Abitibi belt is tholeiitic or calc-alkaline and whether the apparent calc-alkaline character is due to alteration (e.g. Descarreaux, 1973; MacGeehan and MacLean, 1980).

The association of Kuroko-style VMS deposits with grabens (or calderas) and extension tectonics (Scott, 1978; Scott, 1980; Ohmoto et al., 1983) may apply to Hellyer, with the core lava and ore body having a long thin shape in plan possibly controlled by graben walls.

CHAPTER 5 EFFECTS OF HYDROTHERMAL ALTERATION

Introduction

The effects of hydrothermal alteration at Hellyer are evident in both the footwall and the hangingwall. In the footwall, a distinct stringer zone core containing abundant coarse-grained base-metal mineralization (Plate 5) is surrounded by a macroscopically characteristic pyrite-veined envelope zone (Plate 6) which has a sharp boundary with essentially unaltered albite porphyritic andesite. This zoning is depicted in Figure 7, which includes some detail interpreted from the contoured element cross sections in Appendix 1. Geochemical evidence is presented below for the continuation of the hydrothermal process after the extrusion of the hangingwall basalt lavas to produce the plume-shaped zone of calcite-fuchsite (Plate 7) and interpillow pyrite also shown on Figure 7.

Zoning at Hellyer occurs at an ore body scale and also at the scale of several metres where, particularly in the footwall stringer core, major textural, mineralogic and geochemical changes have knife-edge boundaries. To cover broad scale changes, a series of cross sections have been produced showing element distribution around the ore body. Split NQ diamond drill core samples of all major alteration types are used to describe textures and to compare mineralogy with whole-rock analyses. In order to assess the direction and amount of element movement, altered rocks are compared geochemically with unaltered parents using a graphical method that takes account of mass and volume changes (Grant, 1986).

Textures and Mineralogy

Footwall

The footwall andesite has been altered in the stringer zone core dominantly to a quartz-sericite-pyrite \pm sphalerite \pm galena \pm chalcopryrite rock. The core has a quartz-barite rich central zone. A sericite-rich zone grading into a chlorite-rich zone occurs peripherally to the quartz-barite rich core. A detailed description of the zoning in this stringer zone core is beyond the scope of this thesis and descriptions are based on data from exploration holes and do not include detailed examination of underground exposures developed since data in this thesis were collected.

Pyrite is ubiquitous in the stringer zone giving a grey colour to the rock when fine-grained, or it may form coarse recrystallized pyrite veins and aggregates that can constitute 70% of the rock locally. Siliceous patches are complexly intermingled with friable, vertically foliated, sericitic zones (Plate 5). Centimetre to millimetre scale veinlets of sphalerite, galena, chalcopryrite and pyrite occur in highly foliated sericitized or chloritized rock. Anastomosing veinlets and aggregates, at several metre scale, consisting of coarse recrystallized galena, sphalerite, chalcopryrite and pyrite are widespread in underground exposures immediately below the ore body. In the quartz-barite rich central zone, barite occurs in elongate pods and veinlets. At the immediate base of, and penetrating the ore body, these may be mixed with calcite.

Massive Mg chlorite schists (Mg-chlorite identified by microprobe) containing disseminated (1mm across) euhedral pyrite crystals extend

Plate 5:

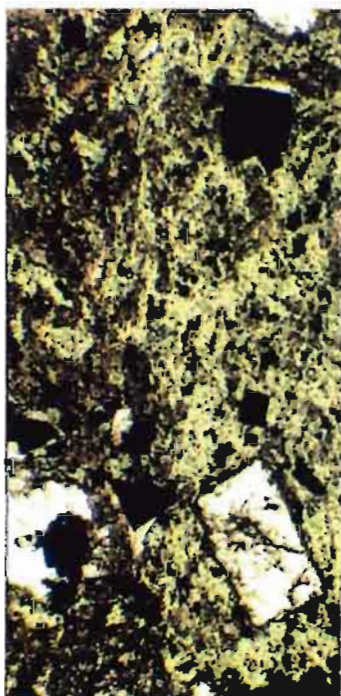
Textures in the
stringer zone core.

Sphalerite and
galena veinlets in
in chlorite-sericite-
quartz rock.

0 5cm
(right)



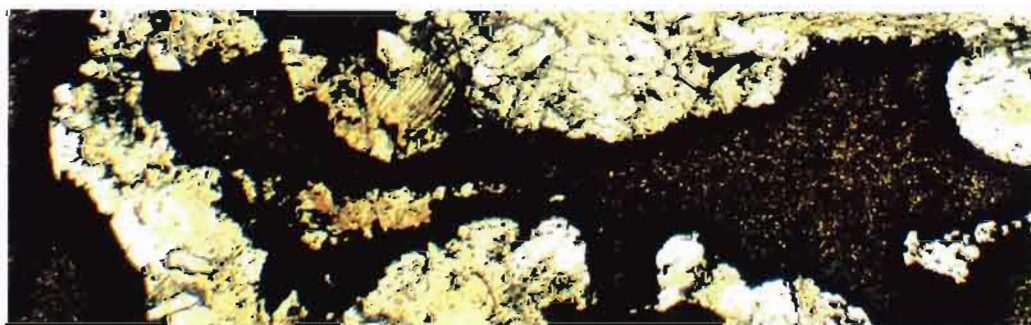
HL035A 398.7m 334086



Left: Sericite and
adjacent chlorite.

Right: Vertical
zones of sericite
quartz and pyrite.

Below: Sphalerite
in quartz rich core.



0 1mm (above)

from deep in the stringer zone possibly in semi-continuous elongate zones a few metres across, up to the ore body. Massive chlorite occurs adjacent to a 50 thousand tonne chalcopyrite-pyrite body toward the top of the stringer zone. Massive chlorite is in places dotted with dolomite disks 1-2cm across.

Almost no relict textures are recognizable in this complex stringer- zone core. Some suggestion of primary lava fragments and occasional pseudomorphed feldspar (albite) are all that remain of the original rock. Occasionally, a polymict component with variably altered and coloured lava fragments is discernable.

Strongly foliated sericite with disseminated euhedral pyrite and accumulations of recrystallized equigranular quartz is dominant microscopically in the stringer zone core (Plate 5). Remnants of variably sericitized lava fragments and occasional albite phenocrysts pseudomorphed by quartz or sericite are discernable in some less altered samples. Other remnant features include sericitized perlitic glass. Both the sericite and the quartz vary markedly in grain size. Sericite can form a fine-grained mat (Plate 5) in which crystalline or coarse recrystallized quartz accumulations or single crystals are set. In some samples within this setting are elongate zones of coarse-grained, highly foliated sericite and patches of very coarse books of sericite. Minor carbonate, usually siderite or dolomite, occurs in patches and veinlets. In chloritic zones chlorite may replace volcanic fragments or pseudomorph augite or albite phenocrysts. These zones are distinct from the chlorite schists which consist almost entirely of uniformly massive Mg-chlorite and fine-grained euhedral pyrite. Minor minerals in Mg-

chlorite are accessory rutile in trains, foliated sericite and accessory quartz grains. Minor barite-sericite veinlets may cut the foliation. Coarse dolomite patches, in places zoned with coarse-grained centres, may also be present in the Mg-chlorite schists.

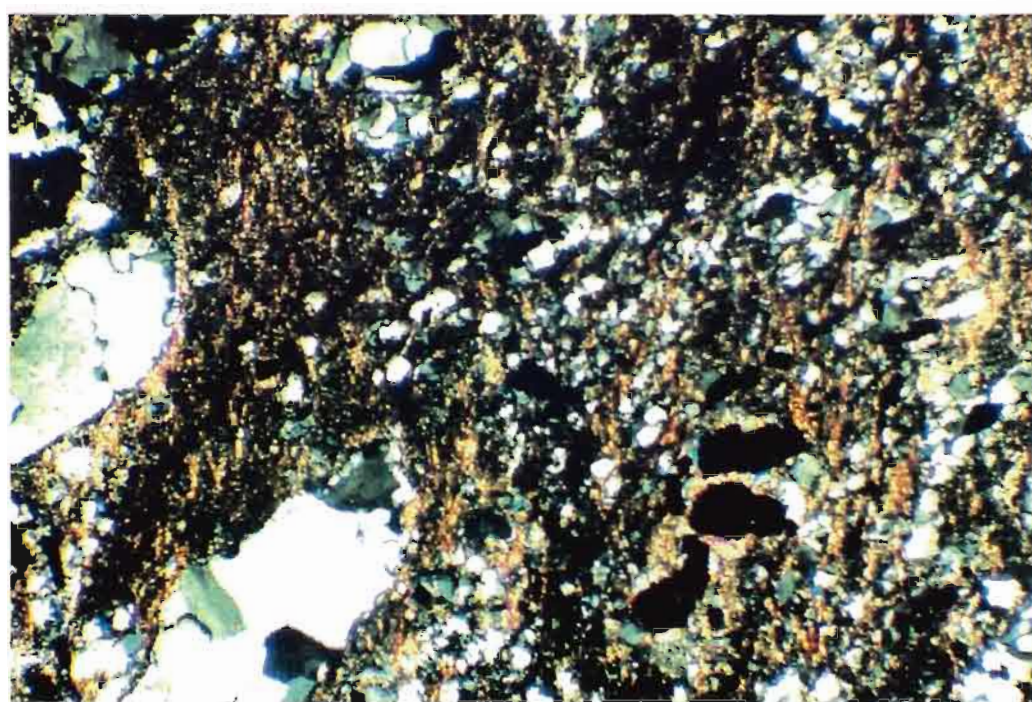
Mineralized zones are highly foliated. Euhedral crystalline pyrite crystals and patches are cut and partially enveloped by galena, chalcopyrite 'diseased', light-brown sphalerite and galena-chalcopyrite veinlets. The veinlets occur with highly foliated chlorite and sericite.

The stringer envelope zone is more uniform than the core with a distinctive brecciated lava with a pyrite stockwork being characteristic (Plate 6). Base metal sulphides are absent. Relict albite phenocrysts and minor small vesicles may be present.

Microscopically, light to colourless foliated sericite occurs with and within fine brown sericite. Quartz may predominate as fine cryptocrystalline grains mixed with sericite or as coarse recrystallised patches (Plate 6). Carbonate-or quartz-filled vesicles are concentrated in patches. Abundant albite phenocrysts are pseudomorphed by quartz and sericite. Pyrite occurs as a fine dusting or as coarse euhedral to subhedral grains in bands or in coarse-grained quartz - sericite veinlets. Patches of K-feldspar extend from this zone across the sharp boundary of this rock type with macroscopically unaltered andesite.

Hangingwall

The hangingwall volcanoclastic rocks are a highly varied unit in which there is abundant sericitization and bedded pyrite and sphalerite.



334236

Plate 6: Textures in the stringer envelope zone.

Note the characteristic pyrite fracturing (top). The photomicrograph shows quartz-sericite-pyrite alteration and quartz filled vesicles (bottom).

0 1mm (above)

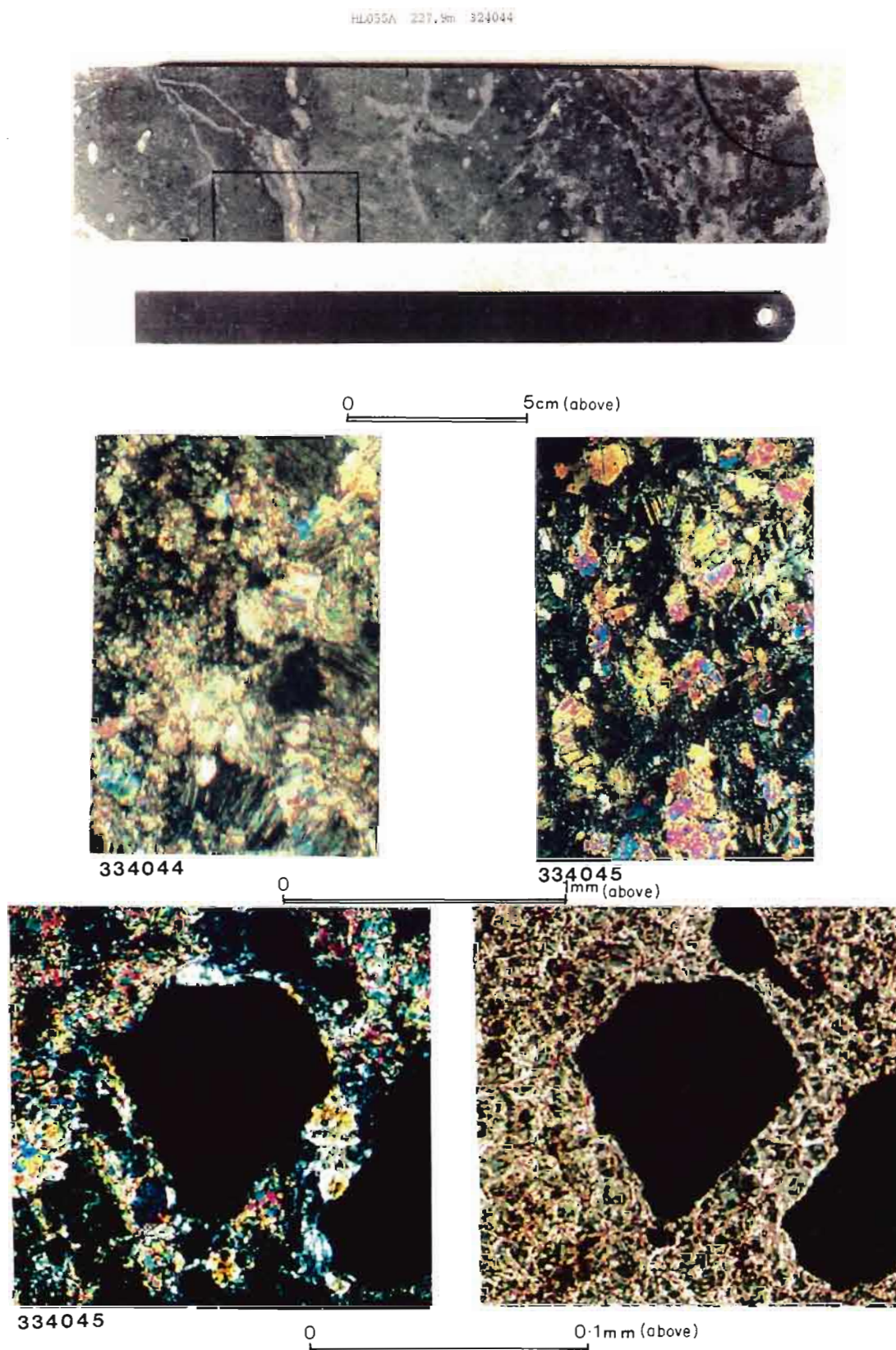
Microscopically, (Plate 3) the sericite occurs either as a fine mat in bedded ash volcanoclastic rocks or in highly foliated zones with sheared volcanic fragments replaced by sericite or calcite, and with trains of pyrite. Some zones contain abundant chalcedonic silica which may dominate the matrix completely or occur in alteration with sericite bands. Angular quartz grains are pervasive as are shard-like fragments replaced by quartz sericite or chlorite. Subsidiary Fe-chlorite identified by microprobe occurs with the sericite especially in the fine ash volcanoclastic rocks. Quartz-and carbonate-filled vesicles occur in the matrix. The larger fragments in breccias are also extensively altered to sericite.

The most striking macroscopic alteration feature in the Hellyer hangingwall basalt is the bright, chrome-green, calcite-sericite-fuchsite alteration (Plate 7). Fe chlorite alteration may accompany this alteration in accessory amounts. The alteration is pervasive throughout the lava. In addition, calcite veinlets are abundant and these may contain extensive pyrite as rims or globular accumulations. Barite is associated with this alteration, and there is a 3 metre x 1 metre white barite lens exposed at surface within the most intensely calcite-fuchsite altered lava.

Interpillow areas are the site of increased pyrite sericite alteration. This is accompanied by a marked increase in pyrite content. The increase in total sulphur within the hangingwall plume (described below under geochemistry) can largely be accounted for by this interpillow pyrite.

Plate 7: Textures in calcite-fuchsite alteration.

Middle: Left; calcite-fuchsite.
 Right; calcite-fuchsite-chlorite
 Bottom: Euhedral chromite in pervasive calcite-fuchsite;
 Left; polars crossed Right; uncrossed

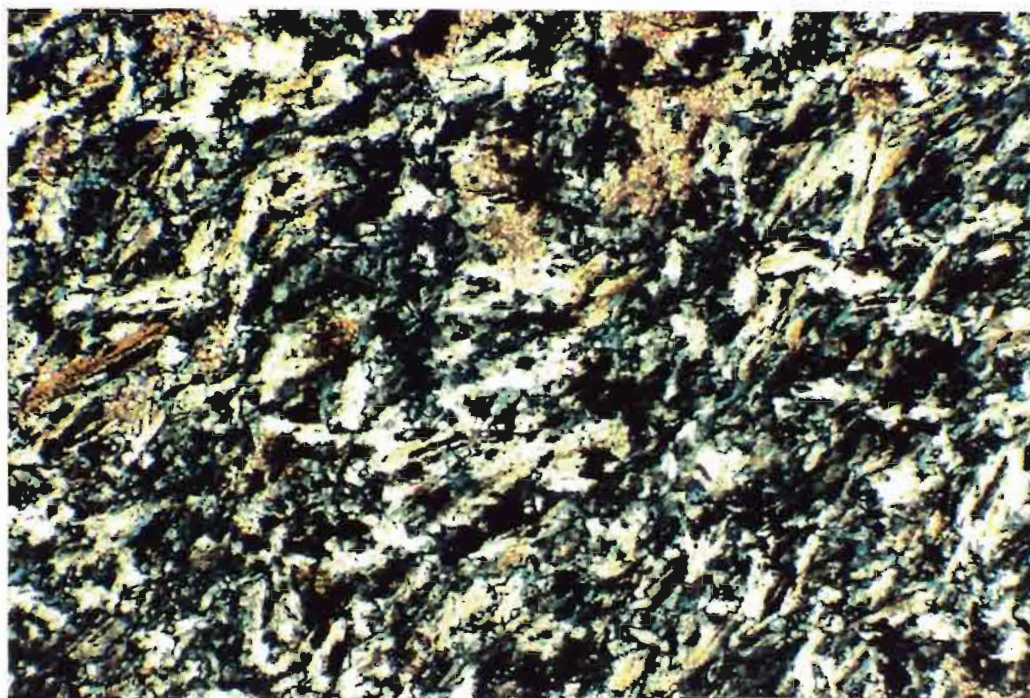


Pink albite is found in patches outside of the hangingwall plume. Where albite alteration occurs with the calcite-fuchsite it is not readily apparent macroscopically other than as micro-phenocrysts of albite and by the light grey colour of the rock.

Close to the Jack fault, small anastomosing veinlets of pyrite, sphalerite, galena and chalcopryrite are disseminated through otherwise uniformly textured rock.

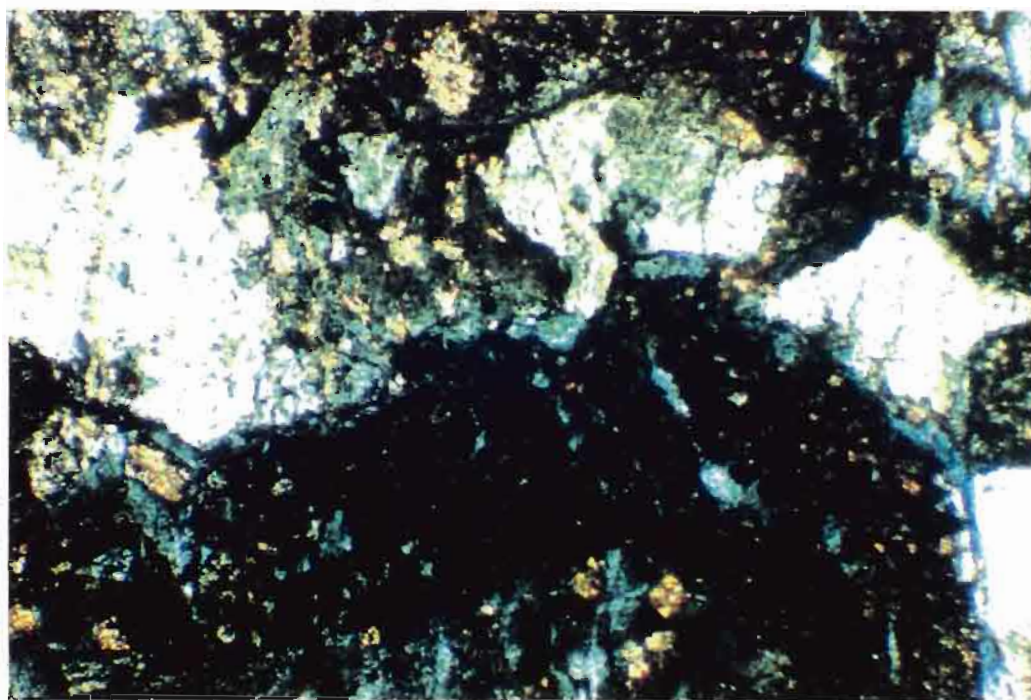
At the contact with the Que River Shale and spreading for several hundred metres away from Hellyer, there is an increase in pyrite content with massive pyrite locally.

Microscopically, in intensely calcite-fuchsite altered rocks there is complete replacement of other minerals by patches of calcite, fine sericite and Fe-chlorite. All primary textures are destroyed. The only other minerals recorded are resistate chromite grains which may remain euhedral (Plate 7), and minor apatite and titanite. Albite alteration occurs with the calcite-fuchsite in patches with complete replacement of all other minerals by a mat of albite crystals (Plate 8), differentiated from the primary albite microlaths by their coarser grain size and the absence of other minerals or textures. Chlorite is most abundant in interpillow areas, in occasional tension gashes and in less altered rocks where glass in the matrix is altered to chlorite. Cryptocrystalline chalcedonic quartz occurs as a subsidiary alteration type as pseudomorphs of albite and augite phenocrysts and in patches in the matrix. Pyrite occurs predominantly in interpillow areas and with calcite veining. Interpillow areas may contain veinlets of K-feldspar (Plate 8).



334017

Plate 8: A mat of albite alteration (above) and a K-feldspar
veinlet in interpillow sediment (below)



334018

0 1 mm

The Que River Shale and the Upper Rhyolitic Sequence

No alteration features in these units are proven to be associated with the Hellyer hydrothermal system of the section studied.

Whole Rock Geochemistry

Introduction

Analyses recalculated to 100% volatile free, analytical methods, and the names of laboratories that performed the analyses are listed in Appendices 2i, 2ii and 2iii.

Element distribution around the ore body is depicted on a pre-Jack fault cross section (Figure 17) constructed from the two sections shown on Figures 5 and 6. Data deep in the stringer system were obtained by projecting HL14 onto this section making allowances for the plunge to the north. All transformations are listed in Table 4 and all holes sampled are shown on the long section already presented as Figure 4. A bias in favour of continuous core grinds was introduced by repeating core grind samples that covered long intervals of uniformly similar rock so that there was a sample point every 5 metres at least. These data were entered, together with the split core samples, into the Apollo computer and using an "Eagle-Condor" gridding and gradient interpolating programme a series of colour images was produced. These were then used, together with the raw data, to hand contour 1:2500 scale cross sections, in the process removing any computer-generated problems such as interpolating into areas with no data or across geological boundaries. A total of 314 analyses were used in the production of the Hellyer Research Section. Split core samples were 15 to 30 cm long NQ core.

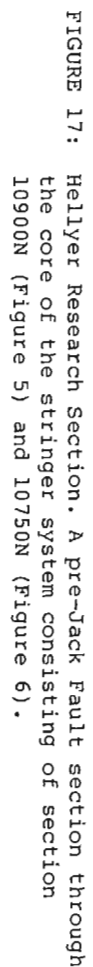


FIG. 17

TABLE 4 Transformations Used in Constructing the Hellyer Pre-Jack Fault Research Section

	North	East	R.L.	
14	+130 10500.9	+0 5350.2	-100 686.8	transformation collar co-ordinates
30	+130 10899.9	+0 5444.3	+30 681.2	transformation collar co-ordinates
31	+0 10900.1	+0 6047.8	+0 685.5	transformation collar co-ordinates
39(1)	+0 10793.9	+0 5910.0	+0 696.4	transformation collar co-ordinates
57	+130 10750.0	+13 5905.2	+0 700.4	transformation collar co-ordinates
61	+130 10750.3	+13 5945.7	+0 694.4	transformation collar co-ordinates
55	+0 10899.9	+0 5927.9	+0 687.9	transformation collar co-ordinates
24(1)	+0 10901.3	+0 5695.2	+0 686.3	transformation collar co-ordinates
28	+0 10901.0	+0 5695.5	+0 686.4	transformation collar co-ordinates
18	+130 10900.9	+0 5694.5	+30 686.4	transformation collar co-ordinates
15	+130 10694.2	+13 6050.1	+0 693.2	transformation collar co-ordinates
39(2)	+130 10793.9	+0 5910.0	+30 696.4	transformation collar co-ordinates
50	+130 10749.9	+13 5906.5	+0 700.2	transformation collar co-ordinates
24(2)	+130 10901.3	+0 5695.2	+30 686.3	transformation collar co-ordinates

The continuous core grind intervals are listed in Appendix 2i and 2ii. These were repeated in the data set according to the sample length and transformed co-ordinates for all sample points are listed in Appendix 2iii. With repeats, a total 554 analyses were used to make the element distribution cross sections.

A second technique used to study the alteration geochemistry is the isocon diagram. This is a graphical method of solution of Greisens (1967) mass (volume) balance equations proposed by Grant (1986). This technique was chosen for its simplicity in comparison with other methods such as those used by Avison (1985), or Naschwitz (1985) which involve a geostatistical approach and suffer from the difficulty of selecting the correct parent rock. Concentrations of elements in product altered-rocks are plotted against concentrations in pristine parent rocks. Elements are scaled by a convenient factor on both axes to plot all the elements on the same graph. Immobile elements plot on a straight line through the origin as mass or volume changes do not affect their ratio. This line is the so called isocon and its slope defines the constant volume or mass changes that have affected the rock. Elements which have been mobile plot above this line for addition and below where they have been depleted. In this thesis, additions and losses are depicted on histograms below the isocon diagrams.

The selection of parent rocks, an intractable problem because of metamorphism and structural complications in many other districts, is simplified at Hellyer where unaltered lava remnants in the Hangingwall basalt, with Ti/Zr ratios identifying individual lava flows, occur within the hangingwall plume (334028 was used as parent for surrounding basalt

and 334038 for the core basalt). In the albite porphyritic andesite footwall, length-weighted continuous core grinds over uniform lava west and east of Hellyer were combined to represent the parent rock (total 277.8 metres of core grind, n=13, sample nos 334114 through to 334124 in HL30 and 334146, 334147 in HL31 - see Appendix 2i).

Element Distribution on Cross Sections through the Hydrothermal Centre

Contoured cross sections showing the distribution of silica, alumina, total iron, manganese, magnesium, calcium, sodium, potassium, sulphur, copper, lead, zinc, chromium and barium on the pre-Jack fault movement section are presented as Figures 18 to 31. These sections were selected from the full range of colour images of the elements and ratios in Appendix 2. Paper copies of all these images are filed in Aberfoyle's files but are not all presented here as omitted images were considered to repeat features visible on the sections chosen.

Major Features

Before discussing the distribution of each element separately, two major zones of alteration need definition.

The stringer zone below Hellyer is reflected in the iron, sulphur, copper, lead, zinc, barium highs and sodium, silica low on Figures 18, 20, 26, 27, 28, 29, 31 and 24.

The hangingwall plume is a plume-shaped zone in the hangingwall basalt above the massive sulphide, directly above the core of the stringer zone. It is defined by a major calcium and sulphur high (Figures 23 and 26) associated with calcite and pyrite development. Fuchsite-sericite is also extensively developed in this plume.

Elements

Silica (Figure 18)

The stringer zone core is outlined by a silica low. A high to the west of the massive sulphide is associated with the stringer envelope zone. Local mobility of silica cannot be depicted at this scale.

Aluminium (Figure 19)

The effect of extensive sericitization at the Hellyer ore position along the hangingwall volcanoclastic rocks is reflected in the aluminium high. Sericite in the hangingwall basalt is more intensely developed closer to the ore body and this causes the broad high immediately above the massive sulphide. Mobility of aluminium in the stringer zone (see isocon diagrams) cannot be depicted at this scale owing to rapid local variation in total aluminium content.

Total iron (Figure 20)

The high pyrite content of the stringer zone causes the iron high. Pyrite at the contact with the Que River shale results in the high there. The hangingwall plume does not result in an iron high in spite of the increase of pyrite content as there is a simultaneous decrease in iron content of the basalt (see isocon diagrams).

Manganese (Figure 21)

There is a manganese low around the massive sulphide with most depletion in the footwall, but extending into the hangingwall where the low exists 300 metres either side of the massive sulphide.

Magnesium (Figure 22)

There is overall depletion in magnesium in the immediate footwall with major increases in the massive chlorite in the stringer zone

difficult to depict at this scale but shown by the vertically elongate highs. The regional scale depletion in magnesium in the hangingwall is complex. Note the >12% MgO highs 300 metres east and west of the ore body.

Calcium (Figure 23)

The increase in calcium in the hangingwall plume with complex but high values >15% CaO is associated with pervasive calcite alteration and also with calcite veining caused by hydrothermal fracturing. The calcium low in the footwall extends outside the section sampled. No footwall carbonate analysed was calcite. Strontium (distribution diagram not included in this thesis) is also regionally depleted in the footwall.

Sodium (Figure 24)

Sodium depletion outlines the stringer zone, but does not extend outside of pervasively mineralized and altered stringer zone rocks in the same way that the calcium and strontium depletion does. The sodium highs in the footwall 100 metres on either side of the ore body reflect the prominently albite porphyritic andesite. Albitization of plagioclase is interpreted to be a metamorphic feature and is widespread regionally in the footwall andesite. This is different to the pervasive hydrothermal albite alteration in the hangingwall basalt which causes the hangingwall highs east of the ore body and close to the Jack fault.

Potassium (Figure 25)

The increase in sericite in the stringer envelope zone is highlighted in a complex potassium distribution. The sericite in the inner stringer zone is difficult to show at this scale because of its

complex mixture with highly silicified or chloritized rocks. Sericite developed in the hangingwall volcanoclastic rocks causes the potassium high at the Hellyer ore position. An altered zone 200 metres west of Hellyer causes the potassium high there, but it is interesting to note the absence of any hangingwall calcium - sulphur enrichment or iron-magnesium depletion above this zone or of any widespread sodium depletion in the zone itself. No massive sulphide has been intersected associated with this zone.

Sulphur (Figure 26)

The hangingwall plume is outlined by the increase in sulphur from <2% outside the plume to 2-6%S inside the plume. This mostly reflects increased interpillow pyrite. The increase in sulphur in the stringer zone is greatest in the core. Pyrite developed at the Que River shale contact west of the section may connect with the hangingwall plume off section. Again the alteration west of Hellyer in the footwall is shown. Localised increases in sulphur close to the Jack fault occur.

Copper (Figure 27)

The stringer zone is outlined using a 200 ppm upper clip. Copper levels are low in massive chlorite-quartz-sericite and silica alteration (see isocon diagram) and the copper high is caused by chalcopyrite development with sphalerite and galena in veinlets. No data on the massive chalcopyrite - pyrite body in the upper stringer zone were included in the data set. The copper low in the hangingwall basalt and extending into the footwall is complex and difficult to represent at this scale. Mineralization west of Hellyer is evident with a 200 ppm upper clip as a broad high, but this is of lower intensity than that in the stringer zone.

Lead (Figure 28)

The stringer zone is outlined by a lead high. Also evident is interpreted stringer type mineralization (see Chapter 6 on sulphur isotopes) close to the Jack fault. A lead low, similar to that of copper, is also evident around the ore body. Elevated lead in the black shale is due to galena in minor veinlets, possibly formed during Devonian remobilization.

Zinc (Figure 29)

The complex increase in zinc in the stringer zone is difficult to represent at this scale. This results from sphalerite (and galena) being concentrated in veinlets adjacent to altered, zinc depleted, rocks. The zinc low above the ore body extends to the shale contact (compare copper and lead). The mineralization west of Hellyer is represented by a zinc high.

Chrome (Figure 30)

This depicts the primary chrome content of the rocks, with the hangingwall basalt having a higher chrome content of 500 - >1000 ppm Cr than the footwall andesite. There is no increase in chrome in the stringer zone and the high above the massive sulphide is probably primary as regional chrome analyses in unaltered basalt analysed in exploration drilling show similar highs. Most chrome is contained in resistate chromes with very little contribution from mobile chrome now in fuchsite. Chrome is essentially immobile (see isocon diagrams) with only minor local redistribution.

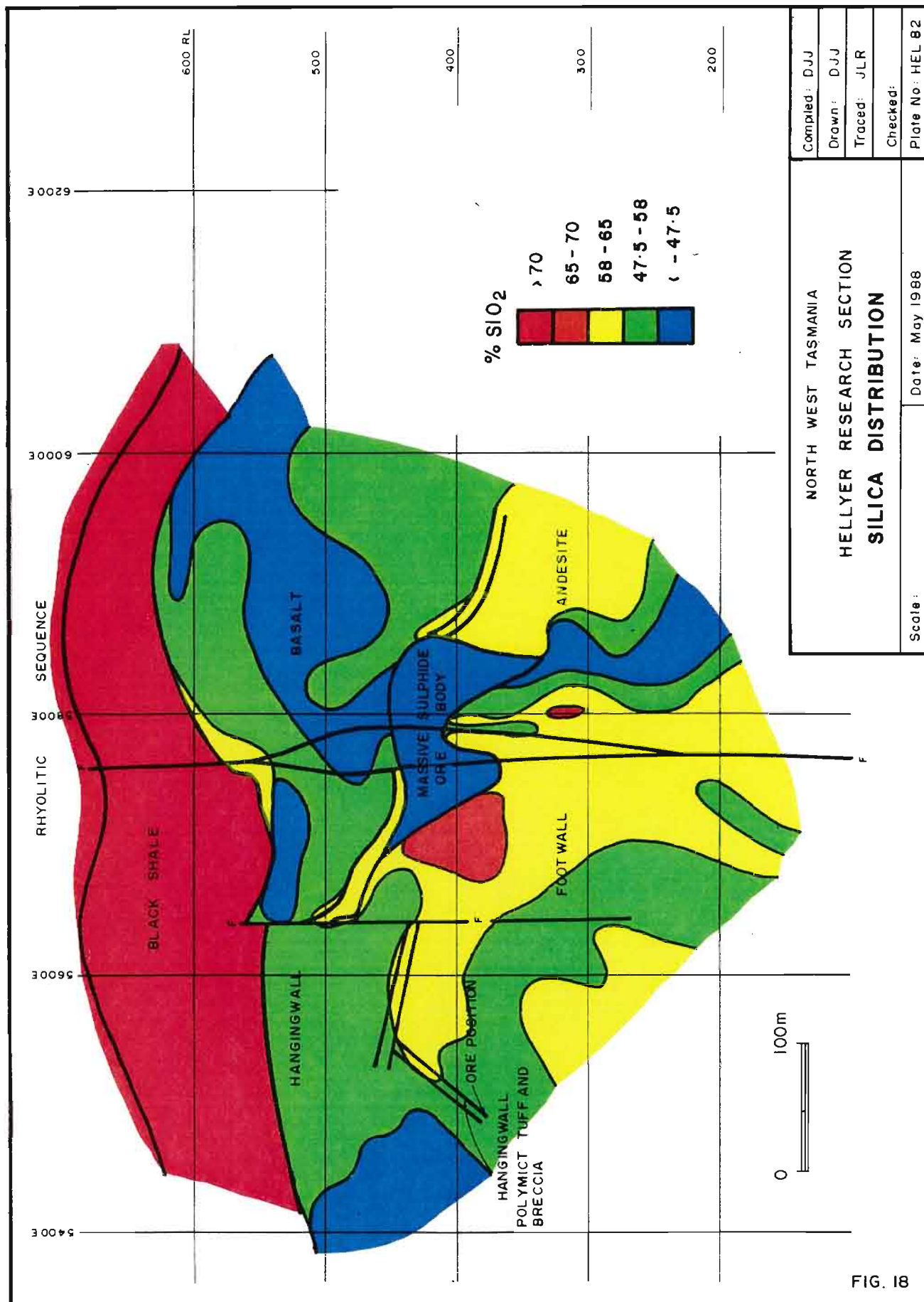


FIG. 18

FIGURE 18: Silica Distribution. Silicification in the stringer envelope zone is reflected in a SiO_2 high west of the massive sulphide. The core of the stringer zone is outlined by a silica low. Local silicification in the stringer zone cannot be depicted at this scale.

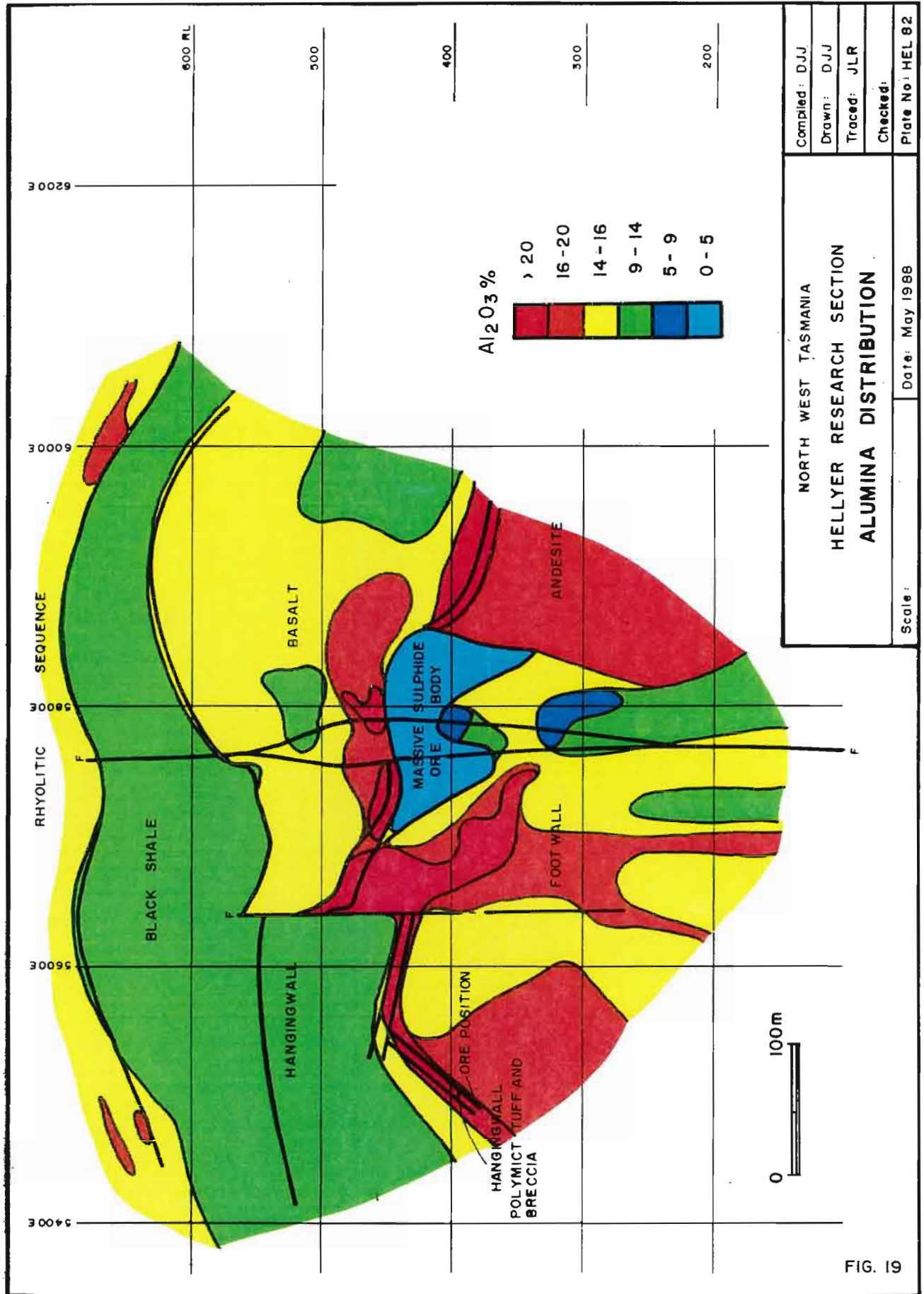


FIG. 19

FIGURE 19: Aluminium Distribution. Sericitization along the Hellyer ore position and in the hangingwall basalt immediately above the massive sulphide causes the highs there.

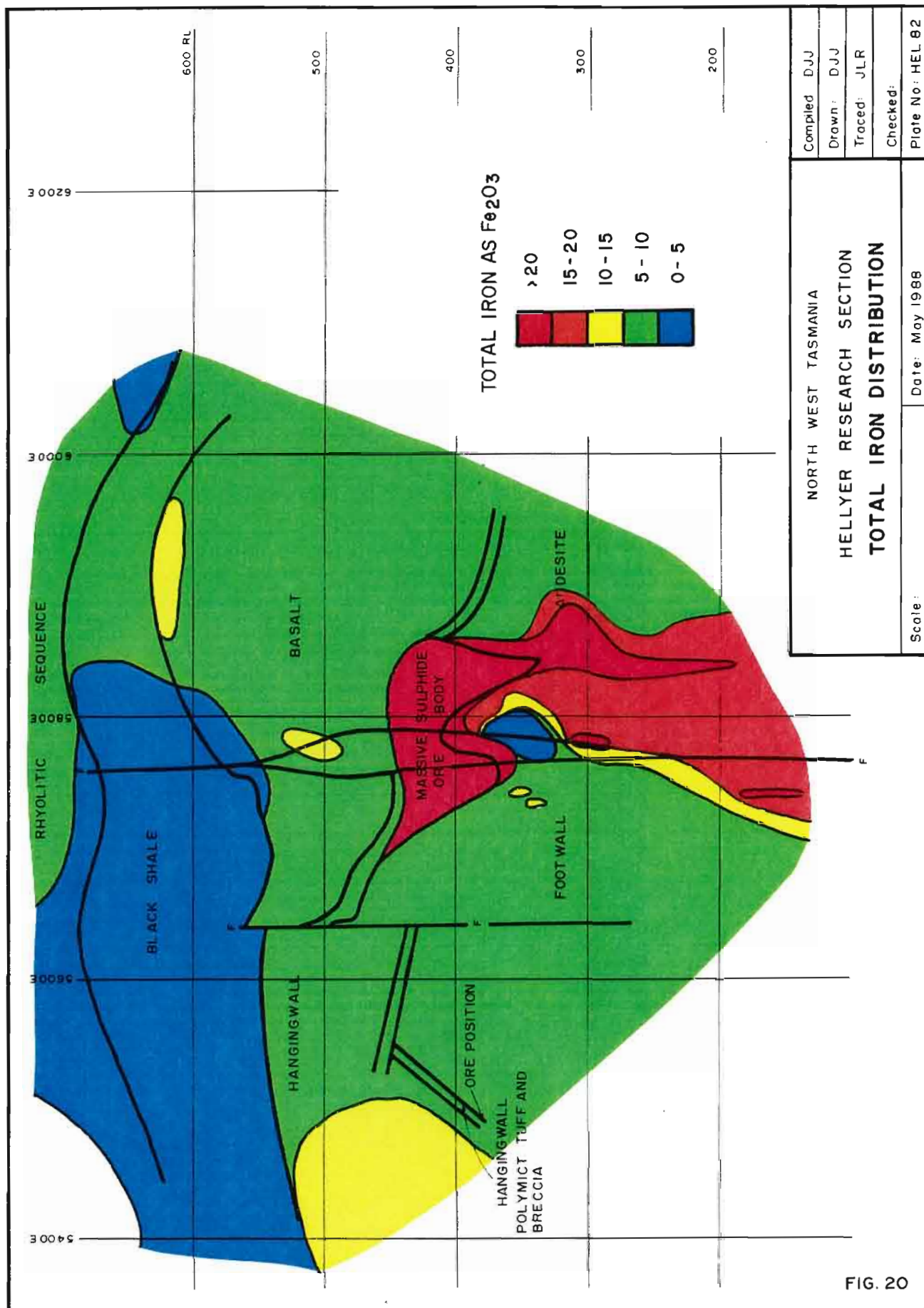


FIG. 20

FIGURE 20: Total Iron Distribution. Increased pyrite content causes the high in the ore body and the stringer zone. A simultaneous decrease in the iron content of the basalt in the hangingwall plume masks the increased pyrite content there.

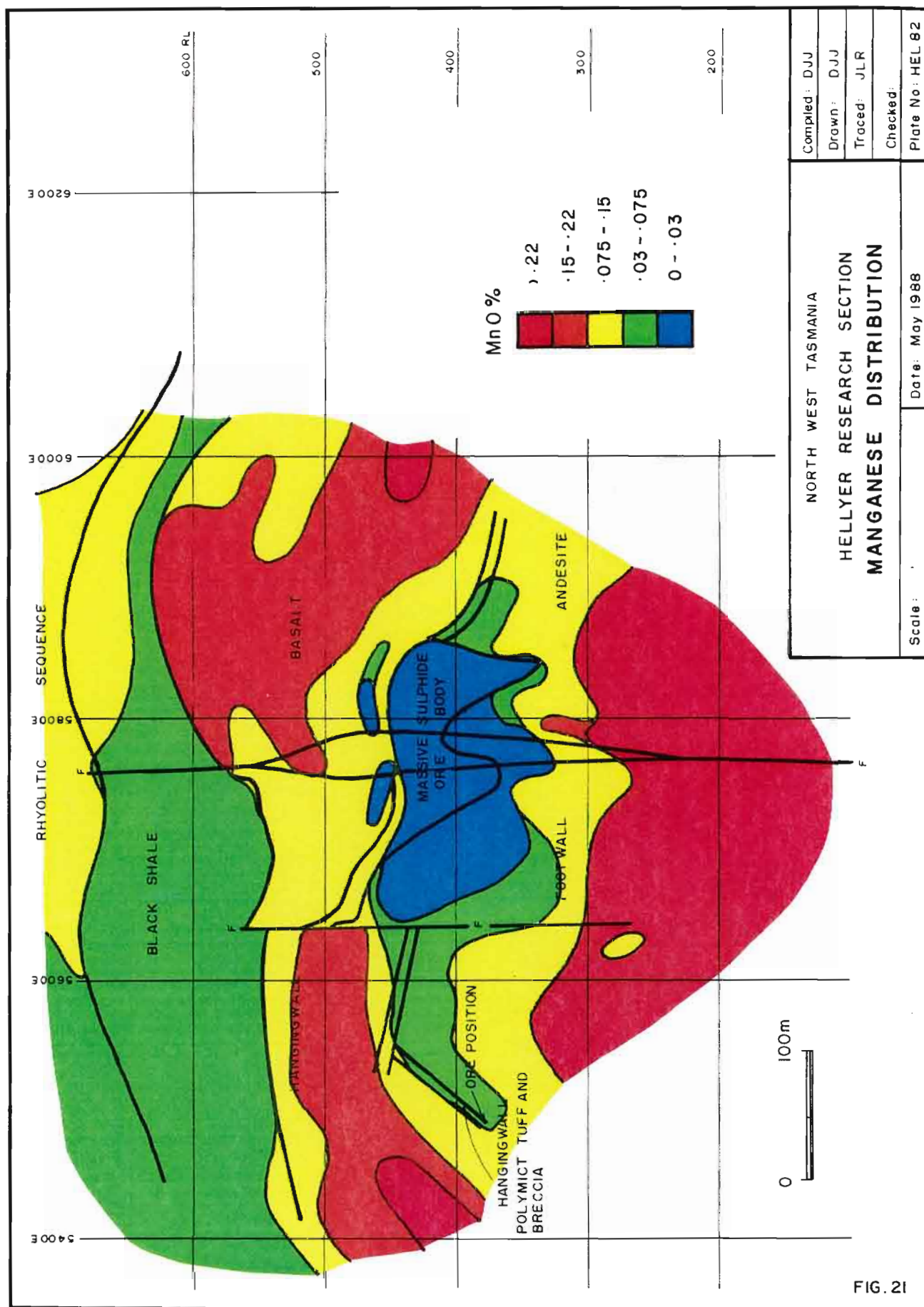


FIGURE 21: Manganese Distribution. Note the manganese low that surrounds the orebody.

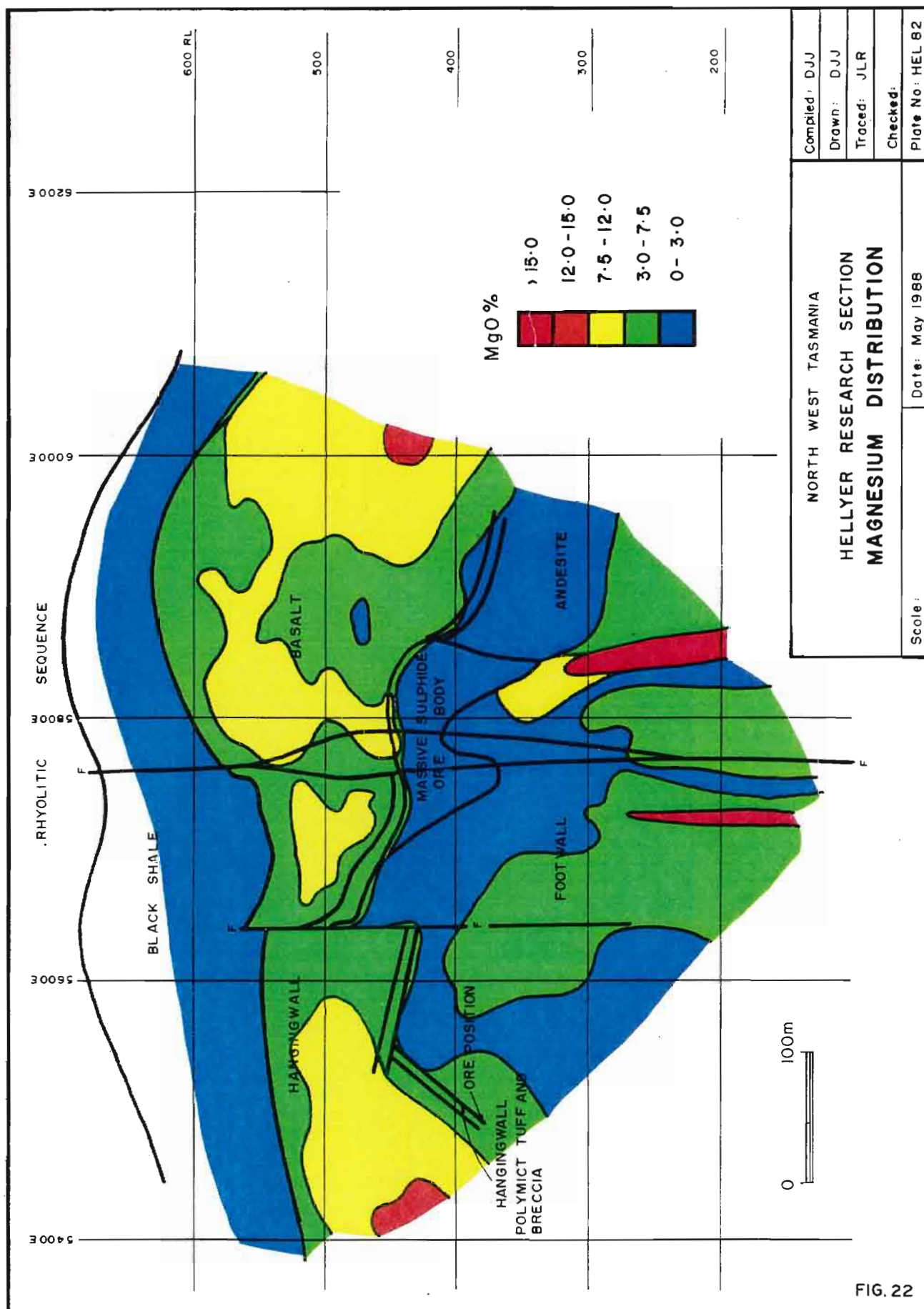


FIGURE 22: Magnesium Distribution. Note the magnesium low in the footwall immediately below the ore position.

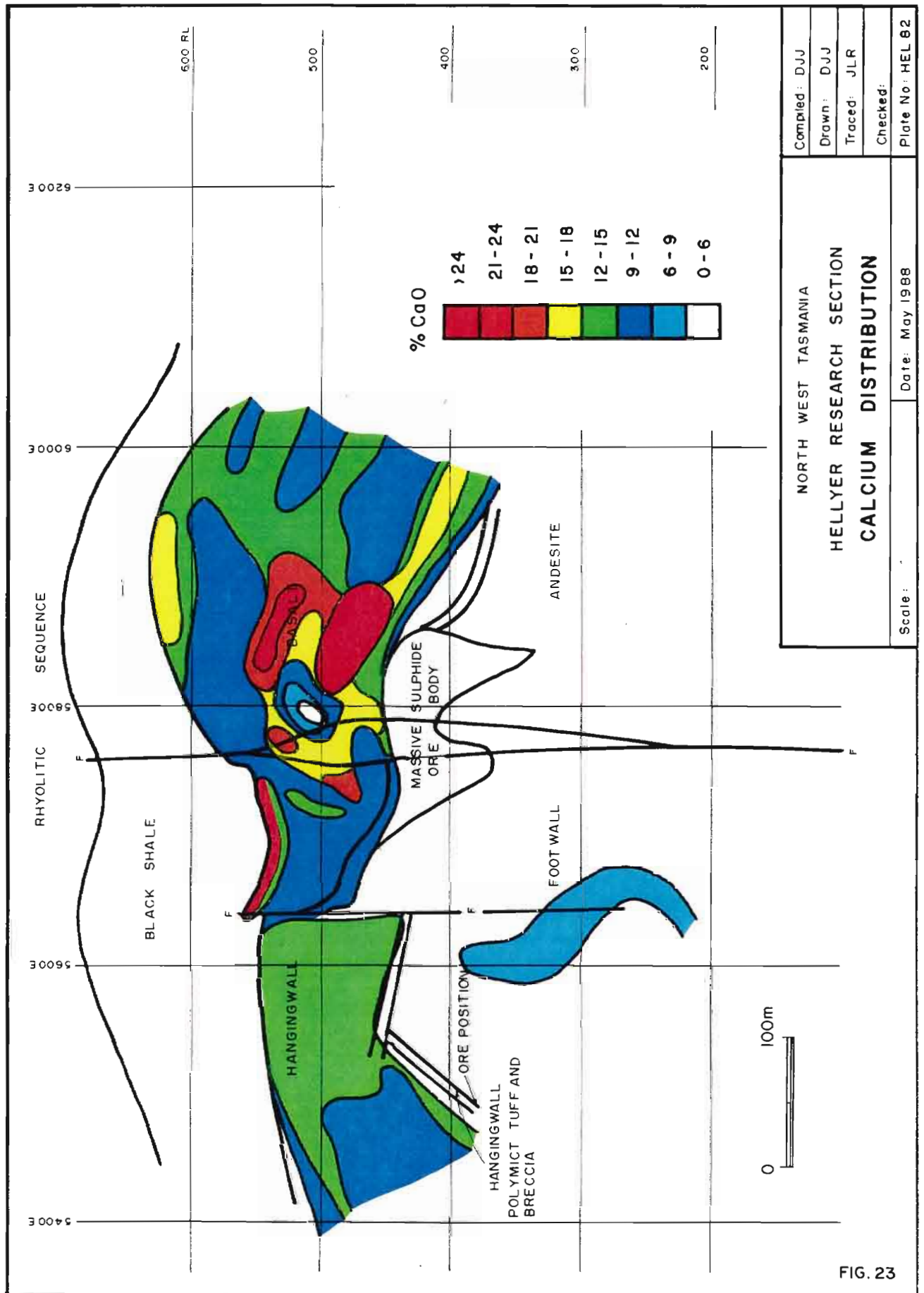


FIGURE 23: Calcium Distribution. There is a complex calcium high in the calcite rich hangingwall alteration plume. Calcium is depleted in the footwall.

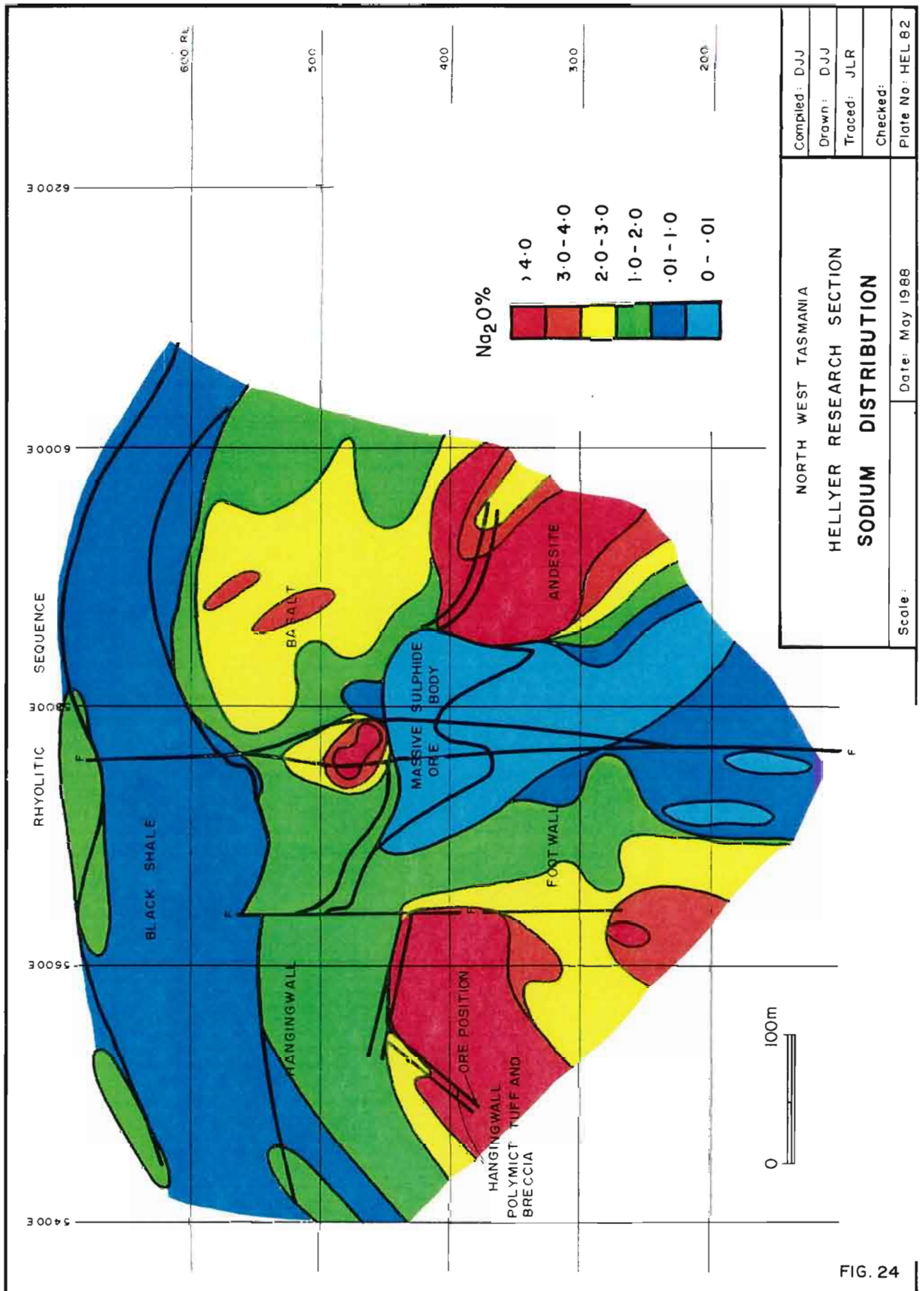


FIGURE 24: Sodium Distribution. Sodium depletion in the footwall outlines the pervasively altered and mineralized stringer zone rocks, but does not extend laterally. Regionally the footwall is characterized by sodium rich albite porphyritic andesite which has produced the sodium highs on either side of the orebody.

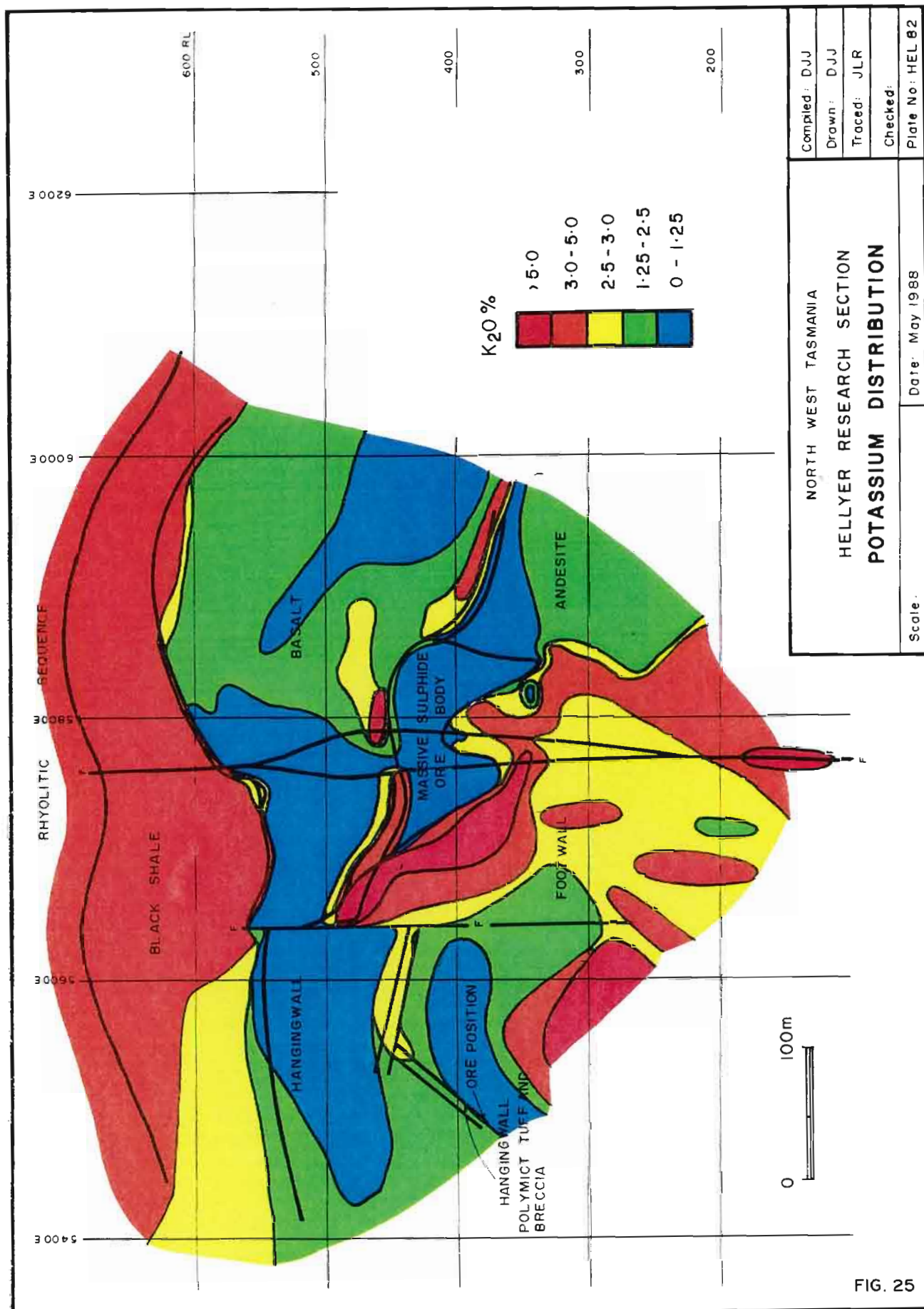


FIG. 25

FIGURE 25: Potassium Distribution. Potassium highs in the stringer zone and along the hangingwall volcanoclastic are caused by sericite development.

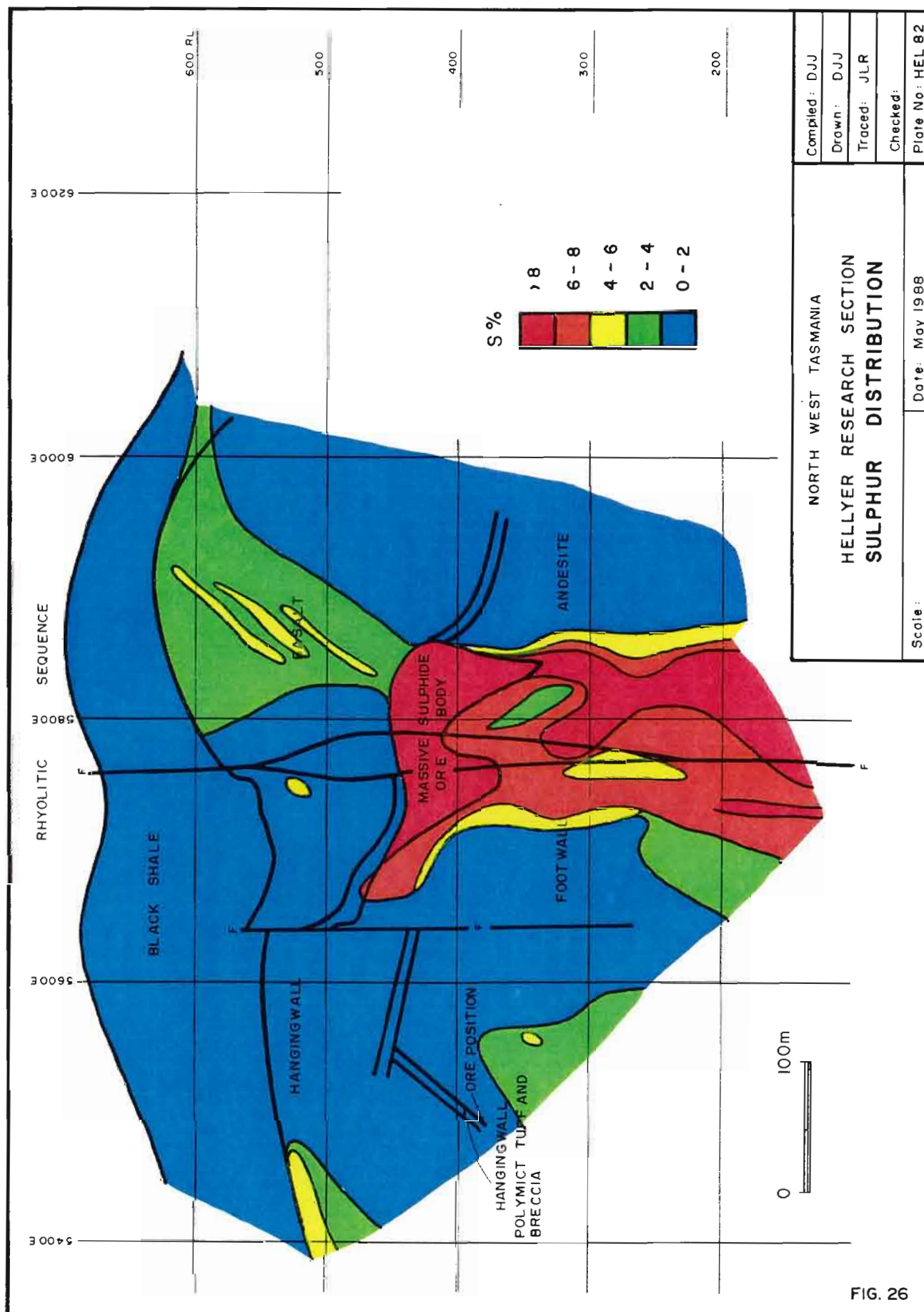


FIG. 26

FIGURE 26: Sulphur Distribution. The increased pyrite content of the hangingwall plume is reflected in the sulphur distribution. The stringer zone is also clearly outlined.

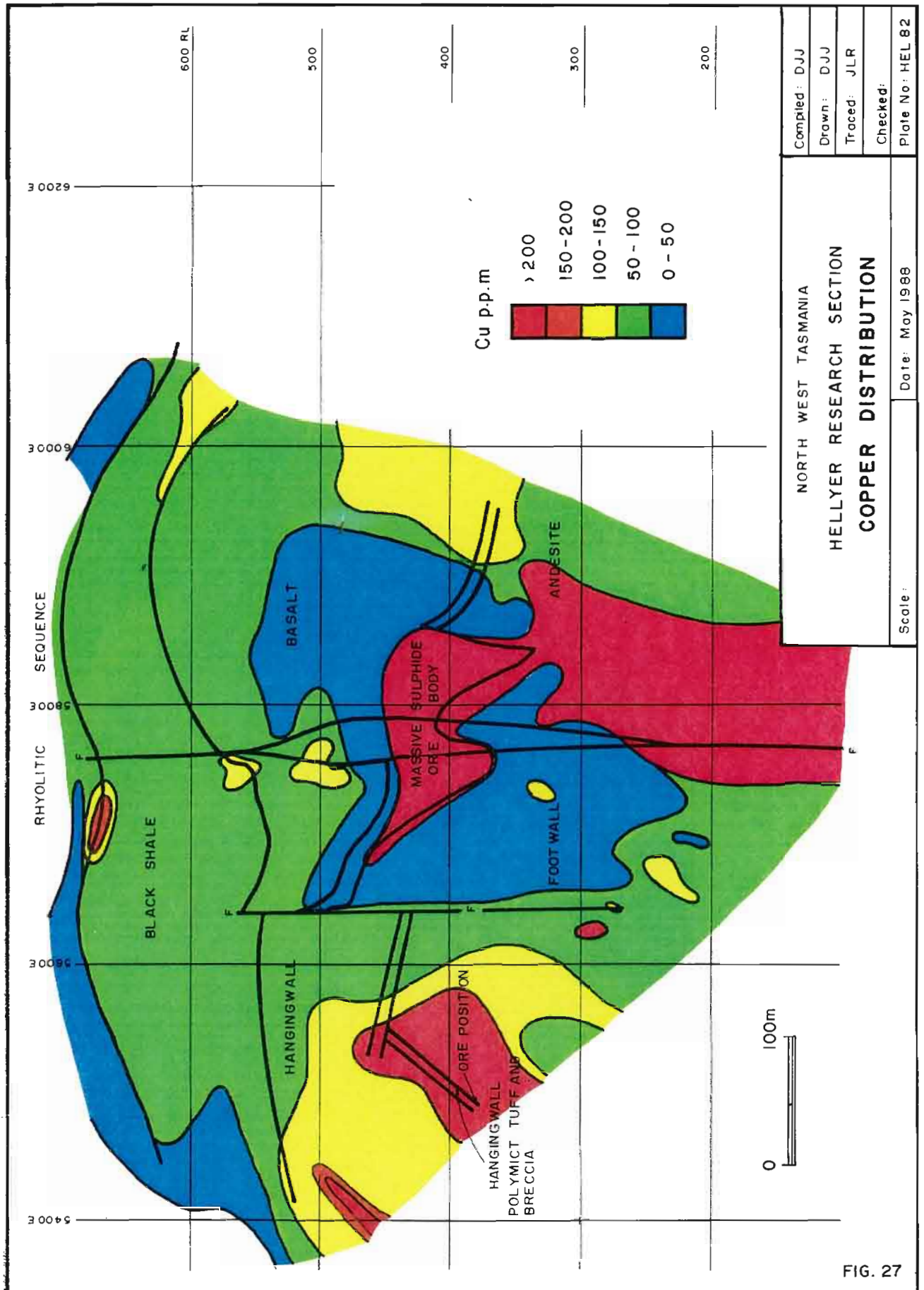


FIGURE 27: Copper Distribution. There is a copper low around the orebody and a copper high in the stringer zone.

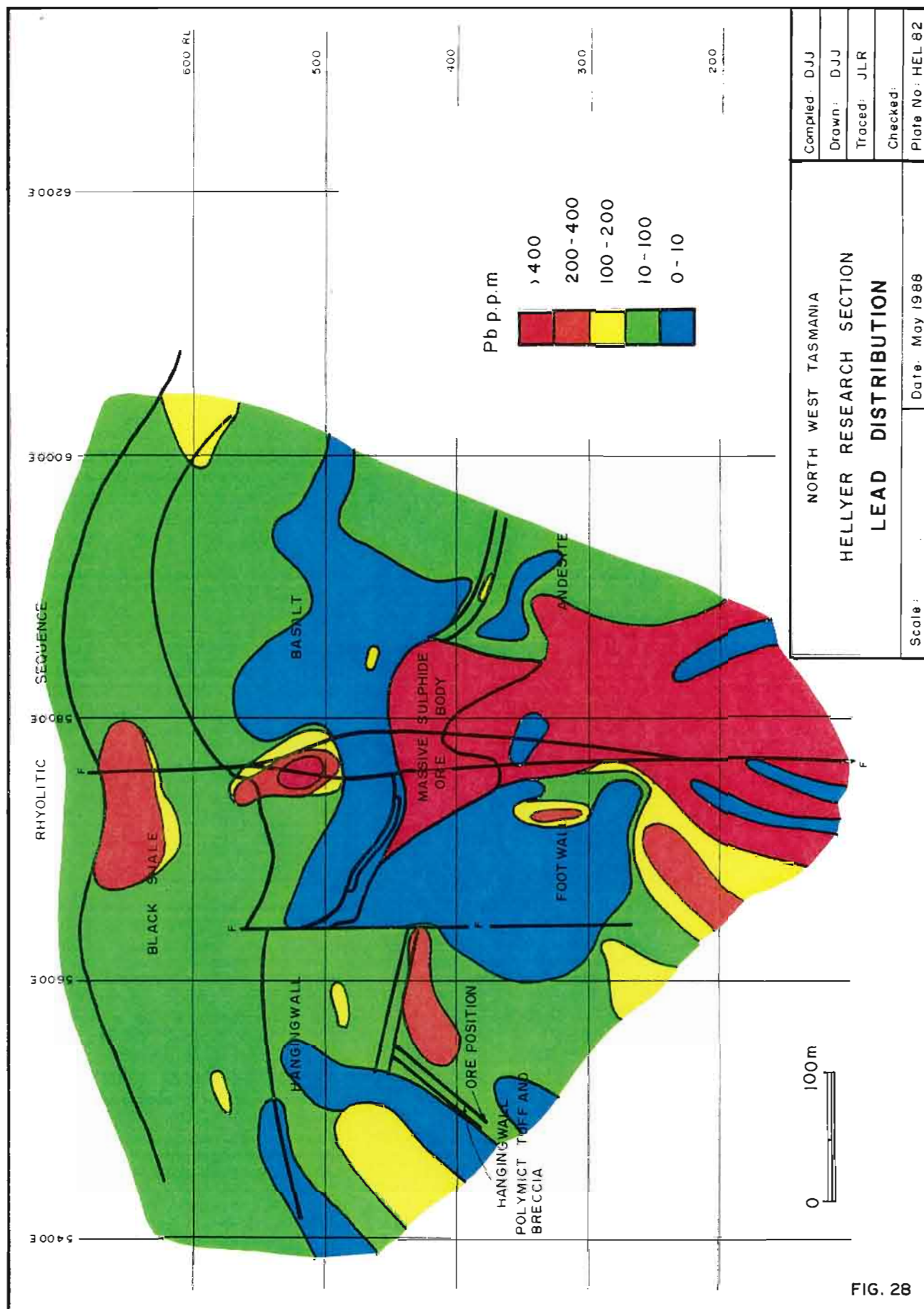


FIGURE 28: Lead Distribution. A lead high results from galena in the stringer zone. There is a lead low around the orebody. Interpreted stringer type mineralization occurs in the hangingwall close to the Jack fault.

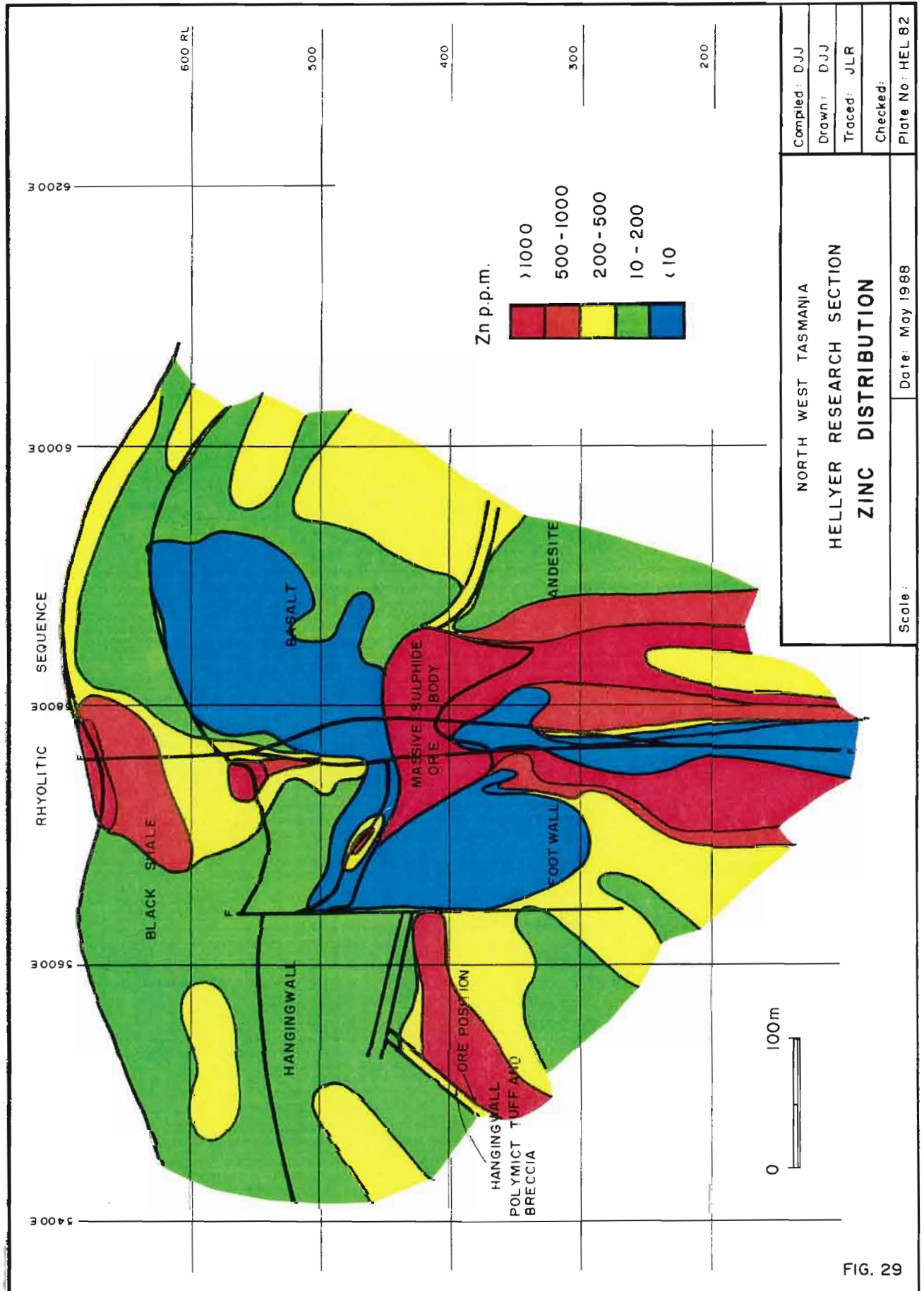


FIGURE 29: Zinc Distribution. The zinc low around the orebody extends all the way to the shale-basalt contact. A complex mixture of highs and lows occurs in the stringer zone.

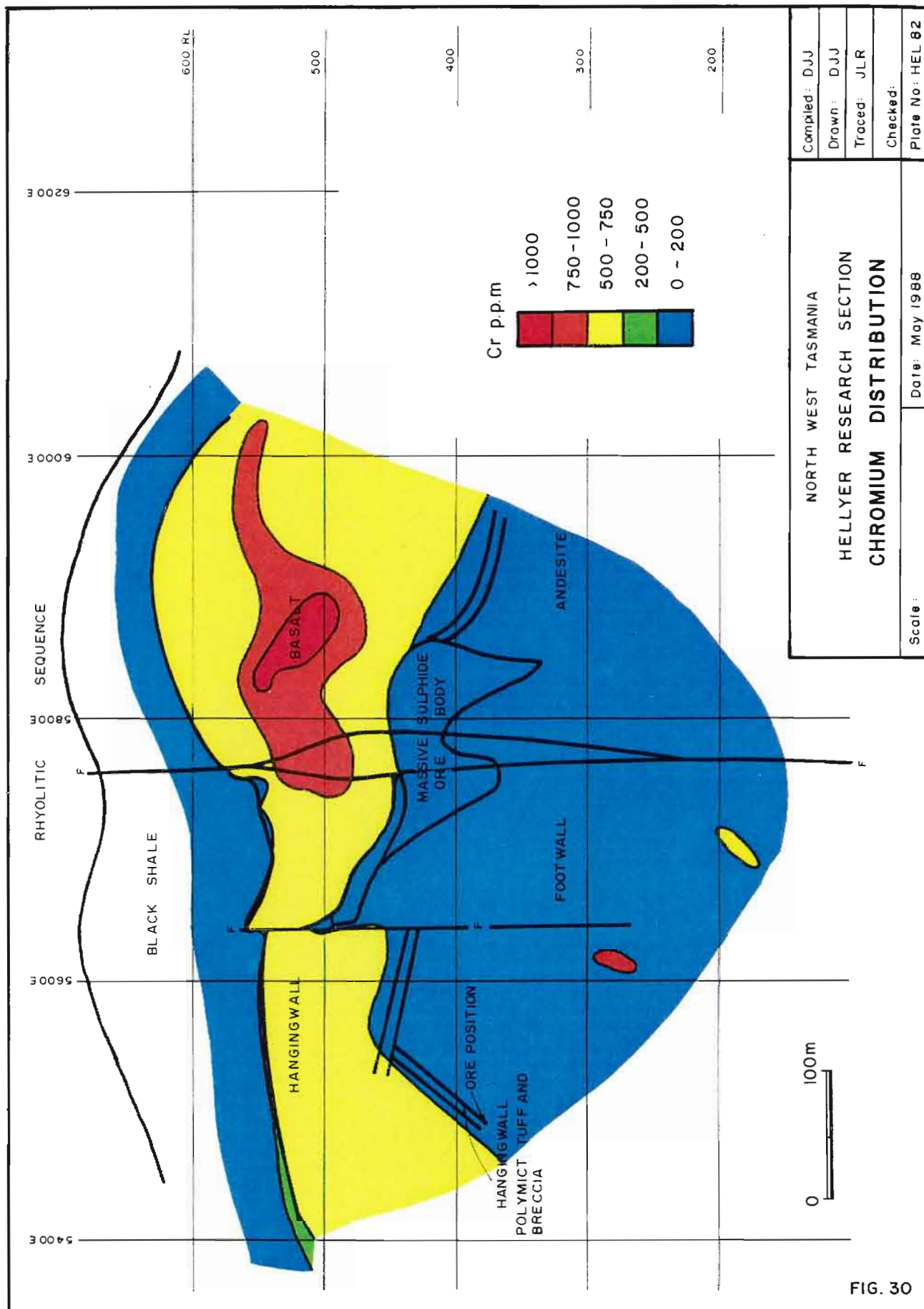


FIGURE 30: Chromium Distribution. The lower primary chrome contact of the andesite relative to the basalt is evident. Most chrome in the basalt is contained in resistate, often euhedral chromites and the chrome high above the orebody is interpreted to be the result of a local primary variation in chromite content.

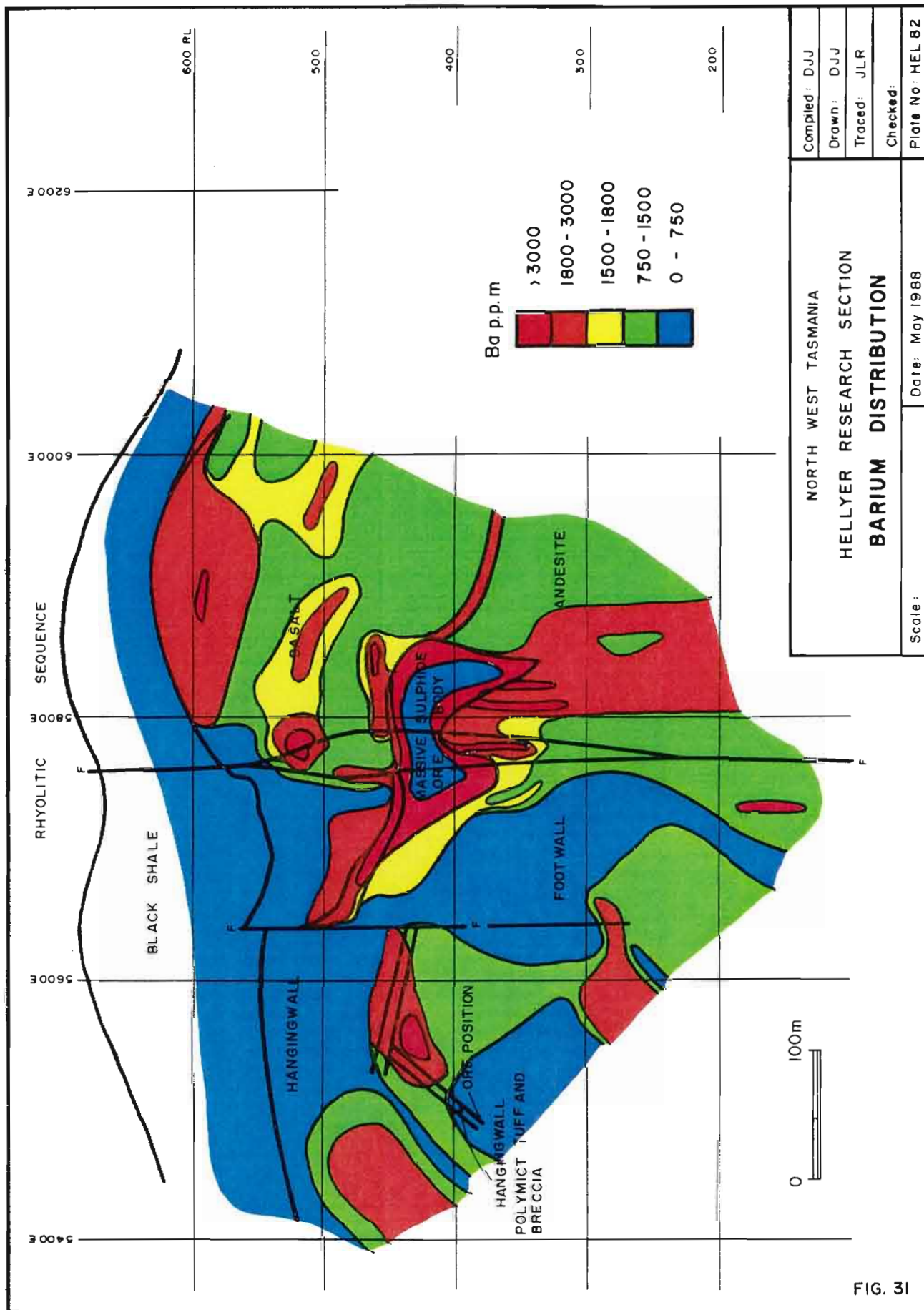


FIG. 31

FIGURE 31: Barium Distribution. There is an increase in barium (barite) in the upper stringer zone, upper orebody, in the hangingwall plume and along the ore position.

Barium (Figure 31)

The increase in barium in the upper stringer zone and in the hangingwall plume is evident. There is also an increase in barium content along the Hellyer ore position in the hangingwall volcaniclastic rocks.

Detailed Sections through the Upper Stringer Zone and Massive Sulphide

There are problems in representing the complexity of the stringer zone at the scale of the sections in this thesis. Therefore, using 2 metre core grinds from underground resource drilling a series of detailed sections were contoured at 1:1000 scale. Reductions of these are presented in Appendix 1 Figures i to viii. Interpretation is kept to a minimum as the distributions, and their significance particularly those in the orebody, are beyond the scope of this thesis.

Copper (Appendix 1 Figure i)

The vein-like nature of the copper highs is represented in the contouring. Copper highs associated with the lower part of the ore body and with the hangingwall gold zone are also apparent.

Lead (Appendix 1 Figure ii)

Two high zones in the stringer zone are interpreted. Lead highs are more pervasive than copper highs. Within the ore body, the concentric zoning around the stringer zone core is well represented in the lead distribution. In particular the zoning is interpreted in the ore body down the eastern side of the Jack fault, confirming that on this section the centre of hydrothermal activity was east of the fault.

Zinc (Appendix 1 Figure iii).

Two zones of elevated zinc are interpreted in the upper stringer zone. These are the two feeder zones represented schematically in Figure 7.

Silver (Appendix 1 Figure iv)

Enrichment in the hangingwall precious-metal zone east of the ore body is the dominant feature. Silver values in the stringer zone are low.

Gold (Appendix 1 Figure v)

Enrichment in the hangingwall precious-metal zone occurs above the silver enrichment. The enrichment at the top of the sulphide mound occurs in glassy silica - pyrite rock. Gold values in the stringer zone are low.

Barium (Appendix 1 Figure vi)

Major features include the occurrence of a barite cap to the orebody, and a major barium low in the centre of the ore body. Barite veinlets occur at the top of the stringer zone.

Arsenic (Appendix 1 Figure vii)

Most arsenic (arsenopyrite) occurs in the central, pyrite-rich, barium-poor parts of the ore body.

Density (Appendix 1 Figure viii)

The density reflects the pyrite content. Increased pyrite is found within the two centres in the stringer zone and in the central, arsenic-rich, barium-poor parts of the ore body.

Isocon Diagrams

Individual alteration types have been analysed for element additions or losses using the isocon method described in the introduction (page no. 66).

Footwall alteration

These are described from the core of the stringer zone outwards. The results are summarized in Table 5.

Figure 32 is an isocon plot for quartz-barite alteration and shows the dominance of these two minerals, reflecting the major mass addition of SiO_2 and Ba. K_2O , Rb (sericite) and As (arsenopyrite) are also enriched.

Sericite-pyrite alteration (Figure 33), as expected, shows enrichment in K_2O , Fe_2O_3 and S. Al_2O_3 and TiO_2 , as in the Mg-chlorite alteration, plot above the isocon drawn through Nb, Y and Zr. Ba enrichment is marked, as is the CaO and Na_2O depletion.

Mg chlorite alteration (microprobe data; $\text{MgO} = 26.2\%$ $n=4$ for 334063) shows the expected MgO enrichment on the isocon diagram (Figure 34), with a major depletion in Ba, SiO_2 , CaO, Sr, Rb, Cu, Pb, Zn. Enrichment in Mn is marked in percentage change, but is not significant in mass addition. TiO_2 , Cr and Al_2O_3 plot off the selected isocon reflecting some mobility of "immobile" elements. Whitford (1986) used the relative "immobility" of Al_2O_3 in Mg chlorite at Que River in support of (as suggested by McLeod and Stanton, 1984), the hypothesis that chlorite formed at pre-existing aluminium sites and was not sedimentary in origin.

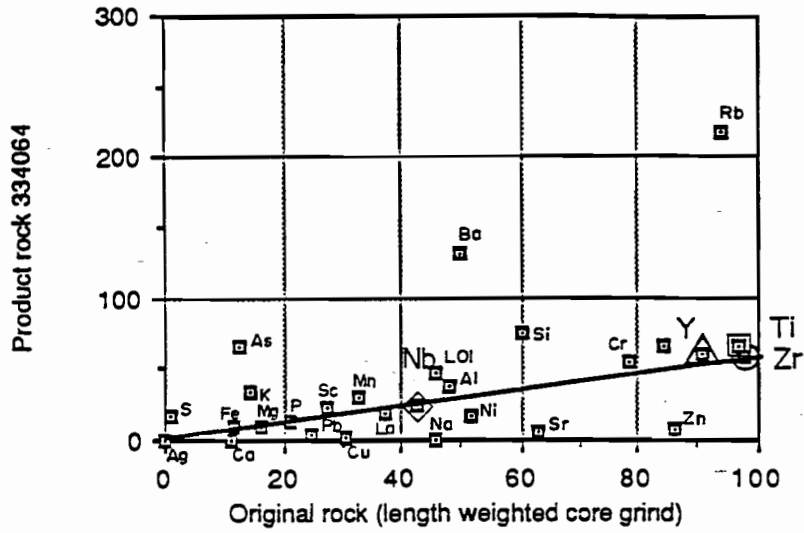
Quartz-sericite alteration in the envelope zone again presents problems with selecting an isocon. Two alternatives are presented in Figure 35; Y (and Ti) immobile, and Zr (and Nb) immobile. In both cases, SiO_2 , Al_2O_3 , and K_2O are added while MgO, CaO and Na_2O are removed. There is an increase in volume from parent to product in both cases.

TABLE 5 Major Additions and Losses of Elements During Alteration

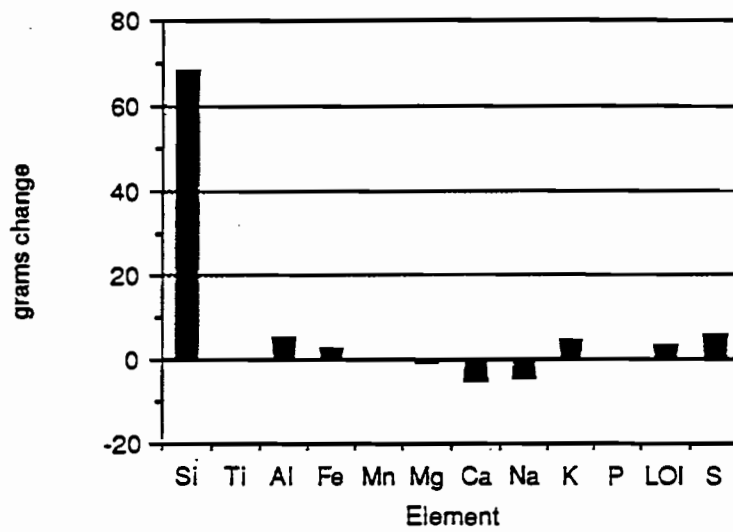
	Alteration type	For original 100 gram rock Addition (grams)	Loss (grams)
Hangingwall	Calcite-fuchsite	18 CaO, 16 CO ₂ , 6 Al ₂ O ₃ 3 K ₂ O, .23 Ba	13 SiO ₂ , 11 MgO, 4 Fe ₂ O ₃
	Albite	13 SiO ₂ , 12 CaO, 11 CO ₂ , 6 Na ₂ O, .07 Pb, .03 Zn	8 MgO, 5 Fe ₂ O ₃ , .13 Ba
Inner stringer Zone	Quartz barite	68 SiO ₂ , .35 Ba	5 CaO, 4 Na ₂ O
Footwall	Sericite - Pyrite	22 Fe ₂ O ₃ , 18 S, 12 Al ₂ O ₃ 8 K ₂ O, .35 Ba	6 CaO, 5 Na ₂ O
	Mg - chlorite	23 MgO	30 SiO ₂ , 5 CaO, 4 Na ₂ O
Outer stringer Zone	Quartz sericite envelope	66 SiO ₂ , 18 Al ₂ O ₃	2 CaO, 2 Na ₂ O, 2 MgO, .04 Zn

Silica alteration

90.



Zr immobile



Zr immobile

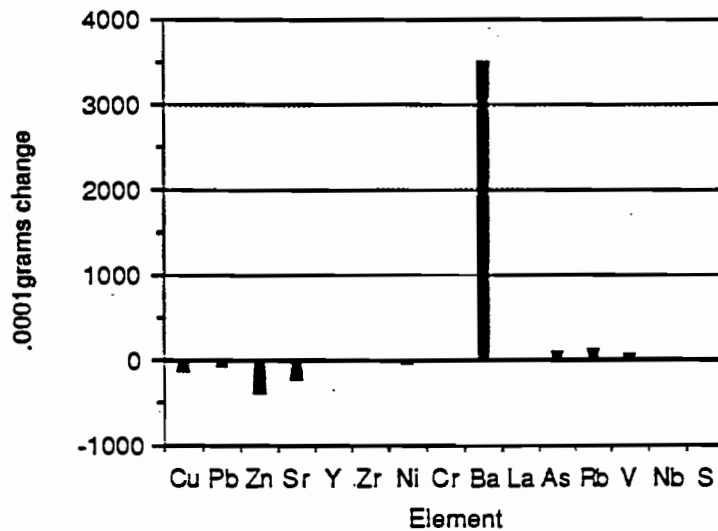


FIG. 32

Quartz barite alteration

FIGURE 32: Quartz-barite Alteration Isocon. Barium and silica are the only elements added in detectable quantities.

Sericite pyrite alteration 334065

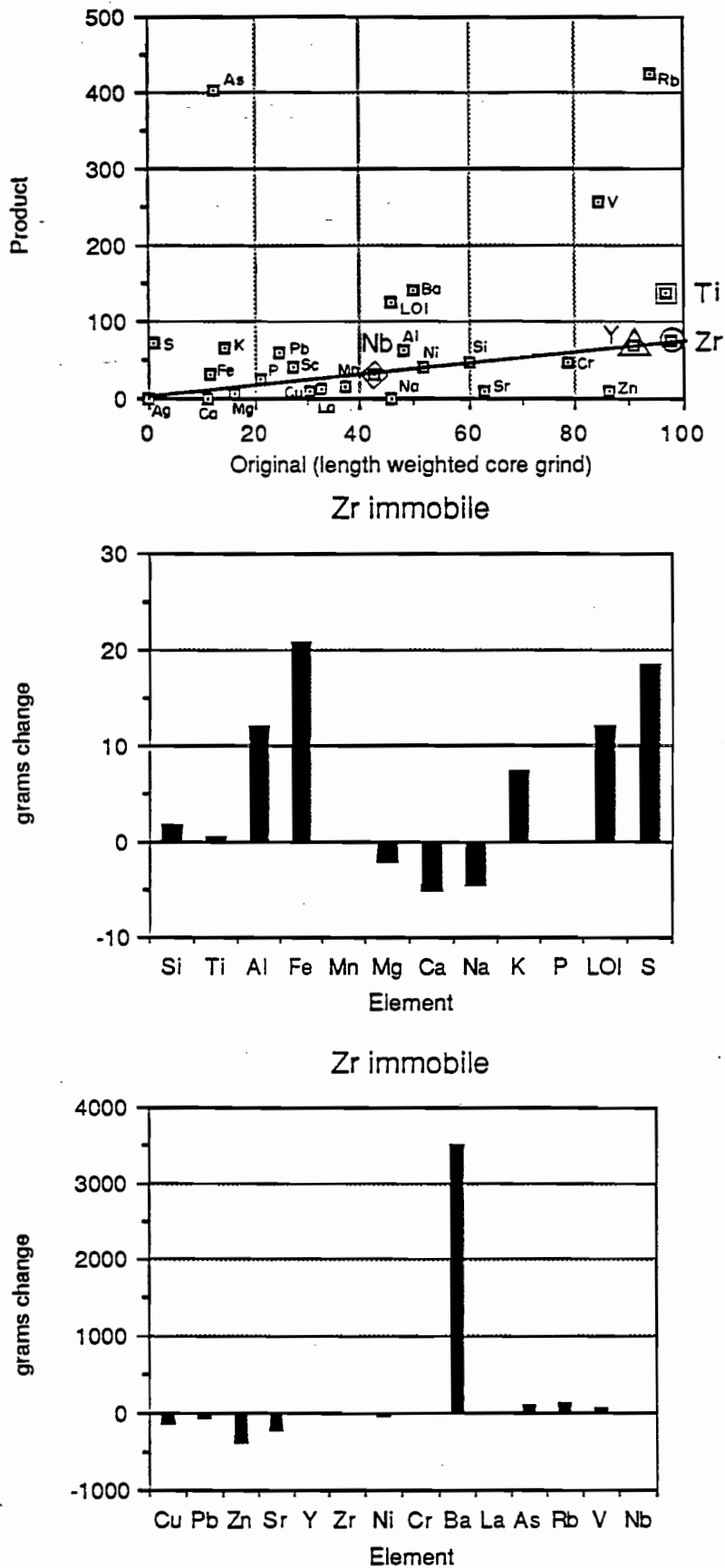


FIG. 33

FIGURE 33: Sericite-pyrite Alteration Isocon. Aluminium, iron, potassium, sulphur and barium are added. Calcium and sodium are removed.

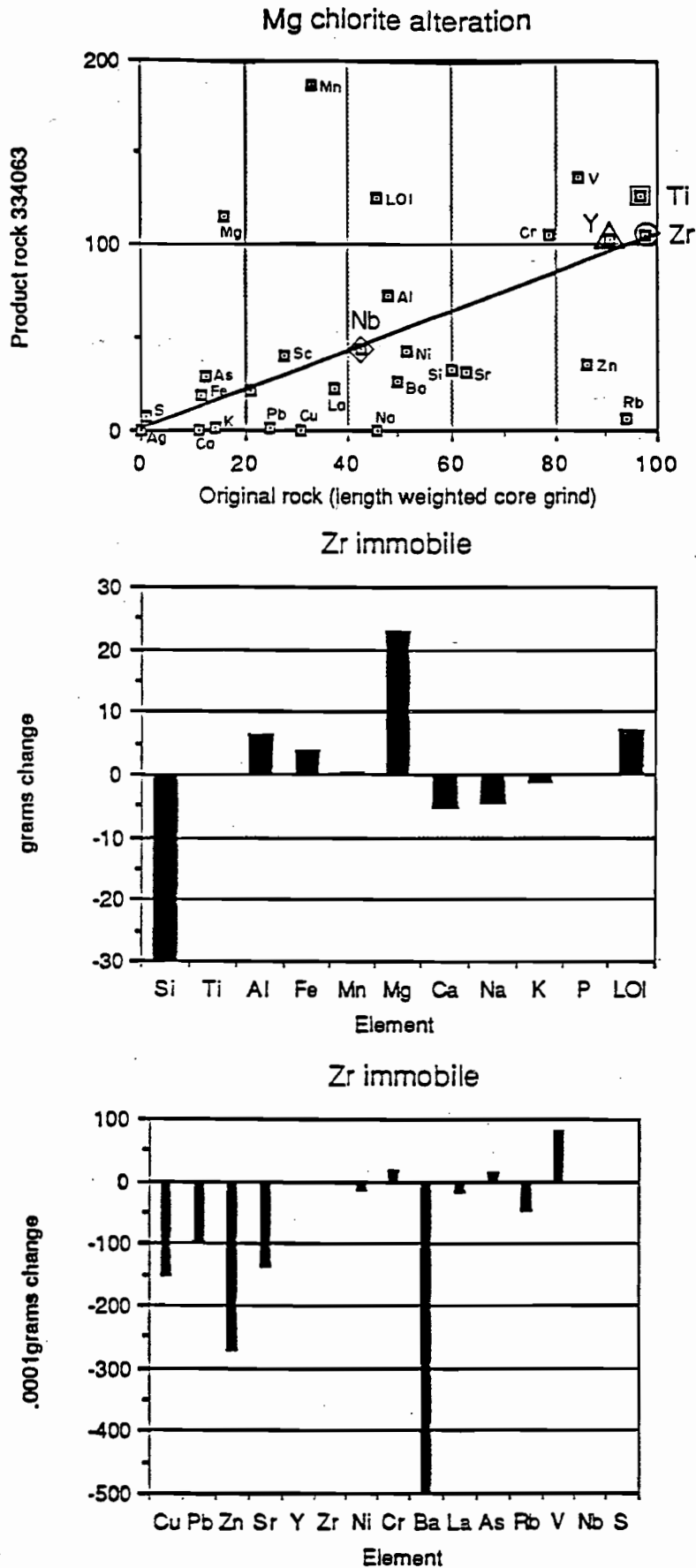
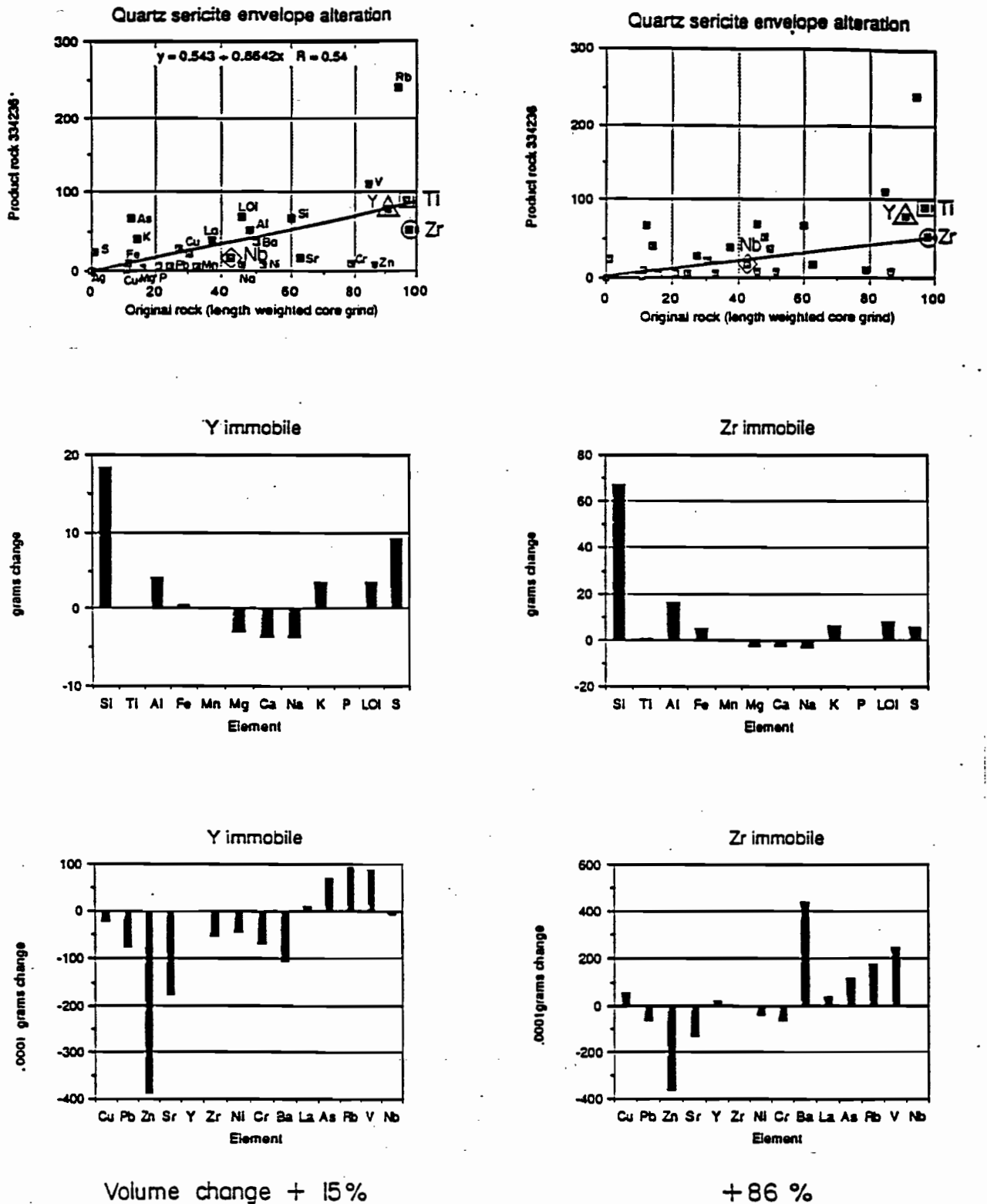


FIG. 34

FIGURE 34: Mg-chlorite Alteration Isocon. Magnesium is added while silica, barium (and copper, lead, zinc and strontium) are removed.



For total mass of elements
in parent rock 100g
Altered mass 116.5g
S.G. ratio 2.81/2.84=0.989
Volume change 0.989(1.165) - 1 = 15%

100g
188.8g
0.989
0.989(1.888) - 1 = 86%

FIG. 35

FIGURE 35: Quartz-sericite Stringer-envelope-zone Alteration Isocon. Depending on whether yttrium or zirconium are chosen as immobile elements, different volume increases and element additions are calculated.

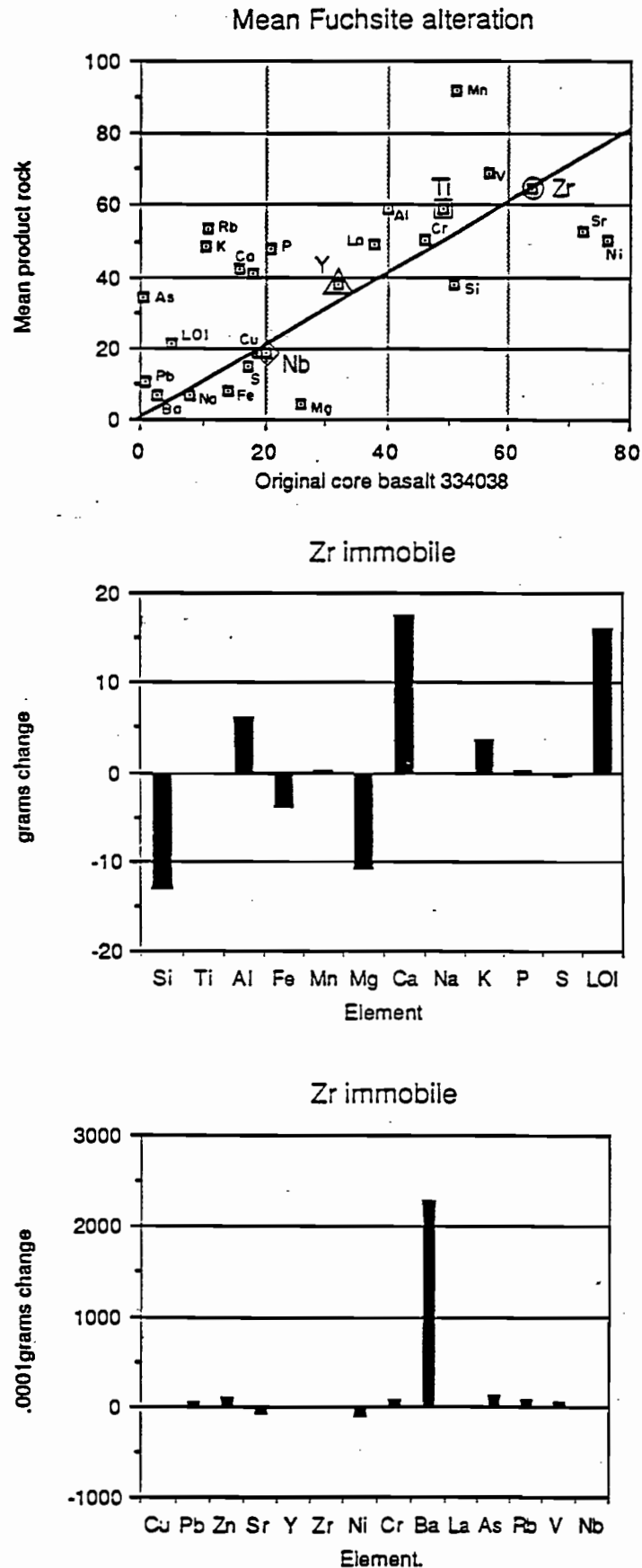


FIG. 36

Mean product rock : Mean of sample no.s 334171, 334044, 334045, 334206, 334194, 334221

FIGURE 36: Mean Fuchsite Alteration Isocon. Calcium, aluminium, potassium, carbonate and barium are added while silica and magnesium are removed.

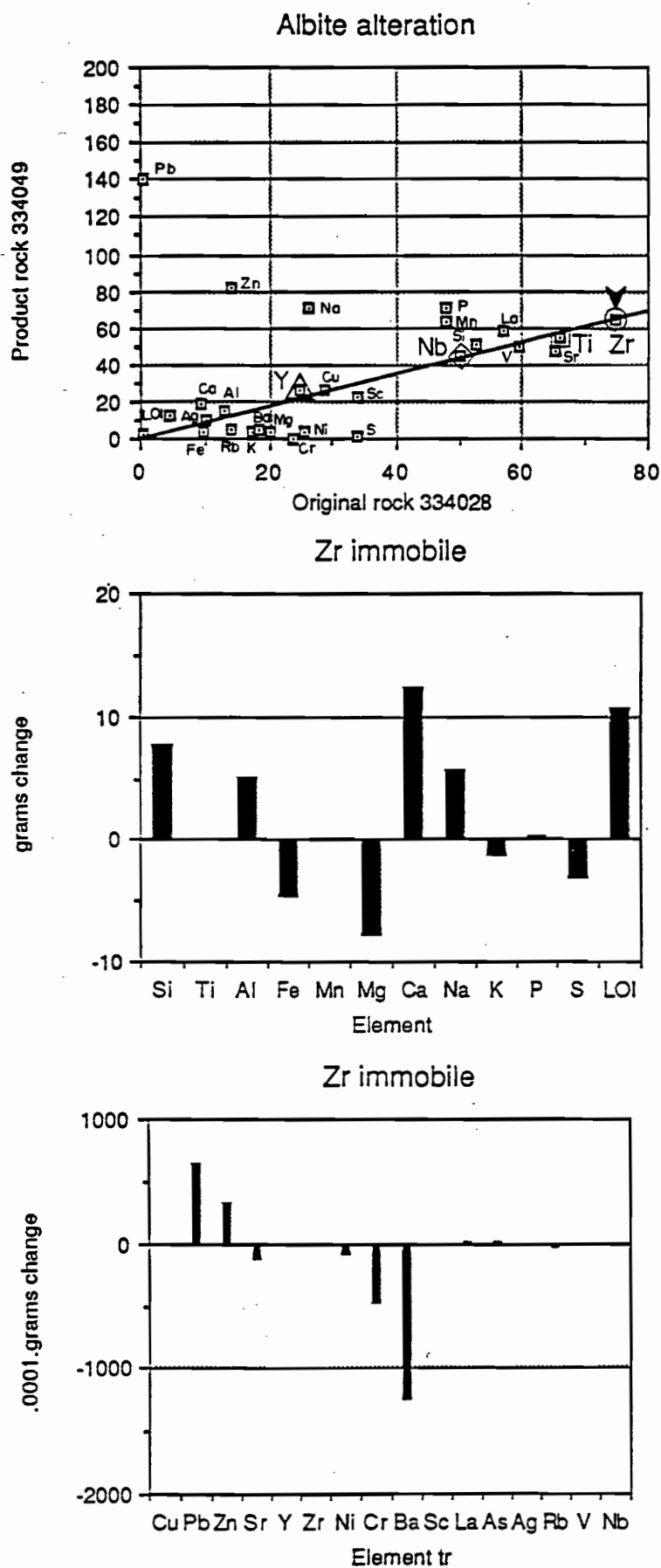


FIG. 37

FIGURE 37: Albite Alteration Isocon. Silica,aluminium, calcium, sodium and carbonate are added; iron,magnesium and barium are removed.

There is no association of base metals with any of these silicate alteration effects. Base metal (Cu, Pb, Zn) mineralisation in the footwall is concentrated in veinlets, probably formed by open space filling. Construction of isocon diagrams for these zones would therefore be meaningless.

Hangingwall alteration

In the hangingwall a mean of six calcite fuchsite altered rocks in the core basalt lava was used in the isocon plot (Figure 36). Enrichment in CaO , K_2O , Al_2O_3 and Ba and depletion in Fe_2O_3 , MgO and SiO_2 is evident. There is also relative (but only small mass) enrichment in As, Rb and Mn.

Albite alteration in the hangingwall basalt is depicted on an isocon plot in Figure 37. Besides the Na_2O enrichment, there is also some calcite and quartz alteration giving CaO and SiO_2 mass gains. There is also a small mass gain in Pb and Zn. Mass losses of Fe_2O_3 , MgO , Cr and Ba occur. Measured in percentage change CaO and SiO_2 additions are small. Pb, Zn, Na_2O , P_2O_5 and Mn show large gains.

Rare Earth Elements

REE analyses are listed in Table 3. Figures 38 and 39 depict chondrite-normalized rare-earth element patterns for rocks in the footwall stringer system. Rare-earth elements are considered to be immobile in the hangingwall, and these samples were therefore discussed in Chapter 4.

Comparison with the unaltered, Hellyer footwall-andesite parent-rock, also plotted on Figures 38 and 39, shows that the REE pattern

REE for the Hellyer Stringer Zone

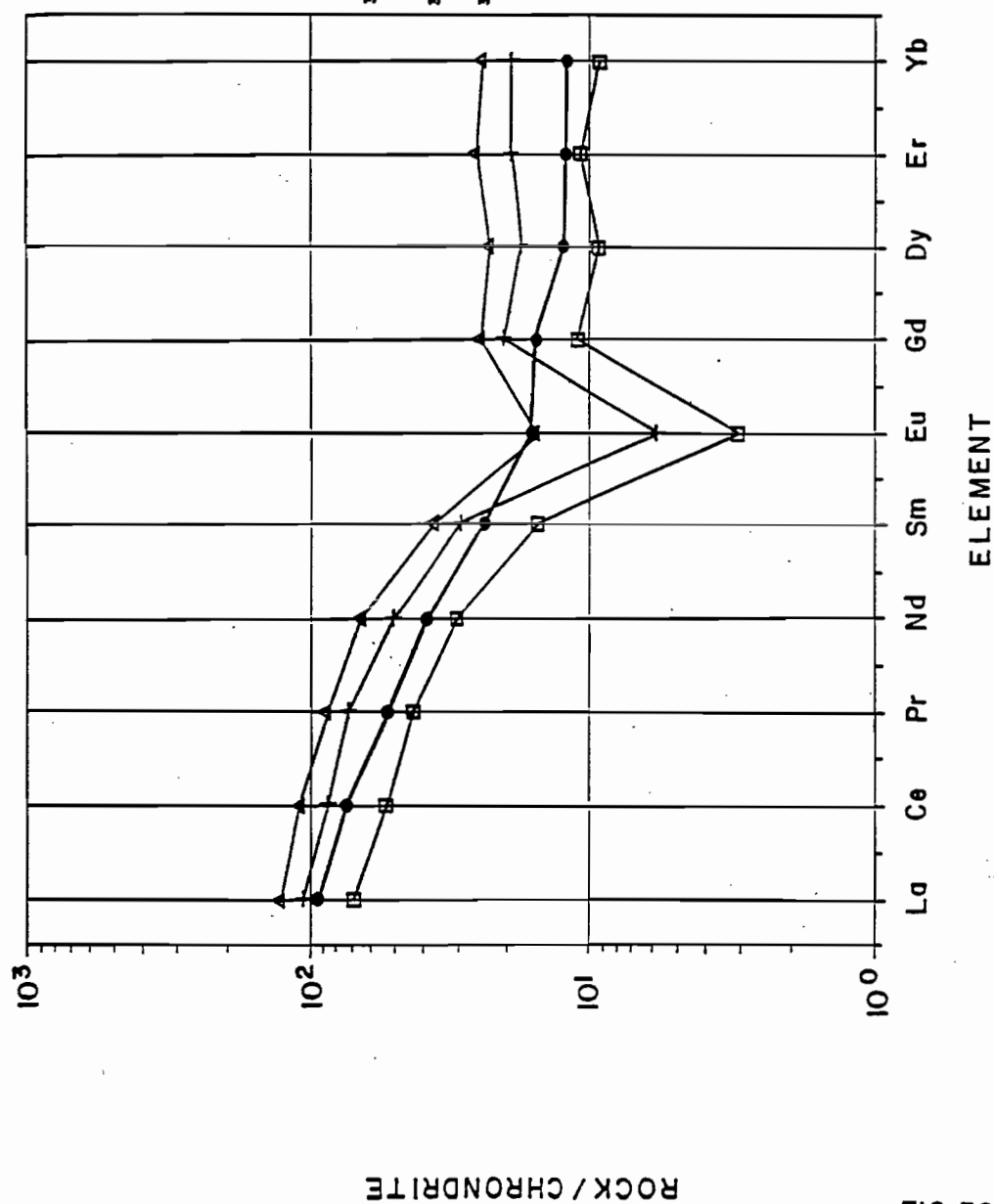


FIG.38.

FIGURE 38: Rare-earth Element Chondrite-normalized Spidergram for Stringer Zone Rocks. There is a pronounced negative europium anomaly relative to unaltered parent andesite.

REE for the Hellyer Stringer Zone

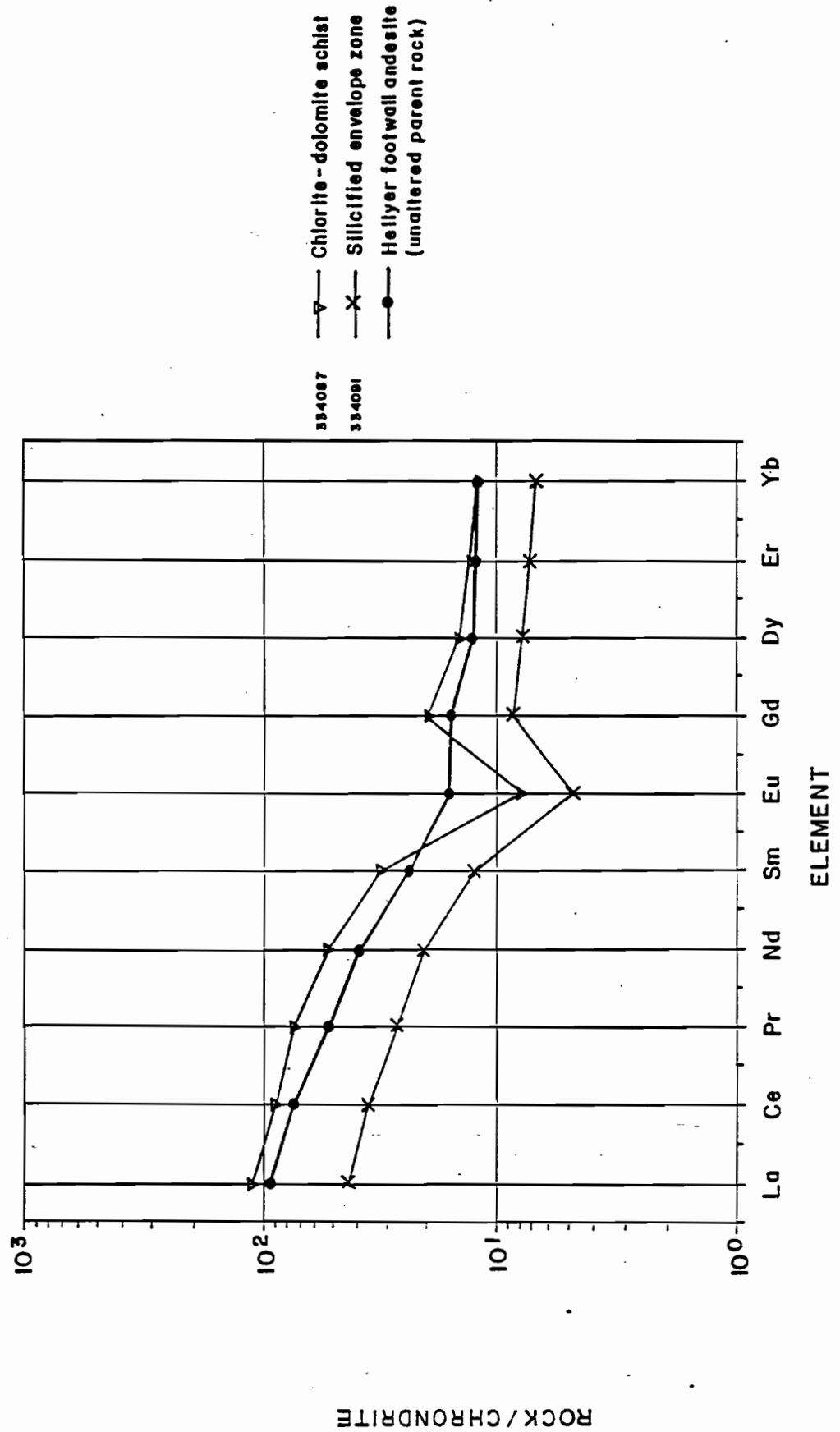


FIG.39.

FIGURE 39: Rare-earth Element Chondrite-normalized Spidergram for Stringer Zone Rocks. In addition to the negative europium anomaly, there is an overall depletion in rare-earth elements relative to unaltered parent andesite.

remains similar except for a pronounced negative Eu anomaly. This is most extreme in the silicified zones. The overall depletion in rare earth relative to the parent in the quartz altered rocks is consistent with a similar result obtained by Whitford et al. (1988) for Que River host rocks, where siliceous alteration showed a similar more extreme depletion than chloritic or phengitic stringer-zone rocks.

Whitford et al. (1988), interpreted that phengitic rocks represented a less intense, lower-temperature alteration than siliceous rocks at Que River. Chlorite-quartz zones, especially the quartz-rich rocks, similarly represent more intense, higher-temperature alteration in the core of the stringer zone at Hellyer and consequently have larger negative Eu anomalies (Figure 38), with some suggestion of overall rare earth element depletion in the siliceous zones.

Interpretation

In the footwall the major volume change calculated in Figure 35 is considered important as accommodating this sort of expansion has to have contributed to the present morphology.

The element abundances down drill hole HL55, through the hangingwall calcite-fuchsite-pyrite plume presented in Figures 40 to 43, exhibit a scattering of elements in the core lava not present in the surrounding lava. It is interpreted that a fluid emanating from the VMS mound has locally remobilized elements in the core lava to cause the variation in element abundances, but that as there is much less variation in element abundances in the later lava (see upper part of hole HL55 in Figures 40 to 43), early remobilization by hydrothermal fluids had ceased by the

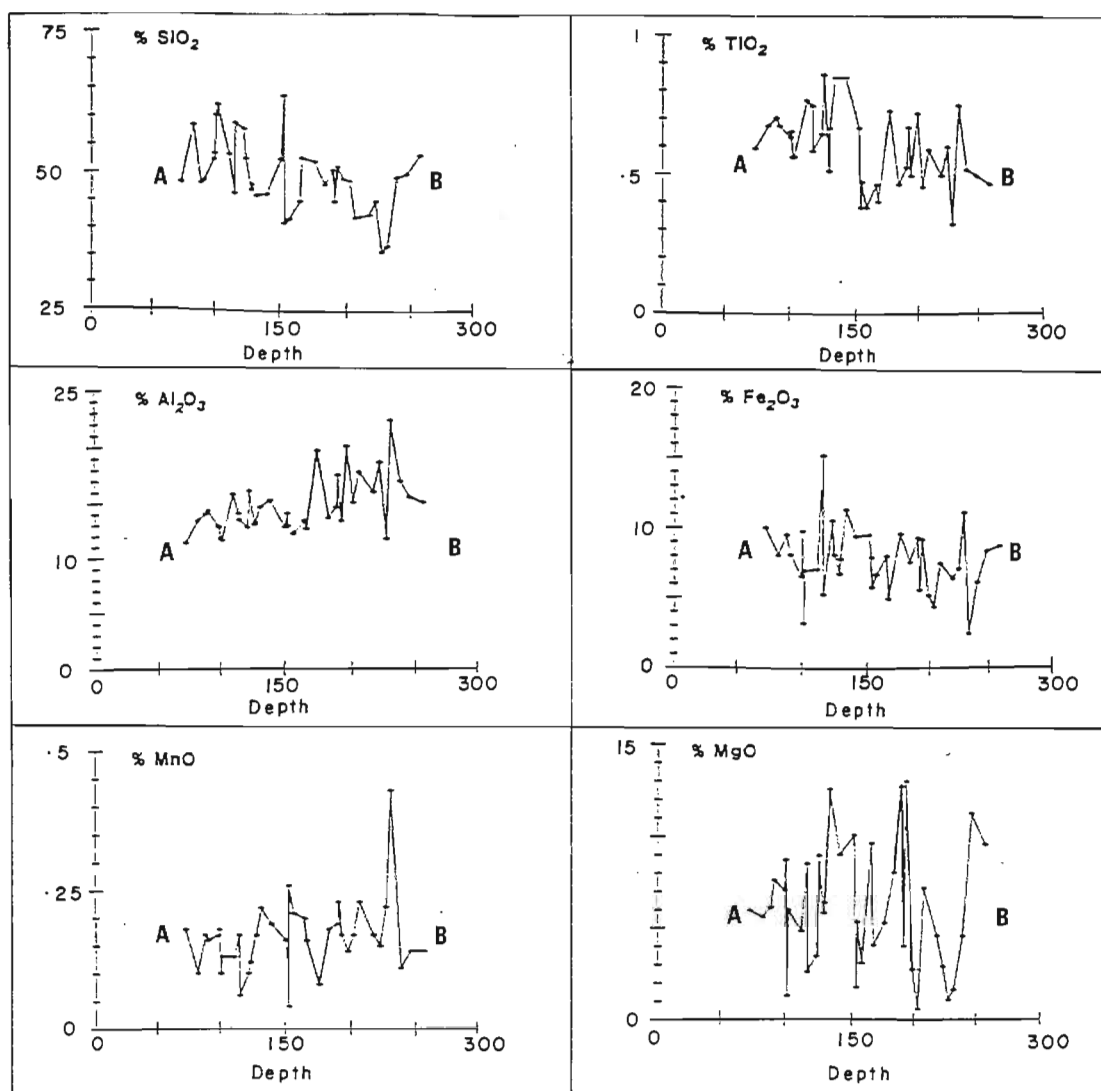
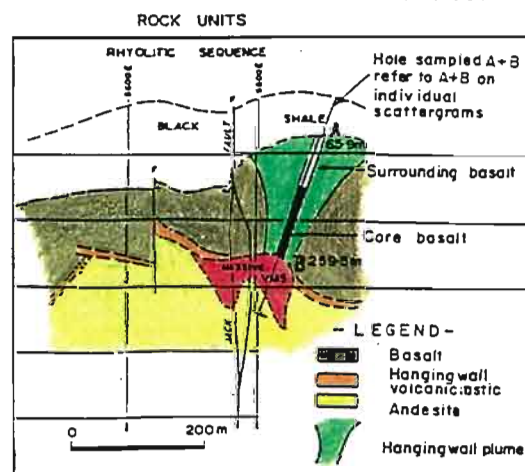


FIGURE 40 Element abundances in DDH HL55 through the calcite-fuchsite-pyrite plume - Major Elements. A and B on the graphs refer to A and B on the inset diagram below right. Note the scattering of elements in the core basalt (between 150 and 300 metres depth)

FIG. 40.



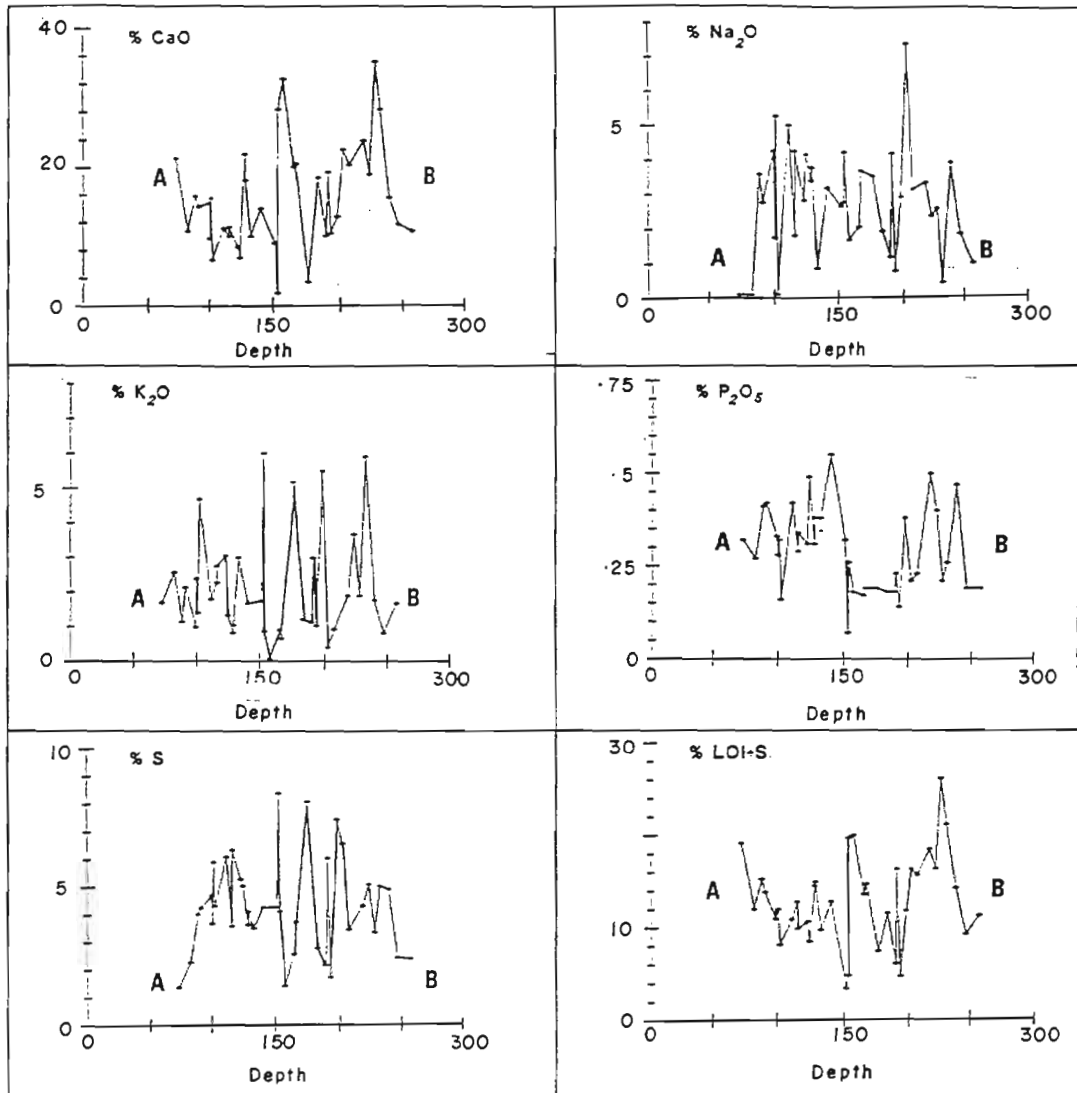
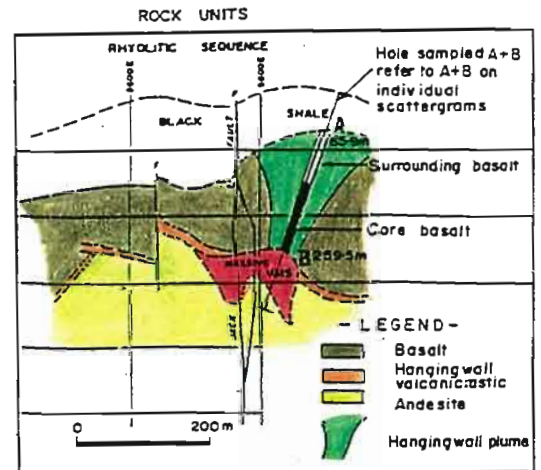


FIGURE 41 Element abundances in DDH HL55 through the calcite-fuchsite-pyrite plume - Major Elements. A and B on the graphs refer to A and B on the inset diagram below right. Note the scattering of elements in the core basalt (between 150 and 300 metres depth)

FIG.41.



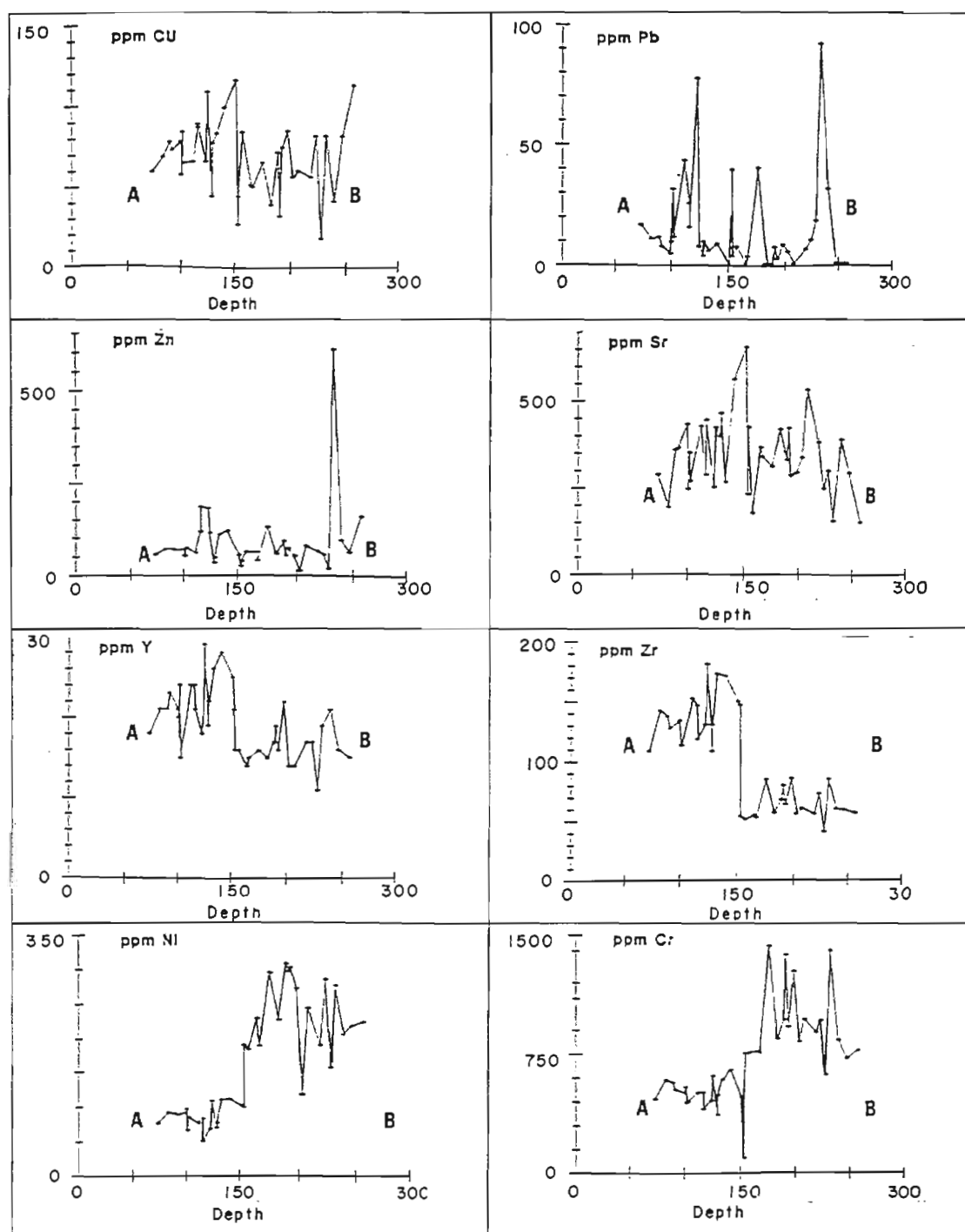
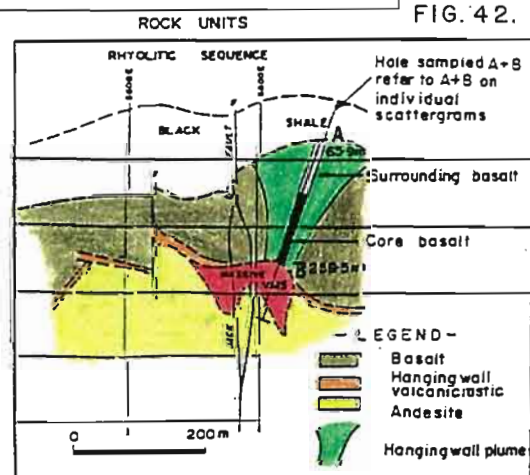


FIG. 42.

FIGURE 42 Element abundances in DDH HL55 through the calcite-fuchsite-pyrite plume - Trace Elements. A and B on the graphs refer to A and B on the inset diagram below right.
Note the scattering of elements in the core basalt (between 150 and 300 metres depth)



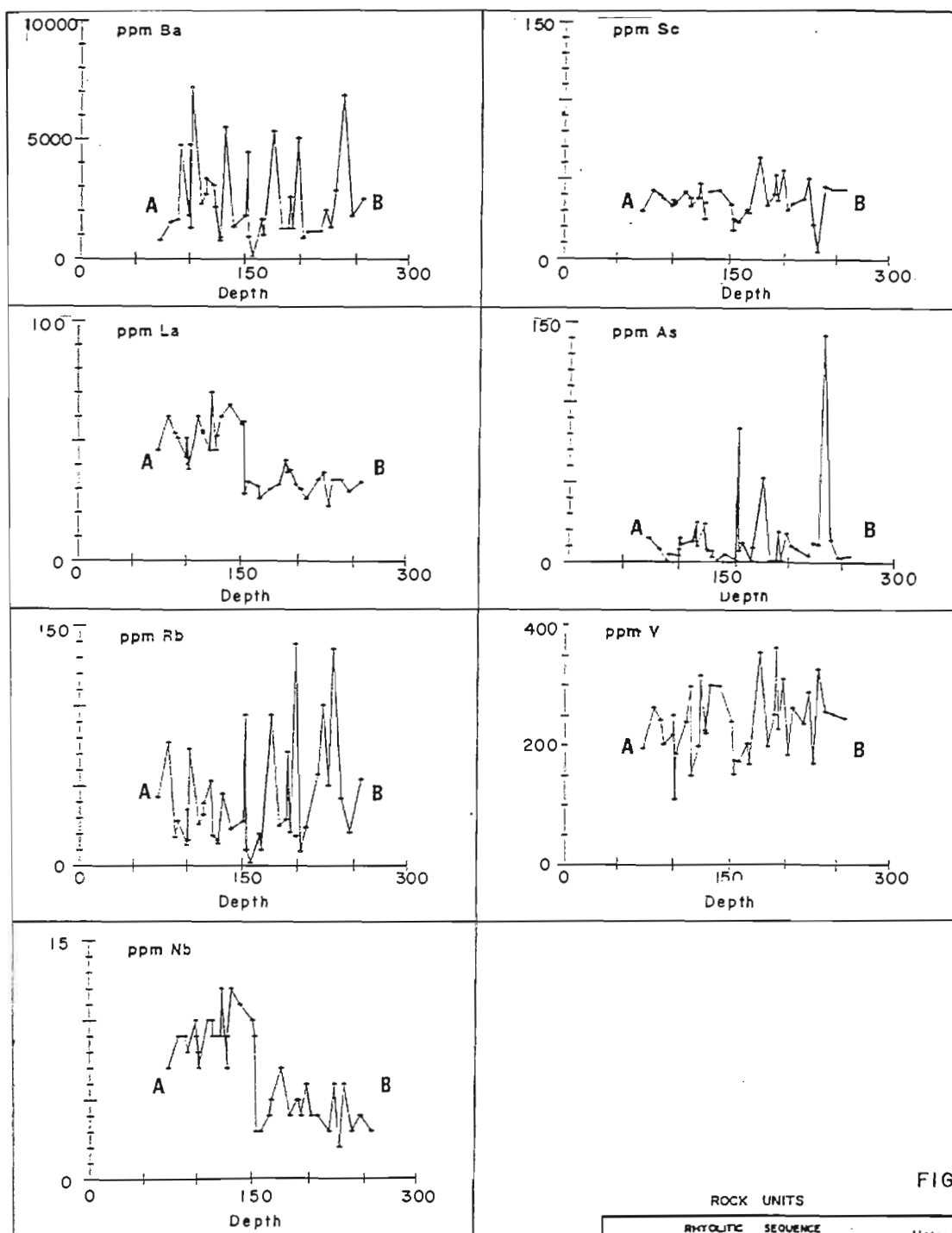
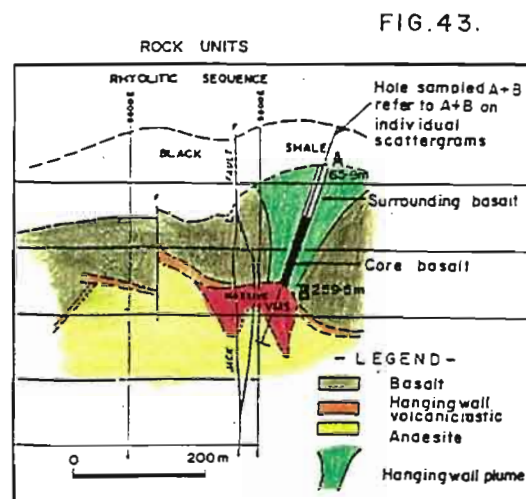


FIGURE 43 Element abundances in DDH HL55 through the calcite-fuchsite-pyrite plume - Trace Elements. A and B on the graphs refer to A and B on the inset diagram below right. Note the scattering of elements in the core basalt (between 150 and 300 metres depth)



time that the surrounding lava was extruded. Combined with the positioning of the calcite-fuchsite, sulphur-enriched plume directly above the core of the stringer zone, this is considered to be powerful evidence that the Hellyer hangingwall basalt extruded while the hydrothermal system was still active.

The evidence of calcite gangue in the ore body, and the major CaO alteration in the hangingwall, suggests that CaO has been removed from the footwall (where it is depleted) and transported through the ore body into the hangingwall (where it is now concentrated). Cation exchange, involving loss of Mg in seawater to the footwall andesite in exchange for Ca, could supply Mg for the Mg-chlorite schists and supply the Ca for the hangingwall plume. The depletion of Mg in the hangingwall provides a further possible source for Mg in the Mg-chlorite schists.

Mineral Chemistry

Micas

Microprobe data on the micas in the hangingwall plume are tabulated in Table 6. XRD scans of highly fuchsite-altered rocks indicate that both 2M and 1M polytypes are present. The low Cr levels confirm the findings of Whitford and Creelman (1984), who obtained similar low levels for many micas at Que River. Only bright fuchsite-feldspar pseudomorphs contain percentage level of Cr. Whitford and Creelman (1984) advocate the use of the term phengite for the micas at Que River. However, they recognise problems with the present terminology of Cr-micas. Illites have an idealized structural formula as shown in Table 7 from Deer et al. (1966).

TABLE 6 Mica Microprobe Analyses

Rock No.	Description	SiO ₂	TiO ₂	Al ₂ O ₃	V ₂ O ₃	Cr ₂ O ₃	FeO	MgO	CaO	Na ₂ O	K ₂ O	Sum
334171	Calcite	44.9	0.5	31.2	0.2	0.5	0.9	1.0	4.5		9.9	93.7
	Fuchsite	47.0	0.6	33.4		0.4	1.3	1.3	0.2		10.0	94.2
	Altered	49.1	0.5	35.1	0.2	0.7	0.9	1.2			10.5	98.1
	Hangingwall	47.7	0.5	34.2	0.2	0.9	0.9	1.1			10.6	96.0
	core basalt	47.8	0.3	32.0		0.3	1.0	1.2	0.2	0.2	8.7	91.6
		48.0	1.0	29.0		0.3	1.1	1.1	0.5		8.5	89.4
		40.7	0.6	31.7	0.2	0.2	1.1	1.2	3.6		9.1	88.3
		45.4	0.3	31.2	0.2		0.9	1.2	0.3	0.2	8.7	88.3
		50.4	0.2	33.3			1.0	1.2	0.2		8.9	95.2
		48.5	0.7	34.0	0.2		1.2	1.4	1.2		10.8	97.9
		47.9	0.5	33.2		0.2	1.1	1.3	0.2		9.5	93.9
		51.0	0.6	35.2	0.2	0.2	1.0	1.3	0.2		9.8	99.5
		49.7	0.5	33.9			1.2	1.3	0.3		10.1	97.0
	adjacent to chromite	50.2	0.7	31.3	0.2	0.8	1.2	1.2	0.2		9.9	95.8
	1mm from chromite	48.6	0.7	31.7	0.2	1.0	1.3	1.3	0.2		10.0	95.1
	3mm from chromite	46.0	0.7	32.1		0.7	1.4	1.1	0.2		10.4	92.6
334051	Hangingwall	45.2	0.4	33.4			1.1	0.6			10.1	90.8
	ash	46.3	0.2	32.0			1.8	1.3			10.2	91.8
	volcani-	45.5	0.3	30.0			3.3	2.2	0.2		9.9	91.4
	clastic	46.1	0.3	32.0			1.7	1.3			10.3	91.8
		48.6	0.4	24.5	0.2		3.8	2.2	0.2		8.1	87.9
334230	Stringer	51.9		30.5			0.3	2.5	0.3		9.3	94.7

TABLE 7 Variations in Illite Composition with Reference to Muscovite

	X	[Y] ^a	[Z] ^a	(OH) ⁻	(O) ⁻²
1. Muscovite	K ₂	Al ₄	Si ₆ Al ₂	4	20
2. (a) Hydro-	[K, (H ₃ O) ⁺] ₂	Al ₄	Si ₆ Al ₂	4	20
(b) muscovite	K _{2-x}	Al ₄	Si ₆ Al ₂	4+x	20-x
3. Illite	K _{2-x}	Al ₄	Si _{6+x} Al _{2-x}	4	20
4. Phengite	K ₂	Al _{4-x} (Mg, Fe ⁺²) _x	Si _{6+x} Al _{2-x}	4	20

Z = tetrahedral site Y = octahedral site
after Deer et al. (1966).

Phengites have Si to Al ratio >3:1 in the tetrahedral sites. Fe and Mg maintain charge balance by substituting in the octahedral sites. Hellyer tetrahedral Si:Al ratios range from 2.85:1 to 5.15:1 (mean 4.01:1). Whitford and Creelman (1984) analysed phengites at Que River and these data have a mean of 5.24:1.

The K₂O content in the fuchsite at Hellyer is less than the theoretical limit of 2, and similar low K₂O values lead to the use of the term hydro-muscovite-illite at Que River (van de Boom and Washausen, 1980). As pointed out by Whitford and Creelman (1984), the decrease in K₂O is not matched by an increase in H₂O content. In this thesis, the term fuchsite is used throughout for mica that is light-chrome green macroscopically.

Offler et al. (1987), differentiate metamorphic and hydrothermal mica. Mica is considered by them to be hydrothermal if it shows no preferred orientation and is colourless, and metamorphic if it is foliated and wraps around minerals of hydrothermal origin. Samples in the hangingwall used in this study are not foliated, but are often colourless in thin section. Their concentration in the hangingwall plume without prominent schistosity suggests that they are hydrothermal.

Microprobe data on micas in the hangingwall volcanoclastic rocks, and a single analysis in the footwall envelope zone, are tabulated in Table 6. The consistently lower TiO_2 in the micas (0.33% TiO_2 n=6) from the hangingwall tuff compared with the fuchsite (0.54% TiO_2 n=16), in the hangingwall plume and the absence of Cr in any of the mica samples from the hangingwall tuff and footwall are the most notable differences.

Chlorite

Microprobe data on chlorites are tabulated in Table 8. Chlorites in the hangingwall basalt may be either Fe or Mg rich. All chlorites in the hangingwall volcanoclastic rocks are Fe rich. Massive chlorite schists in the stringer zone are Mg rich, whereas chlorites from the footwall lavas outside the stringer zone are Fe rich.

Chromite

Microprobe data for chromite are presented in the section on primary chemistry. The chromites are unzoned, with similar Cr levels obtained along traverses from the centre of grains to the edge (Table 2). Cr in the fuchsites is not thought to originate from the chromite. The resistate character of the chromites, with euhedral grains preserved in calcite-fuchsite altered lavas supports this conclusion. Cr-rich augites which are readily pseudomorphed by calcite or quartz are a more likely source of the Cr in fuchsite.

Carbonate

Carbonate analysed in the fuchsite-calcite altered plume is exclusively calcite, and selected analyses are presented in Table 8. All carbonate analysed in the hangingwall volcanoclastic is also

calcite. No systematic study of the carbonate in the footwall was undertaken. No carbonate samples microprobed in the footwall were calcite. The carbonate in the Mg-chlorite schists are all dolomite.

Table 8 also contains selected analyses of albite in the footwall lavas, and of titanite in the hangingwall basalt.

TABLE 8 Chlorite Carbonate Albite Apatite and Titanite Microprobe Analyses

Rock No.	Description	Mineral	SiO ₂	TiO ₂	Al ₂ O ₃	Cr ₂ O ₃	V ₂ O ₃	FeO	MnO	MgO	CaO	Na ₂ O	K ₂ O	P ₂ O ₅	NiO	SO ₃	Cl	Sum
334051	Hangingwall bedded ash volcaniclastic	Calcite						1.1 0.5	1.4 1.3	0.5	54.8 51.1				0.3			58.1 53.0
334171A	Extreme calcite fuchsite altered hangingwall basalt	Calcite 7 microns from nearest chromite	3.8		3.1	1.6		1.3	0.7	0.4	52.0				0.4			64.1
334020	Edge of pillow - hangingwall basalt	Titanite	31.8 31.5	28.0 28.7	6.3 6.9	0.3 0.3		1.7 0.5			30.3 30.2		0.1 0.1	0.2 0.2		0.2		98.9 98.3
334051	Hangingwall bedded ash volcaniclastic	Apatite	0.6		0.4			0.7		0.2	52.5		0.2	39.3			0.5	94.4
334063	Chlorite pyrite schist in stringer zone	Chlorite	25.9 27.6 27.0		19.9 20.5 20.7			7.7 7.7 3.7 4.8	0.5 0.4 0.5	24.6 26.3 26.7	0.3 0.1					0.4	0.1	79.6 82.7 83.8
334089			28.5 26.9		21.7 21.1			9.8 16.2	0.6 0.5	27.0 23.0							0.5	65.8 87.8
334083	Footwall albite porphyritic andesite	Chlorite	26.7 25.8		19.4 17.7			24.4 0.9 23.1	0.4 0.5	17.1 16.3								88.0 84.3
334254		Chlorite	27.3		18.6			25.3	0.9	16.7								88.8
334051	Hangingwall bedded ash volcaniclastic. Alteration of glass shards	Chlorite	25.0 30.4 25.9 24.9 28.5 28.0 25.5		20.6 22.7 20.2 19.9 20.9 20.8 18.1			25.8 29.7 27.5 26.4 21.5 26.8 25.9		13.6 14.4 13.4 14.0 14.4 17.8 14.7			0.3 0.6 0.5					85.3 98.4 87.5 85.3 86.2 93.7
334038	Hangingwall core basalt	Chlorite	32.2 31.7 31.3		16.2 15.8 16.1			15.5 15.3 15.3	0.3 0.2	23.7 23.7 23.1	0.4 0.4 0.4							88.3 87.2 86.2
338024	Hangingwall basalt	Chlorite	28.7		23.2			17.4		20.2								89.5
338045	Interpillow hangingwall basalt	Chlorite	27.6 27.4		22.1 22.4			24.4 25.2	0.4 0.6	12.2 13.2			0.7 0.4					87.4 89.1
338045	Hangingwall core basalt	Albite	63.5		18.9			1.6		0.7	0.2	9.6						94.5
334083	Footwall albite porphyritic andesite	Albite	69.0 68.5		20.4 20.1						0.4 0.3	10.9 10.9	0.1				0.1	100.8 99.7

Comparison with other Volcanogenic Massive Sulphide Alteration

Like the Kuroko deposits (Date et al., 1979, Urabe et al., 1983), Hellyer has been subjected to low grades of metamorphism and minimal structural overprint. The prominent stringer zone directly below Hellyer is also characteristic of the Kuroko and Noranda Deposits (e.g. Franklin et al., 1981). However, Hellyer is unusual in that the stringer system is wider in cross section than the massive sulphide body above. The zoning within the stringer zone differs from the Kuroko and other Zn-Pb-Cu deposits, such as those interpreted from the metamorphic assemblages in the Noranda district, in that Hellyer has a silica-rich core surrounded by chlorite and then by sericite. Kuroko (e.g. Shirozu, 1974; Date et al., 1983) and Noranda (e.g. Riverin and Hodgson, 1980) deposits have a sericitic inner zone grading outwards into chlorite. The barite at the top of the silica core at Hellyer is also atypical. No montmorillonite clays or zeolites, such as have been described for the Kuroko deposits, (e.g. Date et al., 1983), occur at Hellyer. The Hellyer hydrothermal alteration is carbonate rich. Other CO₂-rich systems include the Archean Mattabi copper-zinc deposit (Franklin et al., 1975). There, high carbonate content occurs in the footwall in dolomite and siderite. No larger scale, semiconformable, regional alteration zone occurs below Hellyer, as has been described in the Precambrian Shield of Canada (e.g. Descarreaux, 1973, Franklin et al., 1975; Spooner and Fyfe, 1973).

Hellyer is noteworthy in that there is a clearly defined zone of hangingwall alteration in the basalt above the ore body. Other deposits

that have hangingwall alteration include some Kuroko deposits (Franklin et al., 1981; Shirozu, 1974), but this alteration is the same as that in the footwall whereas at Hellyer there is a unique calcite-fuchsite phase and an isotopically distinctive interpillow pyrite that is developed only in the hangingwall and not in the footwall. Pervasive albite alteration in the hangingwall at Hellyer, is contrasted with regional 'spilitization' that has been described in Cyprus deposits (Constantinou, 1980), or at Garon Lake in the Canadian Archaean (MacGeehan, 1978). Regional metamorphic albitization of plagioclase that occurs throughout the Mount Read Volcanics, but especially in the Hellyer andesites and basalts, may be more analagous to the Cyprus and Garon Lake 'spilitization'.

The Amulet lower A deposit at Noranda (e.g. Knuckley et al., 1982), like Hellyer, is in a mafic volcanic package and also has an altered hangingwall but, like the Kuroko deposits, alteration in the hangingwall (dalmatianite) is similar to that in the footwall.

Geochemically, Hellyer has the same depletion in Na_2O , CaO , Sr in the footwall that has been described in the Kuroko (Date et al., 1983; Hashigushi et al., 1983) and Noranda deposits (Riverin and Hodgson, 1980; Roberts and Reardon, 1978). Pervasive and widespread depletion in CaO and Sr with more focussed Na_2O depletion in the stringer pipe at Hellyer contrasts with many Noranda and Kuroko district deposits where Na_2O depletion in the footwall is regional (Noranda), or several times wider than the ore bodies (Kuroko). Eastoe et al. (1987), recognise a district-wide zonation in Tasmania in the Central Volcanic Complex

between sodic + calcic versus non-sodic, non-calcic assemblages in felsic volcanics. Na_2O depletion is broader than in the Kuroko deposits. Sericitic alteration in post-ore volcanics is recognised, but this does not have the associated calcite and albite alteration that occurs at Hellyer. Minor barite and pyrite replacing haematite distinguish the hangingwall alteration and Prince Lyell from the footwall (Walshe and Solomon, 1981). Chalcopyrite is abundant in both the footwall and hangingwall. Green et al. (1981), note a marked depletion in Na and Sr and enrichment in Rb, K, Mg, Mn and H_2O in the footwall pyroclastics under Rosebery, but the alteration in the host rock grades into the footwall (Brathwaite, 1974; Naschwitz, 1985), and there is no distinct hangingwall alteration as at Hellyer. At Que River, the development of a strong footwall stringer zone and hangingwall calcite-fuchsite alteration, especially in basaltic lava fragments under the hangingwall dacite wedge, is broadly analagous to the alteration at Hellyer.

CHAPTER 6 SULPHUR ISOTOPES

Introduction

Sulphur isotopes, mostly in pyrite, were examined at Hellyer to test for relationships between the alteration in the host rocks and the sulphur isotopic signature. The orebody was also sampled as a basis for comparison. Sulphur isotopic signatures in mineral deposits can provide valuable information about the chemistry of formation of the deposit and also about the source of sulphur (Ohmoto and Rye, 1979). In practice, problems in determining whether mineral pairs have co-precipitated in equilibrium can lead to ambiguous interpretations, especially if the data show a spread of $\delta^{34}\text{S}$ values (Ohmoto and Rye, 1979).

Interpretation needs support from other isotopic studies, fluid inclusion studies and careful observations on the mode of occurrence of the minerals both in handspecimen and microscopically. At Hellyer however, a systematically variable set of sulphur isotope results was obtained which allows for a relatively straightforward interpretation of the data.

Results

Isotopic analyses at Hellyer are presented in Table 9 and displayed on Figure 44. Analyses were done at the Central Science Laboratory, University of Tasmania, by Richie Woolley, and at the University of Queensland by Dr. Sue Golding. Fifty-nine samples, mostly of pyrite, were analysed, one in Que River black shale, twenty-three in Hellyer hangingwall basalt, two in the hangingwall volcanoclastic rocks at the ore position, nine in the massive VMS, seven at the VMS base and top of the stringer zone, ten in the stringer zone and five in the footwall lavas.

TABLE 9 SULPHUR ISOTOPE DATAQUE RIVER SHALE

<u>Sample No.</u>	<u>Hole</u>	<u>Depth</u>	<u>Rock Description</u>	<u>Sample Description</u>	<u>Location</u>	<u>S³⁴_p permil</u>
2	HL28	73.45m	Pyritic bedded black shale	Pyrite	Hangingwall	+15.7

BASALT LAVA-CLOSE TO JACK FAULT (excluding interpillow samples)

<u>Sample No.</u>	<u>Hole</u>	<u>Depth</u>	<u>Rock Description</u>	<u>Sample Description</u>	<u>Location</u>	<u>S³⁴_p permil</u>
3	HL28	146.44m	Basalt. Carbonate veined. Adjacent to strongly albitized rock.	Pyrite-coarse recrystallised.	Hangingwall	+16.1
CSIRO 1	1983 surface sample 10700N.		Basalt.	Pyrite	Hangingwall	+9.1

INTER-PILLOW BASALT

<u>Sample No.</u>	<u>Hole</u>	<u>Depth</u>	<u>Rock Description</u>	<u>Sample Description</u>	<u>Location</u>	<u>S³⁴_p permil</u>
12	HL31	242.7	Basalt. Pyrite with interpillow chert.	Pyrite	Hangingwall east of plume.	-14.6
29	HL5	153.7m	Basalt. Pyritized cherty interpillow area with cross cutting brown sphalerite-carbonate veinlet.	Pyrite	Hangingwall west of Jack fault.	-14.5
30	HL5	153.7m	Basalt. Pyritized cherty interpillow area with cross cutting brown sphalerite-carbonate veinlet.	Coarse brown sphalerite veinlet.	Hangingwall west of Jack fault.	-13.2
24	HL3	149.0m	Basalt. K feldspar altered brecciated area.	Pyrite	Hangingwall west of Jack fault.	-14.0
HELL1 333994	Adit 851 Metres from portal		Basalt. Highly pyritic interpillow area major K feldspar alteration.	Pyrite	Hangingwall east of Hellyer	-13.5

INTER-PILLOW BASALT IN HANGINGWALL PLUME

<u>Sample No.</u>	<u>Hole</u>	<u>Depth</u>	<u>Rock Description</u>	<u>Sample Description</u>	<u>Location</u>	<u>S³⁴_p permil</u>
4	HL28	171.3m	Basalt. Inter-pillow pyritized chert. Carbonate veining.	Pyrite	Hangingwall close to Jack fault. Core lava.	-13.8
5	HL28	232.5	Inter-pillow basalt, intensely fuchsite calcite altered. K feldspar alteration.	Pyrite	Hangingwall. Core lava.	-9.6
7	HL50	293.1	Inter-pillow Basalt. Abundant calcite but only minor fuchsite.	Pyrite	Hangingwall close to Jack fault.	-12.4
55 334029	HL55		Basalt. Cherty inter-pillow area.	Pyrite	Hangingwall. Core lava.	-16.2, -16.4
57 334034	HL55		Basalt - vesicular. Cherty area is possible inter-pillow area.	Pyrite	Hangingwall. Core lava.	-15.5

HANGINGWALL PLUME BASALT

<u>Sample No.</u>	<u>Hole</u>	<u>Depth</u>	<u>Rock Description</u>	<u>Sample Description</u>	<u>Location</u>	<u>S³⁴ permil</u>
53 334020	HL55		Basalt. Pyrite in intensely chlorite altered inter-fragment area. (vein?).	Pyrite	Hangingwall. Core lava.	+8.8
54 334022	HL55		Basalt. Albite-quartz alteration.	Pyrite	Hangingwall. Core lava.	+9.8
56 334031	HL55		Basalt. Extreme calcite veining - alteration.	Pyrite	Hangingwall. Core lava.	-0.3
58 334040	HL55		Basalt. Extreme calcite alteration.	Pyrite	Hangingwall. Core lava.	+3.0
59 334044	HL55		Basalt. Extreme calcite fuchsite alteration.	Pyrite	Hangingwall. Core lava.	+0.3
6	HL28	239.45m	Basalt - intense fuchsite and carbonate veining.	Pyrite	Hangingwall. Core lava.	-1.8
26	Surface 10700N 5750E.		Massive white barite	Barite	Hangingwall. Core lava.	+28.8

BASALT - QUE RIVER SHALE CONTACT

<u>Sample No.</u>	<u>Hole</u>	<u>Depth</u>	<u>Rock Description</u>	<u>Sample Description</u>	<u>Location</u>	<u>S³⁴ permil</u>
1	HL5	88.9M	Basalt.	Pyrite	Hangingwall. West of Hellyer.	-7.9

HANGINGWALL BASALT

9	HL31	143.95m	Basalt. Intensely chlorite altered fragments in carbonate rich matrix. Pyrite rims chloritized lava fragments.	Pyrite	Hangingwall. East of Hellyer.	+1.4
75 HELL 2A 333995	ADIT	823m from portal	Basalt. Centre of pillow.	Pyrite	Hangingwall. East of Hellyer.	+4.9
76 HELL 5 333998	ADIT	790m from portal	Basalt. Pyrite, carbonate altered.	Pyrite	Hangingwall. East of Hellyer.	+1.2

BARREN ORE POSITION. HANGINGWALL VOLCANICLASTIC

8	HL50.	299.95m	Polymict poorly sorted breccia.	Pyrite	Above VMS close to Jack Fault.	+31.3
13	HL31	342.25m	Polymict poorly sorted breccia.	Pyrite	East of Hellyer.	+6.3

VOLCANOGENIC MASSIVE SULPHIDE

<u>Sample No.</u>	<u>Hole</u>	<u>Depth</u>	<u>Rock Description</u>	<u>Sample Description</u>	<u>Location</u>	<u>S³⁴ permil</u>
27 325755	HL75	250.1	Grey massive barite	Barite	Barite zone ore body hangingwall.	+42.1
	HL29	195.0	Grey massive barite	Barite	Barite zone ore body hangingwall.	+42.9
	HL29	195.0	Sphalerite with barite	Sphalerite	Barite zone ore body hangingwall.	+7.1
	HL29	214.0	Barite	Barite	Barite in massive VMS West of Jack Fault south of ore body 10500N.	+40.4
	HL29	214.0	Pyrite with barite	Pyrite	Barite zone in massive VMS West of Jack fault south of ore body 10500N.	+8.0
28	HL55a	268.9	Banded sphalerite galena pyrite.	Pyrite	Hangingwall enriched zone.	+7.1
31	HL55a	268.9	Banded sphalerite galena pyrite.	Brown sphalerite	Hangingwall enriched zone.	+6.3
23	HL75	262.9	Banded sphalerite galena pyrite	Pyrite	Hangingwall enriched zone.	+7.5
32 325773	HL75	267.9	Massive fine-grained VMS.	Fine-grained pyrite	Central Ore body	+7.2
33 326773	HL75	267.9	Recrystallized brown sphalerite.	Sphalerite	Central orebody.	+7.0

VOLCANOGENIC MASSIVE SULPHIDE BASE AND UPPER STRINGER ZONE

<u>Sample No.</u>	<u>Hole</u>	<u>Depth</u>	<u>Rock Description</u>	<u>Sample Description</u>	<u>Location</u>	<u>S³⁴ permil</u>
15	HL39	241.1	Coarse recrystallized "grainy" pyrite.	Pyrite	Base of orebody	+8.6
22	HL55A	315.9	"Grainy" pyrite in massive VMS.	Pyrite	Base of orebody	+10.6
34	HL55A	319.9	"Grainy" recrystallized pyrite in chalcopyrite rich VMS.	Pyrite (some chalcopyrite?)	Base of orebody	+7.8
68	HL29	282.5	Chalcopyrite, pyrite rock	Pyrite	Hellyer upper stringer zone - chalcopyrite, pyrite zone.	+7.8
69	HL29	282.5	Chalcopyrite, pyrite rock	Chalcopyrite	Hellyer upper stringer zone - chalcopyrite, pyrite zone.	+7.9
21 258007	HL6	399.3	Chalcopyrite, pyrite rock	Pyrite	Hellyer upper stringer zone - chalcopyrite, pyrite zone.	+7.7
25	Footwall Development		Massive grey barite	Barite	Hellyer upper stringer zone.	+40.5
14	HL39	246.65	Envelope zone. Silica sericite pyrite altered lava.	Pyrite	Hellyer upper stringer zone.	+8.3

MIDDLE STRINGER ZONE

17	HL15	427.2	Carbonate - chlorite vein with coarse brown sphalerite and coarse recrystallized pyrite.	Pyrite	Hellyer middle stringer zone.	+11.4
18	HL15	438.9	Pyrite in chlorite rich stringer.	Pyrite in cross cutting "grainy" pyrite vein.	Hellyer middle stringer zone	+8.9
19	HL15	462.7	Chlorite rich stringer with fine pyrite.	Pyrite	Hellyer middle stringer zone.	+12.2
16	HL15	427.2	Carbonate - chlorite vein with coarse brown sphalerite and coarse recrystallized pyrite.	Sphalerite	Hellyer middle stringer zone.	+13.2

LOWER AND OUTER STRINGER ZONE

<u>Sample No.</u>	<u>Hole</u>	<u>Depth</u>	<u>Rock Description</u>	<u>Sample Description</u>	<u>Location</u>	<u>S³⁴ permil</u>
65 333988	HL14	522.5	Envelope zone. Silica sericite pyrite altered lava.	Pyrite	Hellyer lower stringer zone.	+12.7
66 333990	HL14	555.82	Stringer	Pyrite	Hellyer lower stringer zone.	+9.1
67 333991	HL14	581.6	Stringer	Pyrite	Hellyer lower stringer zone.	+14.6
10	HL31	490.0	Chlorite schist with Fine-grained pyrite.	Pyrite	Hellyer lower stringer zone.	+12.1
11	HL31	494.6	Sericite pyrite schist	Pyrite	Hellyer lower stringer zone.	+16.9, +16.6
20	HL15	520.8	Chlorite carbonate pyrite rich stringer.	Pyrite	Hellyer lower stringer zone.	+32.2

FOOTWALL LAVAS OUTSIDE STRINGER ZONE

<u>Sample No.</u>	<u>Hole</u>	<u>Depth</u>	<u>Rock Description</u>	<u>Sample Description</u>	<u>Location</u>	<u>S³⁴ permil</u>
60 333980	HL14	282.49	Albite porphyritic andesite	Pyrite	200 metres S.W. of Hellyer.	+24.3
61 333981	HL14	313.85	Albite porphyritic andesite	Pyrite	200 metres S.W. of Hellyer.	+23.0
62 333983	HL14	367.43	Non porphyritic andesite?	Pyrite	200 metres S.W. of & below Hellyer.	+27.0
63 333985	HL14	430.0	Fawn brown basalt dyke	Pyrite	200 metres S.W. of & below Hellyer.	+32.0* *two replicate analyses of 32.06 and 31.98.
64 333986	HL14	454.0	Lava. Basalt dyke?	Pyrite	200 metres S.W. of & below Hellyer.	+19.45

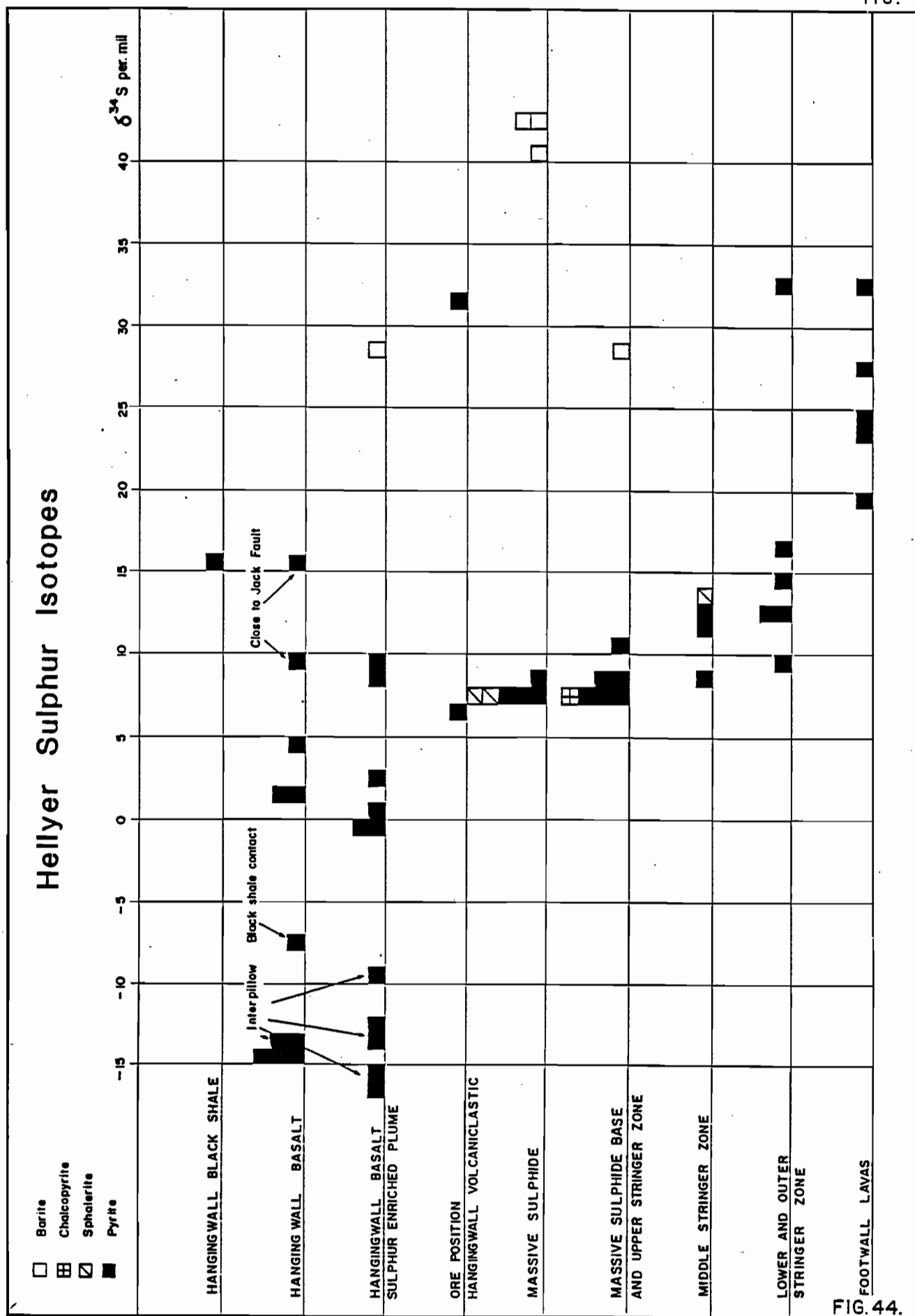


FIGURE 44: Hellyer Sulphur Isotopes-Histogram. There is an overall decrease in $\delta^{34}\text{S}$ (pyrite) inwards and upwards from the footwall lavas into the stringer zone. Massive sulphide values are consistent at around 7 per mil. Very light sulphur occurs in pyrite in interpillow areas in the hangingwall.

Table 10 summarises the data grouped by rock type and position in the ore environment. The results (Figure 44) show an input of heavy sulphur in pyrite on the margins of the stringer system, especially outside of the envelope zone, in the footwall lavas (range from +19.4 to 32.0 per mil for pyrite). This pyrite is normally associated with K-feldspar. There is an erratic decrease in $\delta^{34}\text{S}$ per mil (pyrite) values from the bottom and outside of the stringer zone (mean 13.05 per mil) to the ore body base (mean $\delta^{34}\text{S}$ pyrite 8.4 per mil). The massive sulphide itself has $\delta^{34}\text{S}$ (pyrite) values that cluster closely around 7 per mil. In the hangingwall, very light sulphur in pyrite occurs in interpillow areas both inside and outside the plume. Interpillow pyrite is associated with K-feldspar, sericite and chlorite. Interpillow pyrite accounts for most of the increase in total sulphur content from <2%S outside of the plume to ~4%S in the plume. Sulphur in the hangingwall is also associated with albite alteration where it occurs in pyrite, sphalerite, galena and chalcopyrite ($\delta^{34}\text{S} = 10.9$ per mil), and with the pervasive calcite-sericite alteration as disseminated pyrite or as colloform pyrite on the edges of calcite veinlets ($\delta^{34}\text{S} = 1.2$ per mil). Barite in the massive sulphide hangingwall and in the footwall at the top of the stringer zone has very heavy $\delta^{34}\text{S}$ values (massive ore; hangingwall +41.8 n=3, footwall +40.5 n=1).

Interpretation

Perhaps the best evidence for the primary source of sulphur in stratiform sulphide deposits was provided by Sangster (1976) who noted the correlation between the $\delta^{34}\text{S}$ value in deposits of a given geologic age with coeval seawater. He found that the average $\delta^{34}\text{S}$ value for a

TABLE 10 Sulphur Isotopes Summary

Rock Type	Range $\delta^{34}\text{S}$ per mil	Mean $\delta^{34}\text{S}$ per mil
Pyrite in basalt at shale contact		-7.9 (n=1)
Albite pyrite altered basalt	+8.8 to +16.1	10.9 (n=4)
Disseminated pyrite in fuchsite calcite albite altered basalt.	-1.8 to +3.0	1.2 (n=4)
Interpillow hangingwall basalt (both in and out of H/W plume)	-16.3 to -9.6	-13.7 (n=10)
Hangingwall volcanoclastic rocks	+6.3 and +31.3	
Massive Sulphide	+7.0 to +8.0	7.2 (n=7)
Massive Sulphide Base and Upper Stringer Zone	+7.7 to +10.6	8.4 (n=7)
Middle Stringer Zone	+8.9 to +13.2	11.4 (n=4)
Lower and Outer Stringer Zone	+9.1 to +16.9	13.0 (n=5)
Footwall Andesite Lavas	+19.45 to 32.0	25.1 (n=5)

deposit was ~15 per mil less than coeval sulphate values in seawater, corresponding to what would be produced by the bacterial reduction of seawater sulphate under normal biological conditions. Inorganic reduction, more likely for proximal deposits such as those in Tasmania, would produce a similar correlation (Sangster, 1976).

Rock sulphur is likely to have contributed to the sulphur in the system (Stanton and Rafter, 1966; Shanks et al., 1981; Green et al., 1981; Green, 1983; Solomon et al., in press), and the fact that many volcanic-hosted massive sulphides have $\delta^{34}\text{S}$ values close to rock sulphur values supports this conclusion. Solomon et al., (in press), suggest that to obtain the 10^{13} g S in the Rosebery deposit, a rock sulphur as well as a sulphate-reduction component is required.

Figure 45 compares the $\delta^{34}\text{S}$ (pyrite) in the massive sulphide at Hellyer with other Tasmanian volcanogenic massive sulphide deposits. Solomon et al. (1988) interpret the lack of zoning of $\delta^{34}\text{S}$ in massive sulphide at Que River and Mount Lyell to be the product of a system dominated by rock sulphur (+6 to +10 per mil). The Rosebery massive sulphide shows a progressive increase in $\delta^{34}\text{S}$ (pyrite) values upwards in the ore body (+8 to +17 per mil) and this has been interpreted (Green et al., 1981) as being due to a declining content of rock sulphur with time. Hellyer shows a similar lack of zoning to that displayed by Que River and Mount Lyell suggesting, if this interpretation is adhered to, a domination by rock sulphur.

Any interpretation of the sulphur isotopic data at Hellyer has to account for the following observations :

1. the decreasing $\delta^{34}\text{S}$ values inwards and up the stringer zone.

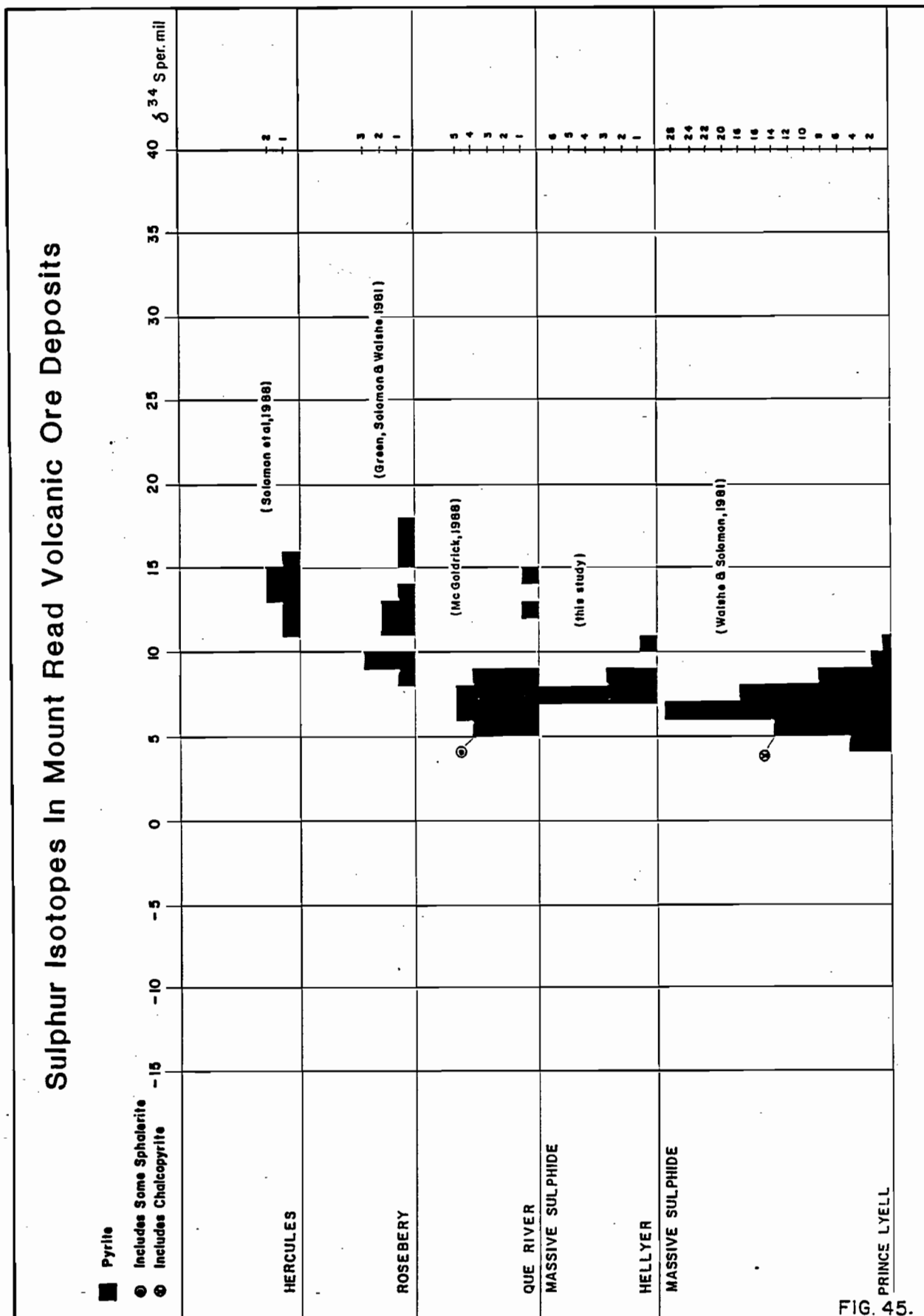


FIGURE 45: Sulphur Isotopes in Mount Read Volcanic Ore Deposits. Values around 7 per mil at Hellyer are similar to those at Que River but are lower than at Rosebery and Hercules and higher than at Prince Lyell.

2. the consistent values around 7 per mil in the massive sulphide.
3. the very heavy pyrite on the margins of the stringer zone.
4. the very light pyrite in the hangingwall interpillow areas.
5. the stringer zone-like values in the hangingwall, especially close to the Jack fault.
6. ^{34}S values close to zero in calcite-fuchsite altered rocks.

Two models may explain these observations and these are presented in Figure 46.

Model 1 has most sulphur precipitating in the orebody in the narrow oxygen fugacity range between B and C on Figure 47. The decrease in ^{34}S per mil values up the stringer zone is explained by an increase in oxygen fugacity up the stringer zone, but especially at the top in the quartz barite rich, low iron sphalerite rich core. In this model, most sulphur is sourced from equilibrium reduction from Cambrian seawater sulphate. Initial values of +13 per mil, produced by reduction from seawater sulphate, precipitate in minor quantities deep in the system, but most sulphur precipitates in the upper stringer zone and finally in the orebody where optimum conditions for deposition are attained. Input of seawater sulphate at the top of the stringer zone may be the mechanism for increasing the oxygen fugacity. The presence of light brown, iron-poor sphalerite at the top of the stringer zone supports the suggestion that oxygen fugacity was elevated in this locality.

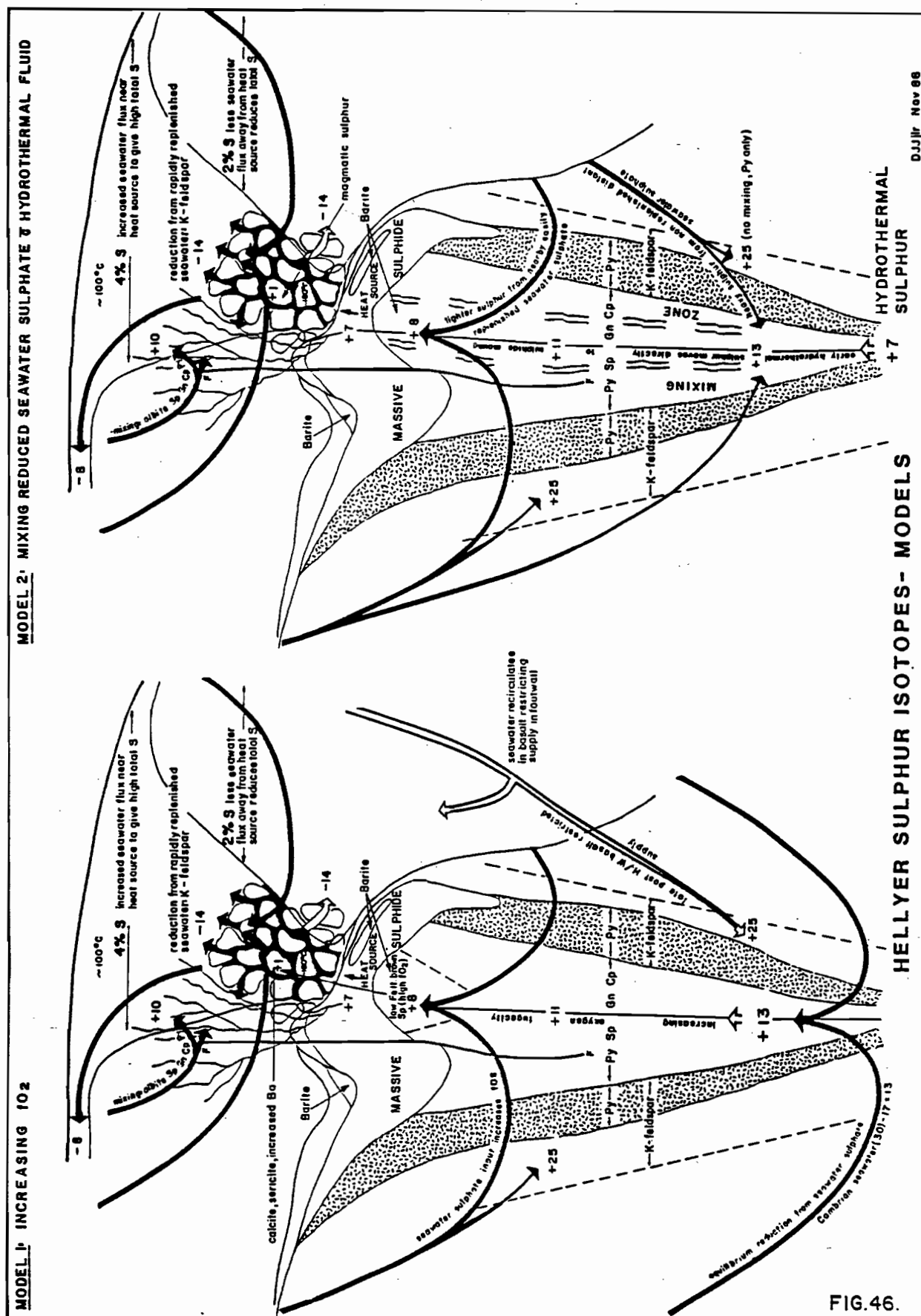
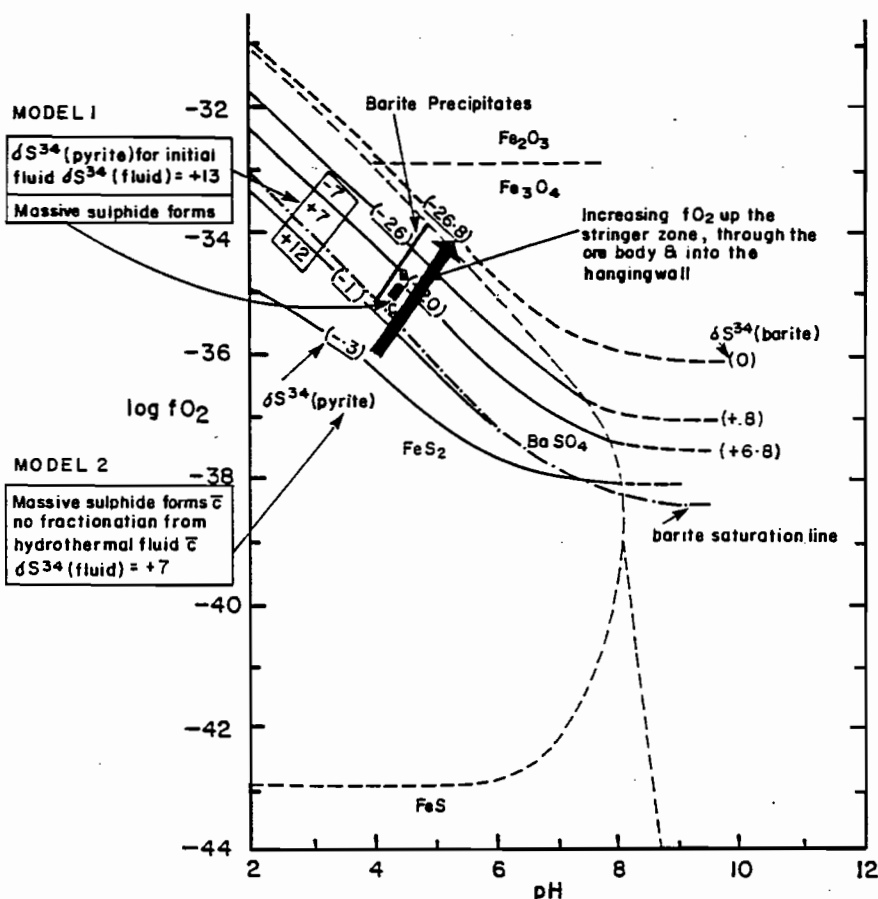


FIGURE 46: Hellyer Sulphur Isotopes-Models. Mixing seawater sulphate with hydrothermal fluid and increasing oxygen fugacity at the top of the stringer zone may both occur to produce the observed isotopic distribution. (see text and diagram for detailed explanation).



Bose diagram from Ohmoto & Rye, 1979 Fig 21-5 $T = 250^\circ C$, ionic strength = 1.0

Aberfoyle Resources Limited

EXPLORATION DIVISION

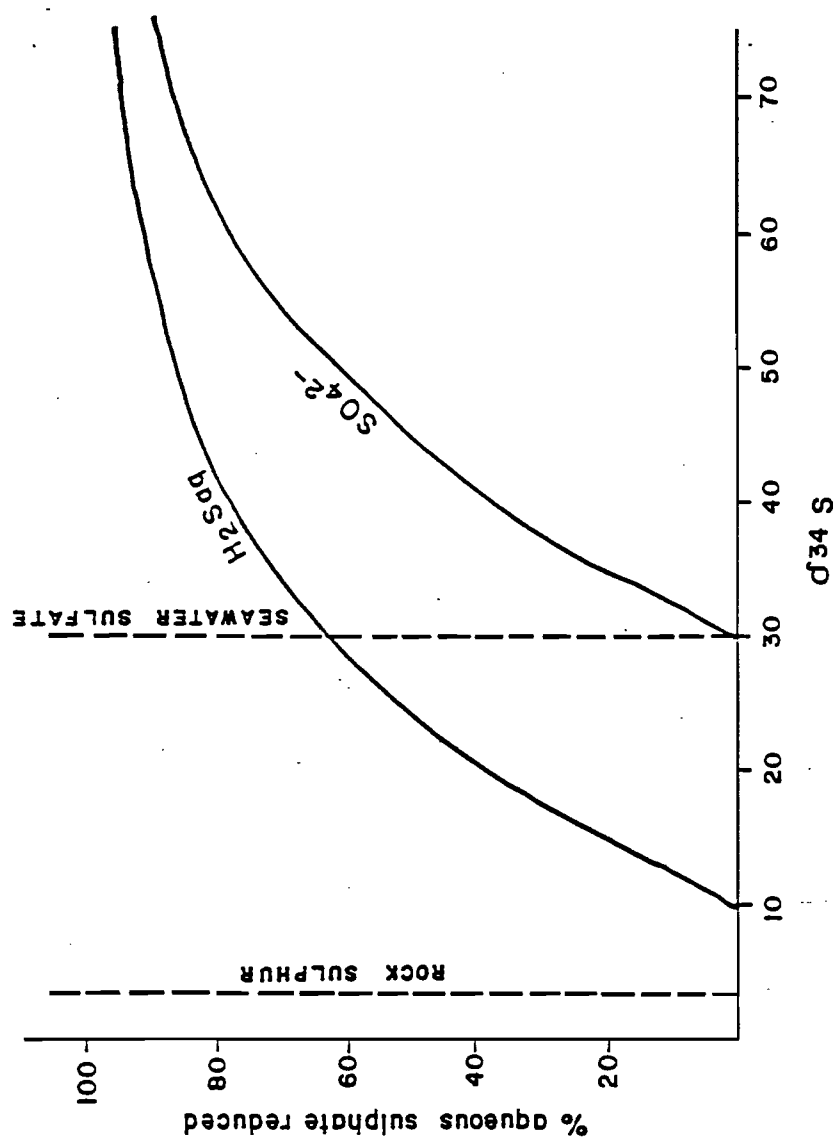
FIG. 47.

REVISIONS				NORTH WEST TASMANIA		Compiled : DJJ	
Init.	Date	Init.	Date	ISOTOPIC COMPOSITION OF SULPHUR IN PYRITE FOR TOTAL SULPHUR IN THE SYSTEM EQUAL TO ZERO PER MIL.		Drawn :	
						Traced : JLR	
						Checked :	
						Plate No. : HEL 106	
Location Code :		Scale :		Date : June, 1988			

FIGURE 47: Log fO_2 versus pH at 250° Showing the Isotopic Composition of Sulphur in Pyrite. In model 1 massive sulphide forms in a narrow range of fO_2 to produce the consistent value around 7 in the orebody. In model 2 massive sulphide forms with no fractionation from hydrothermal fluid with a sulphur isotopic signature of 7 per mil.

Progressive reduction of seawater of $\delta^{34}\text{S} = +30$ per mil at 300°C

Rayleigh fractionation assuming non replenishment of water supply



modified after Solomon et al (in press)

FIG. 48.

FIGURE 48: Progressive Reduction of Seawater with a Non-replenished Supply by Rayleigh Fractionation. With successive reductions sulphur becomes heavier.

This model has elements in common with model 2 that explain the light interpillow hangingwall pyrite, the very heavy sulphur on the margins of the stringer system and the stringer zone-like values in the hangingwall and these are discussed below.

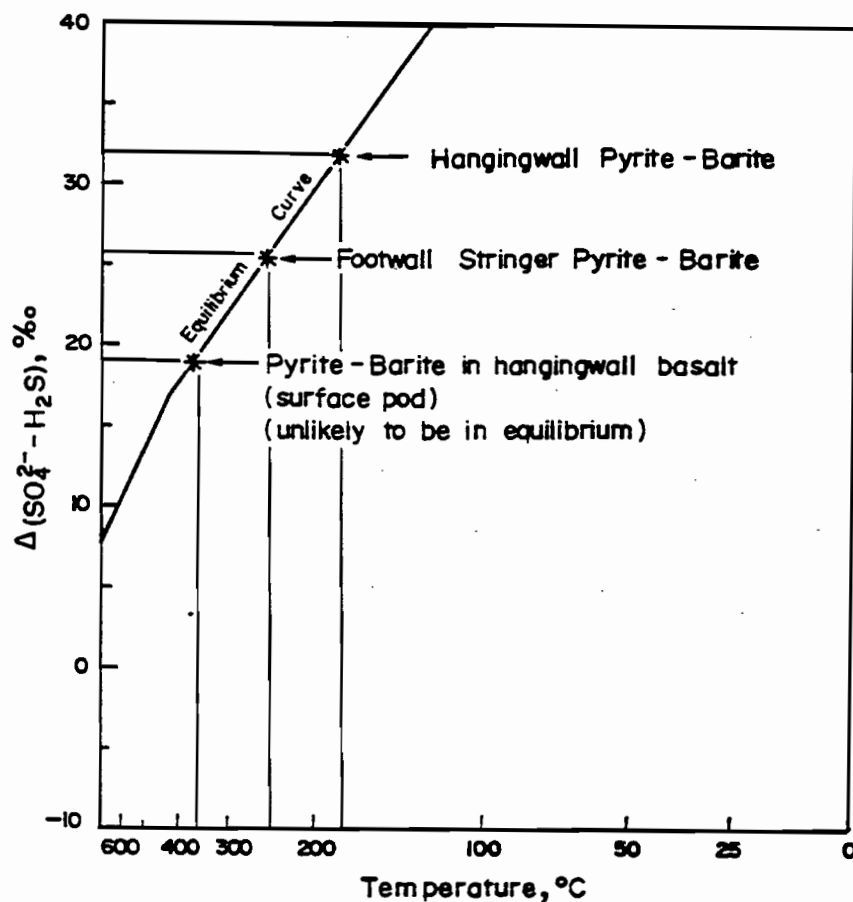
Model 2 (Figure 46) emphasises the consistent values of +7 per mil in the orebody, the site of most sulphur deposition. Early hydrothermal sulphur with a value of +7 per mil moves directly to the sulphide mound where most sulphur precipitates in the massive sulphide orebody. Deposition in the orebody maintains the hydrothermal signature as this occurs in the acid pH, low oxygen fugacity field (Figure 47) where there is virtually no fractionation of sulphur isotopes between fluid and pyrite. Later mixing of hydrothermal sulphur with varying amounts of variably replenished seawater sulphate accounts for the observed decrease in $\delta^{34}\text{S}$ (pyrite) values inwards and upwards in the stringer system. In order to explain this concept, reference should be made to Figure 48 modified from Solomon et al. (1988). A non-replenished supply of seawater drives the $\delta^{34}\text{S}$ values up as a Rayleigh fractionation. Successive reductions of sulphate result in the remaining sulphate becoming heavier and, if the supply is not replenished, very heavy pyrite is produced. Deep in the system, where the seafloor is more distant and supply is not easily replenished, mixing hydrothermal fluid with the heavy sulphur produced from a restricted supply of seawater results in the $\delta^{34}\text{S}$ (pyrite) values around +13 per mil. By contrast, the top of the stringer zone is close to the seawater supply and reduction produces lighter sulphur which, on mixing with the hydrothermal fluid, results in the $\delta^{34}\text{S}$ (pyrite) values around +8 per mil.

Both models account for the very heavy sulphur on the margins of the stringer system and the very light sulphur in the interpillow areas by reduction of seawater sulphate under different conditions. Green et al. (1981) suggested that reduction could be achieved by oxidation of Fe^{2+} to Fe^{3+} . Fe is leached from calcite-fuchsite altered basalt and this is reflected in the isocon diagram in the previous chapter (Figure 36). In the footwall, very heavy sulphur produced from a restricted supply of seawater sulphate does not mix with hydrothermal fluid on the margins of the stringer system and $\delta^{34}\text{S}$ (pyrite) values around +25 result. In support of the lack of mixing are the low levels of base metal sulphides in and just outside of the envelope zone. This is thought to be due to the exclusive sourcing of sulphur from seawater sulphate with no base-metal rich hydrothermal input. K-feldspar may reflect the higher pH of seawater alteration (Rye and Ohmoto, 1974). In the hangingwall, very light sulphur occurs in pyrite in the interpillow areas. Oxygen and carbon isotope data on calcite in the hangingwall lavas indicate temperatures of between 100 and 200°C, increasing towards the orebody (G.R. Green pers. comm., 1987). At the lower end of these temperatures, such as might be expected in interpillow conduits cooled by seawater influx, fractionation from Cambrian seawater with an estimated $\delta^{34}\text{S}$ per mil value of +30 (Kaplan 1975) would result in light pyrite in the range 0 to -20 per mil (Figure 10.3 Ohmoto and Rye, 1979), providing the supply was rapidly replenished. A high flux of seawater driven by heat emanating from the sulphide mound results in a greater volume of water and increased reduction causing higher total sulphur content in the hangingwall plume. The presence of K-feldspar veinlets

in interpillow areas, Plate 8 may be indicative of higher pH seawater influence (Henley et al., 1984). As in the stringer envelope zone, pyrite is the only sulphide to develop in interpillow areas reflecting the lack of base-metal rich hydrothermal input.

Both models account for the stringer zone like values in the hangingwall of $\delta^{34}\text{S}$ (pyrite) = +10 by mixing of hydrothermal sulphur close to the position of the Jack Fault, with seawater. This subsidiary sulphur is associated with base-metal mineralization and early albite alteration.

The consistent values in the ore body, at between 6.3 and 7.5 per mil, suggest that any changes in oxygen fugacity or pH (for a given temperature) were minimal and that the fluid remained within the narrowly constrained field between B and C on Figure 48. The absence of any Ba in the centre of the ore body (Figure vi in Appendix 1) confirms this interpretation, as the field concerned is below the barite saturation boundary. Precipitation of barite in the hangingwall of the ore body must still be constrained at moderate oxygen fugacity near the field B-C, as $\delta^{34}\text{S}$ values in pyrite remain at near 7 per mil. Variation in Ba content of the fluid has to be invoked to shift the saturation boundary and accommodate the presence of barite at the top of the stringer zone and in the hangingwall of the ore body. Figure 49 supports a separate origin for pyrite in calcite-fuchsite-barite enriched lava and pyrite in interpillow areas. Reasonable temperatures are obtained for barite-pyrite pairs in the top of the footwall stringer-zone (240°C), and at the top of the orebody (190°C) where



$(\text{SO}_4^{2-} - \text{H}_2\text{S})$ - sulphate-sulphide isotopic fractionation
versus T (from Ohmoto and Rye 1979)

FIGURE 49: $(\text{SO}_4^{2-} - \text{H}_2\text{S})$ - Sulphate-sulphide Isotopic Fractionation versus T. Pyrite-barite pairs in the hangingwall barite-rich zone of the orebody give a temperature of 280°C whereas in the core of the stringer zone, directly below the orebody temperatures of 240°C are indicated. Barite-pyrite pairs in the barite pod in hangingwall basalt at surface is unlikely to be in equilibrium. (Base diagram from Ohmoto and Rye, 1979.)

FIG. 49

equilibrium co-precipitation is possible. 350°C indicated in the barite pod at surface is too high. Sulphur in this barite is interpreted to be sourced from the end stages of a process of increasing oxygen fugacity in contrast to the interpillow pyrite which has a separate seawater sulphate source.

CHAPTER 7 CONCLUSIONS AND RECOMMENDATIONS

Hellyer occurs in primary calc-alkaline, arc-like, intermediate lavas at the time break between an albite-porphyritic andesite-lava-breccia and a series of hangingwall basalt flows. The primary low Ti and Nb and notable K-group enrichment (K, Ba, Rb, LREE) of the Hellyer hangingwall basalt is typical of high-K, calc-alkaline, arc basalts.

A more-primitive core basalt-lava-flow directly above Hellyer has regionally high Ti/Zr ~ 53 and higher primary MgO, Ni, Cr with lower SiO₂, TiO₂, P₂O₅, Y, Zr, La and Nb than the surrounding basalt, and this deeper sourced lava is thought to have extruded up the same structure that localized the Hellyer hydrothermal system.

Alteration in the footwall consists of a stringer pipe wider than the orebody, with a quartz-barite centre top grading outwards into quartz-sericite and then chlorite, including mono-mineralic Mg-chlorite, schists. Veins and accumulations of base-metal sulphide increase in intensity towards the quartz-barite core. A uniform and distinctive quartz-sericite-pyrite envelope zone surrounds the core. The hangingwall volcanoclastic is altered to sericite, Fe-chlorite and calcite. The hangingwall basalt is altered, in a bright-green, plume-shaped zone directly above the core of the stringer zone, to calcite-fuchsite with increased interpillow pyrite and accessory Fe-chlorite. Albite alteration occurs in and outside of the plume.

Geochemically, the stringer zone is marked by a pronounced Na₂O low, with CaO and Sr depletion being more widespread. In the hangingwall, there is a K₂O, Al₂O₃ and Ba high along the hangingwall volcanoclastic rocks and a pronounced CaO, Ba and S high in the hangingwall plume.

Isocon plots indicate that in the stringer zone all elements are mobile to some extent. In the hangingwall, TiO_2 , Zr, Y, Nb and the rare earth elements remain immobile. In calcite-fuchsite alteration, there is major mass addition of CaO and CO_2 with subsidiary Al_2O_3 , K_2O and Ba addition. SiO_2 , MgO and Fe_2O_3 are removed from the rock. Fe_2O_3 and MgO are also removed in hangingwall albite alteration, but SiO_2 is added here with Na_2O and CaO. Cu, Pb and Zn are not enriched in the hangingwall plume.

A scattering of element abundances in the hangingwall core lava is not evident in the surrounding lava as early hydrothermal processes locally mobilized elements in the earlier core lava, whereas hydrothermal activity had waned by the time the surrounding lava extruded.

Major Eu depletion is strongest in silica altered rocks as these were at the centre of highest temperature and most intense alteration (Whitford et al., 1988).

Chrome in the calcite-fuchsite plume is locally remobilized from chrome-rich augites into fuchsite. Most chrome is contained in resistate chromites and is essentially immobile.

A trend of decreasing $\delta^{34}\text{S}$ (pyrite) values in the core of the stringer zone occurs inwards and upwards from +13 per mil three hundred metres below the massive sulphide to +8 per mil in the quartz-barite rich core of the stringer zone directly below the massive sulphide. This may be due to increasing oxygen fugacity, or to mixing seawater sulphate, heavier at depth due to restricted supply, with hydrothermal

fluids with a primary value of +7 per mil. The massive sulphide has consistent δ^{34} (pyrite) of +7 per mil, implying deposition in a very narrow oxygen fugacity range for a given temperature, or from hydrothermal fluid with a +7 per mil value without fractionation between fluid and pyrite.

Reduced seawater sulphate is thought to be the source of isotopically light sulphur ($\delta^{34}\text{S}$ (pyrite) = -14 per mil) in the interpillow areas in the hangingwall. The rapid replenishment of supply caused by a high flux of seawater through interpillow conduits ensures that the sulphate isotopic signature does not increase by successive fractionation. This is in contrast to the situation in the footwall where a restricted supply, the result of a lack of physical conduits and distance from the seafloor, has resulted in isotopically heavy pyrite ($\delta^{34}\text{S}$ (pyrite) = +25 per mil) on the fringes of the stringer zone. Both interpillow areas and the stringer envelope zone and its fringes contain K-feldspar reflecting higher pH in seawater and do not contain base metal as no mixing with mineralized hydrothermal sulphur has occurred.

It is recommended that the primary characteristics of the Que-Hellyer volcanics, especially the calc-alkaline character should be used in the selection of further belts of volcanics in which to explore for volcanogenic massive sulphides in Tasmania. The special characteristics of the core basalt can further focus exploration, as this occurs close to deep-sourced structures that may have localized a hydrothermal system and orebody.

The characteristics of hangingwall alteration should become an exploration target. The occurrence of calcite-fuchsite and barite are particularly prospective and large negative sulphur isotope signatures

may indicate that a heat source is close and that the sulphides are in a hangingwall alteration system above a VMS deposit. By contrast, isotopically heavy pyrite is more likely in the footwall and, as this can occur outside obvious stringer-zone rock, it can be used in the absence of other evidence to position pyrite relative to a target orebody. This information should be used to focus exploration activity and to aid targeting of drill holes.

The data base established should be used to compare and assess future prospects with Hellyer, and should be utilized in conjunction with ongoing research.

REFERENCES

- Avison, M., 1985, Metasomatism in the Lough Guitane volcanic complex (Southwest Ireland) - An application of composition - volume computations : Chemical Geology v.48, p.79-92.
- Beaty, D.W., and Taylor Jr., H.P., 1982, Some petrologic and oxygen isotopic relationships in the Amulet mine, Noranda, Quebec, and their bearing on the origin of Archean massive sulfide deposits. Econ. Geol., v.77, p. 95-108.
- Berry, R.F., 1986, The Structure of the Henty fault zone at Tullah (abs.): in Collins, P.L.F., and Large R.R., eds., The Mount Read Volcanics and associated ore deposits: Geol. Soc. Austr., Tasmanian Divn. Abstracts, p.31-32.
- Berry, R.F. and Crawford A.J., 1988, The tectonic significance of Cambrian allochthonous mafic - ultramafic complexes in Tasmania : Australian Jour. Earth Sci., v.35, p.523-533.
- Brathwaite, R.L., 1974, The geology and origin of the Rosebery ore deposit, Tasmania : Econ. Geol., v.69, p.1086-1101.
- Brown, A.V., 1986, Geology of the Dundas-Mount Lindsay-Mount Youngbuck region. Tasmania Geol. Surv. Bull. 62, 221p.
- Brown, R., 1987, Determination of mineralogy by XRD: AMDEL Limited Adelaide Unpub. report to Aberfoyle Resources Ltd. 3p.
- Campana, B., Dickson, S.B., King, D. and Matheson, R.S., 1958, The mineralized rift valleys of Tasmania: F.L. Stilwell anniversary v., Australasian Inst. Min. Metall., p.41-60.
- Campana, B., and King, D., 1963, Palaeozoic tectonism, sedimentation and mineralization in west Tasmania : Geol. Soc. Australia Jour., v.10, p.1-53.
- Collins, P.L.F., and Williams, E., 1986, Metallogeny and tectonic development of the Tasman fold belt system in Tasmania : Ore Geology Reviews 1, p.153-201.
- Constantinou, G., 1976, Genesis of the conglomerate structure, porosity and collomorphic textures of the massive sulphide ores of Cyprus : Geol. Assoc. Canada, Spec. Paper 14, p.187-210.
- 1977, Hydrothermal alteration of basaltic lavas of the Troodos ophiolite complex associated with the formation of the massive sulphide ores of Cyprus: Geol. Assoc. Canada Spec. Paper 14, p.187-210.
- Corbett, K.D., 1979, Stratigraphy, correlation and evolution of the Mount Read Volcanics in the Queenstown, Jukes-Darwin and Mount Sedgwick area: Tasmania Geol. Surv. Bull. 58, 75p.

- 1981, Stratigraphy and Mineralization in the Mt. Read Volcanics, Western Tasmania : Econ. Geol. v.76, p.194-208.
- 1986, The Geological setting of mineralization in the Mt. Read Volcanics. in: Collins, P.L.F., and Large, R.R. (eds.), The Mount Read Volcanics and associated ore deposits: Hobart, Geol. Soc. Australia, Tasmanian Div., Abstracts, p.1-10.

Corbett, K.D., and Lees, T.C., 1987, Stratigraphic and structural relationships and evidence for Cambrian deformation at the western margin of the Mt. Read Volcanics, Tasmania: Austr. J. Earth Sci. 34, p.45-67.

Corbett, K.D. and Solomon, M., (in press), The Cambrian Mount Read Volcanics and Mineral Deposits. Chapter 4. in: Burrett, C.F., ed. The Geology and Ore Deposits of Tasmania : Geol. Soc. Aust. Tas. Divn.

Date, J., Watanabe, Y., Iwata, S., and Horiuchi, M., 1979, A consideration on the alteration of dacite below the Fukazawa ore deposits, Fukazawa Mine, Akita Prefecture : Mining Geology, v.29, p.187-196 (in Japanese with English abs only).

Date, J., Watanabe, Y., and Saeki, Y., 1983, Zonal Alteration around the Fukazawa Kuroko deposits, Akita prefecture, Japan : in Econ. Geol. Monograph 5, p.365-386.

Davies, J.L., 1980, Geology of the Bathurst-Newcastle area : Geol. Assoc. Canada, Ann. Mtg., Halifax, May 1980, Field Trip Guidebook 16, p.1-16.

Deer, W.A., Howrie, R.A., Zussman, J., 1966, An introduction to the rock forming minerals : Longman, 528p.

Descarreaux, J., 1973, A Petrochemical Study of the Abitibi volcanic belt and its bearing on the occurrences of massive sulphide ores : CIM Bulletin for February, 1973, p.61-69.

Dick, H.J.B., and Bullen, J., 1984, Chromian spinel as a petrogenetic indicator in Abyssal and Alpine-type peridotites and spatially associated lavas : Contrib Mineral Petrol. v.86, p.54-76.

Eadie, E.T., Silic, J., and Jack, D.J., 1985, "The Application of geophysics to the discovery of the Hellyer ore deposit, Tasmania" : Explor. Geophys., v.16, no. 2/3 : p.207-209.

Eastoe, C.J., Solomon, M. and Walshe, J.L., 1987, District scale alteration associated with massive sulfide deposits in the Mount Read Volcanics, western Tasmania : Econ. Geol., v.82, p.1239-1258.

- Eldridge, C.S., Barton, P.B., Jr., and Ohmoto, H., 1983, Mineral textures and their bearing on formation of the Kuroko orebodies : Econ. Geol. Mon. 5, p.241-281.
- Fander, H.W., 1984, Central Mineralogical Services Reports on Hellyer Rocks. Unpub. reports to Aberfoyle Exploration Ltd.
- Franklin, J.M., Kasarda, J., and Poulsen, K.H., 1975, Petrology and chemistry of the alteration zone of the Mattabi massive sulfide deposit : Econ. Geol. v.70 p.63-79.
- Franklin, J.M., Lydon, J.W., and Sangster, D.F., 1981, Volcanic associated massive sulphide deposits : Econ. Geol., 75th Anniv. v., p.485-627.
- Gee, C.E., Jago, J.B., and Quilty, P.G., 1970, The age of the Mt. Read Volcanics in the Que River Area, western Tasmania : J. Geol. Soc. Aust., 16(2) : p.761-763.
- Gemmel, J.B., 1988, Hellyer stringer zone project progress report No. 1: Unpub. Aberfoyle Resources Ltd. - University of Tasmania report (Dec. 88) 40p.
- Grant, J.A., 1986, The Isocon Diagram - A simple solution to Gresens' equation for metasomatic alteration : Econ. Geol. v.81, p.1976-1982.
- Green, G.R., 1983, The geological setting and formation of the Rosebery volcanic-hosted massive sulphide orebody, Tasmania. Unpub. PhD Thesis, Univ. Tasmania 200p.
- Green, G.R., Solomon, M., and Walshe, J.L., 1981, The formation of the volcanic-hosted massive sulfide ore deposit at Rosebery, Tasmania: Econ. Geol. v.76, p.304-338.
- Gresens, R.L., 1967, Composition - volume relationships of metasomatism : Chem. Geology, v.2, p.47-55.
- Harris, P., 1986, The hangingwall volcanoclastic sequence, Hellyer : Unpub. Aberfoyle Exploration Ltd. Report, 30p.
- Hashiguchi, H., Yamada, R., and Inoue, T., 1983, Practical application of low Na₂O anomalies in footwall acid lava flow for delimiting promising areas around the Kosaka and Fukazawa Kuroko deposits, Akita prefective, Japan : Econ. Geol. Mon. 5 p.387-394.
- Henley, R.W., Truesdell, A.H. and Barton, P.B., 1984, Fluid-mineral equilibria in hydrothermal systems. Reviews in Economic Geology 1.
- Ishikawa, Y., Sawaguchi, T., Iwaya, S., and Horiuchi, M., 1976, Delineation of prospecting targets for Kuroko deposits based on modes of volcanism of underlying dacite and alteration haloes : Mining Geology, v.26, p.137-152 (in Japanese with English abstract).

- Jack, D.J., 1983, A model for the Hellyer base metal sulphide deposit and a suggested morphology - future drilling : Unpub. Aberfoyle Exploration Pty. Ltd. Report, 11p.
- 1984, Report on exploration on the Mackintosh EL2/70 during the period January 1983 to April 1984 : Unpub. Aberfoyle Exploration Pty. Ltd., report to Tasmanian department of mines, 52p.
 - 1985a, b, c, 1987a, b, Hellyer alteration study progress reports : Unpub. Aberfoyle Exploration Pty. Ltd. reports, 492p.
- Jaques, A.L., and Green, D.H., 1980, Anhydrous melting of peridotite at 0-15 kb pressure and the genesis of tholeiitic basalts. *Contrib. Mineral. Petrol.* v.73, No.3, p.287-310.
- Jago, J.B., 1979, Tasmanian Cambrian biostratigraphy - a preliminary report : *Australian Journal of Earth Sciences*, 26. p.223-230.
- Kaplan, I.R., 1975, Stable isotopes as a guide to biogeochemical processes. *Royal Soc. London Proc.*, B189, p.183-211.
- Knuckley, M.J., Comba, C.D.A., and Riverin, G., 1982, Structure, metal zoning and alteration at the Millenbach deposit, Noranda, Quebec : in *Precambrian sulphide deposits*, H.S. Robinson memorial volume, Edited by R.W. Hutchinson, C.D. Spence and J.M. Franklin, *Geol. Ass. Can. Special Paper* 25, p.255-295.
- Knuckley, M.J., and Watkins, J.J., 1982, The geology of the Corbet massive sulphide deposit Noranda, Quebec : in *Precambrian sulphide deposits*, H.S. Robinson Memorial v., Edited by R.W. Hutchinson, C.D. Spence and J.M. Franklin, *Geol. Ass. Can. Special Paper* 25, p.296-317.
- Komyshan, P., 1986, Geology of the Hellyer-Mt. Charter area : In: Large R.R., ed., *The Mount Read volcanics and associated ore deposits*, *Geol. Soc. Aust., Tasmanian Divn. Abstracts*, p.53-55.
- Large, R.R., 1977, Chemical evolution and zonation of massive sulfide deposits in volcanic terrains : *Econ. Geol.*, v.72, p.549-572.
- Large, R.R., Carswell, J., Creelman, R., Huston, D.L., McArthur, G., McGoldrick, P., Purvis, G., Ramsden, T., and Wallace, D., in press, *Gold in western Tasmania*, in *Mineral Resources of Australia : Aus. Inst. Min. Metall. Bicentennial Vol.*
- Large, R.R., Herrmann, W., and Corbett, K.D., 1987a, Base metal exploration of the Mount Read Volcanics, western Tasmania : PT. 1 *Geology and Exploration, Elliott Bay : Economic Geology*, v.82, p.267-290.
- Large, R.R., McGoldrick, P.J., and Young, C.H., 1987b, A tightly folded, gold rich, massive sulfide deposit : Que River Mine, Tasmania : *Econ. Geol.* v.83, p.681-693.

- Lees, T., 1987, Geology and mineralization of the Rosebery-Hercules area, Tasmania: Unpub. M.Sc. Thesis, Univ. of Tasmania, 164p.
- MacGeehan, P.J., 1978, The geochemistry of altered volcanic rocks at Matagami, Quebec : A geothermal model for massive sulphide genesis : Can. J. Earth Sci., 16, p.551-570.
- MacGeehan, P.J., and Maclean, W.H., 1980, Tholeiitic basalt - rhyolite magmatism and massive sulphide deposits at Matagami, Quebec : Nature v.283, p.153-157.
- McArthur, G.J., 1985, "Geological resources of the Hellyer deposit". Unpub. Aberfoyle Resources Ltd. Report, 67p.
- 1986, The Hellyer massive sulphide deposit, in: Collins P.L.F., and Large, R.R., eds., The Mount Read Volcanics and associated ore deposits : Geol. Soc. Austr. Tasmanian Div., Abstracts, p.11-14.
- McArthur, G.J., and Dronseika, E.V., (in press), The Que River and Hellyer volcanogenic Ag-Pb-Zn sulfide deposits: in 'The Geology of Mineral Deposits of Australia and Papua New Guinea'. Australasian Inst. Min. Metall.
- McClenaghan, M.P., and Corbett, K.D., 1985/63, Geochemical diagrams of Cambrian volcanic rocks and associated intrusives from western Tasmania : Unpub. Tasmania Department of Mines Report, p.19.
- McGoldrick, P., 1988, Sulphur isotope studies at Que River : in Controls on Gold and Silver Grades in Volcanogenic Sulphide Deposits : Unpub. Final Research Report, AMIRA - Univ. Tas., p.47-52.
- McLeod, R.L., and Stanton, R.L., 1984, Phyllosilicates and associated minerals in some Paleozoic stratiform sulfide deposits of south eastern Australia : Econ. Geol. v.79, p.1-22.
- Morrison, G.W., 1980, Characteristics and tectonic setting of the shosonitic rock association. Lithos v.13, p.97-108.
- Naschwitz, W., 1985, Geochemistry of the Rosebery Orebody : Unpub. PhD. Thesis, Univ. Tasmania 276p.
- Offler, R., Hand, M., and Whitford, D.J., 1987, A study of white micas in "Fuchsite - Carbonate" rocks adjacent to mineralization, Que River, Tasmania : CSIRO Division of Mineral Physics and Mineralogy Restricted Investigation Report 1684R 11p.
- Ohmoto, H., and Rye, R.O., 1979, Isotopes of sulfur and carbon, in Barnes, H.L., ed., Geochemistry of hydrothermal ore deposits, 2nd ed., : New York, John Wiley and Sons, p.509-567.

- Ohmoto, H., Tanimura, S., Date, J., Takahashi, T., 1983, Geologic setting of the Kuroko deposits, Japan parts I, II and III : in: The Kuroko and Related Volcanogenic Massive Sulfide Deposits, Econ. Geol. Mon. 5, p.9-54.
- Pearce, J.A., and Cann, J.R., 1973, Tectonic setting of basic volcanic rocks determined using trace element analyses : Earth Planet. Sci. Lett., 19, p.290-300.
- Ramsay, W.R.H., Crawford, A.J., and Foden, J.D., 1984, Field setting, mineralogy, chemistry and genesis of arc picrites, New Georgia, Solomon Islands. Contrib. Mineral Petrol. 88 p.386-402.
- Ramsden, A.R., and Creelman, R.A., 1984, Precious metal mineralogy of Hellyer and Que River Ores : Unpub. CSIRO, Institute of Energy and Earth Resources, Division of Mineralogy and Geochemistry, Restricted Investigation Report 1561R, 27p.
- Ramsden, A.R., Kinealy, K.M. and Creelman, R.A., 1986, Mineralogical characteriation of Hellyer ore in HL56 and comparison with results from HL38A, CSIRO, Institute of Energy and Earth Resources, Division of Mineral Physics and Mineralogy, Restricted Investigation Report 1627, 13p.
- Riverin, G., and Hodgson, C.J., 1980, Wall-rock alteration at the Millenbach Cu-Zn mine, Noranda, Quebec : Econ. Geol., v.75, p.424-444.
- Roberts, R.G., and Reardon, E.J., 1978, Alteration and ore-forming processes at Mattagami Lake Mine, Quebec : Can. J. Earth Sci., 15, p.1-21.
- Robinson, P., Higgins, N.C., and Jenner, G.A., 1986, Determinations of rare - earth elements, yttrium and scandium in rocks by an ion exchange - x-ray fluorescence technique. Chem. Geol., 55, p.121-137.
- Rye, R.O., and Ohmoto, H., 1974, Sulfur and carbon isotopes and ore genesis : A review : Econ. Geol., v.69, p.826-842.
- Sangster, 1976, Sulphur and lead isotopes in strata-bound deposits, in Wolf, K.H., ed., Handbook of strata-bound and stratiform ore deposits : Amsterdam, Elsevier, v.2, p.219-266.
- Sato, T., 1974, Distribution and geological setting of the Kuroko deposits : Soc. Mining Geologist Japan, Spec. Issue 6, p.1-9.
- Scott, S.D., 1978, Structrual control of the Kuroko deposits of the Hokuroku district, Japan : Mining Geology, 28, p.301-311.
- Scott, S.D., 1980, Geology and structrual control of Kuroko-type massive sulphide deposits : The Continental Crust and its Mineral Deposits, ed. D.W. Strangway, Geological Association of Canada Special Paper 70, p.705-722.

- Shirozu, H., 1974, Clay minerals in altered wall rocks of the Kuroko-type deposits : Soc. Mining Geologists Japan, Spec. Issue 6, p.303-311.
- Shanks, W.C., Bischoff, J.L., and Rosenbauer, R.J., 1981, Seawater sulfate reduction and sulfur isotope fractionation in basaltic systems : Interaction of seawater with fayalite and magnetite at 200-350°C : *Geochem. Cosmochim. Acta*, v.45, p.1977-1995.
- Sise, J.R., and Jack, D.J., 1984, Exploration case history of the Hellyer deposit. in : P.W. Baillie and P.L.P. Collins eds., *Mineral Exploration and Tectonic Processes in Tasmania*, Geol. Soc. Aust., Tasmanian Div., Abstracts, p.48-49.
- Solomon, M., 1981, An introduction to the geology and metallic ore deposits of Tasmania. *Econ. Geol.*, v.76, p.194-208.
- Solomon, M., Eastoe, C.J., Walshe, J.L., and Green, G.R., in press, Mineral deposits and sulfur isotope abundances in the Mt. Read Volcanics between Que River and Mt. Darwin, Tasmania: *Econ. Geol.*
- Solomon, M., and Walshe, J.L., 1979, The formation of massive sulphide deposits on the sea floor : *Econ. Geol.* v.74, p.797-813.
- Spence, C.D., 1975, Volcanogenic features of the Vauze sulfide deposit, Noranda, Quebec : *Econ. Geol.* v.70, p.102-114.
- Spooner, E.T.C., and Fyfe, W.S., 1973, Sub-seafloor metamorphism, heat and mass transfer : *Contr. Mineralogy Petrology*, v.42, p.287-304.
- Stanton, R.L., and Rafter, T.A., 1966, The isotopic constitution of sulphur in some stratiform lead-zinc ores : *Mineral Deposita*, v.1, p.16-29.
- Thurlow, J.G., Swanson, E.A., and Strong, D.F., 1975, Geology and lithogeochemistry of the Buchans polymetallic sulphide deposits, Newfoundland : *Econ. Geol.*, v.70, p.130-144.
- Urabe T., Scott, S.D., and Hattori, K., 1983, A comparison of footwall-rock alteration and geothermal systems beneath some Japanese and Canadian volcanogenic massive sulphide deposits : *Econ. Geol. Mon. 5*, p.345-364.
- van de Boon, G., and Washausen, G., 1980, Hydrothermal alteration zones of the Que River volcanic sulphide deposit outlined by mineralogical, petrological and geochemical investigations. Unpubl. Report Federal Institute of Geosciences and Natural Resources (BGR) West Germany.
- Varne, R., and Foden, J.D., 1987, Tectonic setting of Cambrian rifting, volcanism and ophiolite formation in western Tasmania : *Tectonophysics*, v.140, p.275-295.

- Vivallo, W., 1987, Early Proterozoic bimodal volcanism, hydrothermal activity, and massive sulphide deposition in the Boliden - Landal Area, Skellefte District, Sweden : Econ. Geol., v.82, p.440-456.
- Wallace, D.B., 1984, "Developments in the geological understanding of the Que River deposit", in: Baillie, P.W. and Collins, P.L.F., eds., Mineral Exploration and Tectonic Processes in Tasmania. Geol. Soc. Aust. Tasmanian Div., p.55-56.
- Wallace, D.B., and Green, G.R., 1982, Que River mine and aspects of the Mount Read Volcanics in the Pieman River area. in: D.C. Green, ed. Geology, Mineralization, Exploration : Western Tasmania, Nov. 1982. Geol. Soc. Aust., Tasmanian Div., p.52-66.
- Walshe, J.L., and Solomon, M., 1981, An investigation into the environment of formation of the volcanic - hosted Mt. Lyell Copper deposits using geology, mineralogy, stable isotopes, and a six-component chlorite solid solution model. Econ. Geol. v.76, p.246-280.
- Waters, J., 1988, Eruptive activity, products and depositional setting of the cambrian volcanic - sedimentary succession hosting massive sulphide mineralization (VMS) at Hellyer and Que River Mines, Mt. Read Volcanic Belt, Western Tasmania : Unpub. Progress Reports 1, 2 and 3. PhD student Monash Uni, 44p.
- Webb, A.W., 1985, Uranium-lead isotope age determination on the Mt. Charter dolerite AMDEL Limited Adelaide Unpubl. Report to Aberfoyle Resources Ltd, 3p.
- Webster, S.S., and Skey, E.H., 1979, Geophysical and geochemical case history of the Que River deposit Tasmania, Australia. in: P.J. Hood ed., Geophysics and Geochemistry in the Search for Metallic Ores. Geol. Surv. Can., Econ. Geol. Rep., 31:p.697-720.
- Whitford, D.J., and Craven, S.J., 1983, Petrological and geochemical studies at Que River, Part 4 : Unpub. CSIRO, Institute of Energy and Earth Resources, Division of Mineralogy, Restricted Investigation Report 1387R, 26p.
- Whitford, D.J. and Creelman, R.A., 1984, Petrological and geochemical studies at Que River, Part 5: Unpub. CSIRO, Institute of Energy and Earth Resources, Division of Mineralogy, Restricted Investigation Report 1498R, 21p.
- Whitford, D.J., Creelman, R.A. and Ramsden, A.R., 1985, Petrological, geochemical and mineragraphic studies at Que River and Hellyer, Part 6 : Unpub. CSIRO, Institute of Energy and Earth Resources, Division of Mineralogy, Restricted Investigation Report 1544R, 38p.

- Whitford, D.J., Korsch, M.J., Porrit, P.M., and Craven, S.J., 1988, Rare-earth element mobility around the volcanogenic polymetallic massive sulphide deposit at Que River, Tasmania, Australia : *Chemical Geology*, 68 p.105-119.
- Whitford, D.J., Nicholls, I.A., Taylor, S.R., 1979, Spatial variations in the geochemistry of Quaternary lavas across the Sunda arc in Java and Bali. *Contributions to Mineralogy and Petrography* 70 (3), p.341-356.
- Whitford, D.J., Offler, R., Creelman, R.A., Ramsden, A.R., and Skilton, B., 1985, Petrological, geochemical and mineralogical studies at Que River and Hellyer, Part 7 : Unpub. CSIRO, Institute of Energy and Earth Resources, Division of Mineralogy, Restricted Investigation Report 1573R, 33p.
- Whitford, D.J., and Sun, S.S., 1981, Petrological and geochemical studies at Que River, Part 1 : Unpub. CSIRO, Institute of Earth Resources, Division of Mineralogy, Restricted Investigation Report 1234R, 21p.
- Whitford, D.J., Sun, S.S., and Gulson, B.L., 1982, Petrological and geochemical studies at Que River, Part 2 : Unpub. CSIRO, Institute of Energy and Earth Resources, Division of Mineralogy, Restricted Investigation Report 1281R, 26p.
- Whitford, D.J., Sun, S.S., and Togashi, Y., 1982a, Petrological and geochemical studies at Que River, Part 3 : Unpub. CSIRO, Institute of Energy and Earth Resources, Division of Mineralogy, Restricted Investigation Report 1332R, 29p.
- Williams, E., 1978, Tasman fold belt system in Tasmania. *Tectonophysics*, 48, p.159-206.
- Winchester, J.A., and Floyd, P.A., 1977, Geochemical discrimination of different magma series and their differentiation products using immobile elements : *Chemical Geology*, 20 p.325-343.
- Young, C.H., 1980, Que River - A synclinally folded stratiform volcanogenic sulphide deposit. Unpub. Report, Aberfoyle Exploration Pty. Ltd., 23p.

APPENDIX 1

Cross Sections through Stringer Zone Core and Orebody

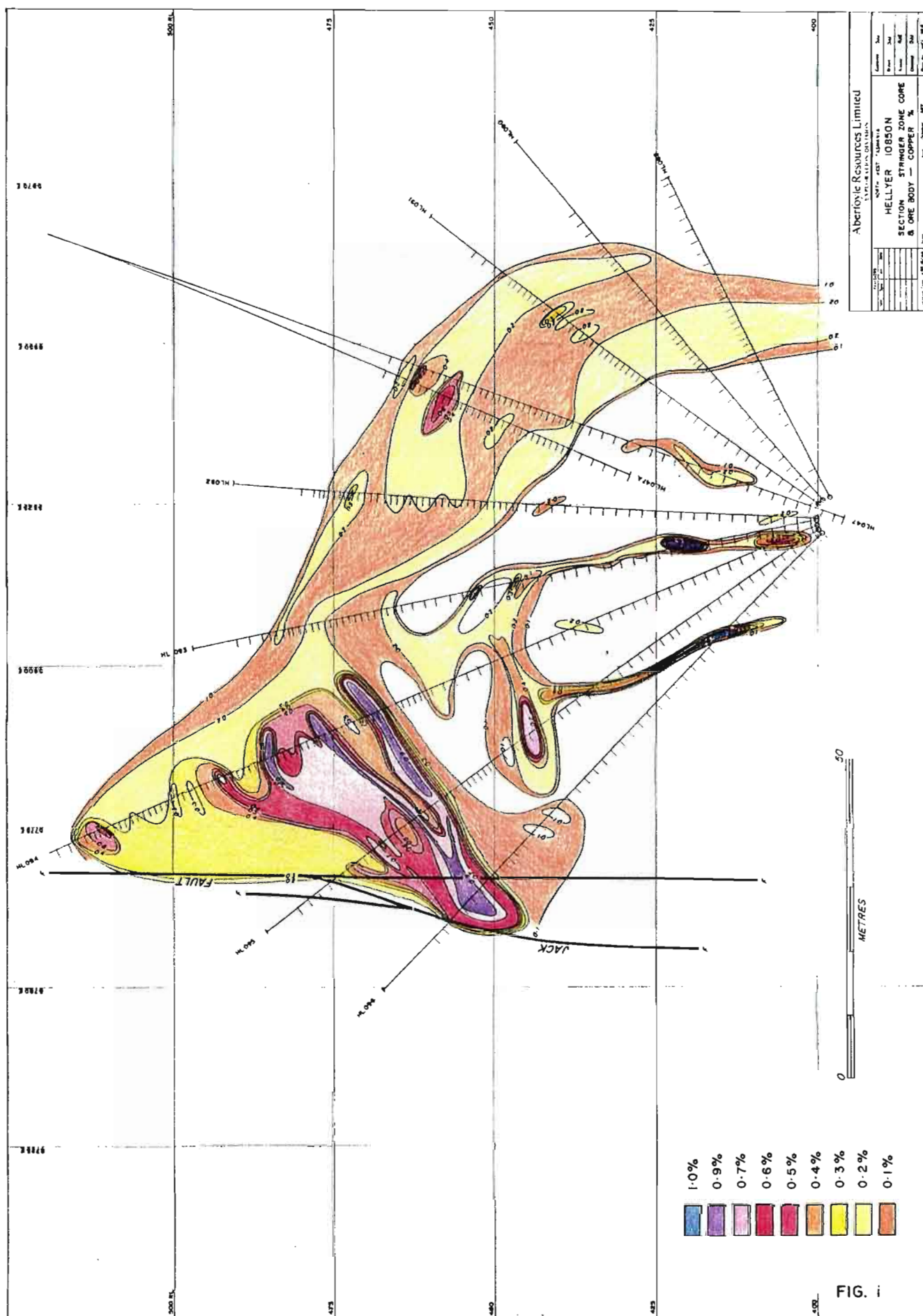


FIGURE 1: Orebody and Upper Stringer Zone- Copper Distribution.
Copper highs are associated with the lower orebody and
the hangingwall gold zone.

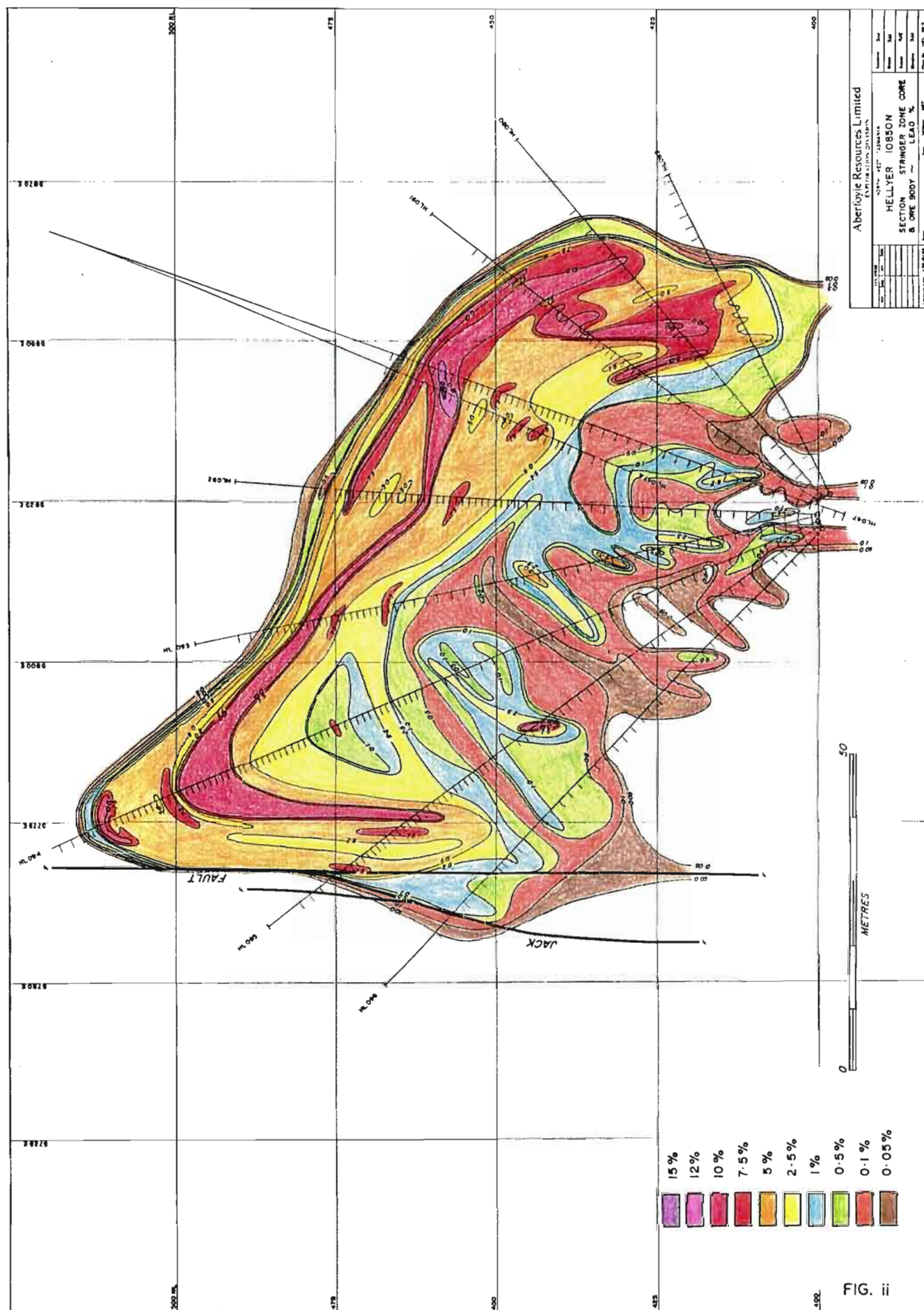


FIGURE ii: Orebody and Upper Stringer Zone- Lead Distribution. Two lead highs are interpreted in the stringer zone. On this section the hydrothermal centre was east of the Jack Fault and a halo of high lead around this is interpreted.

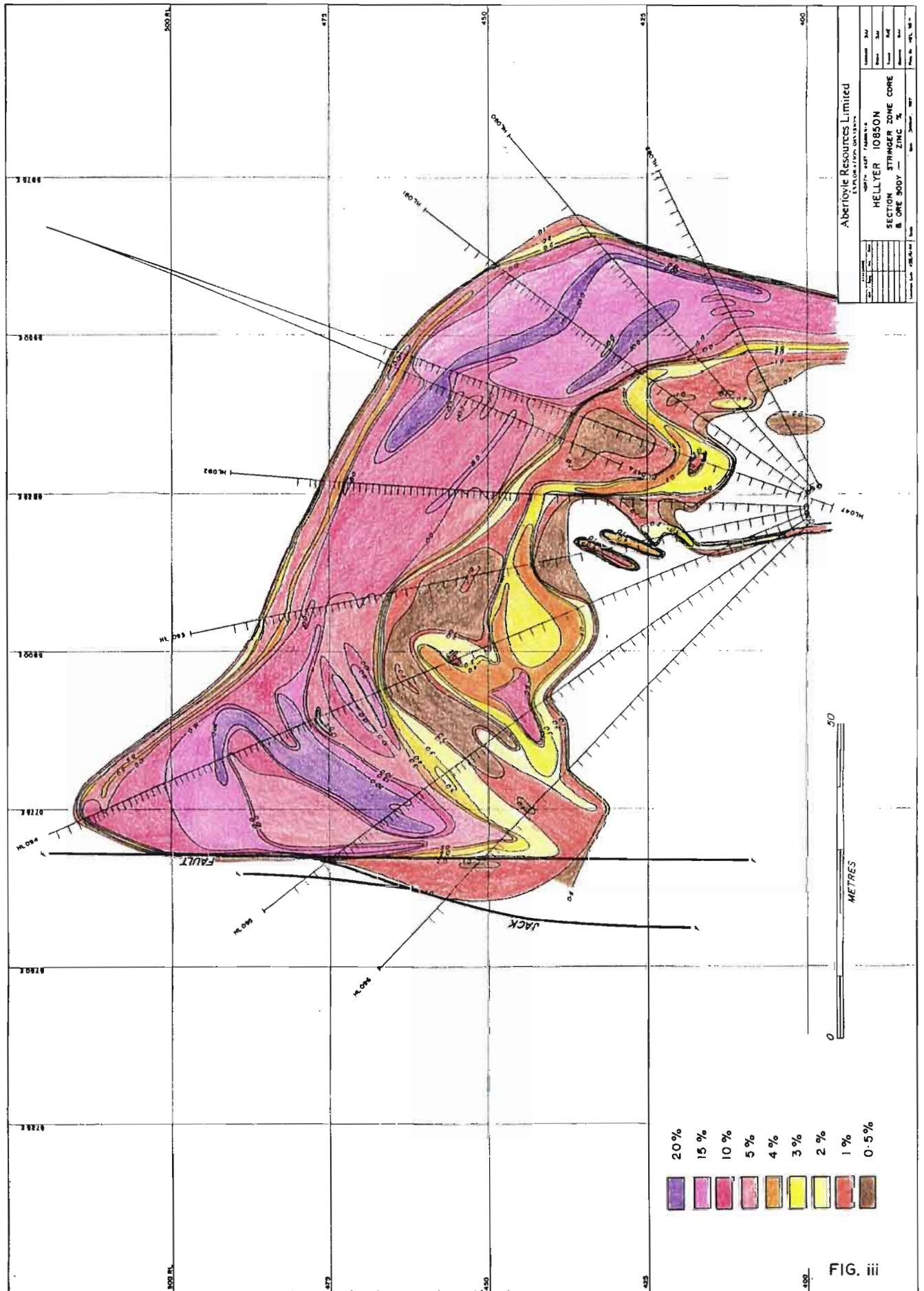


FIGURE iii: Orebody and Upper Stringer Zone- Zinc Distribution. There are two zones of elevated zinc in the upper stringer zone interpreted to be separate feeder zones- see Figure 7.

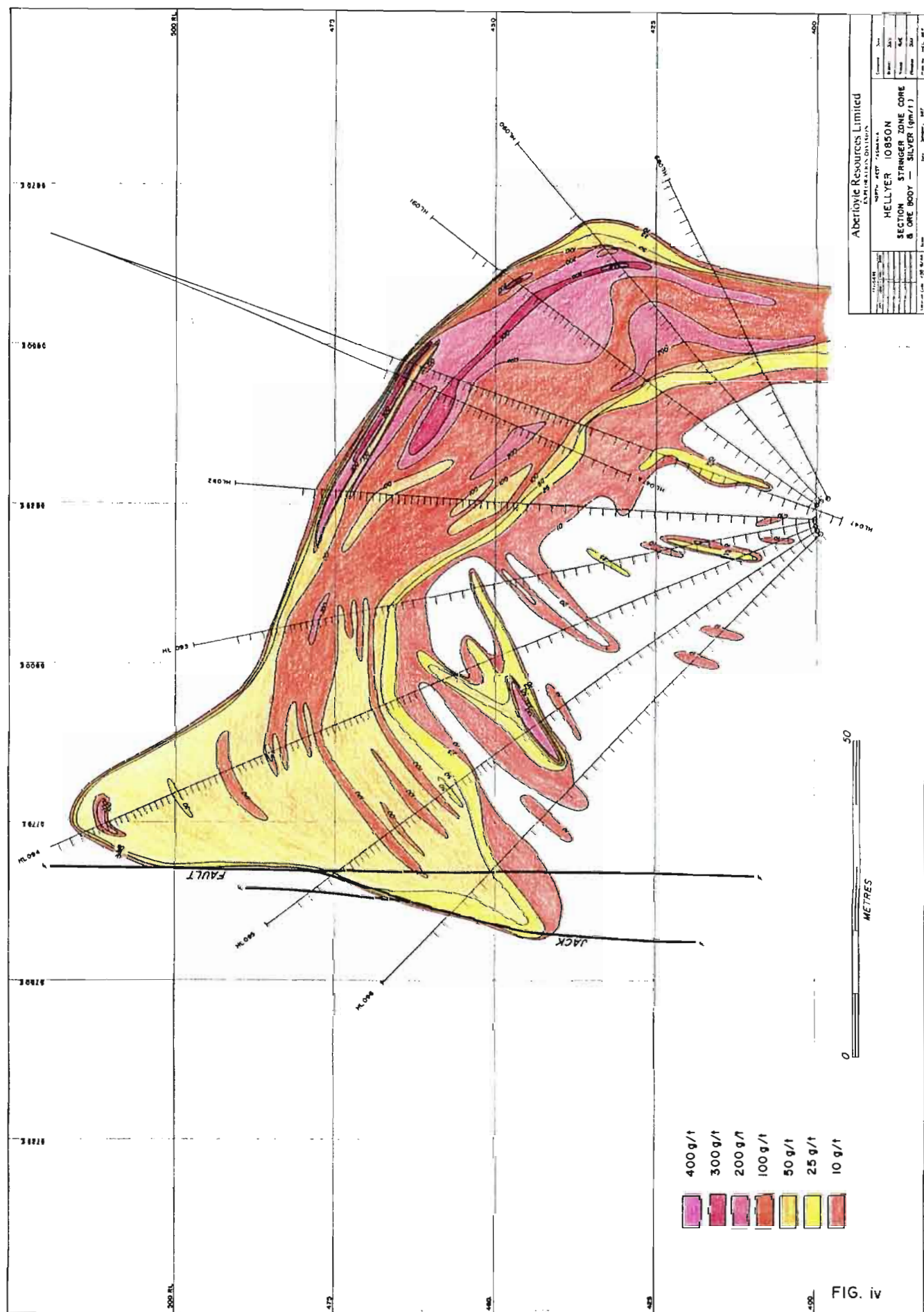


FIGURE iv: Orebody and Upper Stringer Zone- Silver Distribution. Enrichment in the precious metal zone in the Eastern hangingwall of the orebody is the dominant feature.

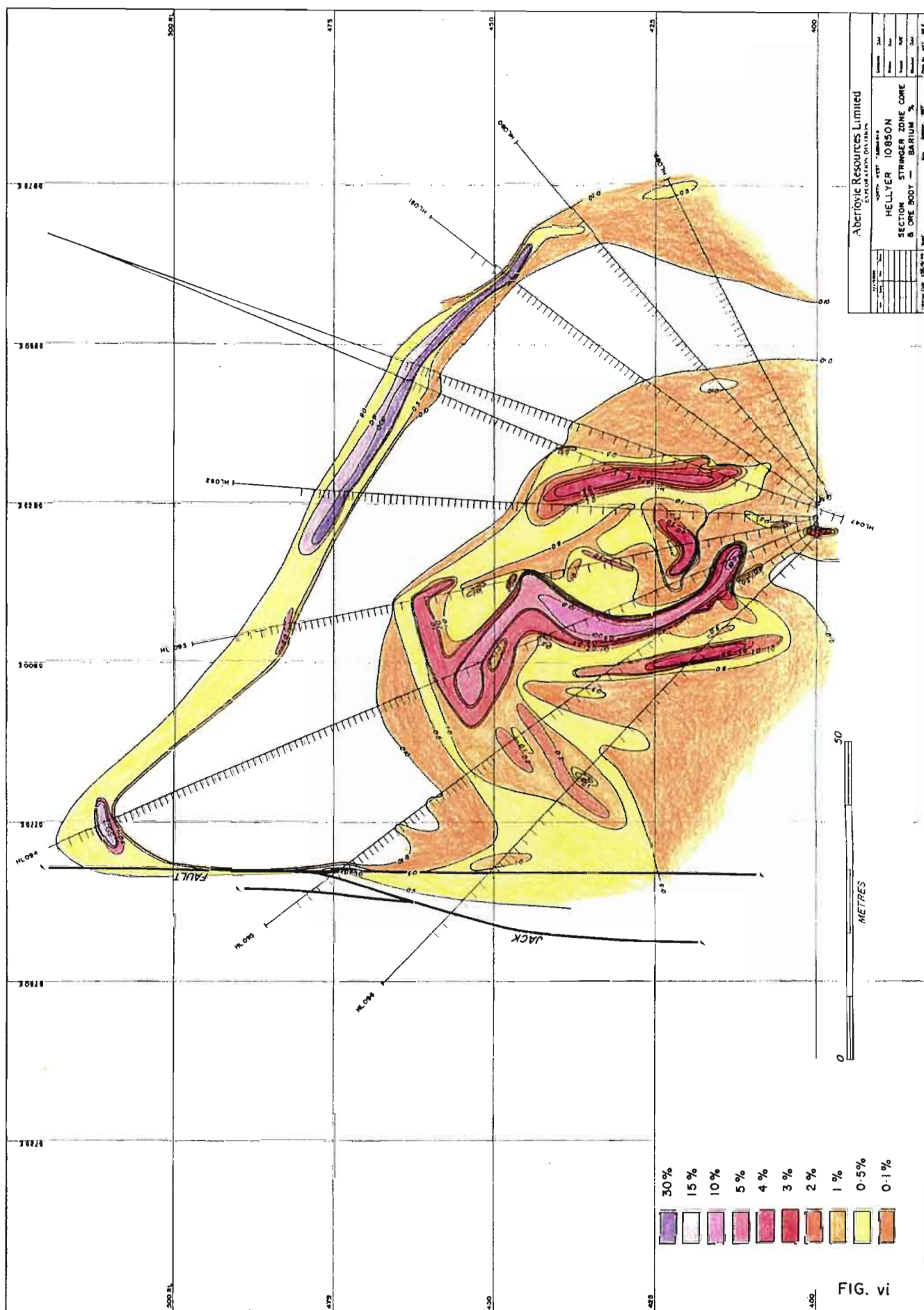


FIGURE vi: Orebody and Upper Stringer Zone- Barium Distribution. Barium is concentrated in the upper stringer zone and at the top of the orebody. There is a barium low in the central part of the orebody.

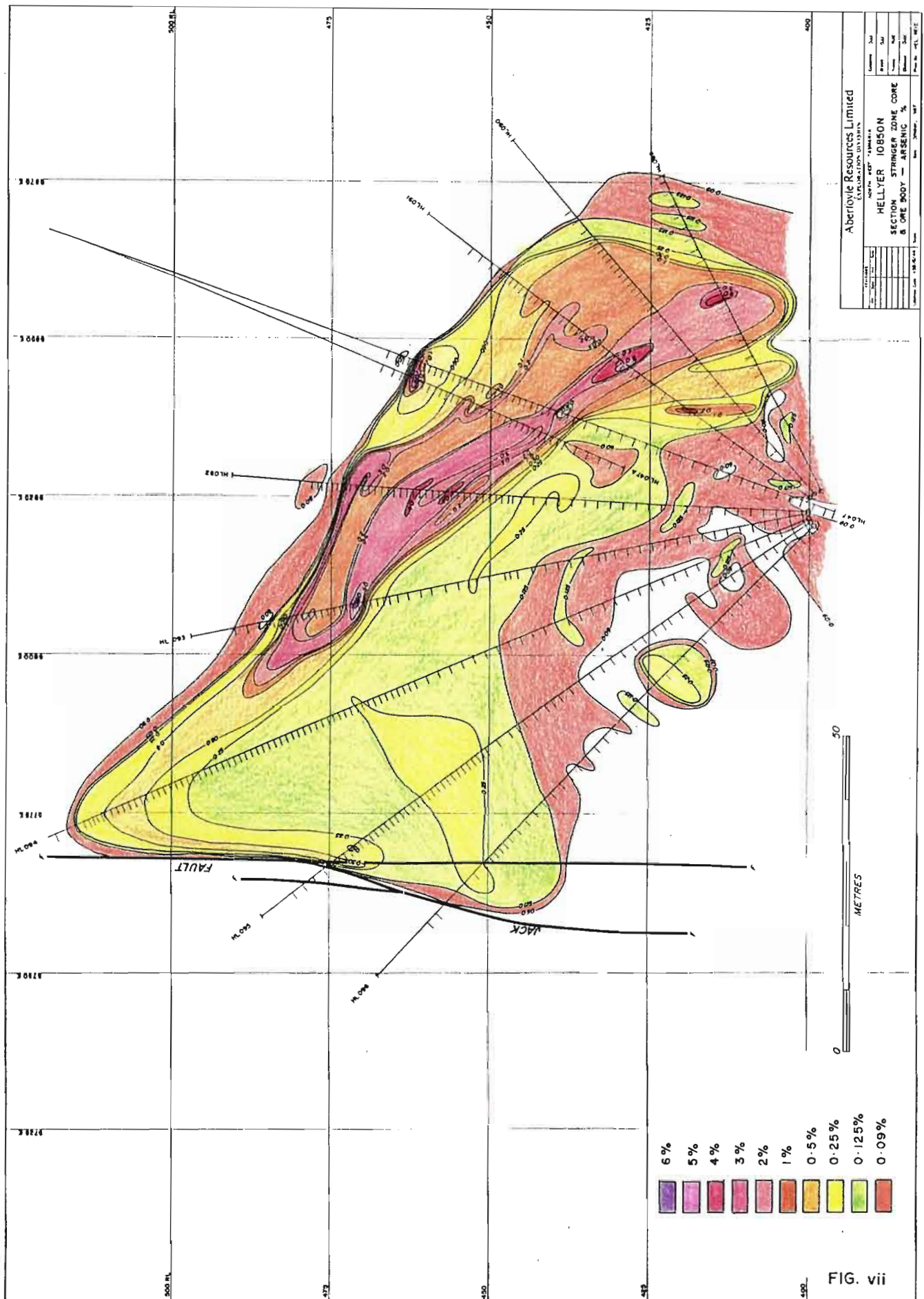


FIGURE vii: Orebody and Upper Stringer Zone- Arsenic Distribution. Arsenic is concentrated in the hangingwall within and more especially just below the precious metal enriched zone.

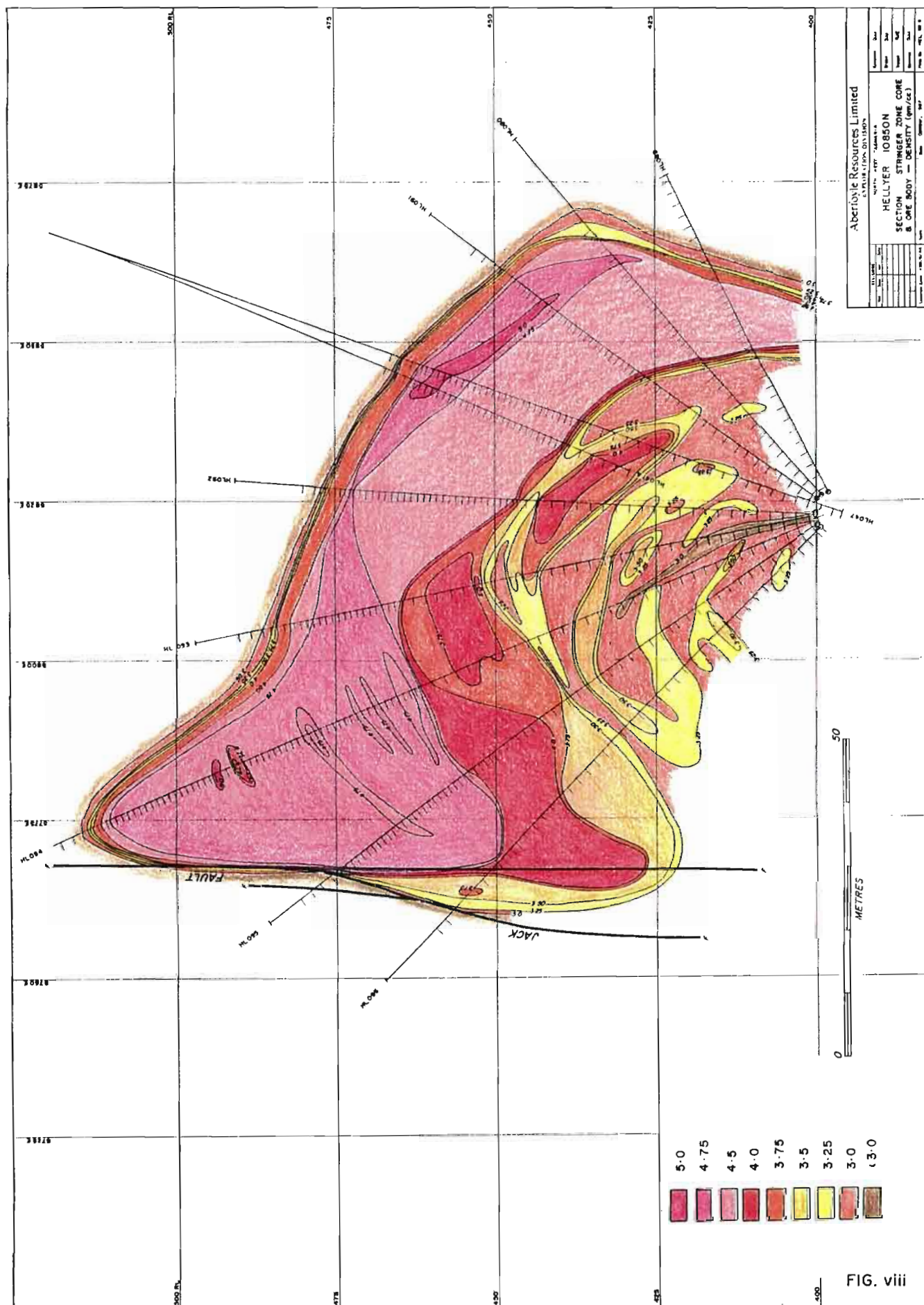


FIGURE viii: Orebody and Upper Stringer Zone- Density Distribution. Density reflects the pyrite content. This is especially high in the lower grade central parts of the orebody.

Appendix 2i

Element Analyses, Holes, Sample Intervals,
Rock Description

Group 1 (URS)

Samp.No	SiO2	TiO2	Al2O3	Fe2O3	MnO	MgO	CaO	Na2O	K2O	P2O5	LOI	HE	Sum	Co	Pb	Zn	Sr	Y	Zr	Ni	Cr	Ba	Sc	La	As	Ag	Rb	V	Nb	S	HOLE	DEPTH	ROCK TYPE	SL
334100	68.73	.56	14.31	6.51	.20	2.30	1.75	2.07	2.73	.11	5.44	99.51	45	32	102	92	31	125	44	50	582	15	36	14	1	199	92	12	.62	HL30	25.6-37.7	Y.R.SH.1	TC	
334101	68.01	.47	16.70	6.40	.13	2.16	1.32	.71	3.63	.10	5.79	99.67	75	58	150	49	38	159	45	53	777	14	52	25	1	140	89	16	.46	HL30	37.9-55.0	Y.R.SH.1	TC	
334102	76.56	.19	15.71	2.80	.03	1.19	.26	.66	3.26	.04	4.05	99.94	6	13	42	42	38	150	6	7	336	5	73	5	1	124	15	19	.15	HL30	55.0-64.5	Y.R.SH.1	TC	
333993	77.61	.10	12.19	1.87	.01	.76	2.00	3.48	1.52	.00	3.52	99.76	9	28	43	200	24	125	1	37	740	1	70	10	1	92	27	12	.26	ADIT	67.2	Y.R.SH.1	HR	
334103	74.91	.24	15.16	1.79	.04	.85	1.47	2.27	2.96	.05	4.19	99.78	19	26	50	171	34	147	8	16	963	5	65	8	1	112	22	16	.35	HL30	64.5-78.9	Y.R.SH.1	TC	
334104	63.50	.45	19.26	5.33	.11	2.42	3.05	.40	4.77	.17	9.12	100.29	55	44	342	95	43	189	30	72	1182	14	64	28	1	173	102	15	1.45	HL30	78.9-83.8	Y.R.SH.1	TC	
334256	69.64	.62	15.61	6.91	.16	1.98	.75	.55	3.92	.16	5.25	100.40	90	52	130	39	46	155	72	110	360	1	85	15	1	120	150	14	.52	HL24	3.0-24.0	BSH.SS.1	AG	
334257	75.00	.22	14.14	1.00	.00	.84	2.12	2.12	3.22	.07	3.06	99.70	25	60	260	74	38	125	16	50	330	1	110	11	1	94	40	14	.18	HL24	24.0-53.4	Y.R.1	AG	
334258	76.77	.28	7.55	3.82	.26	1.75	4.63	.60	2.16	.26	5.85	98.10	3860	74	3340	120	32	60	950	125	250	1	55	31	1	52	85	6	.54	HL24	53.4-54.5	BSH.Y.R.1	AG	
334125	70.90	.52	16.22	5.46	.10	1.55	.78	.47	3.65	.12	5.24	99.81	109	45	183	54	50	163	65	61	675	15	57	16	1	130	110	12	.50	HL31	7.0-20.0	BSH.1	TC	
334126	65.96	.39	17.72	4.75	.10	2.38	3.27	.41	4.66	.16	7.81	99.85	50	21	74	164	40	212	27	50	980	12	72	13	1	171	67	16	.31	HL31	20.0-26.0	BSH.SS.1	TC	
334127	74.43	.22	16.57	1.60	.02	.75	.54	1.20	3.95	.06	4.00	99.46	90	52	124	65	36	149	15	9	934	5	79	8	1	143	21	18	.11	HL31	26.0-31.0	Y.R.1	TC	
334128	73.10	.20	17.36	1.73	.03	1.05	.96	1.10	3.86	.03	4.56	99.47	105	43	127	44	27	160	18	7	896	4	73	4	1	147	16	18	.25	HL31	31.0-34.0	Y.R.1	TC	
334129	71.19	.25	18.54	2.22	.06	.97	.85	.39	4.95	.05	4.90	99.52	179	30	284	38	41	164	27	11	1120	5	96	7	1	177	18	19	.11	HL31	34.0-35.0	BSH.1	TC	
334130	69.43	.20	20.39	1.82	.02	.80	.62	1.42	5.05	.03	4.55	99.57	256	20	243	53	45	198	36	12	1071	5	73	8	1	193	20	24	.13	HL31	35.0-41.5	Y.R.1	TC	
334131	71.00	.25	17.46	2.66	.05	1.15	.96	1.19	4.35	.16	5.39	100.84	186	42	316	135	39	172	21	14	981	5	72	9	1	147	21	18	.36	HL31	41.5-51.5	Y.R.1	TC	
334179	70.05	.14	12.95	1.45	.05	1.04	2.09	.15	3.32	.03	4.44	99.34	6	19	32	180	24	110	1	43	580	1	74	1	1	135	15	11	.09	ADIT	595.0	SS.1	HR	
334180	70.36	.13	12.34	1.42	.05	.96	2.46	.23	3.18	.02	4.49	99.19	4	24	20	79	22	98	1	38	620	1	75	1	1	120	9	11	.07	ADIT	540.0	R.1	HR	
334181	74.50	.42	15.13	3.05	.05	1.02	1.48	.17	3.83	.06	4.31	99.77	23	20	34	49	18	153	14	61	660	11	47	10	1	140	69	8	.35	ADIT	454.0	Y.R.b.m.1	HR	
334182	75.00	.26	12.91	3.18	.09	1.10	3.22	1.32	2.65	.07	5.21	99.93	6	22	26	70	26	150	4	63	575	1	26	1	1	104	32	6	.02	ADIT	430.0	R.ev.1	HR	
334183	70.08	.09	12.34	2.40	.09	.66	2.77	1.56	2.61	.06	4.68	100.62	5	15	20	38	26	130	1	64	250	1	73	11	1	91	4	9	.02	ADIT	392.0	R.1	HR	
334184	77.03	.10	12.23	2.02	.05	.51	1.31	3.74	1.61	.02	2.66	100.26	4	5	23	52	34	130	1	79	210	1	75	17	1	65	3	10	.02	ADIT	310.0	R.1	HR	
334185	72.65	.21	13.98	3.21	.11	.98	4.26	2.56	2.59	.07	6.86	100.67	5	6	23	55	18	140	1	55	280	1	26	11	1	87	28	6	.02	ADIT	237.0	R.1	HR	
334186	72.69	.30	15.18	2.56	.09	.95	2.67	1.16	3.49	.06	5.24	99.10	9	410	2200	33	20	150	1	45	1100	10	30	14	1	130	34	6	.11	ADIT	206.0	SS.1	HR	
334187	67.11	.44	11.98	7.14	.29	2.02	7.44	.30	2.77	.12	10.90	99.64	145	1030	7400	70	24	125	46	86	305	12	24	72	7	100	97	7	.54	ADIT	205.5	BSH.1	HR	
334188	77.50	.18	12.67	2.28	.08	1.29	2.28	.22	3.31	.04	5.03	99.90	8	37	72	34	20	110	5	38	625	1	49	1	1	125	22	9	.07	ADIT	67.0	sed.1	HR	

Group 2 (QRS)

Samp.No	SiO2	TiO2	Al2O3	Fe2O3	MnO	MgO	CaO	Na2O	K2O	P2O5	LOI	HE	Sum	Co	Pb	Zn	Sr	Y	Zr	Ni	Cr	Ba	Sc	La	As	Ag	Rb	V	Nb	S	HOLE	DEPTH	ROCK TYPE	SL
333914	70.34	.68	12.59	6.29	.04	2.75	2.32	.72	2.98	.17	6.25	98.90	100	38	154	64	22	120	106	155	590	1	35	23	2	105	161	8	1.43	HL14	4.6-50.0	BSH.2	AG	
333915	70.46	.65	12.57	6.23	.10	2.66	2.72	.30	3.24	.14	6.15	99.30	73	130	152	58	20	130	100	160	630	1	20	27	1	110	200	8	1.27	HL14	50.0-85.0	BSH.2	AG	
333969	73.39	.66	12.87	5.31	.07	2.00	2.02	.61	2.74	.17	7.65	100.77	71	19	115	55	25	125	65	140	785	15	22	17	1	130	210	11	.95	HL14	49.0	BSH.2	MC	
333970	70.41	.30	10.73	4.04	.08	2.21	1.67	.31	2.39	.12	6.14	100.35	39	25	53	66	24	120	40	88	745	10	41	21	1	10	170	10	.58	HL14	75.01	BSH.2	MC	
334105	71.12	.54	13.34	5.92	.07	2.32	3.15	.03	3.28	.12	8.75	99.95	65	60	176	75	29	140	72	129	738	17	29	29	1	126	140	12	1.64	HL30	83.0-100.0	BSH.2	TC	
333992	71.72	.61	14.48	5.93	.07	2.99	1.51	.61	3.02	.11	7.85	101.11	9	28	43	200	24	125	1	39	740	1	90	10	1	92	27	12	1.14	HL30	120.5	BSH.2	TC	
334106	69.20	.60	13.55	5.96	.06	2.62	4.61	.02	2.96	.13	9.19	99.76	75	46	276	64	33	137	76	142	744	18	26	24	1	119	204	12	1.52	HL30	100.0-150.0	BSH.2	TC	
334107	68.47	.62	12.97	6.93	.06	2.74	4.75	.06	2.69	.15	8.96	99.43	65	40	153	97	30	133	72	135	754	18	20	21	1	110	179	12	1.78	HL30	150.0-186.9	BSH.2	TC	
334066	72.62	.73	13.22	6.67	.03	3.02	.23	.01	2.91	.13	5.24	99.60	56	35	114	24	44	204	70	141	823	20	22	18	1	180	210	19	1.49	HL30	120.5	BSH.2	TC	
334259	68.34	.28	15.77	2.70	.12	1.80	4.09	.03	4.16	.07	6.70	98.50	86	86	420	135	38	140	30	86	470	1	85	36	1	115	65	12	.04	HL24	54.5-57.1	BSH.2	AG	
334260	69.03	.55	13.05	5.45	.07	2.50	2.73	.42	3.51	.14	6.40	97.50	80	215	890	60	34	135	70	135	460	1	55	38	2	105	180	10	1.91	HL24	57.1-100.0	BSH.2	AG	
334261	68.04	.60	12.71	5.92	.35	2.86	3.09	.35	3.18	.12	6.20	99.40	94	52	210	58	32	120	90	145	500	1	65	31	1	96	180	10	1.66	HL24	100.0-150.0	BSH.2	AG	
334262	70.10	.63	12.44	5.90	.09	2.61	3.10	.10	3.21	.11	5.90	98.30	110	185	1140	48	23	125	80	140	490	1	85	68	1	96	180	10	.02	HL24	150.0-176.4	BSH.2	AG	
334132	72.17	.55	13.45	6.50	.08	1.77	.80	.36	3.24	.14	6.90	99.60	104	114	661	37	31	143	75	122	703	17	36	32	1	127	167	11	1.65	HL31	51.5-80.0	BSH.2	TC	
334133	69.80	.61	13.45	6.82	.07	2.33	2.98	.32	3.47	.30	3.62	100.21	145	127	330	51	30	130	86	141	1030	18	32	41	1	123	177	11	2.30	HL31	80.0-102.0	BSH.2	TC	
334178	77.03	.53	13.06	5.21	.02	1.48	.94	.11	3.41	.10	8.45	101.54	28	70	135	29	21	135	70	145	530	12	22	21	1	135	190	8	1.92	ADIT	657.0	BSH.2	MR	
334224	75.74	.53	11.78	5.23	.07	2.90	.52	.00	2.56	.09	4.92	99.60	60	50	155	17	28	115	60	125	690	1	45	21	1	82	220	10	1.08	HL29	136.2	BSH.2	AG	
334264	70.24	.29	9.99	3.10	.12	1.78	8.79	.36	3.10	.04	8.25	97.50	550	32	520	110	26	105	150	135	760	1	85	23	2	72	75	8	1.21	HL24	181.0-183.0	BSH in B2	AG	

Group 3 (D.55 Gnd)

Samp.No	SiO2	TiO2	Al2O3	Fe2O3	MnO	HgO	CaO	Na2O	K2O	P2O5	LOI	ME	Sen	Cu	Pb	Zn	Sr	Y	Zr	Ni	Cr	Ba	Sc	La	As	Ag	Rb	V	Nb	S	HOLE	DEPTH	ROCK TYPE	SL
334001	46.48	.87	16.21	11.78	.25	5.69	15.35	.10	3.26	.45	15.05	99.39	76	41	183	251	27	175	75	733	2376	52	62	27	1	90	317	11	2.77	HL55	64.0-91.2	D.3	TC	
334002	47.00	.94	15.45	11.58	.19	7.73	12.40	2.14	1.91	.41	13.01	100.39	39	27	116	313	27	186	134	711	2764	50	57	9	1	30	336	13	3.54	HL55	91.2-145.0	D.3	TC	
334003	51.92	.74	14.56	9.56	.16	0.71	0.63	2.51	2.10	.28	5.41	99.32	103	37	121	427	24	152	110	559	2150	43	53	52	1	50	272	10	4.37	HL55	145.0-152.0	D.3	TC	
334004	42.01	.58	14.71	8.51	.22	7.73	21.03	3.16	1.04	.19	16.90	100.04	56	34	153	371	21	70	243	1101	1377	44	38	25	1	10	265	4	3.50	HL55	152.0-179.5	D.4	TC	
334005	45.00	.48	14.12	8.32	.23	0.55	19.42	2.40	1.03	.18	13.37	99.77	71	12	82	379	18	63	267	1302	1466	42	37	6	1	23	242	3	2.90	HL55	179.5-210.3	D.4	TC	
334006	39.42	.51	15.99	6.71	.22	3.38	27.66	2.71	2.63	.35	20.50	99.62	69	12	73	327	19	60	225	829	1743	41	37	11	1	60	250	3	4.25	HL55	210.3-225.0	D.4	TC	
334007	37.24	.46	15.25	9.12	.29	2.50	30.02	1.83	3.07	.20	23.36	100.14	73	43	107	223	13	59	210	908	1867	38	36	43	1	75	227	5	3.77	HL55	225.0-233.0	D.4	TC	
334008	47.24	.54	16.17	8.40	.18	6.93	15.77	2.37	1.69	.33	15.76	99.98	85	27	121	307	20	67	219	949	2150	51	36	10	1	47	203	5	3.43	HL55	233.0-241.0	D.4	TC	
334009	40.23	.50	14.80	8.95	.18	10.22	14.47	1.63	1.05	.20	12.50	100.27	80	30	126	323	16	59	210	807	3112	46	30	6	1	29	257	3	2.35	HL55	241.0-250.0	D.4	TC	
334010	52.11	.49	15.63	9.09	.16	5.69	13.20	1.63	1.77	.20	12.69	100.00	61	10	102	200	14	62	200	854	1334	46	29	42	1	57	263	4	2.90	HL55	250.95-259.1	D.4	TC	

Group 4 (D.55 Spt)

Samp.No	SiO2	TiO2	Al2O3	Fe2O3	MnO	HgO	CaO	Na2O	K2O	P2O5	LOI	ME	Sen	Cu	Pb	Zn	Sr	Y	Zr	Ni	Cr	Ba	Sc	La	As	Ag	Rb	V	Nb	S	HOLE	DEPTH	ROCK TYPE	SL
334011	40.34	.59	11.40	9.99	.10	5.94	21.20	.10	1.60	.32	19.10	99.76	59	17	57	291	18	109	77	467	775	30	46	15	1	43	194	7	1.36	HL55	73.5	D.3	TC	
334012	50.50	.67	13.37	8.02	.10	5.56	10.70	.10	2.56	.27	11.97	99.86	68	11	73	195	21	143	93	508	1521	43	60	8	1	77	262	9	2.26	HL55	83.3	D.1P.ch.3	TC	
334013	40.15	.70	13.99	9.51	.17	6.10	15.05	3.50	1.12	.41	15.22	99.63	77	12	72	363	21	130	91	571	1635	40	53	1	1	10	241	9	3.99	HL55	89.3	D.3	TC	
334014	40.67	.67	14.33	8.08	.16	7.60	14.29	2.76	2.12	.42	13.01	99.16	72	8	69	369	23	128	89	527	4734	38	51	5	1	20	201	0	4.21	HL55	92.4	D.3	TC	
334015	52.43	.63	12.85	6.56	.17	7.04	14.00	4.25	.97	.33	10.92	100.17	77	5	71	437	21	134	93	505	1802	33	43	4	1	13	217	10	4.66	HL55	100.05	D.3	TC	
334016	53.47	.65	12.07	9.76	.18	0.71	9.75	1.75	2.37	.20	11.61	99.84	57	10	54	249	20	135	98	545	4753	37	51	8	1	35	249	9	3.65	HL55	100.7	D.1P.3	TC	
334017	60.20	.56	11.02	3.20	.10	1.20	15.56	5.27	1.30	.32	11.96	99.02	83	32	54	355	24	114	67	445	1290	34	40	15	1	16	110	0	5.06	HL55	101.0	D.1P.ab.3	TC	
334018	62.13	.56	11.64	6.95	.13	5.76	6.67	.10	4.67	.16	0.14	98.91	64	12	76	273	15	114	36	453	7162	35	38	11	1	73	105	7	4.29	HL55	102.9	D.co.3	TC	
334019	53.20	.76	15.70	7.09	.13	4.00	11.21	5.00	1.70	.42	10.07	100.29	65	44	61	431	24	153	77	509	2203	42	60	13	1	26	230	10	6.05	HL55	112.0	D.ab.3	TC	
334020	46.30	.74	14.06	15.16	.17	9.53	10.06	1.01	2.26	.29	12.76	99.39	86	26	119	291	21	147	84	519	2601	38	54	25	1	32	297	10	3.55	HL55	116.45	D.1P.cl.3	TC	
334021	50.94	.50	13.50	5.27	.36	2.50	11.41	4.25	2.74	.34	9.06	99.72	86	16	106	440	21	119	51	406	3341	33	53	10	1	39	149	9	6.30	HL55	116.7	D.co.3	TC	
334022	57.07	.64	12.00	10.54	.10	3.44	8.40	2.02	3.04	.31	10.59	100.09	65	70	102	255	18	131	69	460	3056	38	46	24	1	53	198	9	5.25	HL55	123.5	D.1P.ed.3	TC	
334023	52.53	.85	16.07	8.12	.12	0.95	6.97	4.15	1.31	.49	8.40	99.59	100	0	115	427	29	101	110	615	2153	47	70	0	1	19	315	12	5.00	HL55	125.45	D.3	TC	
334024	46.93	.51	13.05	6.77	.17	5.00	22.03	3.39	.00	.31	14.49	99.01	44	4	35	402	19	109	71	371	755	25	46	3	1	16	224	7	3.59	HL55	129.2	D.3	TC	
334025	47.00	.66	13.25	7.03	.17	6.37	10.22	3.77	1.02	.38	14.91	99.69	76	10	49	467	22	131	70	495	697	35	52	7	1	14	219	9	4.00	HL55	129.65	D.3	TC	
334026	45.05	.84	14.62	11.35	.22	12.57	10.02	.05	2.99	.30	9.73	99.74	82	6	110	270	26	173	112	592	5492	42	60	1	1	45	299	12	3.47	HL55	133.7	D.3	TC	
334027	46.14	.04	15.24	9.43	.19	9.00	14.45	3.10	1.65	.55	12.70	100.31	90	9	121	563	20	171	113	654	1334	43	65	5	1	23	297	11	4.22	HL55	141.2	D.3	TC	
334028	52.46	.66	12.01	9.50	.16	10.07	9.02	2.64	1.73	.32	3.40	99.50	115	1	55	655	25	150	103	476	1013	34	57	1	1	20	230	10	4.23	HL55	151.7	D.3	TC	
334029	63.04	.30	14.06	7.96	.44	1.75	1.03	2.76	6.00	.07	4.01	98.74	27	40	26	235	21	147	101	97	4444	10	50	04	1	94	151	9	0.34	HL55	153.6	D.1P.ch.3	TC	
334030	40.95	.47	12.94	5.02	.26	5.31	20.50	4.22	.05	.26	19.61	99.64	44	4	39	426	16	54	193	757	929	25	20	7	1	10	174	3	4.00	HL55	154.2	D.4	TC	
334031	41.64	.30	12.21	6.74	.21	3.05	33.00	1.67	.07	.10	19.91	99.20	83	0	64	100	16	51	107	761	117	23	33	12	1	2	172	3	1.40	HL55	157.05	D.co.vn.4	TC	
334032	44.05	.46	13.40	8.07	.20	9.62	20.10	2.04	.09	.17	13.55	99.06	51	1	63	369	14	55	232	771	1655	31	31	1	1	20	202	4	2.54	HL55	165.5	D.4	TC	
334033	52.62	.40	12.67	5.00	.16	4.04	20.55	3.60	.64	.19	14.62	100.00	50	4	40	342	15	53	192	759	999	29	26	9	1	10	160	5	3.70	HL55	167.1	D.4	TC	
334034	51.92	.72	19.63	1.66	.03	5.26	3.44	3.51	5.17	.19	7.40	99.63	65	41	130	314	16	05	290	1417	5327	64	30	53	1	94	353	7	0.04	HL55	176.0	D.4	TC	
334035	47.70	.46	13.62	7.63	.18	0.02	10.50	1.91	1.20	.10	11.51	99.53	39	1	50	420	15	57	230	040	1247	34	32	1	1	25	190	4	2.76	HL55	183.55	D.4	TC	
334036	50.31	.52	14.61	9.37	.19	12.63	10.10	1.17	1.11	.10	6.06	100.22	71	1	92	334	17	60	311	965	1262	41	42	1	1	29	250	5	2.15	HL55	189.6	D.4	TC	
334037	44.60	.66	17.46	5.64	.23	3.99	19.34	4.10	2.90	.23	16.24	99.45	32	0	53	424	19	00	300	1363	2504	53	37	19	1	71	361	5	6.00	HL55	191.15	D.4	TC	
334038	50.94	.49	13.35	9.25	.17	12.90	10.47	.76	1.02	.14	4.70	99.56	74	3	72	290	16	64	306	922	1258	37	38	1	1	21	226	4	1.71	HL55	193.5	D.4	TC	
334039	40.72	.71	20.03	5.25	.14	2.72	12.06	2.90	5.49	.30	11.76	99.24	04	9	52	290	22	06	276	1261	5052	56	32	10	1	130	309	6	7.00	HL55	198.4	D.4	TC	
334040	40.30	.45	14.99	4.41	.17	.57	22.50	7.39	.39	.21	16.25	99.52	56	6	13	341	14	56	120	030	359	31	30	10	1	9	103	4	6.52	HL55	203.0	D.ab.4	TC	
334041	41.75	.50	17.72	7.57	.23	7.16	20.33	3.12	.92	.23	15.55	99.67	60	1	79	533	14	61	247	967	1133	35	26	0	1	24	261	4	3.42	HL55	207.65	D.4	TC	
334042	42.30	.49	15.94	6.45	.17	4.56	23.07	3.33	1.00	.50	10.37	99.53	56	7	64	304	17	56	193	006	1154	38	34	4	1	57	235	3	4.26	HL55	210.5	D.4	TC	
334043	44.67	.59	10.56	7.10	.15	2.09	10.95	2.35	3.66	.40	16.24	99.47	61	11	56	252	17	73	267	757	2030	51	37	12	1	100	207	6	5.04	HL55	223.35	D.1P.4	TC	
334044	35.71	.32	11.72	11.18	.22	1.07	35.37	2.57	1.06	.21	25.99	100.32	10	19	19	303	11	41	160	022	1312	22	23	11	1	50	169	2	3.31	HL55	227.9	D.co.fun4	TC	
334045	36.70	.74	22.27	2.46	.43	1.64	20.36	.41	5.09	.26	21.01	99.29	01	72	004	150	19	05	200	1307	2053	5	34	142	1	135	325	6	4.90	HL55	232.2	D.1P.4	TC	

Samp.No	SiO2	TiO2	Al2O3	Fe2O3	MnO	MgO	CaO	Na2O	K2O	P2O5	LOI	HE	Sum	Co	Pb	Zn	Sr	Y	Zr	Ni	Cr	Ba	Sc	La	As	Ag	Rb	V	Nb	S	HOLE	DEPTH	ROCK TYPE	SL
334146	48.95	.51	16.85	6.19	.11	4.35	15.52	3.91	1.75	.47	14.15	58.86	41	32	95	353	21	68	239	837	6823	46	34	14	1	42	235	3	4.85	HL55	239.4	D.4	TC	
334147	49.23	.49	15.43	3.43	.14	11.11	11.71	1.53	.80	.17	7.17	99.75	31	1	63	297	16	59	221	721	1788	44	29	3	1	21	258	4	2.48	HL55	247.8	D.4	TC	
334148	52.81	.46	14.92	3.73	.14	7.45	10.71	.97	1.66	.19	11.19	100.17	112	1	159	154	15	56	227	778	2587	44	33	4	1	54	243	3	2.35	HL55	257.5	D.4	IC	

Group 1 S (D.50285724)

Samp.No	SiO2	TiO2	Al2O3	Fe2O3	MnO	MgO	CaO	Na2O	K2O	P2O5	LOI	HE	Sum	Co	Pb	Zn	Sr	Y	Zr	Ni	Cr	Ba	Sc	La	As	Ag	Rb	V	Nb	S	HOLE	DEPTH	ROCK TYPE	SL
334191	45.21	.59	15.44	6.27	.16	8.88	21.23	.68	2.14	.19	17.38	101.84	84	4	88	288	20	58	188	883	1163	1	45	10	1	52	260	2	.82	HL58	243.83	D.4	AC	
334192	42.76	.48	16.18	9.58	.12	11.18	17.48	2.14	.99	.20	15.58	101.88	58	2	78	195	28	54	288	738	768	1	73	4	1	13	258	4	.82	HL58	262.22	D.4	AC	
334193	48.36	.58	17.18	6.39	.14	7.92	14.27	5.64	.13	.19	11.88	100.78	475	5	53	388	22	54	175	888	688	1	58	11	1	1	248	4	.82	HL58	282.9	D.4	AC	
334194	39.26	.46	15.78	6.83	.23	3.56	31.85	.32	3.35	.34	20.98	100.58	62	16	62	245	22	44	155	728	3928	1	45	288	1	78	288	4	.14	HL58	299.89	D.4	AC	
334195	45.59	.38	13.42	8.22	.21	9.55	19.47	1.63	1.19	.19	17.38	99.98	78	8	54	315	18	48	248	1128	358	1	55	18	1	23	188	2	2.24	HL28	137.6	D.4	AC	
334196	55.58	.74	15.93	8.73	.12	8.73	6.86	3.31	.74	.31	9.18	101.88	29	32	748	155	32	155	74	358	358	1	75	17	1	11	188	8	1.87	HL28	145.5	D.3	AC	
334197	53.79	.67	15.14	7.94	.15	11.88	3.81	2.82	.17	.34	18.38	100.98	115	2	78	248	28	145	118	578	248	1	75	1	1	1	218	8	.82	HL28	157.96	D.3	AC	
334198	58.66	.58	13.31	11.99	.11	3.53	4.87	1.91	1.45	.88	9.28	100.68	78	38	62	178	18	64	275	818	1928	1	45	76	1	31	238	2	4.16	HL28	169.61	D.4	AC	
334199	51.95	.63	17.68	8.58	.14	18.76	5.76	4.99	.88	.28	8.85	100.78	88	2	88	395	24	76	288	1888	238	1	65	1	1	1	268	4	.86	HL28	178.32	D.4	AC	
334200	49.85	.47	14.18	6.69	.22	7.53	19.36	2.16	.31	.19	16.58	100.98	44	22	54	388	22	58	178	828	278	1	25	11	1	1	288	6	.16	HL28	173.32	D.4	AC	
334201	43.89	.45	13.31	7.58	.28	11.81	20.38	2.18	1.88	.19	13.88	101.88	76	18	82	428	22	58	288	838	4688	1	65	1	1	18	228	4	.82	HL28	187.96	D.4	AC	
334212	51.42	.44	13.47	8.32	.14	2.57	2.12	1.52	.54	.15	11.88	100.78	88	2	62	195	18	52	238	818	1388	1	56	1	1	5	228	4	.82	HL28	288.27	D.4	AC	
334213	51.35	.46	14.33	7.75	.13	13.16	11.82	1.39	1.88	.18	6.68	100.58	18	4	58	318	22	58	198	788	918	1	65	1	1	19	238	4	.82	HL28	228.87	D.4	AC	
334214	48.97	.68	22.88	4.62	.26	2.94	22.73	.63	5.47	.48	17.98	100.88	68	2	36	158	22	78	225	1188	2368	1	78	22	1	118	298	2	.12	HL28	234.63	D.4	AC	
334215	48.62	.43	14.19	7.39	.14	9.16	18.45	.31	1.95	.16	15.68	100.88	86	2	88	188	28	42	175	668	1588	1	55	6	1	38	228	2	.82	HL28	249.14	D.4	AC	
334216	37.18	.78	23.36	6.78	.36	3.37	22.63	.12	5.92	.34	18.48	100.88	135	128	225	288	22	76	198	1148	6888	1	98	225	1	148	318	4	.21	HL28	265.76	D.4	AC	
334217	56.86	.51	14.84	8.51	.14	15.92	3.84	.76	.91	.16	9.65	100.98	62	18	98	185	22	68	225	838	1828	1	66	18	1	18	228	4	.82	HL57	222.53	D.4	AC	
334218	51.48	.49	13.82	8.53	.14	18.98	12.93	1.41	.94	.14	18.48	100.88	74	2	68	215	22	56	235	828	1448	1	65	48	1	7	218	4	.82	HL57	229.19	D.4	AC	
334219	54.48	.59	15.67	9.81	.11	3.84	9.47	4.55	.62	.25	11.38	99.68	84	1188	295	165	6	74	315	1828	698	1	45	135	4	37	266	6	5.36	HL57	245.43	D.4	AC	
334220	52.25	.43	14.35	8.65	.15	12.48	9.96	1.16	1.22	.17	8.88	100.98	84	2	66	175	22	58	185	668	1968	1	78	5	1	24	248	4	.85	HL57	271.3	D.4	AC	
334211	48.62	.44	14.26	7.57	.15	9.58	16.89	3.21	.73	.17	12.58	100.98	88	28	68	478	22	44	175	718	2548	1	85	2	1	3	218	2	.15	HL57	286.82	D.4	AC	
334212	58.94	.44	14.57	8.23	.13	18.95	12.79	1.66	1.86	.17	18.28	101.88	92	2	62	178	24	46	175	648	1848	1	65	2	1	21	228	2	.82	HL57	296.5	D.4	AC	
334213	47.39	.45	15.11	8.58	.15	14.15	11.19	1.51	.86	.18	8.88	99.88	185	8	84	495	28	52	185	748	3388	1	78	13	1	6	218	6	.82	HL57	345.14	D.4	AC	
334214	51.34	.43	14.26	7.82	.19	18.16	12.92	3.68	.61	.17	11.18	100.98	39	2	68	68	14	2	135	38	1388	1	35	2	1	1	158	2	.82	HL57	312.88	D.4	AC	
334215	49.37	.47	15.48	7.78	.28	9.96	13.13	4.47	.38	.19	11.88	100.98	94	24	215	458	22	52	198	728	1848	1	65	52	1	1	238	2	.82	HL57	317.68	D.4	AC	
334216	89.97	.82	1.43	.61	.87	.54	7.67	.18	.28	.83	6.25	100.88	138	32	12	468	28	46	8	678	2688	1	58	28	1	1	18	2	.86	HL57	322.25	D.4	AC	
334217	44.93	.58	18.58	6.15	.23	4.52	19.24	3.49	2.48	.34	14.98	100.98	158	2	49	538	22	68	198	848	2988	1	68	13	1	1	268	6	.82	HL57	217.43	D.4	AC	
334218	48.11	.52	16.77	8.33	.25	18.11	11.77	4.42	.38	.28	18.18	100.98	19	6	155	218	22	62	288	968	1338	1	55	1	1	56	248	4	.82	HL24	232.62	D.4	AC	
334219	48.31	.49	16.36	9.14	.16	13.65	7.42	2.73	.29	.19	11.58	100.88	185	14	98	288	22	56	288	768	578	1	68	1	1	1	258	2	.82	HL24	246.1	D.4	AC	
334220	52.99	.52	17.88	7.45	.14	7.89	9.27	4.57	.17	.15	9.45	100.28	17	92	138	255	28	62	235	838	558	1	35	96	1	1	288	2	.41	HL24	249.31	D.4	AC	
334221	41.58	.58	19.96	8.69	.15	18.51	14.88	3.26	1.13	.21	15.18	100.98	288	8	148	228	22	64	235	878	1228	1	58	318	1	18	278	2	.82	HL24	252.8	D.4	AC	
334223	45.82	.67	14.32	11.31	.17	7.84	14.89	.84	1.62	.22	11.58	95.48	758	14	738	155	28	125	235	448	788	1	68	28	1	38	218	8	3.58	HL24	176.4-181.8	D.4	AC	
334265	45.84	.49	11.84	14.18	.16	6.55	12.24	.83	.87	.26	7.75	98.88	475	338	2848	145	22	98	188	435	278	1	88	54	2	7	168	6	6.78	HL24	183.8-187.9	D.4	AC	
334266	46.43	.57	15.67	8.55	.28	8.81	16.83	.81	1.88	.16	15.48	97.58	38	128	768	225	22	66	225	888	548	1	65	58	1	11	248	4	1.88	HL24	187.9-199.5	D.4	AC	
334267	44.79	.48	14.93	8.19	.28	4.66	21.68	.88	3.85	.19	17.38	98.28	94	1	76	225	16	38	218	778	788	1	75	24	1	62	258	4	.35	HL24	199.5-203.9	D.4	AC	
334268	45.81	.47	14.68	7.42	.19	9.32	18.48	2.22	.88	.17	15.68	98.78	138	6	82	275	22	38	198	728	1148	1	65	1	2	5	228	4	.14	HL24	203.9-211.2	D.4	AC	
334269	48.68	.49	15.58	6.78	.26	4.77	25.58	2.13	2.18	.18	18.88	98.28	88	1	72	238	28	38	288	688	1188	1	58	17	1	43	248	1	.25	HL24	211.2-223.8	D.4	AC	
334270	43.37	.47	14.53	7.62	.21	8.34	19.54	3.43	.42	.22	15.88	98.28	92	42	155	358	16	36	195	698	1268	1	68	35	1	1	228	4	.18	HL24	228.8-251.6	D.4	AC	
334271	37.59	.38	11.86	9.57	.19	6.84	18.88	1.88	1.58	.16	9.38	87.18	1828	1858	2-522	268	2	56	168	748	2548	1	68	588	18	45	188	6	5.95	HL24	251.6-253.9	D.4	AC	

Group 1 S (D.14 Gnd)

Samp.No	SiO2	TiO2	Al2O3	Fe2O3	Mn
---------	------	------	-------	-------	----

Samp.No	SiO2	TiO2	Al2O3	Fe2O3	MnO	MgO	CaO	Na2O	K2O	P2O5	LOI	HE	Sum	Co	Pb	Zn	Sr	Y	Zr	Ni	Cr	Ba	Sc	La	As	Ag	Rb	V	Nb	S	HOLE	DEPTH	ROCK TYPE	SL
333917	42.12	.41	14.59	18.83	.11	7.82	9.69	.42	2.69	.10	9.85	76.00	92	16	93	220	4	.60	290	930	870	1	10	36	2	80	210	2	8.85	HL14	89.6-92.3	D.5	AC	
333918	47.94	.33	12.32	12.51	.16	7.77	10.76	1.14	1.70	.10	7.65	95.10	124	8	101	246	2	.53	296	940	570	1	31	23	1	56	213	2	4.45	HL14	92.3-112.0	D.5	AC	
333919	49.22	.35	14.53	9.50	.16	7.72	11.79	.41	1.91	.37	12.50	78.90	165	4	130	255	14	135	186	340	570	1	35	13	1	54	260	8	.27	HL14	112.0-110.3	D.5	AC	
333920	51.70	.78	14.35	13.10	.41	11.23	4.38	.33	1.60	.22	9.85	78.40	224	6	238	62	16	135	211	630	510	1	30	10	1	52	245	4	.66	HL14	110.3-121.3	D.5	AC	
333921	48.86	.69	12.76	10.17	.17	7.86	11.41	2.43	1.17	.24	9.68	78.10	173	26	142	245	12	136	171	560	330	1	45	7	1	42	243	4	.61	HL14	121.3-144.3	D.5	AC	
333922	47.79	.77	13.35	11.59	.24	10.04	10.92	1.75	1.43	.35	9.25	78.30	144	140	274	266	12	150	151	570	1940	1	25	52	2	45	242	4	1.13	HL14	144.3-137.3	D.5	AC	
333923	47.33	.77	14.85	10.60	.16	11.16	9.89	.52	2.03	.27	10.20	78.00	164	20	111	205	14	140	138	570	2630	1	50	36	2	54	240	6	.14	HL14	187.0-189.0	D.5	AC	
333924	46.58	.83	13.34	9.67	.18	10.33	13.89	2.89	1.32	.41	10.00	99.50	154	14	119	270	16	160	130	540	2300	1	65	40	1	33	255	8	.15	HL14	189.0-197.0	D.5	AC	
333925	53.47	.53	14.67	15.21	.83	2.36	5.88	2.75	3.65	.16	7.85	98.20	156	44	185	130	10	115	183	230	1200	1	20	215	1	120	170	6	9.15	HL14	199.0-231.0	D.5	AC	
333926	47.11	.55	15.74	8.49	.12	7.81	14.25	4.22	1.12	.20	12.20	98.90	84	2	111	240	10	58	297	990	520	1	10	43	2	38	222	2	.94	HL14	201.0-213.0	D.5	AC	
333927	45.85	.51	14.53	8.22	.18	9.52	16.11	4.01	.42	.10	11.20	99.60	82	2	97	395	20	54	290	860	820	1	25	34	1	16	217	2	.85	HL14	213.0-223.0	D.5	AC	
333928	52.71	.57	17.20	8.55	.10	5.89	7.52	4.84	1.71	.10	7.55	99.20	188	46	201	320	8	70	259	840	990	1	30	37	2	58	266	2	.88	HL14	223.0-225.4	D.5	AC	

Group 7 (D.AMIRA20)

Samp.No	SiO2	TiO2	Al2O3	Fe2O3	MnO	MgO	CaO	Na2O	K2O	P2O5	LOI	HE	Sum	Co	Pb	Zn	Sr	Y	Zr	Ni	Cr	Ba	Sc	La	As	Ag	Rb	V	Nb	S	HOLE	DEPTH	ROCK TYPE	SL
334162	55.60	.77	18.60	10.50	.23	4.60	3.08	4.12	1.93	.57	3.99	100.00	50	33	224	595	302	187	17	5	3407	31	47	24	1	46	237	11	.02	HL6	208.4	D.5	TC	

Group 8 (D.Licence)

Samp.No	SiO2	TiO2	Al2O3	Fe2O3	MnO	MgO	CaO	Na2O	K2O	P2O5	LOI	HE	Sum	Co	Pb	Zn	Sr	Y	Zr	Ni	Cr	Ba	Sc	La	As	Ag	Rb	V	Nb	S	HOLE	DEPTH	ROCK TYPE	SL
334164	52.57	.49	13.78	9.72	.14	10.16	9.51	2.63	.55	.22	11.14	99.87	76	1	90	228	24	135	151	544	288	32	50	1	1	13	182	9	.02	HAI5	418.0	D.L.6	TC	
334165	63.24	.35	12.72	5.86	.12	5.26	6.92	4.22	.72	.17	7.41	99.63	27	15	86	225	22	112	140	519	337	25	37	3	1	15	138	8	.31	HAI5	305.1	D.L.6	TC	
334166	49.43	.57	13.87	9.70	.15	11.84	10.98	1.11	1.12	.68	4.74	99.49	85	9	74	536	31	188	223	961	2106	30	105	1	1	26	247	7	.22	HAI1	87.0	D.U.6	TC	
334167	53.34	.57	16.82	9.90	.18	5.64	8.02	4.85	.92	.30	9.12	99.73	91	3	85	310	18	64	68	200	452	44	43	1	1	30	340	3	.02	HAI5	173.3	D.U.6	TC	
334168	44.11	.65	15.64	13.75	.27	13.89	9.55	.86	.36	.28	12.35	97.06	6	7	176	125	33	192	235	754	293	41	72	1	1	21	191	13	.02	HAI5	345.0	D.L.6	TC	
334169	59.08	.47	12.94	6.81	.22	6.87	8.76	5.48	.11	.19	4.90	100.14	43	516	382	474	20	124	119	494	445	28	45	8	1	2	177	8	.02	HAC4	97.5	D.U.6	TC	
334170	61.46	.48	12.86	7.41	.15	6.67	7.43	2.90	.08	.17	8.72	99.66	17	78	441	218	19	122	111	515	154	30	46	4	1	25	224	2	.02	HAC4	113.6	D.U.6	TC	

Group 9 (D.Fu HL5)

Samp.No	SiO2	TiO2	Al2O3	Fe2O3	MnO	MgO	CaO	Na2O	K2O	P2O5	LOI	HE	Sum	Co	Pb	Zn	Sr	Y	Zr	Ni	Cr	Ba	Sc	La	As	Ag	Rb	V	Nb	S	HOLE	DEPTH	ROCK TYPE	SL
334171	37.67	.65	22.74	1.90	.34	1.84	28.37	.10	6.52	.35	21.51	99.62	90	5	45	210	18	73	203	1878	4865	59	34	222	1	136	365	4	.16	HL5	284.5	D.fu.4	TC	

Group 10 (D.Adlt)

Samp.No	SiO2	TiO2	Al2O3	Fe2O3	MnO	MgO	CaO	Na2O	K2O	P2O5	LOI	HE	Sum	Co	Pb	Zn	Sr	Y	Zr	Ni	Cr	Ba	Sc	La	As	Ag	Rb	V	Nb	S	HOLE	DEPTH	ROCK TYPE	SL
334172	54.44	.70	14.58	8.34	.11	5.63	13.35	.10	2.06	.34	13.64	99.60	25	10	87	147	24	141	47	371	558	39	31	5	1	49	237	8	1.39	ADIT	697.0	D.7	HR	
334174	54.87	.74	14.62	9.87	.11	6.75	11.73	.10	1.57	.28	13.20	99.75	27	9	84	198	25	149	47	339	417	37	49	5	1	43	230	9	1.07	ADIT	717.0	D.pc.7	HR	
334177	56.22	.68	14.98	6.58	.12	5.17	12.33	.44	2.35	.29	12.82	99.23	30	10	48	225	20	140	34	425	596	33	42	1	7	79	245	8	1.10	ADIT	719.0	D.7	HR	
334175	52.10	.76	15.76	11.00	.11	7.70	10.57	.10	1.45	.30	12.47	100.00	31	5	98	148	26	157	55	399	400	42	49	5	1	38	257	10	.90	ADIT	737.0	D.7	HR	
334176	49.85	.73	15.69	8.38	.17	7.39	13.55	2.86	.56	.39	12.73	98.82	37	7	97	415	19	145	45	415	470	37	39	1	6	34	265	8	.51	ADIT	755.0	D.7	HR	
333999	48.74	.77	15.26	8.08	.19	8.67	13.24	3.39	.55	.39	11.28	99.33	42	5	83	605	16	140	57	495	720	35	42	1	1	25	265	8	.74	ADIT	782.0	D.7	HR	
333998	34.60	.41	6.32	31.47	.22	4.36	23.41	1.80	.35	.35	20.87	105.27	54	74	135	275	6	60	41	390	275	28	25	41	8	43	165	1	14.30	ADIT	790.0	D.7	HR	
333997	58.88	.46	12.23	5.64	.13	3.73	10.15	1.73	2.79	.25	6.45	96.04	64	7	65	265	13	125	67	475	3853	26	45	1	1	82	195	4	.57	ADIT	805.0	D.gy.7	HR	
333996	55.77	.63	15.15	9.55	.17	6.73	8.00	1.13	3.34	.31	11.87	101.64	90	10	93	230	15	160	66	590	2650	34	72	1	5	110	255	8	.15	ADIT	805.0	D.gn.7	HR	
333995	52.54	.56	13.47	6.64	.16	5.35	15.33	3.19	1.70	.53	12.56	98.81	61	11	89	365	17	130	80	638	1134	32	42	1	7	53	245	6	.77	ADIT	823.0	D.pc.7	HR	

Samp.No	SiO2	TiO2	Al2O3	Fe2O3	MnO	H2O	CaO	Na2O	K2O	P2O5	LOI	ME	Sum	Cu	Pb	Zn	Sr	Y	Zr	Ni	Cr	Ba	Sc	La	As	Ag	Rb	V	Mb	S	HOLE	DEPTH	ROCK TYPE	SL
333994	49.96	.74	21.83	13.65	.84	1.77	2.55	.3810	0.01	1.14	11.21	101.44	110	32	87	240	33	170	23	110	8450	39	94	87	1	265	480	6	7.30	ADIT	857.0	D.tfd.Py.7 HR		

Group 0 11 (Picrite)

Samp.No	SiO2	TiO2	Al2O3	Fe2O3	MnO	H2O	CaO	Na2O	K2O	P2O5	LOI	ME	Sum	Cu	Pb	Zn	Sr	Y	Zr	Ni	Cr	Ba	Sc	La	As	Ag	Rb	V	Mb	S	HOLE	DEPTH	ROCK TYPE	SL
272844	56.18	.36	12.62	7.75	.14	8.49	11.34	1.36	1.40	.14	12.20	99.84	55	3	70	245	14	55	239	1897	5300	40	24	3	1	25	224	2	1.46	HL7	66.4	D.parich.5 TC		

Group 0 12 (D.HL31 Spt)

Samp.No	SiO2	TiO2	Al2O3	Fe2O3	MnO	H2O	CaO	Na2O	K2O	P2O5	LOI	ME	Sum	Cu	Pb	Zn	Sr	Y	Zr	Ni	Cr	Ba	Sc	La	As	Ag	Rb	V	Mb	S	HOLE	DEPTH	ROCK TYPE	SL
334049	51.32	.55	15.17	4.26	.21	1.90	18.16	7.05	.37	.47	12.70	99.78	185	560	327	466	26	128	17	11	490	22	59	10	1	10	198	9	.14	HL31	316.15	D.ab.8 TC		

Group 0 13 (D.HL38 Spt)

Samp.No	SiO2	TiO2	Al2O3	Fe2O3	MnO	H2O	CaO	Na2O	K2O	P2O5	LOI	ME	Sum	Cu	Pb	Zn	Sr	Y	Zr	Ni	Cr	Ba	Sc	La	As	Ag	Rb	V	Mb	S	HOLE	DEPTH	ROCK TYPE	SL
334067	52.35	.68	16.96	11.86	.11	5.72	8.28	3.39	1.22	.39	11.12	100.22	44	16	82	239	22	149	74	629	534	46	54	17	1	41	292	10	2.66	HL38	188.0	D.5 TC		
334068	48.87	.58	13.64	8.89	.18	7.69	17.28	2.06	.70	.30	15.38	100.17	80	1	66	357	17	114	120	581	450	72	46	1	1	23	245	6	.81	HL38	204.4	D.5 TC		
334069	52.72	.49	13.10	8.86	.17	7.63	13.59	2.13	.50	.28	13.35	99.53	61	6	113	374	18	113	129	554	470	73	41	5	1	16	231	7	.13	HL38	210.1	D.5 TC		
334070	50.21	.50	12.31	7.26	.18	6.68	20.78	.56	1.51	.34	17.17	100.39	98	1	57	243	15	112	93	516	749	39	42	4	1	40	235	5	.33	HL38	243.0	D.5 TC		
334071	53.62	.60	13.82	9.83	.18	9.29	9.74	1.26	1.83	.35	9.27	99.77	98	15	71	290	21	148	82	489	1838	45	48	4	1	32	266	9	.63	HL38	268.5	D.5 TC		
334072	71.35	.31	15.13	3.58	.04	1.94	2.98	.71	3.92	.85	5.37	99.97	17	13	79	47	33	221	19	32	1233	9	65	22	1	151	51	14	.77	HL38	274.5	D.pcp.MOPS TC		

Group 0 14 (D.HL38 Gnd)

Samp.No	SiO2	TiO2	Al2O3	Fe2O3	MnO	H2O	CaO	Na2O	K2O	P2O5	LOI	ME	Sum	Cu	Pb	Zn	Sr	Y	Zr	Ni	Cr	Ba	Sc	La	As	Ag	Rb	V	Mb	S	HOLE	DEPTH	ROCK TYPE	SL
334100	48.57	.55	14.90	16.25	.15	6.10	15.93	1.51	1.43	.32	16.60	99.61	65	40	153	353	21	125	182	572	884	39	45	21	1	49	249	7	2.55	HL38	186.7-200.0	D.5 TC		
334109	50.69	.55	13.88	9.42	.17	8.27	15.45	1.16	.87	.32	15.15	100.43	102	14	182	320	19	121	127	683	541	40	47	4	1	27	258	7	.25	HL38	200.0-263.0	D.5 TC		
334119	52.37	.58	13.56	9.34	.17	7.67	12.94	1.72	.98	.37	13.02	100.24	115	15	96	299	21	142	85	420	776	42	53	11	1	36	261	8	1.20	HL38	263.0-272.4	D.5 TC		

Group 0 15 (D.HL31 Gnd)

Samp.No	SiO2	TiO2	Al2O3	Fe2O3	MnO	H2O	CaO	Na2O	K2O	P2O5	LOI	ME	Sum	Cu	Pb	Zn	Sr	Y	Zr	Ni	Cr	Ba	Sc	La	As	Ag	Rb	V	Mb	S	HOLE	DEPTH	ROCK TYPE	SL
334174	47.18	1.35	20.36	9.22	.12	2.82	12.28	.57	5.14	.56	15.23	99.35	245	43	341	196	33	211	92	828	2839	68	68	37	1	129	359	13	3.32	HL31	182.0-185.0	D.8 TC		
334135	45.76	.73	14.81	10.41	.14	8.04	15.76	1.42	1.71	.37	16.46	99.37	87	15	99	268	24	147	96	691	1277	43	61	10	1	68	388	13	1.87	HL31	185.0-126.0	D.8 TC		
334136	46.29	.97	16.65	10.88	.12	9.41	11.36	1.68	2.25	.48	13.43	99.94	80	91	243	249	28	260	126	879	1514	25	64	7	1	68	388	13	.64	HL31	126.8-142.3	D.8 TC		
334137	46.95	.78	15.16	9.51	.16	8.24	14.67	1.16	2.48	.39	14.93	99.55	79	84	350	274	24	164	184	652	1532	48	54	9	1	62	298	18	.70	HL31	142.0-172.5	D.8 TC		
334138	48.96	.98	16.12	10.23	.13	8.79	18.30	1.78	2.13	.42	11.93	99.80	96	10	127	264	28	194	110	645	1657	58	66	5	1	45	349	12	.22	HL31	172.5-180.0	D.8 TC		
334139	52.67	.68	13.31	9.27	.11	9.71	18.46	1.53	1.74	.33	7.65	100.82	76	7	87	488	25	152	89	477	1497	48	59	1	1	37	254	9	.84	HL31	186.8-195.1	D.8 TC		
334140	47.99	.76	14.68	7.15	.15	7.72	12.88	1.95	2.86	.37	12.21	99.96	96	11	657	419	25	158	100	587	1929	42	56	3	1	36	288	9	.34	HL31	195.1-205.0	D.8 TC		
334141	49.25	.64	12.61	8.29	.18	6.68	15.67	2.38	1.92	.35	11.72	100.47	92	49	154	493	25	135	91	473	1769	37	52	7	1	33	247	7	.38	HL31	205.0-220.7	D.8 TC		
334142	51.89	.43	13.85	9.36	.23	14.45	12.16	1.91	.43	.17	14.28	100.12	114	97	296	381	19	92	173	676	1438	36	39	18	1	27	226	6	.48	HL31	220.9-284.3	D.8 TC		
334143	51.11	.43	13.65	9.32	.21	18.64	12.26	1.79	.43	.18	13.13	99.97	102	57	203	294	16	56	244	852	376	42	31	33	1	13	235	3	.82	HL31	284.0-288.4	D.8 TC		
334144	46.50	.50	14.75	8.17	.22	6.89	18.18	4.13	.73	.27	14.37	100.33	123	93	467	378	17	75	205	734	1147	36	39	22	1	19	242	4	.34	HL31	288.4-318.6	D.8 TC		
334145	50.22	.68	19.17	8.76	.22	4.11	11.25	4.34	1.71	.51	7.83	100.42	148	74	387	410	29	160	44	11	1516	31	77	13	1	58	388	8	.26	HL31	318.6-324.2	D.8 TC		

Group 0 16 (D.HL14 Spt)

Sam.No	SiO2	TiO2	Al2O3	Fe2O3	MnO	HgO	CaO	Na2O	K2O	P2O5	LGI	ΔE	Sun	Cu	Pb	Zn	Sr	Y	Zr	Ni	Cr	Ba	Sc	La	As	Ag	Rb	V	Nb	S	HOLE	DEPTH	ROCK TYPE	SL
333971	52.17	.34	11.96	5.37	.27	6.64	20.60	2.28	.38	.35	13.65	130.46	66	1	43	545	11	75	140	760	235	29	17	1	1	20	165	1	.26	HL14	186.97	D.5	HC	
333973	53.15	.62	12.19	7.67	.16	6.77	11.69	1.75	1.93	.30	7.55	70.79	104	1	70	565	17	50	115	525	5150	37	30	1	1	41	260	6	.60	HL14	139.27	D.5	HC	
333974	54.33	.60	12.18	5.25	.18	6.46	14.96	3.95	.22	.32	8.64	98.51	109	1	47	305	19	144	115	595	455	33	49	23	1	7	210	6	.67	HL14	177.38	D.5	HC	
333975	50.68	.69	13.46	7.06	.20	7.18	16.40	2.84	.82	.49	13.62	99.14	97	1	78	295	19	140	91	510	1050	29	39	18	1	23	225	5	.82	HL14	198.66	D.5	HC	
333976	54.23	.76	19.37	9.02	.16	6.41	4.68	2.21	2.79	.13	8.37	99.02	72	7	159	270	11	105	240	1460	1485	60	21	36	1	145	325	5	.40	HL14	224.5	D.5	HC	

Group 0 17 (D.HL79)

Sam.No	SiO2	TiO2	Al2O3	Fe2O3	MnO	HgO	CaO	Na2O	K2O	P2O5	LOI	HE	Sun	Cu	Pb	Zn	Sr	Y	Zr	Ni	Cr	Ba	Sc	La	As	Ag	Rb	V	Nb	S	HOLE	DEPTH	ROCK TYPE	SL
334099	63.51	.30	12.42	3.27	.08	1.55	13.67	3.86	.57	.10	9.83	99.38	131	10	34	160	10	49	138	531	234	28	18	12	1	18	223	4	.79	HL79	379.1	Wagtail6	TC	

Group 0 18 (HVS)

Sam.No	SiO2	TiO2	Al2O3	Fe2O3	MnO	HgO	CaO	Na2O	K2O	P2O5	L01	ME	Sun	Cu	Pb	Zn	Sr	Y	Zr	Ni	Cr	Ba	Sc	La	As	Ag	Rb	V	Nb	S	HOLE	DEPTH	ROCK TYPE	SL
333977	52.31	.77	21.91	8.66	.17	6.50	3.68	.31	4.73	.33	7.79	99.55	104	20	257	51	24	185	59	230	2575	40	114	1	1	220	355	11	.02	HL14	226.5	T.b.d.9	HC	
333978	61.51	.63	18.65	7.33	.10	3.93	1.48	3.28	2.43	.22	4.93	99.80	13	9	140	340	25	170	10	52	1355	24	80	15	1	140	140	9	.72	HL14	234.0	L.b.9	HC	
333929	58.11	.63	18.98	7.58	.08	5.15	3.28	2.37	4.22	.29	5.75	100.70	113	26	201	100	22	160	55	150	1660	1	100	21	1	160	184	10	.35	HL14	225.4-230.87	T.b.d.9	AC	
333930	59.65	.59	18.42	7.54	.05	3.74	2.20	5.57	2.24	.16	3.96	100.20	167	42	243	365	21	170	50	59	840	1	45	20	1	90	82	8	.79	HL14	230.87-234.1	L.b.9	AC	
334222	44.76	.49	16.68	8.10	.20	9.22	17.39	1.72	1.17	.20	15.60	100.74	90	1	170	210	22	54	185	760	1340	1	50	155	1	21	250	4	.02	HL57	323.53	D.4	AC	
334223	60.40	.45	22.17	3.76	.03	2.12	2.56	.37	5.38	.07	6.96	97.40	27	48	46	50	38	225	8	28	6450	1	110	60	1	190	40	14	1.91	HL57	326.62	L.b.9	AC	
334072	71.35	.31	15.13	3.50	.04	1.94	2.98	.71	3.92	.05	5.37	99.97	17	13	79	47	33	221	19	32	1233	9	65	22	1	151	51	14	.77	HL30	274.4	D.9	TC	
334072	75.97	.43	10.20	4.72	.15	2.43	2.92	.01	2.32	.15	4.99	99.13	23	21	83	26	23	92	38	79	682	12	29	17	1	99	119	14	.67	HL30	274.5	OSH.9	TC	
334073	72.73	.30	15.77	3.10	.02	1.92	.57	.66	4.22	.05	3.65	99.37	12	10	50	31	33	236	13	28	1377	7	61	15	1	169	42	16	.52	HL30	275.3	OSH.9.9	TC	
334074	49.18	.65	21.37	5.75	.24	2.78	11.82	3.86	4.72	.55	11.64	100.18	85	14	145	130	32	87	126	1034	1520	58	33	75	1	164	346	5	.80	HL30	278.7	OSH.9.9.9	TC	
334111	68.83	.37	17.21	3.99	.04	2.05	2.50	.13	4.33	.07	5.68	99.57	70	17	116	43	40	260	27	49	1503	10	54	22	1	187	61	17	.91	HL30	272.4-278.3	OSH.9	TC	
334112	55.61	.72	21.25	8.42	.06	2.64	4.04	1.36	5.53	.13	8.44	99.80	104	26	201	65	30	122	134	801	1074	54	72	115	1	213	363	10	3.54	HL30	278.3-278.8	A.b.9	TC	
334113	56.86	.91	21.95	6.57	.04	1.55	4.08	2.89	4.63	.20	7.46	99.73	43	35	90	220	45	230	16	20	2472	25	62	54	1	197	119	10	3.35	HL30	278.8-283.4	A.b.9	TC	
334050	56.98	.77	24.06	4.99	.04	2.72	.76	3.41	5.59	.30	4.84	99.78	44	16	206	226	44	224	5	22	2669	20	61	7	1	243	135	15	.26	HL31	325.5	A.9	TC	
334051	61.16	.57	16.25	8.82	.12	4.27	3.86	.57	3.60	.27	6.30	99.55	82	66	962	111	27	135	61	279	1452	38	77	66	1	143	232	10	.73	HL31	338.0	T.b.d.ch.9	TC	
334052	56.26	1.01	25.64	2.65	.06	1.91	.74	1.99	6.95	.28	5.96	99.55	3	12	328	127	39	217	13	46	3129	40	04	12	1	250	183	15	.24	HL31	341.95	L.b.9	TC	

Group 0 19 (FPS HL14)

Sam.No	SiO2	TiO2	Al2O3	Fe2O3	MnO	MgO	CaO	Na2O	K2O	P2O5	L01	HE	Sun	Cu	Pb	Zn	Sr	Y	Zr	Ni	Cr	Ba	Sc	La	As	Ag	Rb	V	Nb	S	HOLE	DEPTH	ROCK TYPE	SL
333979	58.65	.65	19.09	7.83	.11	4.10	1.91	6.14	.22	.10	3.90	98.24	66	1	140	280	23	135	31	123	290	41	10	43	1	26	320	9	1.12	HL14	270.42	FPA.10	HC	
333980	57.35	.60	18.22	11.54	.17	3.73	3.34	3.73	1.97	.16	9.17	100.60	47	24	156	320	22	115	26	110	315	36	26	29	1	115	310	5	3.44	HL14	282.49	FPA.10	HC	
333981	66.81	.50	17.85	5.89	.07	.98	1.79	3.54	3.24	.13	6.29	100.64	34	17	71	330	12	84	25	180	765	30	8	74	1	160	240	4	3.45	HL14	313.85	FPA.10	HC	
333931	57.34	.70	20.12	7.44	.04	2.99	1.99	5.65	3.83	.12	4.60	99.70	75	74	488	290	22	150	43	65	1300	1	75	41	1	160	203	6	3.35	HL14	234.1-235.3	FPA.10	AG	
333932	53.80	.71	17.42	9.43	.09	4.72	3.50	7.93	.41	.09	2.94	98.30	7283	44	5311	345	18	124	1630	175	580	1	30	62	1	17	247	8	1.01	HL14	235.3-250.4	FPA.10	AG	
333933	55.56	.65	17.22	8.48	.11	5.30	3.82	7.19	.78	.11	4.76	99.43	2165	66	1789	340	14	110	436	94	1020	1	10	40	1	24	236	8	.73	HL14	250.3-275.3	FPA.10	AG	
333934	56.30	.65	18.75	7.92	.09	3.87	3.27	8.08	1.01	.13	3.52	100.20	407	62	560	305	10	115	41	120	410	1	45	39	2	46	252	6	1.81	HL14	275.0-284.0	FPA.10	AG	
333935	56.53	.61	18.29	7.11	.07	2.22	4.96	5.50	2.39	.10	3.72	98.50	30	94	221	215	18	115	34	38	630	1	16	53	3	130	255	6	3.70	HL14	284.0-304.5	FPA.10	AG	
333936	50.59	.50	16.75	21.16	.02	.84	1.39	4.84	3.37	.11	11.60	97.60	312	130	284	190	8	96	75	141	853	1	10	250	4	140	212	1	13.90	HL14	304.5-316.8	FPA.10	AG	
333937	57.12	.52	17.25	8.36	.15	1.12	4.27	5.09	3.36	.07	4.80	97.20	89	115	244	220	14	115	40	76	810	1	10	120	3	140	196	6	5.70	HL14	306.8-314.1	FPA.10	AG	

Group 0 20 (FPS HL30cg)

Sam.No	SiO2	TiO2	Al2O3	Fe2O3	MnO	HgO	CaO	Na2O	K2O	P2O5	LOI	ME	Sum	Cu	Pb	Zn	Sr	Y	Zr	Hf	Cr	Ba	Sc	La	As	Ag	Rb	V	Nb	S	HOLE	DEPTH	ROCK TYPE	SL
334114	61.58	.83	18.91	6.37	.95	1.73	2.70	5.08	2.53	.20	5.06	100.83	62	28	77	444	45	216	13	1	1197	21	55	18	1	112	91	16	1.76	HL30	283.4-288.2	FPA.10	TC	
334115	66.94	.35	15.82	5.31	.44	1.06	2.67	4.61	2.49	.14	4.42	99.66	90	35	154	478	35	171	17	8	4322	17	45	18	1	68	72	13	2.83	HL30	238.2-514.3	FPA.10	TC	
334116	65.19	.67	16.71	5.28	.47	1.63	1.38	7.58	.44	.15	2.63	99.66	344	739	2450	374	28	183	58	2	289	17	53	12	1	22	81	16	.76	HL30	314.3-326.2	FPA.10	TC	
334117	58.86	.65	15.58	7.84	.13	4.39	6.37	4.73	1.47	.13	5.83	100.12	171	117	460	254	29	128	58	95	1256	28	34	21	1	43	181	11	.34	HL30	326.2-382.6	FPA.10	TC	
334118	57.98	.60	15.87	8.51	.12	4.97	7.26	3.44	1.50	.12	4.40	100.37	187	28	214	236	27	115	52	117	948	32	31	9	1	47	216	9	.11	HL30	382.6-458.2	FPA.10	TC	
334119	63.31	.46	14.57	6.82	.18	4.08	5.21	3.93	.88	.18	5.98	99.43	340	20	453	177	23	97	106	71	393	27	29	5	1	33	178	7	.36	HL30	450.2-454.3	FPA.10	TC	
334120	61.43	.55	16.88	6.84	.11	3.65	5.96	2.65	1.67	.11	4.11	100.89	326	37	370	173	25	103	81	81	1827	29	38	6	1	53	245	8	.44	HL30	454.3-460.1	FPA.10	TC	
334121	60.70	.59	18.09	6.57	.12	3.68	3.77	4.69	1.59	.15	5.99	99.92	239	163	566	192	23	125	73	82	353	33	27	6	1	53	243	9	.48	HL30	460.1-463.8	FPA.10	TC	
334122	61.91	.51	16.43	6.36	.12	3.23	5.44	3.18	2.15	.13	3.95	99.43	228	32	269	238	26	118	66	76	1334	28	28	6	1	65	188	8	.33	HL30	463.8-469.4	FPA.10	TC	
334123	58.96	.61	18.78	6.56	.07	3.03	3.29	6.94	1.66	.12	4.71	100.82	246	79	326	253	26	122	66	83	1196	33	35	1	1	42	237	8	.73	HL30	469.4-478.6	FPA.10	TC	
334124	61.63	.59	17.13	7.22	.11	2.86	3.23	6.55	.82	.18	3.97	100.26	372	55	462	243	26	118	100	74	565	38	38	7	1	26	289	9	1.13	HL30	478.6-484.4	FPA.10	TC	

Group 0 21 (FPS HL30sc)

Sam.No	SiO2	TiO2	Al2O3	Fe2O3	MnO	HgO	CaO	Na2O	K2O	P2O5	LOI	ME	Sum	Cu	Pb	Zn	Sr	Y	Zr	Hf	Cr	Ba	Sc	La	As	Ag	Rb	V	Nb	S	HOLE	DEPTH	ROCK TYPE	SL
334075	55.44	1.05	24.32	6.14	.82	1.79	1.62	3.61	5.82	.22	5.24	99.99	32	38	80	288	49	264	5	18	2503	26	58	45	2	242	117	20	3.12	HL30	280.8	FPA.10	TC	
334076	70.38	.57	13.94	3.27	.83	.20	4.83	5.63	1.51	.15	4.15	99.56	18	11	14	541	33	155	3	18	1749	16	27	19	1	48	62	11	1.77	HL30	291.8	FPA.10	TC	
334077	79.23	.59	13.54	5.76	.81	.17	1.43	3.78	3.19	.15	3.51	99.23	22	27	114	584	38	162	3	7	5691	17	38	59	1	97	68	12	3.56	HL30	302.2	FPA.10	TC	
334078	78.13	.64	15.17	3.97	.85	1.37	.78	6.98	.71	.15	1.75	99.87	16	462	786	324	29	167	2	3	257	17	31	13	1	38	75	13	.32	HL30	319.7	FPA.10	TC	
334079	55.61	.55	14.71	3.45	.11	4.51	6.15	3.69	1.89	.15	3.31	99.67	61	14	60	160	25	114	33	126	1513	34	38	25	1	54	198	9	.76	HL30	370.6	FPA.10	TC	
334080	63.15	.55	11.53	7.25	.12	3.97	7.35	1.78	1.61	.12	4.73	100.23	56	3	61	283	22	97	27	165	738	27	25	6	1	56	167	7	.84	HL30	418.8	FPA.10	TC	
334081	61.82	.55	15.53	6.28	.12	3.11	6.71	2.24	1.99	.15	3.71	99.25	49	9	84	323	25	112	25	66	1054	26	25	12	1	58	187	8	.11	HL30	446.25	FPA.10	TC	
334082	59.02	.59	17.88	5.75	.13	3.15	3.33	5.37	1.47	.13	3.92	99.79	22	12	36	247	31	131	26	77	1871	31	42	11	1	35	179	18	1.12	HL30	467.4	FPA.10	TC	
334083	64.36	.55	16.86	5.87	.88	2.23	1.86	3.98	.56	.11	2.62	99.68	55	15	112	221	25	111	22	73	12	1	22	11	1	2	179	7	.77	HL30	483.9	FPA.10	TC	

Group 0 22 (FPS HL31)

Sam.No	SiO2	TiO2	Al2O3	Fe2O3	MnO	HgO	CaO	Na2O	K2O	P2O5	LOI	ME	Sum	Cu	Pb	Zn	Sr	Y	Zr	Hf	Cr	Ba	Sc	La	As	Ag	Rb	V	Nb	S	HOLE	DEPTH	ROCK TYPE	SL
334053	64.56	.61	16.89	5.77	.11	3.89	2.41	6.38	.51	.13	3.95	99.63	5	9	84	257	22	125	29	84	323	26	35	16	1	16	151	9	.22	HL31	347.7	FPA.11	TC	
334054	65.85	.66	17.09	2.99	.87	1.88	3.55	9.48	.11	.16	3.17	100.28	67	5	45	326	35	178	4	12	211	19	37	9	1	1	77	13	.18	HL31	355.15	FPA.Dfr.11	TC	
334055	65.38	.62	14.71	6.86	.12	3.56	3.89	4.56	.85	.13	4.64	99.94	18	8	95	276	29	138	15	58	1149	25	36	9	1	24	128	11	.88	HL31	357.3	FPA.mts.11	TC	
334056	72.26	.51	12.88	3.18	.88	1.28	3.91	4.28	1.43	.12	4.47	99.81	28	11	51	214	23	138	3	9	774	16	42	6	1	57	58	18	.21	HL31	383.75	Y.FPA.11	TC	
334146	59.82	.76	19.97	6.88	.89	2.48	4.43	2.59	4.53	.21	7.38	100.21	172	142	484	285	58	181	56	72	1948	31	57	38	1	164	167	.2	1.39	HL31	324.2-346.2	Y.FPA.11	TC	
334147	63.46	.69	16.73	6.27	.88	2.76	2.98	5.13	1.46	.17	4.74	99.78	144	32	236	242	34	173	43	31	934	23	45	7	1	57	128	11	.82	HL31	346.2-481.8	Y.FPA.11	TC	

Group 0 23 (FPS ADIT)

Sam.No	SiO2	TiO2	Al2O3	Fe2O3	MnO	HgO	CaO	Na2O	K2O	P2O5	LOI	ME	Sum	Cu	Pb	Zn	Sr	Y	Zr	Hf	Cr	Ba	Sc	La	As	Ag	Rb	V	Nb	S	HOLE	DEPTH	ROCK TYPE	SL
334254	70.58	.58	14.68	1.17	.84	.68	3.54	6.52	.32	.18	1.92	98.18	16	290	238	388	38	135	16	56	158	1	45	14	1	1	55	18	.11	ADIT		FPA.Dfr.11	AC	
334255	63.37	.54	15.99	5.53	.21	3.44	2.89	5.33	.63	.18	2.44	98.18	11	798	698	435	32	175	8	34	518	1	55	4	1	1	98	12	.18	ADIT		FPA.mts.11	AC	

Group 0 24 (YVL HL14)

Samp.No	SiO2	TiO2	Al2O3	Fe2O3	MnO	Na2O	K2O	P2O5	LOI	HE	Sum	Co	Pb	Zn	Sr	Y	Zr	Ni	Cr	Ba	Sc	La	As	Ag	Rb	V	Nb	S	HOLE	DEPTH	ROCK TYPE	SL
333902	67.08	.67	16.62	6.31	.29	2.21	1.22	1.80	3.35	.15	5.13	99.74	100	1	115	60	12	96	14	61	830	26	13	50	1	190	310	3	1.54	HL14 340.99	L.12	HC
333930	58.87	.65	19.72	8.62	.18	2.83	1.80	3.46	4.15	.69	4.70	99.80	50	18	157	180	13	130	22	94	710	1	10	90	2	160	219	6	2.45	HL14 314.1-315.6	L.fv.12	AG
333939	66.66	.70	15.67	6.47	.17	1.38	2.71	1.14	4.51	.16	4.28	99.60	72	16	131	98	21	165	18	26	730	1	30	66	3	160	76	10	2.85	HL14 315.6-336.4	Y.b.11.12	AG
333940	60.69	.81	19.38	7.36	.12	1.68	1.62	2.71	5.61	.14	5.50	.14	126	38	95	80	24	115	40	46	861	1	40	255	4	210	257	6	3.85	HL14 336.4-345.8	Y.11.12	AG
333941	57.19	.67	17.27	8.47	.30	5.11	3.56	2.92	3.20	.10	5.00	98.60	159	80	179	135	12	74	118	275	770	1	10	68	2	115	802	1	1.60	HL14 345.8-361.6	Y.11.12	AG
333903	60.53	.84	18.07	5.55	.21	2.81	2.65	4.30	3.56	.26	4.97	98.83	20	18	59	230	23	160	20	46	1400	25	42	24	1	125	280	6	1.50	HL14 367.33	L.12	HC
333942	59.68	.64	16.27	7.30	.19	3.90	3.52	2.92	4.82	.12	4.14	99.10	264	14	241	145	20	94	113	185	1310	1	33	60	1	145	253	1	2.35	HL14 360.6-363.0	Y.b.1.12	AG
333984	69.67	.52	13.23	4.43	.18	1.60	1.50	1.34	6.69	.25	3.55	99.40	17	19	45	18	17	145		26	3200	10	58	17	1	185	125	6	.69	HL14 390.93	L.12	HC
333943	57.49	.84	10.11	8.46	.12	2.55	3.03	4.41	4.79	.18	4.50	99.70	91	41	184	190	18	145	41	44	1340	1	35	49	1	145	234	8	3.90	HL14 363.3-368.3	L.Q.12	AG
333944	58.73	.74	17.42	8.34	.20	4.29	2.44	2.92	4.79	.16	4.16	100.20	90	88	239	145	14	130	38	88	1560	1	45	31	1	125	230	5	1.01	HL14 368.0-385.0	L.12	AG
333945	64.14	.65	14.82	6.22	.19	2.04	2.39	3.68	4.85	.23	2.86	99.40	181	56	230	145	24	160	27	18	2000	1	55	30	1	115	131	10	1.31	HL14 385.0-391.3	L.gls.12	AG
333946	63.02	.74	16.32	6.89	.18	2.47	2.14	2.05	6.76	.23	3.22	100.10	10	30	189	110	22	175	6	18	2000	1	85	27	1	190	137	10	1.35	HL14 391.3-398.0	L.12	AG
333947	63.17	.65	14.73	7.52	.25	3.41	2.14	2.93	5.46	.20	2.96	99.50	212	34	233	129	22	175	24		2240	1	55	20	1	135	110	13	1.44	HL14 398.0-405.3	L.12	AG
333985	65.59	.63	15.40	6.18	.12	1.74	1.04	2.13	7.09	.25	5.10	100.22	35	210	240	155	14	120	23	145	2915	27	29	28	1	210	290	6	2.87	HL14 430.0	B.(D).12	HC
333948	62.41	.73	15.86	6.11	.19	2.50	3.69	3.17	4.83	.23	3.54	99.60	35	51	114	125	26	190	1	12	1580	1	60	58	1	165	125	10	1.84	HL14 465.3-417.5	L.12	AG
333949	61.50	.72	10.12	7.12	.12	3.03	1.14	2.84	5.76	.13	4.58	100.50	22	26	76	70	12	105	9	30	1300	1	35	47	1	205	243	4	2.60	HL14 419.5-421.0	Y.12	AG
333986	55.07	.60	18.72	7.92	.27	7.12	4.13	3.79	1.97	.18	8.37	99.86	44	63	160	270	14	78	77	520	1090	52	15	27	1	81	360	3	1.74	HL14 454.0	L.11.12	HC
333950	60.56	.57	16.10	6.28	.11	2.05	2.45	2.88	7.51	.18	3.70	98.98	224	80	485	160	16	110	90	98	2940	1	45	64	1	180	234	4	3.05	HL14 421.0-435.4	B.(D).12	AG
333987	55.72	.49	15.70	7.12	.29	7.63	7.64	1.75	2.71	.19	9.86	99.31	83	11	124	170	12	62	65	425	1620	42	7	22	1	87	290	1	1.08	HL14 463.5	L.11.12	HC
333951	56.15	.56	16.40	7.61	.27	4.85	7.24	3.55	4.87	.07	6.20	100.80	100	66	187	185	10	60	60	130	1560	1	10	26	1	100	247	2	1.68	HL14 435.4-450.0	L.12	AG
333952	52.00	.46	15.14	8.75	.32	7.09	7.14	3.45	2.27	.05	6.70	96.70	83	170	232	180	8	50	97	300	1280	1	25	36	1	56	238	2	1.97	HL14 450.0-475.0	L.12	AG
333953	52.50	.46	15.58	8.61	.28	7.79	8.56	2.98	2.41	.05	8.05	99.40	119	220	516	155	6	44	85	279	1436	1	10	30	1	58	220	2	1.43	HL14 475.0-500.0	L.12	AG
333988	58.26	.48	16.70	8.41	.43	10.95	.42	1.0	4.82	.10	7.47	99.93	159	98	478	66	9	61	41	290	2230	44	10	62	1	120	320	2	1.27	HL14 522.5	L.Q.12	HC
333954	51.00	.55	17.31	9.40	.27	6.31	5.52	2.82	4.83	.05	5.70	97.40	97	300	418	130	10	68	47	140	1430	1	10	25	2	105	256	2	2.85	HL14 500.0-519.5	L.12	AG
333955	63.08	.46	15.85	8.24	.37	6.25	1.29	1.0	3.12	.04	7.20	99.10	112	100	221	64	8	48	74	185	640	1	10	110	3	110	224	4	4.00	HL14 519.5-521.0	L.fm.pu.12	AG
333956	53.56	.42	14.73	8.24	.42	7.05	7.25	.89	3.18	.05	8.20	97.76	186	165	252	140	2	40	52	195	1200	1	13	66	2	72	215	2	1.46	HL14 521.0-526.0	L.12	AG
333957	52.99	.46	15.94	8.18	.25	8.77	4.26	.31	5.87	.05	6.95	97.10	143	48	156	98	6	40	65	200	1840	1	10	125	4	130	217	4	3.55	HL14 526.0-530.5	L.fm.pu.12	AG
333989	54.51	.59	15.71	9.20	.27	10.43	.50	.01	.34	.13	8.43	99.67	109	13	114	41	10	65	74	425	425	43	19	46	1	31	205	2	.32	HL14 519.0	Stz.Q.c113	HC
333958	52.80	.47	16.37	9.85	.32	13.77	2.68	.36	1.51	.13	7.60	97.70	89	40	142	92	8	50	55	225	560	1	10	88	2	42	222	2	1.03	HL14 530.5-539.8	Stz.L.13	AG
333990	75.76	.41	11.32	7.87	.86	1.66	.29	.19	3.24	.17	7.50	101.60	515	3630	7270	22	9	91	37	260	870	26	13	85	7	150	200	3	4.37	HL14 555.32	Stz.gls13	HC
333959	53.61	.53	15.98	9.40	.23	15.11	1.53	.34	1.19	.14	7.90	98.10	113	26	135	58	10	60	106	285	310	1	10	165	3	31	245	2	1.24	HL14 539.8-549.8	Stz.Q.13	AG
333960	56.93	.35	9.65	7.14	.07	2.59	.99	.37	2.81	.11	6.75	81.10	3796	#=2	25300	10	26	300	110	610	1500	1	10	50	13	295	121	2	8.05	HL14 549.8-560.2	Stz.Qgls13	AG
333961	55.16	.47	12.49	10.80	.15	2.76	.38	.29	3.21	.20	10.50	94.00	23401	3000	3.32X	10	26	130	69	110	1220	1	30	400	35	145	137	2	11.60	HL14 560.2-561.5	Stz.cl.13	AG
333962	70.69	.57	12.69	7.83	.03	1.16	.41	.29	4.69	.14	6.20	99.80	384	3660	4852	20	26	98	44	225	2020	1	40	180	8	165	158	2	5.65	HL14 561.5-569.3	Stz.gls.13	AG
333963	27.95	.52	14.22	45.92	.36	3.91	.36	.31	2.74	.19	19.20	96.60	512	5500	9244	10	26	100	29	64	1090	1	10	610	11	125	149	4	23.10	HL14 569.3-570.4	Stz.cl.13	AG
333991	71.50	.50	11.44	11.48	.18	1.18	.81	.13	3.18	.14	7.24	100.66	253	3440	3040	34	9	99	21	125	2430	32	6	187	8	160	265	4	5.84	HL14 587.6	Stz.13	HC
333964	63.31	.55	13.69	10.90	.14	2.66	.72	2.58	3.37	.16	6.40	98.40	782	7400	5058	30	26	64	172	275	3700	1	10	94	26	135	176	2	4.90	HL14 570.4-572.2	Stzfm.13	AG
333965	67.69	.57	12.69	10.97	.18	2.47	.62	.30	3.14	.18	7.00	98.80	339	1160	2829	90	26	50	100	12011000	1	30	155	4	120	163	4	6.15	HL14 572.2-578.8	Stz.Q.13	AG	
333966	63.97	.64	14.22	11.34	.20	1.87	1.03	.31	4.15	.21	6.45	98.00	740	8000	5902	40	26	120	41	140	3200	1	25	210	15	160	166	4	5.70	HL14 578.8-599.3	Stz.13	AG
333967	53.57	.54																														

Group 0 25 (Stz HL57)

Samp.No	SiO2	TiO2	Al2O3	Fe2O3	MnO	Na2O	K2O	P2O5	LOI	HE	Sum	Cu	Pb	Zn	Sr	Y	Zr	Ni	Cr	Ba	Sc	La	As	Ag	Rb	V	Nb	S	HOLE	DEPTH	ROCK TYPE	SL
334225	62.37	.61	20.97	5.31	.32	1.68	1.07	.14	5.56	.15	7.35	98.10	34	155	470	56	36	185	2	6	7700	1	140	210	2	195	80	12	4.08	HL57 336.1	Stz.14	AC

Samp.No	SiO2	TiO2	Al2O3	Fe2O3	MnO	MgO	CaO	Na2O	K2O	P2O5	LOI	ME	Sum	Cu	Pb	Zn	Sr	Y	Zr	Ni	Cr	Ba	Sc	La	As	Ag	Rb	V	Nb	S	HOLE	DEPTH	ROCK TYPE	SL
334229	55.39	.81	22.82	9.83	.04	1.99	1.28	3.40	4.02	.09	6.35	98.10	88	68	78	190	32	140	40	170	2580	1	55	37	1	155	260	12	5.45	HL57	355.40	STZ.14	AC	

Group 0 26 (STZ PL61)

Samp.No	SiO2	TiO2	Al2O3	Fe2O3	MnO	MgO	CaO	Na2O	K2O	P2O5	LOI	ME	Sum	Cu	Pb	Zn	Sr	Y	Zr	Ni	Cr	Ba	Sc	La	As	Ag	Rb	V	Nb	S	HOLE	DEPTH	ROCK TYPE	SL
334230	66.95	.53	14.35	5.81	.13	1.34	4.88	.18	4.52	.09	7.00	98.50	36	62	39	62	26	64	8	22	1680	1	45	190	3	155	210	4	3.93	HL61	395.80	STZ.Q.14	AC	
334231	39.52	1.31	29.93	16.52	.01	1.23	1.68	.31	6.32	.09	13.10	77.20	54	111	36	165	48	230	23	56	1520	1	120	5400	2	210	260	18	12.40	HL61	404.65	STZ.Q.14	AC	
334232	52.44	.75	21.38	9.62	.21	7.31	3.21	.12	6.45	.04	11.10	77.66	135	58	115	58	26	92	10	44	980	1	35	200	2	145	250	6	6.20	HL61	408.57	STZ.Q.14	AC	
334233	62.20	.64	14.96	11.64	.06	.84	3.19	.55	3.59	.14	9.63	77.80	66	26	43	52	33	105	20	40	790	1	70	120	1	100	140	8	9.40	HL61	419.64	STZ.Q.14	AC	
334234	56.26	.77	17.86	11.05	.12	2.50	4.30	1.09	3.66	.17	10.20	77.80	54	36	70	80	32	135	29	50	830	1	70	105	1	110	180	10	7.40	HL61	421.2	STZ.Q.14	AC	
334235	68.32	.33	9.25	7.81	.18	1.95	8.41	2.59	.61	.03	9.05	99.40	68	16	41	100	29	38	8	26	170	1	45	130	1	7	100	1	4.10	HL61	426.87	STZ.Q.14	AC	
334236	67.36	.50	17.19	6.71	.02	.81	1.39	.74	4.83	.04	6.85	98.90	110	21	37	64	26	74	8	10	760	1	40	68	1	120	220	4	4.94	HL61	436.56	STZ.Q.14	AC	
334237	74.23	.50	13.86	5.48	.06	1.51	.21	.86	3.51	.05	4.30	98.70	29	380	105	11	26	78	46	265	1300	1	50	130	1	90	190	6	2.62	HL15	453.0	STZ.15	AC	
334238	58.83	.30	7.79	10.16	.21	2.94	.77	.02	1.30	.10	5.80	32.50	11530	10	94	14600	10	26	271	16	240	570	1	70	50	105	150	75	4	6.00	HL15	456.6	STZ.vn.15	AC
334239	65.41	.28	6.15	13.41	.27	2.88	.84	.01	1.85	.02	8.85	98.30	104025000	25200	10	26	110	2	52	520	1	35	200	10	50	50	2	10.90	HL15	464.5	STZ.15	AC		
334240	70.96	.51	12.33	7.96	.14	4.55	.49	.94	2.53	.11	5.15	99.70	11	325	620	14	16	66	14	56	540	1	50	180	1	72	180	4	2.61	HL15	480.6	STZ.gls.15	AC	
334241	39.43	.40	11.69	35.27	.11	2.83	.60	.13	4.79	.04	17.44	94.80	21	830	340	44	4	62	12	54	3200	1	35	500	3	120	95	4	23.40	HL15	491.72	STZ.vn.15	AC	
334242	46.92	.40	14.87	27.89	.40	7.60	.46	.02	1.40	.09	9.15	97.30	17	130	250	22	12	02	12	70	1350	1	40	330	4	30	120	6	6.85	HL15	493.27	STZ.15	AC	
334243	74.69	.37	11.27	5.74	.11	2.80	.56	.03	3.47	.02	5.04	98.30	14	130	56	33	16	68	16	78	1300	1	25	170	2	110	120	4	3.32	HL15	501.2	STZ.gls.15	AC	
334244	73.16	.38	12.47	5.65	.02	1.05	.21	.07	3.82	.04	5.25	76.90	15	80	47	25	28	80	18	66	2040	1	55	285	1	125	150	4	4.38	HL15	508.2	STZ.gls.15	AC	
334245	57.42	.58	17.66	8.18	.14	4.68	4.57	1.71	2.83	.08	7.55	97.90	76	30	54	80	26	90	16	54	590	1	50	54	1	82	210	6	2.44	HL15	513.2	STZ.gls.15	AC	
334246	57.20	.59	17.88	6.46	.11	4.02	4.82	2.26	2.73	.09	6.90	96.20	60	18	54	90	28	92	10	44	660	1	65	23	1	82	230	8	1.69	HL15	518.2	STZ.gls.15	AC	
334247	61.40	.57	17.43	6.25	.10	4.42	4.84	2.80	2.50	.10	6.45	98.90	72	16	43	82	26	82	14	54	450	1	50	38	1	66	220	6	1.28	HL15	525.6	STZ.gls.15	AC	

Group 0 27 (STZ HL50)

Samp.No	SiO2	TiO2	Al2O3	Fe2O3	MnO	MgO	CaO	Na2O	K2O	P2O5	LOI	ME	Sum	Cu	Pb	Zn	Sr	Y	Zr	Ni	Cr	Ba	Sc	La	As	Ag	Rb	V	Nb	S	HOLE	DEPTH	ROCK TYPE	SL
334248	69.23	.61	13.51	5.91	.07	1.77	2.19	.16	3.76	.05	6.80	97.30	74	96	88	28	28	110	14	22	1320	1	70	220	2	125	170	8	4.62	HL50	362.5	STZ.14	AC	
334249	61.82	.77	17.53	8.49	.07	2.36	2.43	.09	4.97	.14	8.55	97.90	80	50	135	31	30	135	20	40	1400	1	70	155	1	165	220	8	6.10	HL50	365.3	STZ.Q.14	AC	

Group 0 28 (STZ HL35A)

Samp.No	SiO2	TiO2	Al2O3	Fe2O3	MnO	MgO	CaO	Na2O	K2O	P2O5	LOI	ME	Sum	Cu	Pb	Zn	Sr	Y	Zr	Ni	Cr	Ba	Sc	La	As	Ag	Rb	V	Nb	S	HOLE	DEPTH	ROCK TYPE	SL
334081	24.28	.40	13.48	52.16	.16	1.23	.71	.01	4.81	.12	21.95	95.95	350027900	9000	15	26	117	21	71	5854	32	3	970	41	152	182	5	30.34	HL35	394.8	STZ.top.16	TC		
334085	70.68	.45	10.60	10.26	.23	5.60	.28	.01	1.27	.09	5.26	99.50	11	385	299	11	16	84	15	60	1051	18	9	112	3	46	129	7	2.22	HL35	396.2	STZ.c1.16	TC	
334086	25.91	.81	19.75	27.85	.54	13.12	.98	.80	2.12	.20	13.67	90.31	3900	7.462	4.87	12	26	260	33	154	3223	42	2	531	58	110	332	9	12.40	HL35	397.7	STZ.c1.16	TC	
334087	25.41	.75	18.49	13.41	1.51	25.91	14.38	.01	.68	.20	23.96	100.80	3	32	250	116	28	119	21	90	680	27	31	24	1	20	100	8	1.18	HL35	408.2	STZ.c1.16	TC	
334088	66.58	.48	11.75	9.67	.51	6.81	2.73	.01	1.78	.09	8.51	100.44	17	213	696	37	22	66	16	71	926	24	21	37	2	66	177	6	2.02	HL35	413.65	STZ.gls.16	TC	
334089	26.17	.79	20.35	30.18	1.36	18.43	1.91	.01	.17	.17	15.55	99.59	31	575	553	21	24	131	38	112	175	24	31	285	5	8	269	11	8.42	HL35	417.2	STZ.c1.16	TC	
334090	36.23	.61	23.47	13.87	1.06	12.06	7.18	.01	5.21	.15	17.34	110.11	23	69	204	68	35	145	29	101	2791	38	34	107	3	165	267	10	4.69	HL35	417.4	STZ.c1.16	TC	
334091	79.88	.34	8.84	6.55	.02	.74	.24	.01	2.72	.07	4.81	99.44	15	358	90	37	15	59	14	51	6192	20	11	161	1	102	111	5	4.65	HL35	425.6	STZ.gls.16	TC	
334092	68.57	.51	15.19	8.25	.23	3.21	.24	.01	3.70	.10	5.51	100.45	20	189	166	23	22	190	18	73	2135	27	24	80	1	131	187	7	3.31	HL35	430.6	STZ.top.16	TC	
334093	72.34	.46	13.29	8.14	.03	.86	.20	.01	3.94	.10	5.88	99.40	14	41	24	26	21	93	16	60	1711	28	20	450	1	134	162	7	5.45	HL35	435.8	STZ.Q.16	TC	

Group 0 29 (STZ HL39)

Samp.No	SiO2	TiO2	Al2O3	Fe2O3	MnO	MgO	CaO	Na2O	K2O	P2O5	LOI	NE	Sum	Cu	Pb	Zn	Sr	Y	Zr	Ni	Cr	Ba	Sc	La	As	Ag	Rb	V	Nb	S	HOLE	DEPTH	ROCK TYPE	SL
334094	64.47	.18	4.05	28.63	.01	.31	.05	.40	1.13	.03	13.55	99.31	74	2682	1964	5	26	46	6	11	1467	5	4	937	8	37	21	3	19.31	HL39	239.0	STZ,qls.16	TC	
334095	59.58	.18	3.38	38.12	.02	.85	.05	.61	.71	.01	13.84	74.58	145423000	5.43%	1	26	60	17	24	1352	6	6	783	27	45	22	1	20.84	HL39	245.7	STZ.16	TC		
334096	5.46	.05	3.32	64.84	.08	.22	.62	5.41	.91	.01	24.12	68.56	50043	4.0%	16.6%	12	26	33	36	53	6448	3	2	1133	86	61	20	1	38.12	HL39	251.7	STZ,ss.16	TC	
334097	81.76	.15	2.72	12.56	.33	.35	.33	.31	.83	.03	6.78	98.95	48	2865	5100	17	26	39	5	13	5677	5	3	227	8	34	38	2	8.92	HL39	254.8	STZ,qls.16	TC	
334098	75.79	.46	11.56	7.24	.31	.75	.34	.01	3.36	.16	5.05	99.59	24	325	18	16	15	98	14	52	5515	19	12	278	1	116	123	8	4.74	HL39	293.7	STZ,qls.16	TC	

Group 0 30 (STZ HL31cg)

Samp.No	SiO2	TiO2	Al2O3	Fe2O3	MnO	MgO	CaO	Na2O	K2O	P2O5	LOI	ME	Sum	Cu	Pb	Zn	Sr	Y	Zr	Ni	Cr	Ba	Sc	La	As	Ag	Rb	V	Nb	S	HOLE	DEPTH	ROCK TYPE	SL
334148	63.82	.74	19.29	6.62	.35	2.54	2.26	4.52	2.29	.24	5.12	100.58	128	41	246	247	37	195	33	16	1786	22	51	7	1	92	94	14	1.01	HL31	401.8-411.5	FPAYSTZ.10	TC	
334149	61.66	.78	18.46	6.92	.85	3.15	2.69	3.61	2.36	.18	5.94	99.32	154	17	227	234	35	173	42	31	1787	24	46	15	1	98	116	11	1.16	HL31	411.5-431.15	FPAYSTZ.11	TC	
334150	68.71	.62	17.83	7.89	.88	3.71	4.74	3.88	1.82	.19	7.51	100.30	233	13	287	233	30	138	67	86	1318	31	34	14	1	68	194	8	.57	HL31	431.15-444.4	FPAYSTZ.11	TC	
334151	54.52	.47	13.15	6.87	.27	7.15	14.73	.71	2.15	.13	16.97	99.44	209	16	258	161	28	92	64	58	312	22	28	44	1	65	136	6	1.47	HL31	444.4-447.5	STZ.Q.17	TC	
334152	62.62	.59	15.33	6.24	.12	4.12	5.77	.59	3.99	.14	11.38	99.56	467	81	521	92	24	123	111	73	1124	26	37	58	1	123	161	8	3.67	HL31	447.5-458.8	STZ.Y.17	TC	
334153	52.83	.71	18.14	9.15	.27	14.14	2.68	.81	2.39	.15	12.00	99.96	259	397	951	49	36	141	65	78	807	35	43	194	1	73	285	18	4.38	HL31	458.8-462.0	STZ.17	TC	
334154	57.43	.51	15.85	8.29	.27	18.82	1.12	3.15	2.23	.13	7.23	99.86	493	2766	3617	31	23	183	59	75	1436	31	26	128	4	62	208	9	3.88	HL31	462.0-478.2	STZ.17	TC	
334155	42.57	.70	21.24	11.62	.51	21.85	.66	.01	1.23	.13	11.22	99.78	143	25	320	36	28	132	58	93	1084	36	27	88	1	36	265	8	2.43	HL31	478.2-483.0	STZ.cl.17	TC	
334156	59.17	.56	17.23	18.41	.38	6.94	1.17	.01	3.74	.10	8.94	99.67	169	57	258	59	25	185	61	72	3788	32	25	126	1	112	215	2	4.98	HL31	483.0-489.8	STZ.17	TC	
334157	38.87	.98	22.37	25.85	.98	15.79	1.86	.01	1.74	.17	14.89	99.69	72	953	977	48	28	119	43	57	1472	36	27	152	5	56	349	9	7.83	HL31	489.8-493.0	STZ.cl.17	TC	
334158	48.84	.78	17.98	28.99	.48	6.28	1.59	.01	3.56	.12	11.72	99.58	166	391	545	45	18	88	57	43	1834	38	31	329	4	113	286	5	9.43	HL31	493.0-502.5	STZ.17	TC	

Group 0 31 (STZ HL31cc)

Samp.No	SiO2	TiO2	Al2O3	Fe2O3	MnO	MgO	CaO	Na2O	K2O	P2O5	LOI	NE	Sum	Cu	Pb	Zn	Sr	Y	Zr	Ni	Cr	Ba	Sc	La	As	Ag	Rb	V	Nb	S	HOLE	DEPTH	ROCK TYPE	SL
334857	62.48	.74	17.48	6.55	.86	2.62	3.86	4.37	2.23	.15	5.49	99.78	18	37	121	239	35	183	3	18	1173	21	56	16	1	84	82	13	1.25	HL31	489.3	FPAYSTZ.11	TC	
334858	68.82	.88	18.44	7.88	.86	4.36	1.64	3.48	2.22	.21	4.52	99.92	22	8	151	218	38	192	18	27	1318	23	32	8	1	86	115	15	.17	HL31	415.45	FPAYSTZ.11	TC	
334859	64.22	.51	15.32	6.87	.89	5.38	3.36	1.73	1.93	.13	6.82	99.38	32	9	188	72	25	122	17	71	955	26	35	38	1	58	161	9	.94	HL31	445.5	FPAYSTZ.11	TC	
334860	36.81	.36	18.93	5.33	.58	12.73	38.91	.68	1.69	.11	28.21	100.23	28	16	65	244	13	64	9	45	583	12	17	31	1	42	96	4	1.29	HL31	446.4	STZ.Qca.17	TC	
334861	66.75	.72	17.77	5.32	.85	2.65	1.46	.43	4.49	.21	7.31	99.68	48	16	39	56	32	147	28	84	1335	28	48	63	1	148	174	11	3.67	HL31	456.3	STZ.Y.Q.17	TC	
334862	68.32	.55	15.82	5.87	.28	7.48	.31	.81	2.79	.09	5.52	99.86	7	48	74	23	23	94	17	67	1321	31	25	39	1	88	287	7	1.32	HL31	475.15	STZ.mv.17	TC	
334863	32.54	.84	24.88	12.28	.62	28.69	.38	.81	.12	.14	12.54	99.71	2	5	174	127	34	158	42	185	531	48	23	29	1	3	272	11	1.54	HL31	482.8	STZ.clc.17	TC	
334864	75.22	.44	12.21	5.67	.18	2.13	.34	.31	3.11	.39	4.68	99.86	8	16	42	26	29	82	16	55	2631	23	19	66	1	187	132	6	3.34	HL31	488.8	STZ.sl.17	TC	
334865	47.88	.92	21.35	21.52	.84	1.58	.34	.01	6.61	.17	12.62	99.56	54	248	51	41	23	186	41	47	2835	41	17	434	5	213	515	8	14.26	HL31	497.15	STZ.ss.17	TC	

Major elements in wt. % recalculated to 100 % . Trace elements in p.p.m.

Appendix 2ii

Northings, Eastings, RLs, Ratios

Group 1 (URS)

Samp.No	HOLE DEPTH	ROCK TYPE	SL	Zn No.	ALT1	ALT2	Ti/Zr	NORTH	EAST	RL	HR	AI/3K
334100	H.30 23.6-37.9	Y.R.SH.1	TC	76.1194	.577901	.812920	19.1035	10901.2	5458.2	646.3	1.51084	
334101	H.30 37.9-55.0	Y.R.SH.1	TC	72.1154	.740449	.882953	17.7206	10901.8	5464.4	630.1	1.41375	
334102	H.30 55.0-64.5	Y.R.SH.1	TC	76.3636	.820678	.912239	7.59346	10902.0	5467.8	621.2	1.48088	
333993	ADIT 67.2	Y.R.SH.1	HR	68.5634	.293723	.707508	8.63257	10402.1	6858.9	382.7	2.46447	
334103	H.30 64.5-70.9	Y.R.SH.1	TC	69.0476	.584636	.862616	9.78749	10902.4	5473.2	607.9	1.57387	
334104	H.30 70.9-83.0	Y.R.SH.1	TC	88.6010	.628497	.908143	14.2734	10902.5	5475.0	603.3	1.24080	
334256	H.24 3.0-24.0	BSH.SS.1	AG	71.4266	.619444	.889084	23.9794	10903.2	5702.7	663.6	1.22371	
334257	H.24 24.0-53.4	Y.R.1	AG	81.2500	.489157	.868093	10.5509	10905.7	5711.8	635.7	1.34945	
334258	H.24 53.4-54.5	BSH.Y.R.1	AG	97.0325	.427790	.859197	27.9759	10905.7	5712.2	634.7	1.07413	
334125	H.31 7.0-20.0	BSH.1	TC	88.2632	.806202	.910875	19.1246	10898.0	6140.1	666.2	1.36559	
334126	H.31 20.0-26.0	BSH.SS.1	TC	77.0947	.656716	.901899	11.0282	10898.4	6038.2	661.4	1.16853	
334127	H.31 26.0-31.0	Y.R.1	TC	78.4545	.720859	.912083	8.85144	10897.9	6036.4	656.7	1.28910	
334128	H.31 31.0-34.0	Y.R.1	TC	74.7059	.704448	.911632	7.49355	10897.5	6035.3	653.9	1.38205	
334129	H.31 34.0-35.0	BSH.1	TC	98.4459	.826816	.947082	9.13248	10897.4	6035.0	653.0	1.15098	
334130	H.31 35.0-41.5	Y.R.1	TC	92.3954	.783355	.932046	8.47755	10896.7	6032.7	647.0	1.24076	
334131	H.31 41.5-51.5	Y.R.1	TC	88.2682	.718954	.906810	8.71341	10895.4	6029.2	637.7	1.23344	
334179	ADIT 595.0	SS.1	HR	62.7451	.668686	.939130	7.62980	10640.1	6355.3	388.1	1.19866	
334180	ADIT 540.0	R.1	HR	45.4545	.606149	.937924	7.95234	10623.7	6407.8	387.6	1.19248	
334181	ADIT 454.0	Y.R.S.M.1	HR	54.8387	.746154	.944984	16.2441	10597.9	6489.8	386.7	1.21396	
334182	ADIT 430.0	R.ev.1	HR	54.1667	.457507	.882519	10.3911	10590.7	6512.7	386.4	1.49707	
334183	ADIT 392.0	R.1	HR	57.1429	.430263	.888666	4.15027	10579.3	6549.0	386.0	1.45290	
334184	ADIT 310.0	R.1	HR	82.1429	.295676	.780728	4.61141	10554.8	6627.2	385.2	2.33433	
334185	ADIT 237.0	R.1	HR	79.3103	.343600	.854737	8.99226	10532.9	6696.9	384.4	1.65871	
334186	ADIT 206.0	SS.1	HR	84.2912	.536800	.910021	11.9097	10523.7	6726.5	384.1	1.33662	
334187	ADIT 205.5	BSH.1	HR	80.1734	.382282	.905345	21.1618	10523.5	6726.9	384.1	1.32904	
334188	ADIT 67.9	sed.1	HR	66.0551	.647887	.723622	7.70765	10482.1	6859.1	382.7	1.17628	

Group 2 (QRS)

Samp.No	HOLE DEPTH	ROCK TYPE	SL	Zn No.	ALT1	ALT2	Ti/Zr	NORTH	EAST	RL	HR	AI/3K
333914	H.14 4.6-50.0	BSH.2	AG	80.2003	.653364	.837547	33.9708	10500.8	5382.5	648.7	1.29829	
333915	H.14 50.0-85.0	BSH.2	AG	53.9007	.655555	.859064	29.9742	10500.2	5405.0	621.9	1.19221	
333969	H.14 49.0	BSH.2	HC	85.8209	.681212	.834754	31.6528	10500.8	5381.7	649.4	1.44341	
333970	H.14 75.81	BSH.2	HC	67.9407	.699088	.854419	18.9837	10500.4	5399.2	629.0	1.37564	
334105	H.30 83.0-100.3	BSH.2	TC	74.5763	.637813	.893761	23.1230	10902.8	5481.1	588.3	1.24981	
333792	H.30 120.5	BSH.2	TC	60.5634	.739237	.810778	29.2548	10903.0	5480.8	569.3	1.47341	
334106	H.30 100.0-150.0	BSH.2	TC	85.7143	.546523	.808809	26.2548	10903.1	5499.8	541.9	1.40673	
334107	H.30 150.0-186.9	BSH.2	TC	79.2746	.530273	.879362	27.9459	10903.0	5511.2	587.6	1.48167	
334066	H.30 120.5	BSH.2	TC	76.5101	.961102	.843734	21.4521	10903.0	5480.8	569.3	1.29605	
334259	H.24 54.5-57.1	BSH.2	AG	83.0040	.547794	.901313	11.9897	10905.9	5713.0	632.2	1.16493	
334260	H.24 57.1-100.0	BSH.2	AG	80.5430	.656114	.860528	24.4234	10908.9	5726.0	591.4	1.14253	
334261	H.24 100.0-150.0	BSH.2	AG	80.1527	.637131	.855340	29.9742	10910.3	5740.4	543.6	1.22623	
334262	H.24 150.0-176.4	BSH.2	AG	86.0377	.645233	.873710	30.2140	10910.3	5747.9	518.3	1.19491	
334132	H.31 51.5-80.0	BSH.2	TC	85.2983	.811994	.891437	23.0571	10892.1	6018.9	611.3	1.27567	
334133	H.31 80.0-102.0	BSH.2	TC	72.2101	.637363	.882483	26.4987	10890.4	6019.6	591.1	1.19112	
334178	ADIT 657.0	BSH.2	HR	63.3803	.823232	.910316	23.5353	10658.7	6296.2	388.8	1.17693	
334224	H.20 136.2	BSH.2	AG	72.0934	.900990	.832960	30.2348	10901.9	5758.5	565.8	1.41406	
334254	H.24 181.0-183.0	BSH in B2	AG	94.2029	.355425	.922420	16.5572	10910.2	5749.9	512.0	.998299	

Group 0 3 (D.55 Gnd)

Sam.No	HOLE	DEPTH	ROCK TYPE	SL	Zn No.	ALT1	ALT2	Ti/Zr	NORTH	EAST	RL	HR	AI/3K
334001	H.55	64.0-71.2	B.3	IG	81.6964	.366803	.857424	29.8029	10896.0	5895.1	603.0	1.52802	
334002	H.55	91.2-145.0	B.3	IG	84.3931	.444614	.712103	30.2965	10893.9	5876.6	552.5	2.42137	
334003	H.55	145.0-152.0	B.3	IG	76.5623	.492483	.693525	29.1854	10893.6	5874.0	545.1	2.14525	
334004	H.55	152.0-179.5	B.4	IG	81.8182	.266080	.771554	44.5770	10893.0	5865.2	519.9	4.34652	
334005	H.55	179.5-210.3	B.0	IG	87.2340	.305096	.759446	45.6750	10892.7	5854.6	491.0	4.21270	
334006	H.55	210.3-225.0	B.4	IG	85.8624	.165201	.803712	58.9561	10892.8	5849.4	477.3	1.86834	
334007	H.55	225.0-233.0	B.4	IG	71.3333	.150667	.916398	46.7394	10892.8	5846.3	469.0	1.52649	
334008	H.55	233.0-241.0	B.4	IG	31.7568	.322123	.784872	46.9161	10892.9	5843.7	462.3	2.99481	
334009	H.55	241.0-258.0	B.4	IG	80.7692	.411765	.718995	58.8037	10893.1	5837.6	445.5	4.33147	
334010	H.55	258.95-259.1	B.4	IG	91.0714	.334679	.806762	46.4117	10893.1	5837.2	445.4	2.71361	

Group 0 4 (D.55 Spt)

Sam.No	HOLE	DEPTH	ROCK TYPE	SL	Zn No.	ALT1	ALT2	Ti/Zr	NORTH	EAST	RL	HR	AI/3K
334011	H.55	73.5	B.3	IC	77.0270	.262759	.854495	32.4491	10896.0	5901.3	619.5	2.18525	
334012	H.55	83.3	B.1P.ch.3	IC	86.9840	.427360	.825147	28.0877	10876.3	5897.9	610.3	1.60492	
334013	H.55	89.5	B.3	IC	85.7143	.270919	.761811	30.4086	10896.0	5895.7	604.5	3.83851	
334014	H.55	92.0	B.3	IC	89.6104	.363893	.747932	31.3792	10895.9	5894.0	602.2	2.07717	
334015	H.55	100.05	B.3	IC	93.4211	.295136	.717679	28.1847	10895.6	5892.0	594.7	4.07893	
334016	H.55	100.7	B.1P.3	IC	84.3750	.490700	.704937	28.0640	10895.5	5891.8	594.1	1.66876	
334017	H.55	101.0	B.1P.ab.3	IC	62.7907	.113240	.814500	29.4403	10895.5	5671.4	593.0	2.63209	
334018	H.55	102.9	B.ch.3	IC	86.3636	.610920	.791322	29.4403	10895.4	5891.1	592.8	.765947	
334019	H.55	112.0	B.ab.3	IC	58.4952	.280723	.745916	29.7783	10895.0	5887.9	583.5	2.72427	
334020	H.55	116.45	B.1P.cl.3	IC	82.4690	.475475	.718997	30.1781	10894.9	5886.4	579.3	1.91179	
334021	H.55	116.7	B.sl.3	IC	92.0792	.253575	.801914	29.2106	10894.9	5886.3	579.1	1.51407	
334022	H.55	123.5	B.1P.sed.3	IC	70.0000	.364455	.795291	29.2878	10894.6	5883.9	572.7	1.29389	
334023	H.55	125.15	B.3	IC	93.4959	.479880	.658200	28.1526	10894.5	5883.4	571.2	3.76970	
334024	H.55	129.2	B.3	IC	89.7436	.206121	.796095	28.0493	10894.4	5882.0	567.3	5.01283	
334025	H.55	129.65	B.3	IC	83.0500	.251532	.762139	30.2030	10894.4	5881.0	566.9	3.99189	
334026	H.55	133.7	B.3	IC	94.0275	.588725	.673082	29.1079	10894.2	5880.5	563.1	1.50258	
334027	H.55	141.2	B.3	IC	93.3769	.381994	.717532	29.4483	10894.3	5877.9	556.1	2.83833	
334028	H.55	151.7	B.3	IC	93.2143	.582984	.649573	26.3773	10893.7	5874.4	546.2	2.27544	
334029	H.55	153.6	B.1P.ch.3	IC	39.3939	.628439	.829167	15.4969	10893.6	5873.7	544.4	.720166	
334030	H.55	154.2	B.4	IC	94.6977	.156436	.816494	52.1773	10893.6	5873.5	543.8	4.67619	
334031	H.55	157.85	B.co.vn.4	IC	88.8089	.825615E-01	.905650	44.6674	10893.5	5872.3	540.4	53.6619	
334032	H.55	165.5	B.4	IC	90.4375	.321899	.746797	50.1387	10893.3	5867.3	533.2	4.62675	
334033	H.55	167.1	B.4	IC	90.9091	.161882	.814334	45.2441	10893.3	5865.3	531.7	6.68353	
334034	H.55	176.0	B.4	IC	76.0234	.600115	.763037	50.7798	10893.0	5866.3	523.3	1.16679	
334035	H.55	183.55	B.4	IC	90.3051	.310333	.770828	40.3794	10892.9	5863.9	516.1	3.48785	
334036	H.55	189.6	B.4	IC	98.9247	.545380	.651691	45.8429	10892.7	5861.9	510.4	4.04473	
334037	H.55	191.15	B.4	IC	86.8853	.226510	.629614	49.4574	10892.7	5861.4	508.9	1.80449	
334038	H.55	193.5	B.4	IC	96.0000	.553479	.645267	45.6530	10892.3	5860.4	506.8	4.82503	
334039	H.55	199.4	B.4	IC	85.2457	.342511	.872273	49.4923	10892.5	5850.0	502.2	1.12117	
334040	H.55	203.0	B.ab.4	IC	68.4211	.310378E-01	.826655	48.1728	10892.6	5857.2	497.7	11.8114	
334041	H.55	207.85	B.4	IC	98.7500	.256264	.791269	57.0001	10892.7	5855.5	493.3	5.91887	
334042	H.55	219.5	B.4	IC	90.1408	.191439	.810863	52.4548	10892.8	5851.7	493.3	2.60551	
334043	H.55	223.35	B.1P.4	IC	83.5821	.235189	.887093	48.4514	10892.8	5850.0	478.0	1.55333	
334044	H.55	227.9	B.co.fvvn.4	IC	50.0000	.721446E-01	.938012	46.7899	10892.8	5848.4	474.6	1.91572	
334045	H.55	232.2	B.fv.4	IC	86.7816	.207438	.964999	52.1904	10892.8	5846.9	470.5	1.16170	

Samp.No	HOLE DEPTH	ROCK TYPE	SL Zn No.	ALT1	ALT2	Ti/Zr	NORTH	EAST	RL	HR AL/3K
334046	HL55 237.4	B.4	TC 74.8031	.244050	.801362	50.9551	10892.9	5844.3	463.8	2.96062
334047	HL55 247.0	B.4	TC 98.4375	.467976	.683464	49.7877	10893.0	5841.6	456.7	5.92705
334048	HL55 257.5	B.4	TC 99.3750	.487495	.723681	49.2433	10893.1	5837.8	446.9	2.76200

Group 6 5 (D.502E5724)

Samp.No	HOLE DEPTH	ROCK TYPE	SL Zn No.	ALT1	ALT2	Ti/Zr	NORTH	EAST	RL	HR AL/3K
334191	HL50 243.83	B.4	AC 95.2381	.318083	.815858	59.9484	10743.0	5775.1	494.9	2.21716
334192	HL50 262.22	B.4	AC 97.5000	.381268	.723533	53.2975	10742.4	5765.4	479.3	5.02231
334193	HL50 282.9	B.4	AC 98.6250	.287911	.699668	55.5078	10741.7	5754.5	461.8	40.4218
334194	HL50 299.09	B.4	AC 79.4872	.180512	.928228	62.6733	10741.1	5745.9	448.8	1.44752
334195	HL29 139.6	B.4	AC 87.8968	.337312	.752983	47.4592	10901.6	5760.0	562.8	3.46552
334196	HL28 145.5	B.3	AC 95.8549	.482179	.661513	28.6245	10901.2	5762.6	557.5	6.61526
334197	HL28 157.96	B.3	AC 77.2232	.525000	.614655	27.7043	10900.2	5753.1	546.4	27.3678
334198	HL28 169.51	B.4	AC 67.3913	.625313	.643321	46.8347	10899.3	5773.3	536.8	2.82080
334199	HL28 170.32	B.4	AC 97.5618	.582084	.598112	49.6941	10899.2	5773.6	535.3	67.6860
334200	HL28 173.32	B.4	AC 71.0526	.267030	.777036	56.3515	10899.0	5774.7	532.6	13.9772
334201	HL28 187.96	B.4	AC 82.0000	.362992	.713786	53.9536	10897.7	5781.3	519.6	4.89816
334202	HL28 208.27	B.4	AC 96.8750	.460741	.797725	58.7256	10895.9	5790.3	501.4	7.66543
334203	HL28 228.87	B.4	AC 92.5726	.533984	.644775	55.1525	10894.2	5799.6	483.1	4.15435
334204	HL28 234.63	B.4	AC 94.7368	.264715	.933686	58.2356	10893.7	5802.2	478.8	1.23594
334205	HL28 249.14	B.4	AC 96.8000	.371945	.765066	61.3757	10892.4	5808.8	465.1	2.23620
334206	HL29 265.76	B.4	AC 65.2174	.289950	.937804	55.2156	10891.1	5816.5	450.5	1.21257
334207	HL57 222.58	B.4	AC 98.8000	.785348	.529743	50.9561	10746.2	5752.4	538.8	4.74120
334208	HL57 229.19	B.4	AC 97.1429	.453922	.698868	52.4548	10746.2	5747.7	531.1	4.51796
334209	HL57 245.43	B.4	AC 28.8000	.287814	.772414	47.7967	10746.2	5736.3	522.6	7.76676
334210	HL57 271.3	B.4	AC 97.8588	.551974	.651774	51.5556	10745.7	5718.1	504.2	3.61455
334211	HL57 286.82	B.4	AC 75.0000	.348237	.788178	59.9464	10745.3	5707.3	493.1	5.78647
334212	HL57 296.5	B.4	AC 96.8750	.453893	.657664	57.3419	10745.0	5700.5	486.2	4.22393
334213	HL57 305.14	B.4	AC 91.3444	.544901	.631308	51.8784	10744.8	5694.4	480.8	5.42442
334214	HL57 312.68	B.4	AC 97.1429	.393497	.667547	1288.89	10744.6	5689.8	474.5	7.18377
334215	HL57 317.68	B.4	AC 89.9582	.373634	.672655	54.1841	10744.5	5685.6	471.1	15.7747
334216	HL57 322.25	Si.4	AC 27.2727	.954598E-01	.936128	2.68645	10744.4	5682.4	467.9	1.56943
334217	HL57 217.43	B.4	AC 96.8784	.235452	.834176	57.9501	10744.5	5685.8	471.3	2.38227
334218	HL24 232.62	B.4	AC 96.2733	.393178	.665593	58.2793	10909.3	5764.3	464.5	13.5616
334219	HL24 246.1	B.4	AC 87.5000	.534304	.614134	52.4548	10909.0	5768.3	451.6	17.3360
334220	HL24 249.31	B.4	AC 58.5586	.368037	.679691	58.2793	10908.9	5769.2	448.6	38.7300
334221	HL24 252.8	B.4	AC 94.5946	.391919	.722714	54.3232	10908.8	5770.3	445.2	5.42806
334263	HL24 176.4-181.8	B.4	AG 98.1183	.401817	.792137	32.1323	10910.2	5749.5	513.1	2.71638
334265	HL24 183.2-187.9	B.4	AG 89.5899	.376841	.785877	32.6386	10910.1	5751.3	507.3	3.89953
334266	HL24 187.9-199.5	B.4	AG 86.3636	.348519	.787572	51.7736	10909.9	5751.7	496.2	4.81537
334267	HL24 199.5-203.9	B.4	AG 98.7813	.262334	.893051	75.7243	10909.8	5755.9	492.8	1.50426
331268	HL24 203.9-211.2	B.4	AG 93.1818	.329213	.745479	74.1467	10909.7	5758.1	485.8	5.64823
334269	HL24 211.2-229.8	B.4	AG 98.6381	.280983	.862228	77.3819	10909.5	5760.6	476.6	2.18493
334270	HL24 220.8-251.6	B.4	AG 79.7181	.276879	.745569	78.2660	10908.9	5769.9	446.4	10.6311
334271	HL24 251.6-253.9	B.4	AG 65.4497	.275786	.820408	48.6793	10908.8	5778.6	444.2	2.42972

Group 6 6 (D.14 Gnd)

Samp.No	HOLE DEPTH	ROCK TYPE	SL Zn No.	ALT1	ALT2	Ti/Zr	NORTH	EAST	RL	HR AL/3K
333916	HL14 65.8-89.6	B.5	AG 83.6956	.262774	.838063	27.5273	10588.1	5408.4	618.3	1.38874

dnap/1888 by data science
page 3

Samp.No	HOLE	DEPTH	ROCK TYPE	SL Zn No.	ALT1	ALT2	Ti/Zr	NORTH	EAST	RL	HR	AL/3K
333917	HL14	89.6-92.0	B.S	AG 35.3211	.489917	.783784	40.9647	13500.0	5409.5	616.5	1.66673	
333918	HL14	92.0-112.0	B.S	AG 92.6606	.443145	.739378	40.6793	10499.4	5422.8	560.7	2.31740	
333919	HL14	112.0-118.0	B.S	AG 77.8149	.408040	.735923	37.7453	10499.2	5425.8	596.2	2.33773	
333920	HL14	118.0-121.6	B.S	AG 97.5410	.731471	.637049	34.6368	10499.0	5427.6	593.9	2.74841	
333921	HL14	121.0-144.0	B.S	AG 84.5238	.443506	.675126	31.3188	10478.0	5442.6	575.4	3.40374	
333922	HL14	144.0-187.0	B.S	AG 66.1836	.475145	.685516	30.7733	10495.8	5469.5	543.8	2.86885	
333923	HL14	187.0-189.0	B.S	AG 84.7328	.578509	.663125	32.9716	10495.6	5470.8	541.5	2.12639	
333924	HL14	189.0-195.0	B.S	AG 89.4737	.409778	.683505	31.3982	10495.1	5477.2	533.0	3.10559	
333925	HL14	199.0-201.0	B.S	AG 80.7860	.428863	.815347	27.6284	10494.9	5479.8	531.6	1.23509	
333926	HL14	201.0-213.0	B.S	AG 98.2301	.385639	.734766	56.8476	10494.3	5486.2	523.1	4.31866	
333927	HL14	213.0-223.0	B.S	AG 97.7798	.330716	.696582	56.6179	10493.7	5492.7	515.5	10.5307	
333928	HL14	223.0-225.4	B.S	AG 81.3765	.380762	.711249	40.8151	10493.5	5494.2	513.7	3.89897	

Group 7 (D.AMIRA20)

Samp.No	HOLE	DEPTH	ROCK TYPE	SL Zn No.	ALT1	ALT2	Ti/Zr	NORTH	EAST	RL	HR	AL/3K
334162	HL6	208.4	B.S	TC 87.1595	.475601	.730281	24.6846	10498.4	5930.1	563.9	2.76151	

Group 8 (D.Licence)

Samp.No	HOLE	DEPTH	ROCK TYPE	SL Zn No.	ALT1	ALT2	Ti/Zr	NORTH	EAST	RL	HR	AL/3K
334164	HATS	418.0	B.L.6	TC 98.9011	.468686	.658850	21.3150	9324.50	2992.2	176.1	7.69926	
334165	HATS	385.1	B.L.6	TC 65.1485	.349279	.682386	18.7339	9328.40	2985.3	308.7	5.42897	
334166	HATS	87.0	B.U.6	TC 89.1566	.517365	.667266	18.1753	6194.10	3504.5	617.5	3.80558	
334167	HATS	173.3	B.U.6	TC 96.5709	.352124	.726657	53.3915	9316.40	2977.6	440.2	5.61825	
334168	HATS	365.0	B.L.6	TC 66.1749	.536335	.638245	28.2950	9320.40	2985.2	208.8	5.35524	
334169	HAC4	97.5	B.U.6	TC 42.5390	.382544	.653361	22.7224	9885.80	5862.6	633.1	36.1379	
334170	HAC4	113.6	B.U.6	TC 84.9711	.375199	.680361	23.5863	9885.40	5855.2	618.8	49.3985	

Group 9 (D.Fo HLS)

Samp.No	HOLE	DEPTH	ROCK TYPE	SL Zn No.	ALT1	ALT2	Ti/Zr	NORTH	EAST	RL	HR	AL/3K
334171	HLS	284.5	B.Fo.4	TC 90.0000	.289825	.980682	53.3787	10787.1	5746.9	466.0	1.87178	

Group 10 (D.Adlt)

Samp.No	HOLE	DEPTH	ROCK TYPE	SL Zn No.	ALT1	ALT2	Ti/Zr	NORTH	EAST	RL	HR	AL/3K
334172	ADIT	677.0	B.7	HR 89.6987	.363765	.839586	29.7616	10678.7	6258.0	389.2	2.17497	
334174	ADIT	717.0	B.pc.7	HR 91.3044	.412903	.802991	28.1637	10676.6	6238.9	389.4	2.85161	
334177	ADIT	719.0	B.7	HR 82.7586	.378626	.840941	29.1178	10677.2	6237.0	389.4	1.95887	
334175	ADIT	737.0	B.7	HR 95.1456	.467033	.776411	29.8196	10682.5	6219.8	389.6	3.34003	
334176	ADIT	755.0	B.7	HR 93.2692	.326355	.744070	33.1809	10688.3	6202.7	389.8	8.60989	
333999	ADIT	782.0	B.7	HR 94.3182	.356673	.786641	32.9716	10696.1	6176.9	394.1	8.52618	
333998	ADIT	798.0	B.7	HR 58.9520	.146866	.845546	48.9647	10698.5	6159.3	390.1	7.36495	
333997	ADIT	805.0	B.gy.7	HR 67.8373	.354318	.821743	22.3610	10703.0	6155.4	390.3	1.34795	
333996	ADIT	805.0	B.gn.7	HR 71.2913	.524477	.776387	23.6447	10703.0	6155.0	390.3	1.46750	
333995	ADIT	823.0	B.pc.7	HR 89.8400	.286935	.881788	25.8237	10708.4	6137.8	390.5	2.43450	

Samp.No	HOLE	DEPTH	ROCK TYPE	SL	Zn No.	ALT1	ALT2	Ti/Zr	NORTH	EAST	RL	HR	AI/3K
333994	ADIT	857.8	B.Lfd.Py.7	HR	73.1093	.807822	.936698	26.0952	10718.6	5185.3	390.8	645606	

Group 0 11 (Picrite)

Samp.No	HOLE	DEPTH	ROCK TYPE	SL	Zn No.	ALT1	ALT2	Ti/Zr	NORTH	EAST	RL	HR	AI/3K
272844	HL7	66.4	B.parich.5	IC	95.8904	.437804	.720250	39.2390	10600.3	5567.0	642.3	2.77009	

Group 0 12 (B.H.31 Spt)

Samp.No	HOLE	DEPTH	ROCK TYPE	SL	Zn No.	ALT1	ALT2	Ti/Zr	NORTH	EAST	RL	HR	AI/3K
334049	HL31	316.15	B.ab.0	TC	36.8658	.826055E-01	.790152	25.7591	10870.4	5923.6	396.5	12.5993	

Group 0 13 (B.H.30 Spt)

Samp.No	HOLE	DEPTH	ROCK TYPE	SL	Zn No.	ALT1	ALT2	Ti/Zr	NORTH	EAST	RL	HR	AI/3K
334067	HL30	180.0	B.5	TC	83.6735	.372910	.743885	27.3590	10902.9	5513.6	506.5	4.27197	
334068	HL30	204.4	B.5	TC	98.5075	.302560	.764322	26.2932	10902.0	5519.4	491.2	5.98796	
334069	HL30	218.1	B.5	IC	94.9580	.340801	.735059	25.9953	10902.7	5524.3	478.4	8.05126	
334070	HL30	243.0	B.5	IC	98.2759	.277345	.826960	26.7627	10902.4	5533.2	455.2	2.50521	
334071	HL30	268.5	B.5	IC	82.5581	.484053	.699772	24.3034	10901.8	5542.5	431.4	4.12319	
334072	HL30	274.5	B.pcp.NOP5	IC	85.8676	.613613	.892626	8.40905	10901.7	5544.7	425.9	1.18608	

Group 0 14 (B.H.30 Gnd)

Samp.No	HOLE	DEPTH	ROCK TYPE	SL	Zn No.	ALT1	ALT2	Ti/Zr	NORTH	EAST	RL	HR	AI/3K
334100	HL30	186.9-200.0	B.5	IC	79.2746	.309854	.803087	26.3773	10902.8	5517.9	495.3	3.20194	
334109	HL30	210.0-263.0	B.5	IC	87.9310	.354951	.762049	27.2493	10902.0	5540.5	436.5	4.90267	
334110	HL30	263.0-272.4	B.5	IC	86.4865	.376436	.743377	24.4860	10901.7	5543.9	427.0	4.34610	

Group 0 15 (B.H.31 Gnd)

Samp.No	HOLE	DEPTH	ROCK TYPE	SL	Zn No.	ALT1	ALT2	Ti/Zr	NORTH	EAST	RL	HR	AI/3K
334134	HL31	102.0-105.0	B.0	TC	80.8021	.382500	.917658	29.0321	10889.0	6009.5	580.3	1.21724	
334135	HL31	105.0-126.0	B.0	TC	86.0421	.366753	.774440	29.7703	10887.0	6001.2	560.3	2.30278	
334136	HL31	126.0-142.0	B.0	TC	72.7545	.472865	.731802	29.0750	10886.2	5995.4	554.3	2.27402	
334137	HL31	142.0-172.5	B.0	TC	80.6452	.403766	.774634	28.5120	10883.1	5983.5	526.4	1.07850	
334138	HL31	172.5-180.0	B.0	TC	92.7047	.474783	.729816	27.0111	10881.4	5977.3	512.2	2.32567	
334139	HL31	180.0-195.0	B.0	TC	92.5532	.494063	.695310	26.0190	10880.7	5974.5	505.7	2.13813	
334140	HL31	195.0-205.0	B.0	TC	98.3533	.446640	.713907	28.0359	10879.6	5979.4	496.0	2.10989	
334141	HL31	205.0-220.9	B.0	TC	75.8621	.366423	.736205	28.4200	10877.9	5963.0	482.5	2.01826	
334142	HL31	220.9-204.0	B.0	TC	77.2846	.436072	.681443	28.0194	10872.2	5937.2	425.5	7.09792	
334143	HL31	204.0-280.4	B.0	TC	70.0769	.440685	.677391	46.3310	10371.9	5935.4	421.5	9.75495	
334144	HL31	208.4-300.6	B.0	TC	83.3929	.255276	.752915	39.5656	10670.0	5926.0	403.3	6.20914	
334145	HL31	300.6-324.2	B.0	TC	81.4574	.271636	.786508	25.4701	10870.0	5920.1	389.2	3.26529	

Group 0 16 (B.HL14 Spt)

Samp.No	HOLE	DEPTH	ROCK TYPE	SL	Zn No.	ALT1	ALT2	T1/Zr	NORTH	EAST	RL	HR	AI/3K
333971	HL14	196.97	D.5	MC	97.7273	.234783	.786989	27.1766	10499.6	5418.7	604.8	9.57166	
333973	HL14	139.27	D.5	MC	98.5916	.443017	.712725	24.7787	10498.2	5439.1	579.7	1.99965	
333974	HL14	177.38	D.5	MC	97.9167	.261839	.724334	25.6922	10496.3	5463.3	558.4	17.0132	
333975	HL14	198.66	D.5	MC	98.7342	.302572	.768722	29.5458	10495.1	5477.8	534.1	5.04422	
333976	HL14	224.5	D.5	MC	94.6429	.571784	.756969	43.3912	10493.6	5493.6	514.4	2.13348	

Group 0 17 (D.HL79)

Samp.No	HOLE	DEPTH	ROCK TYPE	SL	Zn No.	ALT1	ALT2	T1/Zr	NORTH	EAST	RL	HR	AI/3K
334099	HL79	379.1	6Fugls16	TC	65.3846	.107888	.831307	36.7031	11068.8	5971.4	313.3	6.69590	

Group 0 18 (HVS)

Samp.No	HOLE	DEPTH	ROCK TYPE	SL	Zn No.	ALT1	ALT2	T1/Zr	NORTH	EAST	RL	HR	AI/3K
333977	HL14	226.5	T.bd.9	MC	92.7798	.739216	.814835	24.9515	10493.4	5495.8	512.9	1.12346	
333978	HL14	234.8	L.b.9	MC	93.9597	.571942	.759426	22.2162	10493.8	5499.9	507.2	2.38379	
333929	HL14	225.4-230.87	T.bd.9	AC	88.5462	.623835	.778823	23.6047	10493.2	5497.8	509.6	1.38212	
333938	HL14	230.87-234.1	L.b.9	AC	85.2632	.434989	.718600	20.8056	10493.8	5499.9	507.1	2.52699	
334222	HL57	323.53	D.4	AC	99.4152	.349832	.759810	54.3976	10744.4	5681.5	467.8	4.33899	
334223	HL57	326.62	L.b.9	AC	48.9362	.719080	.923620	11.9897	10744.4	5679.3	464.8	1.25633	
334072	HL30	274.4	D.9	TC	85.8696	.613613	.892626	8.40915	10901.7	5544.7	425.9	1.18608	
334072	HL30	274.5	BSH.9	TC	79.2793	.618490	.863535	28.8194	10901.7	5544.7	425.8	1.35165	
334073	HL30	275.3	BSH.D.9	TC	85.2941	.833107	.888505	7.62056	10901.6	5545.0	425.1	1.14837	
334074	HL30	278.7	BSH.D.Fa.9	TC	91.1750	.335121	.866514	44.7899	10901.5	5546.2	421.9	1.39131	
334111	HL30	272.4-278.3	BSH.9	TC	87.2180	.788102	.916857	8.53112	10901.5	5546.1	422.3	1.22139	
334112	HL30	278.3-278.8	A.b.9	TC	88.5462	.602063	.885123	35.3794	10901.5	5546.3	421.8	1.18085	
334113	HL30	278.8-283.4	A.b.9	TC	72.8000	.469962	.873584	23.7187	10901.4	5548.0	417.6	1.45685	
334050	HL31	325.5	A.9	TC	92.7928	.671136	.827708	20.6073	10869.9	5919.6	388.8	1.32265	
334051	HL31	338.8	T.bd.ch.7	TC	93.5798	.639837	.834473	25.3116	10869.2	5914.2	376.8	1.38712	
334052	HL31	341.95	L.b.9	TC	96.4786	.764452	.895246	27.9023	10869.0	5912.5	373.2	1.13369	

Group 0 19 (FPS HL14)

Samp.No	HOLE	DEPTH	ROCK TYPE	SL	Zn No.	ALT1	ALT2	T1/Zr	NORTH	EAST	RL	HR	AI/3K
333979	HL14	278.42	FPA.10	MC	97.2222	.353414	.672796	28.8640	10498.5	5524.8	480.1	26.6653	
333980	HL14	282.49	FPA.10	MC	86.6667	.446357	.759277	31.2774	10489.6	5532.1	471.2	2.84213	
333981	HL14	313.85	FPA.10	MC	60.6618	.441685	.835637	35.6836	10487.8	5553.3	448.2	1.69304	
333931	HL14	234.1-235.3	FPA.10	AC	83.8468	.492063	.753390	27.9757	10492.9	5508.7	506.2	1.61433	
333922	HL14	235.3-251.8	FPA.10	AC	99.1783	.316619	.624049	35.4675	10491.9	5516.4	475.2	13.0565	
333933	HL14	258.8-275.3	FPA.10	AC	95.4420	.363216	.638076	35.4241	10490.1	5527.1	476.7	5.39793	
333934	HL14	275.8-284.8	FPA.10	AC	98.1587	.386678	.656576	33.8837	10489.5	5533.1	478.1	5.70483	
333935	HL14	284.8-304.5	FPA.10	AC	70.1537	.336715	.773341	31.7787	10437.8	5547.8	455.8	1.81694	
333926	HL14	274.5-306.8	FPA.10	AC	68.5990	.484378	.791253	31.2231	10487.6	5548.5	453.4	1.51837	
333937	HL14	306.8-314.1	FPA.10	AC	67.9656	.323699	.860257	27.1871	10467.8	5553.5	448.8	1.57766	

Group 0 20 (FPS HL30cg)

Samp.No	HOLE	DEPTH	ROCK TYPE	SL Zn No.	ALT1	ALT2	Ti/Zr	NORTH	EAST	XL	MR	AL/3K
334114	HL30	283.4-288.2	FPA.10	IG 77.6800	.353821	.779966	23.8257	10901.2	5549.0	413.1	2.29685	
334115	HL30	288.2-314.3	FPA.10	IG 81.4815	.327189	.787482	22.7974	10900.2	5557.8	387.1	1.95244	
334116	HL30	314.3-326.2	FPA.10	IG 76.8266	.187041	.669920	21.9483	10899.8	5584.2	378.8	11.5704	
334117	HL30	326.2-382.6	FPA.10	IG 77.7227	.345519	.719439	38.4425	10897.2	5586.1	326.1	3.24024	
334118	HL30	382.6-450.2	FPA.10	IG 71.4530	.377545	.745067	31.2774	10891.8	5613.5	264.6	3.25123	
334119	HL30	450.2-454.3	FPA.10	IG 95.7717	.348074	.722630	28.4291	10871.3	5615.3	268.9	5.88791	
334120	HL30	454.3-460.1	FPA.10	IG 91.3349	.376534	.790390	30.5293	10890.6	5617.8	255.7	3.10612	
334121	HL30	460.1-463.3	FPA.10	IG 88.3378	.379765	.738733	28.2956	10890.1	5619.4	252.4	3.51837	
334122	HL30	463.3-467.4	FPA.10	IG 87.3688	.386494	.791433	27.7943	10889.3	5621.8	247.4	2.34834	
334123	HL30	467.4-470.6	FPA.10	IG 80.4938	.314343	.703450	29.9742	10889.1	5622.3	246.4	3.46175	
334124	HL30	470.6-484.4	FPA.10	IG 87.9658	.273403	.692081	29.9742	10886.7	5628.4	234.2	6.40833	

Group 0 21 (FPS HL30sc)

Samp.No	HOLE	DEPTH	ROCK TYPE	SL Zn No.	ALT1	ALT2	Ti/Zr	NORTH	EAST	XL	MR	AL/3K
334075	HL30	280.0	FPA.10	IC 67.7966	.589804	.856757	23.8431	10901.5	5546.7	428.7	1.28411	
334076	HL30	291.8	FPA.10	IC 56.8000	.150396	.769656	22.8455	10901.1	5551.1	499.8	2.83693	
334077	HL30	302.2	FPA.10	IC 80.8511	.383124	.814815	21.8331	10900.7	5555.1	400.2	1.31397	
334078	HL30	319.7	FPA.10	IC 62.9008	.216495	.666734	22.9742	10900.8	5561.7	384.8	6.57449	
334079	HL30	379.6	FPA.10	IC 61.8811	.374889	.735057	34.1811	10897.9	5581.4	337.1	2.39174	
334080	HL30	410.8	FPA.10	IC 95.3125	.362929	.800734	33.3914	10895.4	5597.3	300.2	2.77333	
334081	HL30	446.25	FPA.10	IC 87.6712	.355401	.812790	31.8447	10892.3	5611.9	268.1	2.44450	
334082	HL30	469.4	FPA.10	IC 87.5000	.311156	.693834	38.4216	10889.3	5621.8	247.4	3.73777	
334163	HL30	483.9	FPA.10	IC 87.1795	.198374	.644033	29.1784	10886.8	5628.2	234.6	86.3513	

Group 0 22 (FPS HL31)

Samp.No	HOLE	DEPTH	ROCK TYPE	SL Zn No.	ALT1	ALT2	Ti/Zr	NORTH	EAST	XL	MR	AL/3K
334053	HL31	347.7	FPA.11	IC 90.3226	.285366	.669682	29.3828	10868.7	5910.8	368.1	9.69501	
334054	HL31	355.15	FPA.Dfr.11	IC 90.8000	.841584E-01	.664425	23.2741	10868.2	5906.7	361.4	47.7432	
334055	HL31	357.3	FPA.Mix.11	IC 92.2330	.365672	.696675	26.9333	10868.1	5915.8	359.4	5.31818	
334056	HL31	383.75	Y.FPA.11	IC 82.2581	.243866	.767993	22.1548	10866.8	5894.1	335.8	2.75066	
334146	HL31	324.2-346.2	Y.FPA.11	IC 73.9927	.499644	.850882	25.1717	10868.8	5910.8	369.4	1.35470	
334147	HL31	346.2-401.8	Y.FPA.11	IC 88.8597	.342255	.728493	23.9181	10866.3	5886.3	320.4	3.52132	

Group 0 23 (FPS ADIT)

Samp.No	HOLE	DEPTH	ROCK TYPE	SL Zn No.	ALT1	ALT2	Ti/Zr	NORTH	EAST	XL	MR	AL/3K
334254	ADIT		FPA.Dfr.11	AC 44.2308	.837887E-01	.722525	22.2831	10786.0	5900.0	393.0	14.8974	
334255	ADIT		FPA.Mix.11	AC 46.6216	.328980	.690864	21.9240	10786.0	5900.0	393.0	7.79957	

Group 0 24 (Y-L HL14)

Samp.No	HOLE	DEPTH	ROCK TYPE	SL	Zn No.	ALT1	ALT2	TL/Zr	NORTH	EAST	RL	HR	AL/3K
333982	HL14	340.99	L.12	MC	99.1379	.648019	.640873	41.8390	10484.7	5571.8	428.5	1.52457	
333938	HL14	314.1-315.6	L.f.n.12	AG	89.7143	.570261	.803191	29.9712	10486.7	5554.5	447.8	1.46823	
333939	HL14	315.6-336.4	Y.b.11.12	AG	74.0113	.604723	.900926	25.4327	10485.0	5568.7	431.3	1.46771	
333940	HL14	336.4-345.8	Y.11.12	AG	71.4286	.627367	.858387	42.2245	13484.3	5575.1	425.8	1.06158	
333941	HL14	345.8-360.6	Y.11.12	AG	68.8668	.561866	.749532	54.2776	10463.2	5585.2	414.2	1.65846	
333983	HL14	367.33	L.12	MC	76.6234	.478228	.773195	31.4729	10482.7	5587.8	409.3	1.55981	
333942	HL14	360.6-363.0	Y.b.d.1.12	AG	84.5614	.575198	.783010	40.8159	10483.0	5566.8	412.5	1.03730	
333984	HL14	370.93	L.12	MC	70.3125	.744834	.879310	21.4987	10480.0	5605.9	392.2	1.607710	
333943	HL14	363.0-368.0	L.Q.12	AG	70.2703	.496617	.788366	34.7287	10482.6	5590.3	408.9	1.16184	
333944	HL14	368.0-385.0	L.12	AG	73.8687	.628809	.773697	34.1245	10481.3	5601.9	396.5	1.11757	
333945	HL14	385.3-371.3	L.gls.12	AG	80.4196	.527565	.794835	24.3540	10483.9	5606.2	392.0	1.93987	
333946	HL14	371.3-378.0	L.12	AG	70.4173	.687779	.848316	25.3496	10480.3	5613.8	387.1	1.741884	
333947	HL14	378.0-405.3	L.12	AG	67.6559	.609685	.807887	22.2665	10479.6	5615.8	381.9	1.827835	
333985	HL14	430.3	O.(O).12	MC	53.3333	.735833	.858759	31.4729	10477.4	5632.8	364.1	1.667478	
333948	HL14	405.3-419.5	L.12	AG	67.8571	.516561	.811314	23.0328	10478.4	5625.6	371.6	1.00906	
333949	HL14	419.5-421.0	Y.12	AG	74.5098	.588312	.819971	41.1075	10478.2	5626.6	374.5	1.965715	
333986	HL14	454.0	L.11.12	MC	65.8436	.534392	.694654	46.1142	10475.0	5649.3	346.8	2.92013	
333950	HL14	421.0-435.4	O.(O).12	AG	85.8407	.642522	.841019	36.5140	10476.9	5636.3	360.2	1.657043	
333987	HL14	483.5	L.11.12	MC	91.8519	.524798	.735476	47.3786	10472.2	5669.6	325.6	1.76181	
333951	HL14	435.4-450.0	L.12	AG	73.9130	.452562	.767377	55.9518	10475.4	5646.5	349.7	1.23826	
333952	HL14	450.0-475.0	L.12	AG	57.7114	.469173	.699629	55.1525	10473.0	5663.7	331.7	2.04957	
333953	HL14	475.3-500.0	L.12	AG	71.2794	.469181	.711415	62.6733	10478.7	5681.0	313.8	1.98661	
333988	HL14	522.5	L.Q.12	MC	62.9861	.966430	.656726	47.1725	10468.7	5696.6	297.7	1.27659	
333954	HL14	500.0-519.5	L.12	AG	58.2173	.553533	.746318	48.4877	10469.1	5694.6	299.8	1.31994	
333955	HL14	519.5-521.0	L.f.n.pv.12	AG	68.8474	.847197	.752880	57.4585	10468.9	5696.2	298.2	1.56112	
333956	HL14	521.0-526.0	L.12	AG	60.4317	.600393	.715809	62.9458	10468.6	5699.1	295.2	1.42344	
333957	HL14	526.0-530.5	L.f.n.pv.12	AG	76.4786	.762103	.741679	68.9407	10468.2	5702.2	292.0	1.834474	
333989	HL14	549.0	SLZ.Q.c113	MC	89.7638	.973548	.473444	46.1142	10466.8	5715.1	278.7	14.2262	
333958	HL14	530.5-539.8	SLZ.L.13	AG	70.8220	.825854	.595013	56.3515	10467.5	5708.7	285.3	3.33146	
333990	HL14	555.82	SLZ.L.gls13	MC	70.5325	.918781	.389222	27.6197	10466.2	5717.8	273.9	1.87365	
333959	HL14	539.8-549.8	SLZ.Q.13	AG	83.8509	.897083	.547584	52.9544	10466.7	5715.6	278.2	4.12660	
333960	HL14	549.8-560.2	SLZ.Q.gls13	AG	18.0327	.798817	.819622	6.99398	10465.9	5722.3	270.7	1.85532	
333961	HL14	560.2-561.5	SLZ.c1.13	AG	71.4644	.899896	.840565	21.6737	10465.7	5723.8	269.8	1.19569	
333962	HL14	561.5-569.3	SLZ.gls.13	AG	57.8819	.893130	.929680	30.5859	10465.1	5729.2	264.3	1.721980	
333963	HL14	569.3-570.4	SLZ.c1.13	AG	62.6967	.908470	.804885	31.1732	10465.0	5729.9	263.5	1.59482	
333991	HL14	587.6	SLZ.13	MC	46.9136	.822642	.921744	30.2770	10463.6	5742.0	251.2	1.18551	
333964	HL14	570.4-572.2	SLZ.f.n.13	AG	41.9473	.653725	.765719	39.2519	10464.7	5731.2	262.2	1.24035	
333965	HL14	572.2-578.8	SLZ.Q.13	AG	70.9280	.859112	.855879	68.3412	10464.3	5735.8	257.5	1.24152	
333966	HL14	578.8-599.3	SLZ.13	AG	42.4543	.817935	.898990	31.9725	10462.5	5750.1	243.0	1.45297	
333967	HL14	599.3-600.8	Jackf11.13	AG	77.8472	.804488	.679968	64.7443	10462.4	5751.2	241.9	1.96183	
333968	HL14	600.8-601.6	SLZ.13	AG	64.3154	.622299	.763665	95.9174	10462.3	5751.8	241.3	1.82915	

Group 0 25 (SLZ HL57)

Samp.No	HOLE	DEPTH	ROCK TYPE	SL	Zn No.	ALT1	ALT2	TL/Zr	NORTH	EAST	RL	HR	AL/3K
334225	HL57	336.1	SLZ.14	AC	75.2008	.356805	.938137	19.7668	10744.4	5672.6	458.1	1.15901	
334226	HL57	338.4	SLZ.14	AC	47.5004	.761933	.957992	16.7443	10744.4	5671.0	456.4	1.17923	
334227	HL57	342.95	SLZ.14	AC	41.5013	.944180	.936548	35.5694	10744.5	5667.3	453.2	1.15425	
334228	HL57	348.69	SLZ.14	AC	61.1940	.681448	.869949	36.4131	10744.6	5663.8	449.1	1.24246	

dnsp/1000 by data science

Samp. No	HOLE	DEPTH	ROCK TYPE	SL Zn No.	ALT1	ALT2	Ti/Zr	NORTH	EAST	RL	MR	AI/3K
334229	HL57	355.48	STZ.14	AC 53.4247	.562288	.835219	34.6844	10744.8	5659.8	444.3	1.68327	

Group # 26 (STZ HL51)

Samp. No	HOLE	DEPTH	ROCK TYPE	SL Zn no.	ALT1	ALT2	Ti/Zr	NORTH	EAST	RL	MR	AI/3K
334230	HL61	395.88	STZ.Q.14	AC 39.6139	.540590	.943947	49.6448	10758.8	5735.1	359.3	1.00960	
334231	HL61	404.65	STZ.Q.14	AC 24.6575	.795897	.961194	34.1445	10751.8	5730.4	351.8	1.40650	
334232	HL61	468.57	STZ.Q.14	AC 66.4740	.779324	.796271	48.8710	10751.2	5728.3	348.5	1.47642	
334233	HL61	419.64	STZ.Q.14	AC 64.8649	.542228	.939945	36.5400	10751.6	5722.4	339.2	1.28656	
334234	HL61	421.2	STZ.Q.14	AC 71.4286	.533333	.877933	34.1928	10751.6	5721.6	337.9	1.49556	
334235	HL61	426.87	STZ.Q.14	AC 71.9278	.190052	.804103	52.0604	10751.8	5718.5	333.1	4.65786	
334236	HL61	436.56	STZ.Q.14	AC 64.9123	.694465	.935344	48.6068	10752.2	5713.3	325.8	1.31479	
334237	HL15	453.0	STZ.15	AC 21.6495	.948964	.914441	38.4285	10728.3	5785.9	326.4	1.14340	
334238	HL15	456.6	STZ.vn.15	AC // - 8/22	.842942	.769111	6.66093	10728.7	5784.7	323.6	1.34144	
334239	HL15	464.5	STZ.15	AC 50.1992	.822176	.735590	15.2596	10729.7	5779.7	317.5	1.79999	
334240	HL15	480.6	STZ.gls.15	AC 65.6085	.930355	.769609	46.3233	10731.5	5769.7	305.1	1.49763	
334241	HL15	491.72	STZ.sa.15	AC 29.0598	.985886	.388889	38.6764	10732.8	5762.7	296.5	.719987	
334242	HL15	493.27	STZ.15	AC 65.7895	.949367	.687864	29.2431	10733.8	5761.7	295.3	3.26357	
334243	HL15	501.2	STZ.gls.15	AC 30.1475	.902640	.882862	32.6190	10733.9	5756.8	289.2	.998661	
334244	HL15	508.2	STZ.gls.15	AC 37.0079	.945631	.936436	28.4755	10731.7	5752.4	283.8	1.00315	
334245	HL15	513.2	STZ.gls.15	AC 64.2857	.544598	.796320	36.6334	10735.3	5749.2	280.0	1.91764	
334246	HL15	518.2	STZ.gls.15	AC 75.8000	.488869	.801955	38.4452	10735.9	5746.6	276.1	2.41265	
334247	HL15	525.6	STZ.gls.15	AC 72.8813	.533951	.788746	41.6715	10736.8	5741.4	270.5	2.14250	

Group # 27 (STZ HL50)

Samp. No	HOLE	DEPTH	ROCK TYPE	SL Zn No.	ALT1	ALT2	Ti/Zr	NORTH	EAST	RL	MR	AI/3K
334248	HL50	362.5	STZ.14	AC 47.8261	.781777	.909897	33.2441	10739.2	5712.5	394.2	1.10661	
334249	HL50	365.3	STZ.Q.14	AC 72.9738	.744162	.910519	34.1928	10739.1	5711.4	391.8	1.08390	

Group # 28 (STZ HL35A)

Samp. No	HOLE	DEPTH	ROCK TYPE	SL Zn No.	ALT1	ALT2	Ti/Zr	NORTH	EAST	RL	MR	AI/3K
334084	HL35	394.8	STZ.top.16	TC 24.3982	.879195	.936214	20.4952	10916.8	5825.8	361.8	1.03302	
334085	HL35	396.2	STZ.cl.16	TC 43.7134	.959497	.684122	32.1152	10916.1	5824.7	368.7	2.56487	
334086	HL35	397.7	STZ.cl.16	TC 39.4977	.891228	.689484	18.6762	10916.2	5823.9	359.5	2.71787	
334087	HL35	408.2	STZ.clc16	TC 88.9655	.648853	.564158	37.7826	10916.9	5817.2	351.5	0.35585	
334088	HL35	413.65	STZ.gls.16	TC 73.9927	.758164	.704506	33.4596	10917.3	5813.7	347.4	2.02853	
334089	HL35	417.2	STZ.clcn16	TC 49.0240	.986433	.546813	36.1521	10917.6	5811.4	344.7	36.7856	
334090	HL35	417.4	STZ.clc16	TC 74.7253	.786451	.748174	33.4884	10917.6	5811.3	344.5	1.30432	
334091	HL35	425.6	STZ.Qglsl6	TC 20.8893	.932615	.940239	34.5465	10918.3	5805.7	338.3	.998725	
334092	HL35	430.6	STZ.mtx.16	TC 46.7606	.855928	.965984	38.5737	10918.7	5802.7	334.6	1.26157	
334093	HL35	435.8	STZ.Q.16	TC 36.9231	.958884	.952459	29.6519	10919.2	5797.3	338.7	1.03655	

Group 0 29 (STZ HL39)

Samp.No	HOLE	DEPTH	ROCK TYPE	SL	Zn No.	ALT1	ALT2	TI/Zr	NORTH	EAST	RL	NR	AL/3K
334094	HL39	239.0	STZ.gls.16	TC	42.2729	.761905	.880471	23.4531	10804.6	5799.8	464.7	1.10138	
334095	HL39	245.9	STZ.16	IC	59.8602	.941176	.986364	9.99140	10805.3	5795.5	478.7	1.14140	
334096	HL39	251.9	STZ.no.16	IC	67.3008	.167163	.181151	3.61135	10805.9	5793.6	473.4	1.12114	
334097	HL39	254.0	STZ.gls.16	TC	64.0301	.771812	.918367	23.4571	10806.1	5792.5	471.6	1.12165	
334098	HL39	293.7	STZ.gls.16	TC	5.24781	.929864	.952440	28.1353	10810.1	5773.7	436.9	1.45726	

Group 0 30 (STZ HL31cg)

Samp.No	HOLE	DEPTH	ROCK TYPE	SL	Zn No.	ALT1	ALT2	TI/Zr	NORTH	EAST	RL	NR	AL/3K
334148	HL31	401.0-411.5	FPAYSTZ.11	TC	85.7143	.416021	.763360	22.7456	10866.0	5831.3	311.0	2.45437	
334149	HL31	411.5-431.15	FPAYSTZ.11	TC	93.0328	.466554	.756677	24.2566	10865.7	5872.3	293.7	2.10371	
334150	HL31	431.15-444.4	FPAYSTZ.11	TC	95.6667	.410542	.780360	28.5908	10865.4	5866.0	282.0	2.38387	
334151	HL31	444.4-447.5	STZ.Q.17	IC	93.9850	.373909	.792557	30.6256	10865.4	5864.5	279.3	1.87951	
334152	HL31	447.5-458.0	STZ.V.17	IC	86.5448	.566354	.841962	26.7557	10865.2	5859.4	270.1	1.18068	
334153	HL31	458.0-462.0	STZ.17	TC	70.4444	.853636	.623470	30.1868	10865.1	5857.4	266.7	2.37397	
334154	HL31	462.0-478.2	STZ.17	IC	56.6661	.753029	.578662	29.0832	10864.8	5847.4	252.6	2.13417	
334155	HL31	478.2-483.0	STZ.cl.17	IC	92.7536	.970016	.523422	31.7908	10864.7	5846.9	248.5	5.36855	
334156	HL31	483.0-489.0	STZ.17	TC	81.4332	.980506	.761886	31.9725	10864.6	5843.9	243.3	1.11572	
334157	HL31	489.0-493.0	STZ.cl.17	TC	50.6218	.983608	.621733	45.3391	10864.6	5841.8	239.9	3.95075	
334158	HL31	493.0-502.5	STZ.17	TC	53.2265	.853987	.781492	47.6862	10864.5	5835.9	231.7	1.48268	

Group 0 31 (STZ HL31sc)

Samp.No	HOLE	DEPTH	ROCK TYPE	SL	Zn No.	ALT1	ALT2	TI/Zr	NORTH	EAST	RL	NR	AL/3K
334057	HL31	409.3	FPAYSTZ.11	TC	76.5823	.394951	.764488	24.2414	10866.1	5882.3	313.0	2.39777	
334058	HL31	415.45	FPAYSTZ.11	TC	94.7686	.564014	.743333	24.9735	10865.9	5879.7	307.5	2.55253	
334059	HL31	445.5	FPAYSTZ.11	TC	92.3077	.586851	.742868	29.9742	10865.4	5865.5	281.1	2.39153	
334060	HL31	446.4	STZ.Qca.17	TC	80.2469	.312410	.764489	33.7213	10865.4	5865.8	280.3	1.98745	
334061	HL31	456.3	STZ.Y.Q.17	TC	45.8823	.790678	.885075	29.3625	10865.2	5860.2	271.6	1.21620	
334062	HL31	475.15	STZ.no.17	TC	84.9123	.969783	.707536	35.0762	10864.9	5850.9	255.2	1.65435	
334063	HL31	482.0	STZ.cl.17	TC	97.2067	.989427	.457989	33.5711	10864.7	5847.5	249.3	61.4604	
334064	HL31	488.0	STZ.si.17	TC	72.1138	.948577	.881768	32.1674	10864.7	5844.4	244.2	1.18033	
334065	HL31	497.15	STZ.no.17	TC	17.5258	.958629	.949346	52.8307	10864.6	5839.7	236.3	.992565	

Appendix 2iii

Transformed Co-ordinates For Sample Points
used in the Research Section

Flst...File (?TEMP:30)	Date 3:19 PM MON., 27 FE	Flst...File (?TEMP:30)	Date 3:19 PM MON., 27 FE	Flst...File (?TEMP:30)	Date 3:19 PM MON., 27 FE	Flst...File (?TEMP:30)	Date 3:19 PM MON., 27 FE
00001 DJJ030	29.7 11030.9 5455.2 683.6	00058 DJJ030	136.4 11033.0 5494.7 584.5	00115 DJJ055	125.4 10894.6 5883.3 570.8	00172 DJJ055A	227.9 10892.8 5848.4 474.6
00002 DJJ030	33.8 11031.1 5456.7 679.8	00059 DJJ030	140.9 11033.0 5496.4 580.3	00116 DJJ055	130.3 10894.4 5881.6 566.2	00173 DJJ055A	232.2 10892.8 5846.9 470.5
00003 DJJ030	42.2 11031.3 5459.7 672.0	00060 DJJ030	145.5 11033.0 5498.1 576.1	00117 DJJ055	135.2 10894.2 5879.9 561.6	00174 DJJ055A	239.4 10892.9 5844.3 463.8
00004 DJJ030	46.5 11031.5 5461.3 667.9	00061 DJJ030	154.6 11033.1 5501.5 567.6	00118 DJJ055	148.9 10893.8 5875.3 548.8	00175 DJJ055A	247.0 10893.0 5841.6 456.7
00005 DJJ030	50.7 11031.6 5462.8 664.0	00062 DJJ030	159.2 11033.0 5503.2 563.3	00119 DJJ055	157.3 10893.6 5872.5 540.8	00176 DJJ055A	257.5 10893.1 5837.8 446.9
00006 DJJ030	59.8 11031.9 5466.1 655.6	00063 DJJ030	163.8 11033.0 5504.9 559.1	00120 DJJ055	161.7 10893.4 5871.0 536.7	00177 DJJ050	243.8 10873.0 5788.1 495.0
00007 DJJ030	69.3 11032.1 5469.6 646.7	00064 DJJ030	168.4 11033.0 5506.6 554.8	00121 DJJ055	166.2 10893.3 5869.5 532.5	00178 DJJ050	262.2 10872.4 5778.3 479.4
00008 DJJ030	74.1 11032.2 5471.4 642.3	00065 DJJ030	173.1 11033.0 5508.3 550.4	00122 DJJ055	170.6 10893.2 5868.1 528.3	00179 DJJ050	282.9 10871.7 5767.4 461.8
00009 DJJ030	81.4 11032.4 5474.1 635.6	00066 DJJ030	177.7 11033.0 5509.9 546.1	00123 DJJ055	175.1 10893.1 5866.6 524.1	00180 DJJ050	299.1 10871.2 5758.9 448.1
00010 DJJ024(2)	7.2 11031.9 5697.5 709.5	00067 DJJ030	182.3 11032.9 5511.6 541.8	00124 DJJ055A	183.9 10892.9 5863.7 515.8	00181 DJJ028	139.6 10801.7 5760.1 562.8
00011 DJJ024(2)	11.4 11032.2 5698.8 705.5	00068 DJJ030	120.5 11032.9 5488.8 599.3	00125 DJJ055A	188.3 10892.9 5862.2 511.7	00182 DJJ028	145.5 10801.2 5762.7 557.5
00012 DJJ024(2)	15.6 11032.6 5700.1 701.5	00069 DJJ024(2)	55.8 11035.9 5712.5 663.5	00126 DJJ055A	192.7 10892.8 5860.7 507.5	00183 DJJ028	158.0 10800.3 5768.2 546.4
00013 DJJ024(2)	19.8 11032.9 5701.4 697.6	00070 DJJ024(2)	61.9 11036.4 5714.4 657.7	00127 DJJ055A	197.1 10892.8 5859.2 503.4	00184 DJJ028	169.6 10899.3 5773.3 536.0
00014 DJJ024(2)	28.9 11033.7 5704.2 688.9	00071 DJJ024(2)	66.6 11036.7 5715.8 653.2	00128 DJJ055A	201.5 10892.8 5857.7 499.3	00185 DJJ028	170.3 10899.2 5773.6 535.3
00015 DJJ024(2)	33.8 11034.1 5705.7 684.3	00072 DJJ024(2)	71.4 11037.1 5717.3 648.7	00129 DJJ055A	205.9 10892.7 5856.2 495.1	00186 DJJ028	173.3 10899.0 5774.9 532.6
00016 DJJ024(2)	38.7 11034.5 5707.3 679.7	00073 DJJ024(2)	76.2 11037.4 5718.8 644.1	00130 DJJ055A	215.2 10892.7 5852.9 486.4	00187 DJJ028	188.0 10897.7 5781.4 519.6
00017 DJJ024(2)	43.6 11034.9 5708.8 675.0	00074 DJJ024(2)	80.9 11037.8 5720.2 639.6	00131 DJJ055A	220.1 10892.8 5851.2 481.9	00188 DJJ028	208.3 10896.0 5790.4 501.4
00018 DJJ024(2)	48.5 11035.3 5710.3 670.4	00075 DJJ024(2)	85.7 11038.1 5721.6 635.1	00132 DJJ055A	225.0 10892.8 5849.4 477.3	00189 DJJ028	228.9 10894.2 5799.6 483.1
00019 DJJ024(2)	53.9 11035.7 5712.0 665.2	00076 DJJ024(2)	90.5 11038.4 5723.1 630.5	00133 DJJ055A	229.4 10892.8 5847.9 473.2	00190 DJJ028	234.6 10893.7 5802.2 478.0
00020 DJJ031	11.6 10899.5 6043.5 674.8	00077 DJJ024(2)	95.2 11038.7 5724.5 626.0	00134 DJJ055A	237.4 10892.9 5845.0 465.7	00191 DJJ028	249.1 10892.5 5808.8 465.1
00021 DJJ031	16.2 10899.2 6041.8 670.5	00078 DJJ024(2)	104.5 11039.2 5727.3 617.2	00135 DJJ055A	245.2 10893.0 5842.2 458.4	00192 DJJ028	265.8 10891.1 5816.5 458.5
00022 DJJ031	23.4 10898.6 6039.2 663.8	00079 DJJ024(2)	109.1 11039.4 5728.6 612.8	00136 DJJ055A	249.5 10893.0 5840.7 454.4	00193 DJJ057	222.6 10876.2 5765.4 538.8
00023 DJJ031	28.5 10898.1 6037.3 659.1	00080 DJJ024(2)	113.6 11039.6 5730.0 608.5	00137 DJJ055A	253.7 10893.1 5839.1 451.5	00194 DJJ057	229.2 10876.2 5760.7 534.1
00024 DJJ031	33.0 10897.7 6035.7 654.9	00081 DJJ024(2)	118.2 11039.8 5731.3 604.1	00138 DJJ055A	259.0 10893.1 5837.2 445.5	00195 DJJ057	245.4 10876.2 5749.3 522.6
00025 DJJ031	34.5 10897.5 6035.2 653.5	00082 DJJ024(2)	122.7 11039.9 5732.6 599.8	00139 DJJ055	73.5 10896.8 591.3 619.5	00196 DJJ057	271.3 10875.7 5731.2 504.1
00026 DJJ031	38.3 10897.1 6033.9 650.0	00083 DJJ024(2)	127.3 11040.0 5733.9 595.4	00140 DJJ055	83.3 10896.4 5897.9 610.3	00197 DJJ057	286.8 10875.3 5720.3 493.0
00027 DJJ031	44.8 10896.2 6031.6 643.9	00084 DJJ024(2)	131.8 11040.1 5735.2 591.1	00141 DJJ055	89.5 10896.1 5895.7 604.5	00198 DJJ057	296.5 10875.0 5713.6 486.1
00028 DJJ031	48.1 10895.8 6030.5 640.9	00085 DJJ024(2)	136.4 11040.2 5736.5 586.6	00142 DJJ055	92.0 10896.0 5894.8 602.2	00199 DJJ057	305.1 10874.8 5707.5 480.0
00029 DJJ031	9.1 10899.7 6044.4 677.0	00086 DJJ024(2)	141.9 11040.3 5737.8 582.3	00143 DJJ055	100.1 10895.6 5892.0 594.6	00200 DJJ057	312.9 10874.6 5702.0 474.5
00030 DJJ031	13.7 10899.4 6042.7 672.8	00087 DJJ024(2)	145.5 11040.3 5739.1 577.9	00144 DJJ055	100.7 10895.6 5891.8 594.0	00201 DJJ057	317.7 10874.5 5698.7 471.1
00031 DJJ031	18.2 10899.0 6041.0 668.6	00088 DJJ024(2)	154.4 11040.4 5741.6 569.4	00145 DJJ055	101.8 10895.5 5891.4 593.0	00202 DJJ057	322.3 10874.4 5695.4 467.8
00032 DJJ031	22.8 10898.7 6039.4 664.4	00089 DJJ024(2)	158.8 11040.4 5742.8 565.2	00146 DJJ055	102.9 10895.5 5891.0 591.9	00203 DJJ024(1)	217.4 10894.6 5759.9 479.1
00033 DJJ031	27.3 10898.2 6037.8 660.2	00090 DJJ024(2)	163.2 11040.4 5744.1 561.0	00147 DJJ055	112.0 10895.1 5887.9 583.4	00204 DJJ024(1)	232.6 10894.3 5764.3 464.5
00034 DJJ031	31.8 10897.8 6036.2 656.0	00091 DJJ024(2)	167.6 11040.4 5745.4 556.7	00148 DJJ055	116.4 10894.9 5886.4 579.2	00205 DJJ024(1)	246.1 10894.0 5768.3 451.7
00035 DJJ031	36.4 10897.3 6034.5 651.8	00092 DJJ024(2)	172.0 11040.3 5746.6 552.5	00149 DJJ055	116.7 10894.9 5886.3 579.0	00206 DJJ024(1)	249.3 10898.9 5769.2 448.6
00036 DJJ031	40.9 10896.7 6033.0 647.5	00093 DJJ031	56.2 10894.7 6027.6 633.4	00150 DJJ055	123.5 10894.6 5883.9 572.6	00207 DJJ024(1)	252.8 10898.9 5770.2 445.3
00037 DJJ031	45.5 10896.2 6031.4 643.3	00094 DJJ031	61.0 10894.1 6025.9 628.9	00151 DJJ055	125.1 10894.6 5883.4 571.1	00208 DJJ014	87.3 10630.1 5406.5 520.1
00038 DJJ031	54.4 10895.0 6028.2 635.0	00095 DJJ031	65.7 10893.6 6024.2 624.6	00152 DJJ055	129.2 10894.4 5882.0 567.3	00209 DJJ014	90.8 10630.0 5408.0 517.4
00039 DJJ031	58.7 10894.4 6026.7 631.1	00096 DJJ031	70.5 10893.1 6022.5 621.1	00153 DJJ055	129.6 10894.4 5881.8 566.9	00210 DJJ014	96.0 10629.9 5412.0 513.4
00040 DJJ031	63.1 10893.9 6025.2 627.0	00097 DJJ031	75.2 10892.6 6020.7 615.8	00154 DJJ055	133.7 10894.3 5880.4 563.1	00211 DJJ014	100.0 10629.8 5414.5 510.3
00041 DJJ031	67.5 10893.4 6023.6 622.9	00098 DJJ031	84.4 10891.7 6017.3 607.3	00155 DJJ055	141.2 10894.0 5877.9 556.0	00212 DJJ014	104.0 10629.7 5417.0 507.2
00042 DJJ031	71.8 10892.9 6022.0 618.9	00099 DJJ031	88.8 10891.3 6015.7 603.3	00156 DJJ055	151.7 10893.7 5874.4 546.1	00213 DJJ014	108.0 10629.5 5419.6 504.0
00043 DJJ031	76.2 10892.5 6020.4 614.9	00100 DJJ031	93.2 10890.9 6014.0 599.2	00157 DJJ055	153.6 10893.7 5873.7 544.3	00214 DJJ014	115.0 10629.3 5423.9 498.6
00044 DJJ031	80.6 10892.0 6018.7 610.8	00101 DJJ031	97.6 10890.5 6012.3 595.1	00158 DJJ055	154.2 10893.6 5873.5 543.8	00215 DJJ014	119.5 10629.1 5426.7 495.1
00045 DJJ014	49.0 10630.8 5381.9 549.4	00102 DJJ028	136.2 10891.9 5758.5 565.8	00159 DJJ055	157.9 10893.5 5872.3 541.3	00216 DJJ014	125.8 10628.8 5430.7 491.2
00046 DJJ014	75.8 10630.4 5399.2 529.8	00103 DJJ055	68.5 10897.1 5903.0 624.1	00160 DJJ055	165.5 10893.3 5869.8 533.1	00217 DJJ014	130.5 10628.6 5433.6 486.5
00047 DJJ030	87.9 11032.5 5476.6 629.5	00104 DJJ055	73.1 10896.8 5901.4 619.8	00161 DJJ055	167.1 10893.3 5869.2 531.6	00218 DJJ014	135.3 10628.4 5436.7 482.8
00048 DJJ030	91.9 11032.6 5478.1 625.8	00105 DJJ055	77.6 10896.6 5899.9 615.6	00162 DJJ055	176.0 10893.1 5866.3 523.2	00219 DJJ014	140.0 10628.2 5439.6 479.2
00049 DJJ030	95.9 11032.7 5479.6 622.0	00106 DJJ055	82.1 10896.4 5898.3 611.4	00163 DJJ055	183.5 10892.9 5863.9 516.1	00220 DJJ014	149.5 10627.7 5445.6 471.8
00050 DJJ030	120.5 11032.9 5488.8 599.3	00107 DJJ055	86.7 10896.2 5896.7 607.1	00164 DJJ055	189.6 10892.8 5861.9 510.4	00221 DJJ014	154.2 10627.5 5448.6 468.2
00051 DJJ030	104.5 11032.8 5482.8 614.1	00108 DJJ055	92.2 10895.9 5894.8 602.0	00165 DJJ055	191.1 10892.7 5861.4 508.9	00222 DJJ014	158.8 10627.3 5451.5 464.6
00052 DJJ030	109.1 11032.8 5484.6 609.8	00109 DJJ055	96.1 10895.8 5893.4 598.3	00166 DJJ055A	193.5 10892.8 5860.4 506.8	00223 DJJ014	163.5 10627.0 5454.5 461.0
00053 DJJ030	113.6 11032.9 5486.2 605.7	00110 DJJ055	101.0 10895.6 5891.7 593.7	00167 DJJ055A	198.4 10892.8 5858.8 502.2	00224 DJJ014	168.2 10626.8 5457.5 457.4
00054 DJJ030	118.2 11032.9 5488.0 601.4	00111 DJJ055	105.9 10895.3 5890.0 589.1	00168 DJJ055A	203.0 10892.8 5857.2 497.9	00225 DJJ014	172.9 10626.5 5460.5 453.8
00055 DJJ030	122.7 11033.0 5489.6 597.2	00112 DJJ055	110.8 10895.1 5888.3 584.5	00169 DJJ055A	207.9 10892.7 5855.5 493.3	00226 DJJ014	177.6 10626.3 5463.5 450.2
00056 DJJ030	127.3 11033.0 5491.4 593.0	00113 DJJ055	115.7 10894.9 5886.6 579.9	00170 DJJ055A	218.5 10892.8 5851.7 483.3	00227 DJJ014	182.2 10626.0 5466.5 446.7
00057 DJJ030	131.8 11033.0 5493.0 588.8	00114 DJJ055	120.5 10894.7 5885.0 575.4	00171 DJJ055A	223.4 10892.8 5850.0 478.8	00228 DJJ014	186.9 10625.8 5469.5 443.1

Flist...File (TEMP:30)	Date 3:19 PM MON., 27 F	Flist...File (TEMP:30)	Date 3:19 PM MON., 27 F	Flist...File (TEMP:30)	Date 3:19 PM MON., 27 F	Flist...File (TEMP:30)	Date 3:19 PM MON., 27 F
00229 DJ014	188.0 10625.7 5478.2 442.2	00286 DJ031	240.3 10875.9 5955.7 465.0	00343 DJ014	258.3 10621.3 5516.0 389.1	00400 DJ030	446.3 11022.3 5611.9 298.1
00230 DJ014	192.3 10625.5 5472.9 438.9	00287 DJ031	245.0 10875.4 5953.7 460.8	00344 DJ014	262.5 10621.0 5518.8 385.9	00401 DJ030	469.4 11019.2 5621.8 277.4
00231 DJ014	195.7 10625.3 5475.1 436.3	00288 DJ031	250.0 10874.9 5951.6 456.3	00345 DJ014	266.7 10620.7 5521.6 382.8	00402 DJ030	483.9 11016.8 5628.2 264.6
00232 DJ014	200.4 10625.0 5478.1 432.7	00289 DJ031	254.9 10874.5 5949.6 451.8	00346 DJ014	270.8 10620.4 5524.3 379.8	00403 DJ031	347.7 10868.7 5918.0 368.1
00233 DJ014	205.5 10624.7 5481.4 428.8	00290 DJ031	259.7 10874.0 5947.5 447.5	00347 DJ014	279.5 10619.8 5530.1 373.4	00404 DJ031	355.2 10868.2 5906.7 361.4
00234 DJ014	209.3 10624.5 5483.8 425.9	00291 DJ031	264.6 10873.6 5945.5 443.1	00348 DJ014	287.4 10619.2 5535.5 367.6	00405 DJ031	357.3 10868.1 5905.8 359.5
00235 DJ014	216.3 10624.1 5488.4 421.6	00292 DJ031	269.4 10873.2 5943.4 438.7	00349 DJ014	290.8 10618.9 5537.7 365.1	00406 DJ031	383.8 10866.8 5894.1 335.8
00236 DJ014	219.7 10623.8 5490.6 418.0	00293 DJ031	274.3 10872.8 5941.4 434.3	00350 DJ014	294.3 10618.6 5540.1 362.5	00407 DJ031	328.6 10869.8 5918.3 385.3
00237 DJ014	224.2 10623.6 5493.5 414.6	00294 DJ031	279.1 10872.5 5939.3 430.0	00351 DJ014	297.7 10618.4 5542.4 361.0	00408 DJ031	333.0 10869.5 5916.4 381.3
00238 DJ031	316.2 10870.4 5923.6 396.5	00295 DJ031	286.2 10872.0 5936.4 423.6	00352 DJ014	301.1 10618.1 5544.7 357.5	00409 DJ031	337.4 10869.3 5914.5 377.4
00239 DJ030	188.0 11032.9 5513.6 536.5	00296 DJ031	292.4 10871.7 5933.7 418.0	00353 DJ014	305.7 10617.7 5547.8 354.2	00410 DJ031	341.8 10869.0 5912.6 373.4
00240 DJ030	204.4 11032.8 5519.4 521.2	00297 DJ031	296.5 10871.4 5932.0 414.2	00354 DJ014	310.4 10617.3 5551.0 350.7	00411 DJ031	351.2 10868.5 5908.5 365.0
00241 DJ030	218.1 11032.6 5524.3 508.4	00298 DJ031	300.5 10871.2 5930.3 411.6	00355 DJ030	285.8 11031.2 5548.9 445.3	00412 DJ031	356.2 10868.2 5906.3 360.5
00242 DJ030	243.0 11032.3 5533.3 485.1	00299 DJ031	304.6 10871.0 5928.5 406.9	00356 DJ030	292.5 11031.0 5551.4 439.1	00413 DJ031	361.2 10867.9 5904.1 356.0
00243 DJ030	268.5 11031.8 5542.5 461.4	00300 DJ031	308.6 10870.8 5926.8 403.3	00357 DJ030	296.9 11030.8 5553.1 435.0	00414 DJ031	366.1 10867.6 5911.9 351.6
00244 DJ030	274.5 11031.6 5544.7 455.8	00301 DJ031	312.5 10870.6 5925.2 399.8	00358 DJ030	301.3 11030.7 5554.7 431.0	00415 DJ031	371.1 10867.4 5899.7 347.1
00245 DJ030	191.3 11032.9 5514.8 533.4	00302 DJ031	316.4 10870.4 5923.5 396.3	00359 DJ030	305.6 11030.5 5556.3 427.0	00416 DJ031	376.1 10867.2 5897.5 342.6
00246 DJ030	195.6 11032.8 5516.3 529.4	00303 DJ031	320.3 10870.2 5921.8 392.8	00360 DJ030	310.0 11030.3 5558.0 422.9	00417 DJ031	381.1 10866.9 5895.3 338.2
00247 DJ030	204.8 11032.8 5519.6 520.8	00304 DJ014	107.0 10629.6 5418.9 504.8	00361 DJ030	318.3 11030.0 5561.2 415.2	00418 DJ031	386.1 10866.7 5893.1 333.7
00248 DJ030	209.7 11032.7 5521.3 516.2	00305 DJ014	139.3 10628.2 5439.2 479.7	00362 DJ030	322.2 11029.9 5562.7 411.6	00419 DJ031	391.0 10866.6 5890.9 329.3
00249 DJ030	214.5 11032.7 5523.0 511.7	00306 DJ014	177.4 10626.3 5463.4 450.4	00363 DJ030	330.9 11029.5 5566.0 403.6	00420 DJ031	396.0 10866.4 5888.6 324.8
00250 DJ030	219.4 11032.6 5524.8 507.2	00307 DJ014	198.7 10625.1 5477.0 434.0	00364 DJ030	335.6 11029.4 5567.8 399.3	00421 DJ014	341.0 10614.7 5571.9 328.5
00251 DJ030	224.2 11032.6 5526.5 502.7	00308 DJ014	224.5 10623.6 5493.7 414.4	00365 DJ030	340.3 11029.2 5569.6 394.9	00422 DJ014	314.8 10616.9 5554.1 347.5
00252 DJ030	229.1 11032.5 5528.3 498.1	00309 DJ018	178.5 11029.2 5727.0 540.9	00366 DJ030	345.0 11029.0 5571.4 390.6	00423 DJ014	319.8 10616.5 5557.4 343.9
00253 DJ030	233.9 11032.5 5530.0 493.6	00310 DJ018	181.7 11029.1 5727.5 537.8	00367 DJ030	349.7 11028.8 5573.2 386.3	00424 DJ014	323.9 10616.1 5560.2 340.9
00254 DJ030	238.8 11032.4 5531.7 489.0	00311 DJ018	198.0 11028.5 5730.0 521.7	00368 DJ030	354.4 11028.6 5575.1 381.9	00425 DJ014	328.1 10615.7 5563.1 337.9
00255 DJ030	243.6 11032.3 5533.5 484.6	00312 DJ018	208.2 11028.1 5731.5 511.6	00369 DJ030	359.1 11028.4 5576.9 377.6	00426 DJ014	332.2 10615.4 5565.9 334.9
00256 DJ030	248.5 11032.2 5535.2 480.0	00313 DJ018	222.0 11027.6 5733.6 498.0	00370 DJ030	363.8 11028.2 5578.7 373.3	00427 DJ014	341.1 10614.6 5571.9 328.4
00257 DJ030	253.3 11032.2 5537.0 475.5	00314 DJ018	224.5 11027.5 5734.0 495.5	00371 DJ030	368.5 11027.9 5580.5 369.0	00428 DJ014	354.7 10613.9 5578.5 321.4
00258 DJ030	258.1 11032.1 5538.7 471.0	00315 DJ018	238.6 11027.0 5736.2 481.6	00372 DJ030	373.2 11027.7 5582.4 364.7	00429 DJ014	355.7 10613.5 5581.9 317.8
00259 DJ030	267.7 11031.8 5542.2 462.1	00316 DJ018	245.8 11026.8 5737.3 474.5	00373 DJ030	377.9 11027.4 5584.2 361.3	00430 DJ014	367.3 10612.7 5589.8 309.3
00260 DJ031	103.5 10889.9 6010.1 589.7	00317 DJ018	251.5 11026.6 5738.1 468.8	00374 DJ030	387.4 11026.9 5588.0 351.6	00431 DJ014	361.8 10613.1 5586.1 313.4
00261 DJ031	109.4 10889.4 6007.8 584.3	00318 DJ014	226.5 10623.4 5495.0 412.9	00375 DJ030	392.2 11026.6 5589.9 347.2	00432 DJ014	390.9 10610.8 5606.0 292.2
00262 DJ031	113.7 10889.0 6006.2 580.3	00319 DJ014	234.0 10622.9 5499.9 407.2	00376 DJ030	397.1 11026.3 5591.8 342.7	00433 DJ014	365.5 10612.8 5588.6 310.7
00263 DJ031	118.1 10888.6 6004.5 576.3	00320 DJ014	228.1 10623.3 5496.0 411.7	00377 DJ030	401.9 11026.0 5593.7 338.3	00434 DJ014	372.2 10612.3 5593.2 305.8
00264 DJ031	122.4 10888.2 6002.9 572.3	00321 DJ014	232.5 10623.0 5498.9 408.3	00378 DJ030	406.7 11025.7 5595.6 334.0	00435 DJ014	376.5 10612.0 5596.1 302.7
00265 DJ031	130.6 10887.4 5999.8 564.8	00322 DJ030	323.5 10874.4 5694.5 467.0	00379 DJ030	411.6 11025.3 5597.6 329.5	00436 DJ014	380.7 10611.7 5599.0 299.6
00266 DJ031	134.4 10887.0 5998.3 561.3	00323 DJ018	267.4 11026.1 5740.5 453.1	00380 DJ030	416.4 11025.0 5599.5 325.1	00437 DJ014	387.1 10611.1 5603.4 295.0
00267 DJ031	138.2 10886.6 5996.9 557.8	00324 DJ018	270.7 11026.0 5741.0 449.9	00381 DJ030	421.2 11024.6 5601.5 320.7	00438 DJ014	430.0 10607.4 5632.8 264.1
00268 DJ031	146.3 10885.8 5993.8 550.4	00325 DJ030	326.6 10874.4 5692.4 464.8	00382 DJ030	426.0 11024.2 5603.5 316.4	00439 DJ014	394.7 10610.5 5608.6 289.5
00269 DJ031	150.7 10885.4 5992.1 546.3	00326 DJ030	274.4 11031.6 5544.7 455.9	00383 DJ030	430.9 11023.8 5605.5 311.9	00440 DJ014	401.6 10609.9 5613.3 284.5
00270 DJ031	155.1 10884.9 5990.4 542.3	00327 DJ030	274.5 11031.6 5544.7 455.8	00384 DJ030	435.7 11023.3 5607.5 307.6	00441 DJ014	454.0 10605.0 5649.3 246.8
00271 DJ031	159.4 10884.5 5988.7 538.4	00328 DJ030	275.3 11031.6 5545.0 455.0	00385 DJ030	440.5 11022.9 5609.5 303.2	00442 DJ014	488.8 10609.3 5618.3 279.3
00272 DJ031	163.8 10884.0 5987.0 534.3	00329 DJ030	278.7 11031.5 5546.2 452.1	00386 DJ030	445.4 11022.4 5611.5 298.8	00443 DJ014	483.5 10602.2 5669.6 225.6
00273 DJ031	168.1 10883.5 5985.3 534.4	00330 DJ030	275.3 11031.6 5545.0 455.0	00387 DJ030	452.2 11021.6 5614.4 292.7	00444 DJ014	412.4 10609.0 5620.7 276.7
00274 DJ031	176.4 10882.7 5982.0 522.8	00331 DJ030	278.5 11031.5 5546.2 452.1	00388 DJ030	457.2 11020.9 5616.5 288.3	00445 DJ014	415.9 10608.7 5623.1 274.2
00275 DJ031	180.2 10882.3 5980.5 519.4	00332 DJ030	281.1 11031.4 5547.1 449.7	00389 DJ030	461.9 11020.3 5618.6 284.1	00446 DJ014	420.3 10608.3 5626.2 271.0
00276 DJ031	184.1 10881.9 5978.9 515.8	00333 DJ031	325.5 10869.9 5919.6 388.1	00390 DJ030	466.6 11019.6 5620.6 279.9	00447 DJ014	522.5 10598.9 5696.7 197.7
00277 DJ031	191.5 10881.1 5976.0 509.1	00334 DJ031	338.0 10869.2 5914.2 376.8	00391 DJ030	470.0 11019.1 5622.1 276.9	00448 DJ014	425.8 10607.8 5629.9 267.1
00278 DJ031	198.3 10880.4 5973.2 502.9	00335 DJ031	342.0 10869.0 5912.5 373.3	00392 DJ030	475.2 11018.3 5624.4 272.3	00449 DJ014	438.6 10607.3 5633.2 263.6
00279 DJ031	201.7 10880.0 5971.8 499.8	00336 DJ014	278.4 10620.5 5524.0 381.1	00393 DJ030	479.8 11017.5 5626.4 268.2	00450 DJ014	439.1 10606.5 5639.1 257.5
00280 DJ031	209.0 10879.2 5968.8 493.2	00337 DJ014	282.5 10619.6 5532.1 371.2	00394 DJ030	280.0 11031.4 5546.7 450.7	00451 DJ014	442.7 10606.2 5641.6 254.9
00281 DJ031	213.0 10878.8 5967.1 489.6	00338 DJ014	313.8 10617.0 5553.4 348.2	00395 DJ030	291.8 11031.0 5551.1 439.7	00452 DJ014	549.0 10596.7 5715.1 178.7
00282 DJ031	216.9 10878.4 5965.5 486.1	00339 DJ014	234.7 10622.9 5580.4 406.7	00396 DJ030	302.2 11030.6 5555.1 430.1	00453 DJ014	446.3 10605.8 5644.0 252.3
00283 DJ031	225.7 10877.4 5961.8 478.2	00340 DJ014	240.2 10622.5 5584.0 402.6	00397 DJ030	319.7 11030.0 5561.7 413.9	00454 DJ014	555.8 10596.2 5719.8 173.9
00284 DJ031	230.6 10876.9 5959.8 473.7	00341 DJ014	245.1 10622.2 5587.2 398.9	00398 DJ030	370.6 11027.8 5581.4 367.0	00455 DJ014	454.2 10605.8 5649.5 246.6
00285 DJ031	235.5 10876.4 5957.7 469.3	00342 DJ014	254.2 10621.6 5583.2 392.1	00399 DJ030	410.8 11025.4 5597.3 330.2	00456 DJ014	458.3 10604.6 5652.3 243.7

Flist...File (?TEMP::30) Date 3:19 PM MON., 27 F Flist...File (?TEMP::30) Date 3:19 PM MON., 27 FEB.

00457	0DJ014	462.5	10604.2	5655.2	240.7	00514	0DJ035A	394.8	10906.4	5824.6	361.3
00458	0DJ014	466.7	10603.8	5658.1	237.7	00515	0DJ035A	396.2	10906.5	5823.7	360.2
00459	0DJ014	470.8	10603.4	5660.9	234.7	00516	0DJ035A	397.7	10906.6	5822.7	359.1
00460	0DJ014	587.6	10593.6	5742.0	151.2	00517	0DJ035A	408.2	10907.4	5816.0	351.1
00461	0DJ014	479.2	10602.6	5666.7	228.7	00518	0DJ035A	413.7	10907.8	5812.5	346.9
00462	0DJ014	483.3	10602.2	5669.5	225.7	00519	0DJ035A	417.2	10908.1	5810.2	344.2
00463	0DJ014	487.5	10601.8	5672.4	222.7	00520	0DJ035A	417.4	10908.1	5810.1	344.1
00464	0DJ014	491.7	10601.4	5675.3	219.7	00521	0DJ035A	425.6	10908.7	5804.7	337.9
00465	0DJ014	493.8	10601.3	5676.8	218.2	00522	0DJ035A	430.6	10909.2	5801.5	334.1
00466	0DJ014	503.9	10600.4	5683.8	211.0	00523	0DJ035A	435.8	10909.6	5798.0	330.2
00467	0DJ014	507.8	10600.1	5686.5	208.2	00524	0DJ039(2)	239.0	10934.7	5799.8	514.7
00468	0DJ014	511.7	10599.8	5689.2	205.4	00525	0DJ039(2)	245.9	10935.3	5796.5	508.7
00469	0DJ014	515.6	10599.4	5691.9	202.6	00526	0DJ039(2)	251.9	10935.9	5793.6	503.5
00470	0DJ014	520.7	10599.0	5695.4	199.0	00527	0DJ039(2)	254.0	10936.1	5792.6	501.6
00471	0DJ014	523.9	10598.8	5697.7	196.7	00528	0DJ039(2)	293.7	10940.1	5773.7	467.0
00472	0DJ014	528.3	10598.4	5700.7	193.5	00529	0DJ031	406.3	10866.1	5884.0	315.7
00473	0DJ014	535.2	10597.9	5705.5	188.6	00530	0DJ031	416.4	10865.9	5879.3	306.7
00474	0DJ014	543.1	10597.2	5711.0	183.0	00531	0DJ031	421.3	10865.8	5877.0	302.4
00475	0DJ014	546.5	10596.9	5713.4	180.5	00532	0DJ031	426.2	10865.8	5874.7	298.1
00476	0DJ014	553.3	10596.4	5718.1	175.7	00533	0DJ031	435.5	10865.6	5870.3	289.9
00477	0DJ014	556.7	10596.1	5720.5	173.2	00534	0DJ031	440.0	10865.5	5868.2	285.9
00478	0DJ014	560.8	10595.8	5723.3	170.3	00535	0DJ031	446.0	10865.4	5865.3	280.7
00479	0DJ014	565.4	10595.4	5726.5	167.0	00536	0DJ031	451.0	10865.3	5862.9	276.3
00480	0DJ014	569.8	10595.1	5729.6	163.9	00537	0DJ031	454.5	10865.2	5861.2	273.2
00481	0DJ014	571.3	10594.9	5730.6	162.8	00538	0DJ031	460.0	10865.1	5858.5	268.4
00482	0DJ014	575.5	10594.6	5733.5	159.8	00539	0DJ031	466.1	10865.0	5855.5	263.1
00483	0DJ014	582.9	10594.0	5738.7	154.6	00540	0DJ031	470.1	10864.9	5853.5	259.6
00484	0DJ014	587.0	10593.6	5741.6	151.7	00541	0DJ031	474.2	10864.9	5851.4	256.1
00485	0DJ014	591.1	10593.3	5744.4	148.8	00542	0DJ031	480.6	10864.8	5848.2	250.6
00486	0DJ014	595.2	10592.9	5747.3	145.9	00543	0DJ031	486.0	10864.7	5845.5	245.9
00487	0DJ014	600.1	10592.5	5750.8	142.4	00544	0DJ031	491.0	10864.6	5842.9	241.6
00488	0DJ014	601.2	10592.4	5751.5	141.6	00545	0DJ031	497.8	10864.5	5839.4	235.8
00489	0DJ057	336.1	10874.3	5685.7	458.0	00546	0DJ031	409.3	10866.1	5882.6	313.0
00490	0DJ057	338.4	10874.4	5684.0	456.4	00547	0DJ031	415.5	10865.9	5879.7	307.6
00491	0DJ057	343.0	10874.4	5680.8	453.2	00548	0DJ031	445.5	10865.4	5865.5	281.1
00492	0DJ057	348.7	10874.6	5676.8	449.1	00549	0DJ031	446.4	10865.4	5865.1	280.3
00493	0DJ057	355.5	10874.8	5672.0	444.3	00550	0DJ031	456.3	10865.2	5860.3	271.7
00494	0DJ061	395.9	10880.7	5748.1	359.3	00551	0DJ031	475.2	10864.9	5850.9	255.3
00495	0DJ061	404.7	10881.0	5743.4	351.8	00552	0DJ031	482.0	10864.7	5847.5	249.4
00496	0DJ061	408.6	10881.1	5741.4	348.5	00553	0DJ031	488.0	10864.7	5844.4	244.2
00497	0DJ061	419.7	10881.5	5735.4	339.1	00554	0DJ031	497.2	10864.6	5839.8	236.3
00498	0DJ061	421.2	10881.6	5734.6	337.9						
00499	0DJ061	426.9	10881.8	5731.5	333.1						
00500	0DJ061	436.6	10882.2	5726.3	324.9						
00501	0DJ015(1)	453.0	10858.3	5799.9	326.4						
00502	0DJ015(1)	456.6	10858.7	5797.7	323.6						
00503	0DJ015(1)	464.5	10859.6	5792.7	317.5						
00504	0DJ015(1)	480.6	10861.5	5782.7	305.1						
00505	0DJ015(1)	491.7	10862.8	5775.7	296.5						
00506	0DJ015(1)	493.3	10862.9	5774.7	295.3						
00507	0DJ015(1)	501.2	10863.9	5769.8	289.2						
00508	0DJ015(1)	508.2	10864.7	5765.4	283.8						
00509	0DJ015(1)	513.2	10865.3	5762.2	280.0						
00510	0DJ015(1)	518.2	10865.9	5759.0	276.1						
00511	0DJ015(1)	525.6	10866.7	5754.4	270.5						
00512	0DJ050	362.5	10869.2	5725.5	394.2						
00513	0DJ050	365.3	10869.2	5724.0	391.8						

Flist - End of file

Appendix 2iv

Abbreviations. Definition of Ratios
Rock Type Key.

Analyses : Key to Abbreviations

Group Name Abbreviations

URS	Upper Rhyolite Sequence
QRS	Que River Shale
B	Basalt
B.Fu	Calcite fuchsite altered basalt
HVS	Hangingwall Volcaniclastic Sequence
FPS	Feldspar phyrlic sequence - albite porphyritic andesite
Y+L	Polymict units and lava
STZ	Stringer Zone

SL Column Abbreviations

		G continuous core grind
S	= sample type	S split core sample
		R rock grab sample
		A AMDEL ICP, AAS, XRF
L	= Laboratory/Method	T University of Tasmania Geology Dept. XRF
		M Tasmanian Mines Department, Launceston. XRF

Ratios

ALT1	=	$\log \frac{K_2O + MgO}{K_2O + Na_2O + CaO + MgO}$	x 100 after Ishikawa et al (1976)
ALT2	=	$\log \frac{CaO + K_2 + Al_2O}{MgO + K_2O + Na_2O + CaO + Al_2O_3}$	x 100
ZnNo	=	Zinc Ratio = $\frac{Zn \cdot 100}{Zn + Pb}$	
MR Al/3K	=	Molecular ratio Al/3K = K-feldspar indicator.	

Rock Type Key

Y = polymict, R = felsic, BSH = black shale, SS = sandstone/siltstone, sed = sediment, B = basalt, IP = interpillow, Si = silica, Co = carbonate, fu = fuchsite, vn = vein, A = andesite, L = Lava, FPA = albite porphyritic andesite, D = dacite, STZ = stringer zone, Q = stringer envelope zone, gls = glass, cl = chlorite, mx = matrix, ab = albite, se = sericite.